



HAL
open science

Systemes auxiliaires pour les observables : approximation du connecteur dynamique locale pour les spectres d'addition et d'émision d'électrons

Marco Vanzini

► **To cite this version:**

Marco Vanzini. Systemes auxiliaires pour les observables : approximation du connecteur dynamique locale pour les spectres d'addition et d'émision d'électrons. Matière Condensée [cond-mat]. Université Paris Saclay (COMUE), 2018. Français. NNT : 2018SACLX012 . tel-01803435

HAL Id: tel-01803435

<https://pastel.hal.science/tel-01803435>

Submitted on 30 May 2018

HAL is a multi-disciplinary open access archive for the deposit and dissemination of scientific research documents, whether they are published or not. The documents may come from teaching and research institutions in France or abroad, or from public or private research centers.

L'archive ouverte pluridisciplinaire **HAL**, est destinée au dépôt et à la diffusion de documents scientifiques de niveau recherche, publiés ou non, émanant des établissements d'enseignement et de recherche français ou étrangers, des laboratoires publics ou privés.

NNT: 2018SACLX012

THÈSE DE DOCTORAT
de
L'UNIVERSITÉ PARIS-SACLAY
préparée à
L'ÉCOLE POLYTECHNIQUE

École doctorale n°572
Ondes et Matières (EDOM)
Spécialité: PHYSIQUE

par

Marco VANZINI

Auxiliary systems for observables:
dynamical local connector approximation
for electron addition and removal spectra

Thèse présentée et soutenue à Palaiseau le 30 janvier 2018 devant le jury composé de :

Prof. Eric CANCÈS	Président du jury
Prof. Eberhard K. U. GROSS	Rapporteur
Prof. Nicola MARZARI	Rapporteur
Prof. Roi BAER	Examineur
Prof. Silvana BOTTI	Examinatrice
Prof. Simo HUOTARI	Examineur
Dr. Lucia REINING	Co-encadrante
Dr. Matteo GATTI	Directeur de thèse

A chi mi ha portato fin qui.

Contents

	Page
Preface	1
I Background	5
1 The experimental starting point	7
1.1 Photoemission spectroscopy	7
1.1.1 The photoemission process	11
1.1.2 Angle Resolved Photo Emission Spectroscopy (ARPES)	13
1.2 Scanning Tunnelling Spectroscopy	14
2 The many-body problem	17
2.1 The system	17
2.1.1 The Born–Oppenheimer decoupling	18
2.1.2 The electronic system	19
2.2 The problem	19
2.3 Observables	21
2.4 Reformulations of the problem: functionals	24
2.4.1 The Rayleigh–Ritz principle	24
2.4.2 Hohenberg–Kohn Density Functional Theory (DFT)	25
2.4.3 One–body Reduced Density Matrix Functional Theory (RDMFT)	26
2.5 Green’s function	26
2.5.1 Lehmann representation	28
2.5.2 Analytic properties of the Green’s function: the spectral function	29
2.5.3 Standard route to the spectral function: the self energy	30
2.5.4 Dyson and Hedin equations	32
2.6 The Hubbard model	34
II Auxiliary systems	37
3 Auxiliary systems: an introduction	39
3.1 Reduced quantities	40
3.2 How to build auxiliary systems	41
3.2.1 The generalized Sham–Schlüter equation	42
3.2.2 What we have and what we have not	43
3.3 The Kohn–Sham system	43

3.3.1	The Sham–Schlüter equation	45
3.4	An auxiliary system for the density matrix	46
3.5	The spectral potential	47
3.6	DMFT and spectralDFT	52
4	Auxiliary systems: explicit examples	55
4.1	The Hubbard model on the Bethe lattice	55
4.1.1	The auxiliary system	58
4.2	The symmetric Hubbard dimer	61
4.2.1	The auxiliary system	67
4.2.2	Sham–Schlüter equation approach	71
4.3	The homogeneous electron gas	76
4.3.1	Real system viewpoint: HSE06 solution	77
4.3.2	The auxiliary system	82
III	The connector and dynLCA	91
5	The connector	93
5.1	The connector idea: Local Density Approximation (LDA)	93
5.2	Dynamical Mean Field Theory (DMFT)	96
5.3	A generalization	97
5.4	The dynamical local connector approximation (dynLCA)	99
5.5	The connector	102
5.5.1	General structure of the connector	102
5.5.2	Perturbation expansion	104
5.6	Model systems without auxiliary systems	106
5.6.1	Sham–Kohn Quasi Particle LDA	106
6	The connector for the Hubbard dimer	111
6.1	The real system: one–fourth filling solution	112
6.2	Approximations to the self energy	114
6.2.1	Hartree approximation	114
6.2.2	The GW approximation	115
6.3	Dynamical Connector Approach (dynCA)	116
6.3.1	The auxiliary system	116
6.3.2	The model system	117
6.3.3	Different quantities to import	118
7	Dynamical Local Connector Approximation in practice: real systems	125
7.1	Implementation	125
7.2	Fermi energy alignment	129
7.3	A shortcut: local alignment	132
7.4	Band structure correction	136
7.5	External correction	139
7.6	The dynLCA band structure	141
	Conclusion	145
	Acknowledgments	149
	Appendices	151

A	Résumé en français	153
B	Energy contributions	155
C	Bethe lattice CPA solution	159
D	Hubbard dimer at half filling	163
E	Sham–Schlüter for the density matrix	169
F	Homogeneous Electron Gas integrals	173
G	First order perturbation in ν^{ext}	179
H	GW for the Hubbard dimer	183
I	Bilocal functions in Bloch basis	193

Table of main symbols and conventions

\mathbf{r}	real space vector
$n(\mathbf{r}), \bar{n}$	local and average densities
n_{\min}, n_{\max}	minimum and maximum densities
$\omega_p = \sqrt{4\pi n}$	plasma frequency in the homogeneous electron gas
r_s	Wigner–Seitz radius
\mathbf{k}	reciprocal space vector
ε_k	one–particle excitation energy
\mathbf{G}	reciprocal lattice vector
$\{ n, \mathbf{k}\rangle\}$	Bloch basis, with n band index
$\varphi_{n,\mathbf{k}}(\mathbf{r}) = e^{i\mathbf{k}\cdot\mathbf{r}} u_{n,\mathbf{k}}(\mathbf{r})$	Bloch wavefunction
k_F	Fermi wave vector
$v_C(\mathbf{r})$	Coulomb potential
$v^{\text{ext}}(\mathbf{r})$	external potential
$v_H(\mathbf{r})$	Hartree potential
E_H	Hartree energy
E_x	Fock energy
$\gamma(\mathbf{r}, \mathbf{r}')$	one–particle reduced density matrix
$n_2(\mathbf{r}, \mathbf{r}')$	pair density
$n_{xc}(\mathbf{r}, \mathbf{r}')$	exchange–correlation hole
$v_{\text{KS}}(\mathbf{r})$	Kohn–Sham potential
$v_{\text{KS}}^{\text{xc}}(\mathbf{r})$	exchange–correlation part of the Kohn–Sham potential
$\varepsilon_l^{\text{KS}}, \varphi_l^{\text{KS}}(\mathbf{r})$	Kohn–Sham eigenvalue and eigenfunction
ϕ	work function
W	bandwidth
α	parameter of the PBE0 functional
λ	screening length of the HSE06 functional
$ \Psi_0^N\rangle$	ground state of the N –electron system
E_0	ground state total energy
$ \Psi_s^N\rangle$	excited state s of the N –electron system
E_s	total energy of the system described by $ \Psi_s^N\rangle$

ε_s	excitation energy
$\varepsilon_c = -EA$	(minus) electron affinity
$\varepsilon_v = -IP$	(minus) ionization potential
μ	chemical potential / Fermi energy
E_g	fundamental gap
ω	frequency/energy
$\hat{c}_l, \hat{c}_l^\dagger$	annihilation and creation operators
$\hat{\psi}(\mathbf{r}), \hat{\psi}^\dagger(\mathbf{r})$	field operators
$G(\mathbf{r}t, \mathbf{r}'t'), G(\mathbf{r}, \mathbf{r}', \omega)$	one-particle Green's function
$f_s(\mathbf{r})$	Lehmann amplitude
$A(\mathbf{r}, \mathbf{r}, \omega)$	spectral function
$\Sigma(\mathbf{r}, \mathbf{r}, \omega)$	exchange-correlation self energy
Z	renormalization factor
$\nu_{\text{SF}}(\mathbf{r}, \omega)$	spectral potential
$\nu_{\text{SF}}^{\text{xc}}(\mathbf{r}, \omega)$	exchange-correlation part of the spectral potential
$\nu_{\text{x}}^{\text{SR}}(\mathbf{r}, \omega)$	purely frequency-dependent part of the HSE06 spectral potential
$\nu_{\text{SK}}(\mathbf{r}, \omega)$	Sham-Kohn quasi particle potential
t, U	hopping parameter and interaction strength in the Hubbard model
$G_{ii}(\omega) = G_{\text{loc}}(\omega)$	on-site Green's function
$G_{\text{AIM}}(\omega)$	impurity Green's function
$\Delta(\omega)$	impurity hybridization function
$\mathcal{G}_0(\omega)$	impurity reference Green's function
$\mathcal{P.V.} \int$	principal value of the integral
Re, Im	real and imaginary parts
sign	signum
$\theta(x) = \begin{cases} 0 & \text{if } x < 0 \\ 1 & \text{if } x > 0 \end{cases}$	Heaviside theta function

Fourier transforms:

$$f(\mathbf{y}, \tau) = \int \frac{d\omega}{2\pi} \frac{d^3k}{(2\pi)^3} e^{-i(\omega\tau - \mathbf{k}\cdot\mathbf{y})} f(\mathbf{k}, \omega)$$

$$f(\mathbf{k}, \omega) = \int d^3y d\tau e^{i(\omega\tau - \mathbf{k}\cdot\mathbf{y})} f(\mathbf{y}, \tau)$$

Continuum limit:

$$\frac{1}{V} \sum_{\mathbf{k}} \rightarrow \int \frac{d^3k}{(2\pi)^3}$$

*IV. Nous suivons le passage le long du mur.
Il y a du monde, chacun est porteur du terme manquant
d'une équation destinée à rester sans solution. [...]*

*IX. On ne peut voir le mur que par parties,
la totalité est dans l'esprit.
Le texte ne devient complet
que lorsque vous arrivez à la crypte. [...]*

*XI. Certains murs vous incitent à demander:
qu'y a-t-il de l'autre côté ?
Ces murs-ci ne décrivent que leur propre limite.
Ils vous saisissent, mais ne vous demandent rien.*

*JOSEPH KOSUTH
'ni apparence ni illusion'
Murs de l'enceinte de Paris
Carrousel du Louvre*

This thesis is a story, and real stories hardly go straight.
This thesis is no exception: I have tried to condensate in the form of a sequential manuscript three years of research, attempts, many errors, new ideas, trials, some successes, some results, a bit of philosophy, discoveries of old ideas, new implementations, models, derivations, ...
With these ingredients, I have built this story.

Preface

*A quoi bon bouger, quand on peut
voyager si magnifiquement
dans une chaise?*

JORIS-KARL HUYSMANS, À rebours

Condensed matter is an amazing field of research. New phenomena periodically pop up out of nature, asking for an interpretation. It is the case of superconductivity, the quantum Hall effect, Mott insulators, excitons, magnons, ...

Remarkably, all of these are *emergent phenomena*. They cannot easily be explained just by focusing on the properties of the single components involved. On the contrary, they stem from the *collective behaviour* of particles, which is often *more* than just the sum of single-particle effects [1].

Typically, an important contribution to these phenomena is provided by electrons.

If in an extended system most of the electrons are usually attached to their nuclei, some of them can move almost freely through the system. These electrons, called *valence* electrons, wander around, explore and possibly establish coherent connections among themselves. They lose their purely atomic nature, in which their energy is fixed by the atomic quantum numbers n, l, m , and they enter a full *many-body* realm, where plenty of new energy states are available.

Some of these states can be considered as single-particle-like, and the many-electron system behaves as if it were composed of several quasi-independent electrons with renormalized properties. These are the famous Landau *quasiparticles* [2], which explain the success of the free electron gas as a model for metals. Some other states cannot definitely be viewed as single-particle-like, and they are the fingerprint of *correlations* between electrons. These states prove that the many-body system behaves as a whole, and a true many-body approach should be employed for its description.

Such a description exists, it has been developed in the fifties and the sixties, and it relies on the formalism of the Green's functions [3, 4, 5]. It is a very general theory with several ramifications. It yields, in principle, all the information that one could retrieve from the many-body system (*i.e.*, all the information enclosed in the many-particle wavefunction). It is the theory of *everything* of condensed matter.

However, one is usually not interested in everything. *Something* is already enough. In particular, the *spectral function* alone already offers an excellent characterization of the system. Moreover, the spectral function is a measurable quantity, that can be used to benchmark the theoretical approach.

At this stage, this thesis enters the play. The aim of this work is to exactly target, from the

theoretical point of view and in an effective way, the spectral function of a many–electron system, which is measured in photoemission or inverse photoemission spectroscopy.

In particular, throughout the thesis (and explicitly in chapter 1) I refer to angle–integrated photoemission experiments. This is a spectroscopy technique based on the photoelectric effect: schematically, a photon impinges on a sample, it transfers its energy to one of the electrons, which is consequently kicked out of the material and finally collected by an analyzer. By measuring the number of detected electrons at different energies, one has a clear map of the energy distribution of the electrons in the material.

Such a map is of fundamental importance, as it establishes a true window on the microscopic world of electronic states. Describing this map – if it is available – or predict it – when it is not – is the challenge of *theoretical spectroscopy*¹.

In the Green’s functions formalism I mentioned above, the *one–particle* Green’s function $G(\mathbf{r}, \mathbf{r}', \omega)$ exactly describes the physics of *charged excitations*, in which an electron is removed from (photoemission) or added to (inverse photoemission) the system. While the microscopic description requires the full Green’s function, the comparison with experiments is realized through a much simpler quantity. It is the *integrated spectral function* $A(\omega)$, and it is derived from the Green’s function via the following relation:

$$A(\omega) \sim \frac{1}{V} \int d^3r \operatorname{Im}G(\mathbf{r}, \mathbf{r}, \omega).$$

This function is the microscopic quantity that makes the link with experiments possible. In the standard approach (described in chapter 2), one first evaluates the full Green’s function $G(\mathbf{r}, \mathbf{r}', \omega)$, through the introduction of a non–local, complex and frequency–dependent potential, the *self energy* $\Sigma(\mathbf{r}, \mathbf{r}', \omega)$. Once $G(\mathbf{r}, \mathbf{r}', \omega)$ is at hand, all the off–diagonal elements and the real part of the diagonal are discarded. Finally, one integrates $\operatorname{Im}G(\mathbf{r}, \mathbf{r}, \omega)$ over space to obtain $A(\omega)$. At the final stage, a lot of information is removed, and one could question the efficiency of such a method.

In this thesis, an alternative is proposed. It is the joint venture of two *shortcuts*, presented in part II and part III respectively.

The first shortcut deals with the issue just mentioned: instead of using a non–local and complex potential, the self energy $\Sigma(\mathbf{r}, \mathbf{r}', \omega)$, to obtain a non–local and complex object, the full Green’s function $G(\mathbf{r}, \mathbf{r}', \omega)$, and then remove most of the gained information, why not being pragmatic and look for a method that directly focus on $\operatorname{Im}G(\mathbf{r}, \mathbf{r}, \omega)$? Its integral in space would yield the energy spectrum $A(\omega)$, while its integral over frequency returns the local density $n(\mathbf{r})$.

This wish is formalized and realized in chapter 3. There, I introduce an *auxiliary system*, in which fictitious particles interact via a *real, local and frequency–dependent* potential, the *spectral potential* $v_{\text{SF}}(\mathbf{r}, \omega)$ [6]. This is a much lighter object with respect to the self energy. However, if it were known, it would yield the exact values of the integrated spectral function $A(\omega)$ and the density $n(\mathbf{r})$.

In this sense, the spectral potential can be regarded as a dynamical generalization of the Kohn–Sham potential of *density functional theory* (DFT) [7]. Also the latter is an effective potential in an auxiliary system of fictitious particles. If its expression were known, one would have access to the exact density $n(\mathbf{r})$. However, since it is static, even the exact Kohn–Sham (KS) potential could not yield the exact spectral function. KS–DFT can only access the quasi–particle part of the spectrum and, even there, it usually underestimates the fundamental gap of semiconductors or insulators. By contrast, adding the frequency–dependence as an additional

¹www.etsf.eu

degree of freedom, the spectral potential yields in principle both the exact spectrum and the exact density.

It can be shown that a *real* potential is the minimum requirement to have both $A(\omega)$ and $n(\mathbf{r})$. However, a real but dynamical potential may break the usual causality rules (the Kramers–Kronig relations), and it must be considered as no more than a mathematical tool.

A complex generalization of the spectral potential restores causality, and is formally given by the effective potential of *spectral density functional theory* (SDFT) [8], which is in turn a generalization of *dynamical mean field theory* (DMFT) [9]. The latter is a successful approach to treat Hubbard–like systems; by contrast, we here stick to an *ab-initio*, parameter–free system. The former, on the other hand, has never been tested in practice. To complete the review of existing approaches, *time–dependent density functional theory* (TDDFT) [10] focuses on time–dependent phenomena, usually considering a system coupled to a time–dependent external potential. This is not the case within our approach, where frequency is a time difference stemming from a reduced description of a time–independent Hamiltonian [5].

An exact expression for the spectral potential can be found if the self energy is at hand, through the solution of a generalized Sham–Schlüter equation [11, 6]. This is shown in chapter 4, for three prototypical examples.

The first system we consider is the Bethe lattice with infinite coordination number. It describes the Mott metal–insulator transition via the divergence of the imaginary part of the self energy, which is a purely frequency–dependent complex number. The challenge is therefore to describe the same transition via a real spectral potential, whose imaginary part, by definition, is always zero. In a second example we treat the symmetric Hubbard dimer, in which the self energy, besides being complex, is also non–local. As a consequence, the task of the spectral potential is doubled. Finally, we move to continuous system by considering the homogeneous electron gas (HEG), with a purely non–local self energy (the Heyd–Scuseria–Ernzerhof HSE06 one [12]). The challenge is transforming the non–locality of the self energy into the frequency dependence of the spectral potential.

However, this method is efficient if it does *not* require the knowledge of the self energy. Therefore, we propose a second shortcut (part III), which is pretty general and is inspired by the local density approximation (LDA) to the Kohn–Sham potential of DFT.

The strategy consists in evaluating the unknown quantity (the spectral potential) in a model system, and then import it in the auxiliary system through a suitable *connector*, that is a prescription that explains how to use the model system result in the original system.

I explain the general idea of this approach in chapter 5 and I apply it to the study of the asymmetric Hubbard model in chapter 6.

The real challenge, however, is treating *realistic materials* within this method. To this aim we consider the homogeneous electron gas as a model system, like in LDA. The spectral potential is evaluated there for a wide range of densities, and then imported each time a different material is studied. For this task, we propose a very simple connector based on local quantities only, hence the name *dynamical local connector approximation* (dynLCA) for this approach. The results for four prototypical materials, sodium, aluminum, silicon, and solid argon, are presented in chapter 7.

Note that the connector approach has a further practical advantage: in fact, the self energy is used just once in the model system only. Once the latter is solved and the results are stored² for many values of densities, nobody will ever repeat the calculation in the model, nor will he/she perform a self energy calculation in the real material. One can completely abandon the

²<https://etsf.polytechnique.fr/research/connector/dynLCA>

self energy, which is complex-valued and non-local, hence computationally heavy. At the same time, one does not have to build it for every different system; only the local quantities present in the connector are needed, and these can be obtained through a simple DFT calculation.

Besides the theoretical insight that it offers, this approach results in a drastic reduction of the computational cost. Therefore, it is particularly well suited for studying the properties of a large number of materials (*material design*), in which the use of a non-local self energy is usually the most time-consuming part. On the one hand, indeed, a local and real potential is computationally lighter. On the other, this method disentangles general properties due to the electron-electron interaction (accounted for by the calculation in the homogeneous electron gas) from specific properties of the material, that enter the form of the connector.

As I will show in this thesis, it is not easy to design a connector which is generally valid, and more work will have to be done. However, the results of this thesis are meant to show that this is a promising way to go, to answer some open questions and to open new ones.

Part I

Background

*I needed to believe in a tale – however
unlikely – which placed the events
of this most terrible day in a sensible order.*

RICHARD ZIMLER, *The Last Kabbalist of Lisbon*

*La matière ne va pas jusqu'au bout,
et l'isolement n'est jamais complet.
Si la science va jusqu'au bout
et isole complètement,
c'est pour la commodité de l'étude.¹*

HENRY-LOUIS BERGSON, *L'évolution créatrice*

*Though wisdom is common, the many
live as if they had a wisdom of their own.*

HERACLITUS, *Fragments*

¹Matter does not go to the end, and the isolation is never complete. If science does go to the end and isolate completely, it is for convenience of study.

The experimental starting point

The aim of this thesis is to develop an efficient method for the description of observables related to the electronic structure of matter. To validate the approach, we will benchmark it with the existing state-of-the-art theories. Therefore, we will not directly face the comparison with experiments. However, the connection with the experimental world is still of primary importance, as it can guide us on choosing which quantities are important to reproduce theoretically.

All the chapters that follow will focus on one particular measurable quantity, the *spectral function*. This is a key quantity for the interpretation of different crucial experiments, which are based on phenomena that have marked the development of quantum theory itself: the *photoelectric effect* and *quantum tunnelling*.

Indeed, the diagonal of the spectral function in real space is the fundamental observable for describing *scanning tunnelling spectroscopy*. Its diagonal in reciprocal space is the cornerstone of *angle resolved photoemission spectroscopy*. Finally its trace, which is basis independent, is the many-body quantity that is needed for reproducing *photoemission* and *inverse photoemission* experiments.

Tunnelling spectroscopy is essentially a surface-sensitive technique. Also photoemission and its variants, according to the photon energy, are sensitive to the surface. However, they are extremely useful for investigating also the *bulk* properties of a system. In this thesis we concentrate on the bulk, and photoemission will therefore be our primary reference experiment.

1.1 Photoemission spectroscopy

Photoemission experiments are the modern times development of some famous investigations performed by Hertz in 1887, who observed what became known as *photoelectric effect*: under particular circumstances, a beam of monochromatic light is able to knock out electrons, thus called *photoelectrons*, from a solid. The quantum theoretical explanation [13] of this effect earned Einstein his Nobel prize: in an independent-particle picture (see fig. 1.1), a photon of frequency $\omega/2\pi$ is absorbed by one of the electrons of the material, with initial energy $-\varepsilon_B - \phi$, where ϕ is the work function (energy needed to eject an electron from the highest occupied level, namely, in a metal, the vacuum minus the Fermi energy) and $\varepsilon_B > 0$ is the binding energy of the electron, measured with respect to the Fermi energy μ . If the energy gain $\hbar\omega$ is sufficiently large, that is if $\hbar\omega > \varepsilon_B + \phi$, the electron escapes the material into the vacuum, with positive kinetic energy $\varepsilon_{\mathbf{k}} = \hbar\omega - \phi - \varepsilon_B$ and momentum $\hbar\mathbf{k}$, and is then collected by an analyser.

This effect is at the basis of *PhotoEmission Spectroscopy* (PES), whose goal is to determine the energy levels of electrons in materials. Since conservation of energy states that $-\varepsilon_B = \varepsilon_{\mathbf{k}} -$

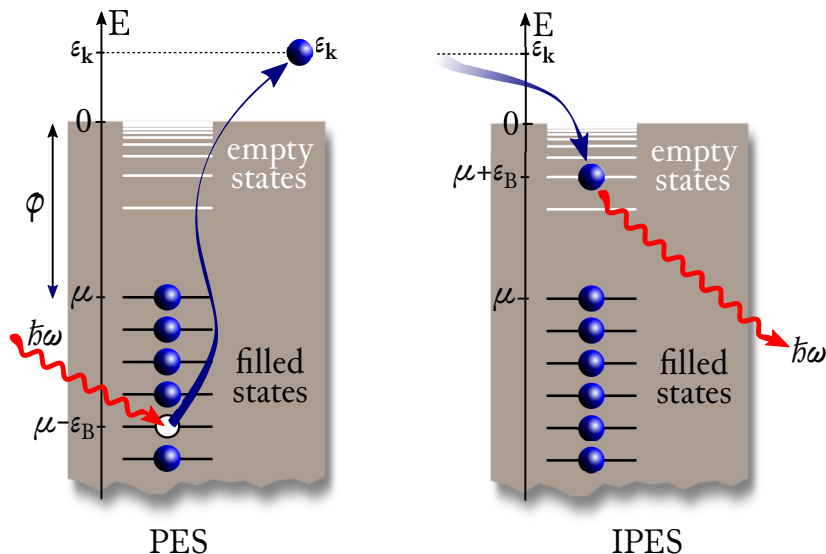


Figure 1.1: *Photoemission (PES) and inverse photoemission (IPES) processes schematically, in an independent particle picture. The wavy red arrow indicates a photon of energy $\hbar\omega$ that enters the sample in PES (and exits in IPES); after the interaction, the sample is left with a hole, indicated by the white circle, and $N - 1$ electrons ($N + 1$ in IPES), indicated by the blue spheres. The photoemitted electron (incoming electron in IPES) has energy ϵ_k . As it is evident from this picture, PES probes the occupied states, while IPES the empty ones.*

$\hbar\omega + \phi$, and since ϵ_k is measured by a detector, $\hbar\omega$ is chosen by the experimentalist and ϕ can be known, the electron binding energy can be determined from the kinetic energy of the photoelectron released in the vacuum.

Plotting the intensity of the signal, which is proportional to the number of photoelectrons, as a function of the binding energy, one obtains an extremely rich spectrum, where a series of distinct features reflects the different electronic energy states allowed in the material.

To make the discussion concrete, I will refer to a particular experiment in which I have taken part. It is an angle resolved photoemission experiment (ARPES, see below) on bulk aluminum, performed at the PEARL beamline of the Swiss Light Source (SLS¹). The aim was collecting experimental data on the electronic structure of aluminum, and use a theoretical approach (the cumulant expansion) to describe them. An overview of the measured angle-integrated photoemission intensity as a function of the binding energy is shown in fig. 1.2, in logarithmic scale.

The most evident isolated sharp peaks are a signature of very localized *core* states, where electrons stick close to nuclei in an atomic-like way; their binding energies do not differ that much from the corresponding isolated-atom energies, hence they are used as evidences of the presence of a particular element in the sample (ESCA: *electron spectroscopy for chemical analysis* [14]). In particular, in fig. 1.2, the most prominent peaks can be identified with the $2s$ and $2p$ atomic states. The line coming from the $1s$ state is at even lower energy and it is not shown.

More complex to interpret is the region of the spectrum close to the vacuum level, the *valence* band. The ARPES spectrum in the valence region at the k -point Γ is shown in fig. 1.3.

In this region, more energetic, less bound electrons are allowed to explore the lattice structure of the solid, exhibiting a stronger itinerant nature. The discrete atomic-like energy levels

¹<https://www.psi.ch/sls/>

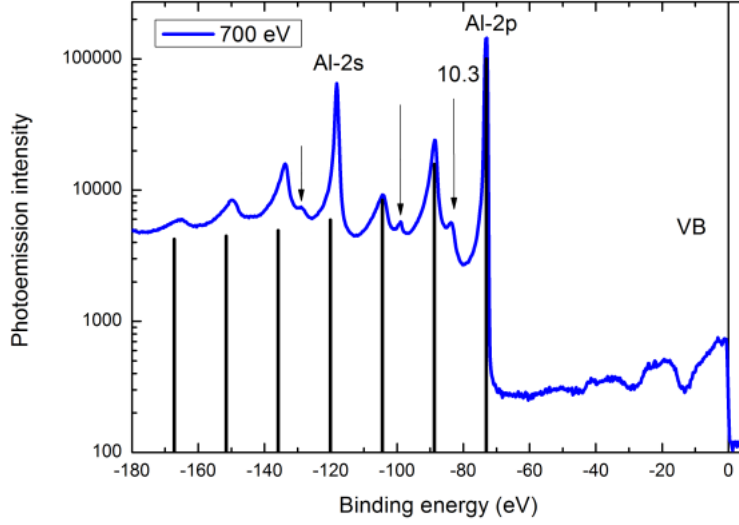


Figure 1.2: Angle integrated X-ray ($\hbar\omega = 700\text{eV}$) photoemission data for aluminum. Intensity (in logarithmic scale) of the photoemitted electrons as a function of the binding energy, in eV. The core levels 2p and 2s yield very sharp peaks in the signal, together with their plasmons. The valence band is, on the contrary, less pronounced; however, it is possible to distinguish, by the Fermi level, the quasiparticle with the characteristic $\sim \sqrt{\omega}$ shape, that creates its own plasmons at lower binding energy (Experiment performed in collaboration, at SLS; figure from ref. [15]).

(3s and 3p in the case of aluminum) merge into a continuous distribution of energy in which electrons are allowed to dwell, the Bloch *bands*. In certain cases (*Fermi liquids*) the band picture is enough to catch the main part of valence spectrum. This is the case when a prominent peak of finite width appears, the one at ~ -10 eV in fig. 1.3 (see also fig. 1.4). It can still be interpreted as the fingerprint of the propagation of one single electron. However, its motion is now affected by the dynamical *polarization* of the medium: as one electron moves, the others are repelled and a *Coulomb hole* in the electron probability distribution surrounds the propagating electron. The interaction of the electron with the Coulomb hole slows it down and thus decreases its kinetic energy once it is ejected. In particular, from the relation $-\varepsilon_B = \varepsilon_{\mathbf{k}} - \hbar\omega + \phi$, such a photoelectron will appear red-shifted with respect to the single-particle state to which it corresponds.

The higher the number of processes by which the electron can be decelerated, the wider the peak in the resulting spectrum. The width of the peak is thus interpreted as the inverse lifetime of the electron-plus-Coulomb-hole entity. The latter is called *quasiparticle* as long as it still exhibits a particle-like behaviour, namely as long as it can be thought of as a *dressed* particle with renormalized energy and mass. Quasiparticles, see fig. 1.4, get sharper and sharper as they approach the Fermi level, as the possibilities of decaying into non-coherent features is reduced by the kinematics of the process; on the contrary, well inside the Fermi sea (but still in the valence region), their lifetime is smaller and one does not see, nor one does talk about, quasiparticles there.

Bloch electrons in the valence band are an extraordinary source of other non-trivial many-body effects. One of these explains the series of smaller features that appear to the left of each

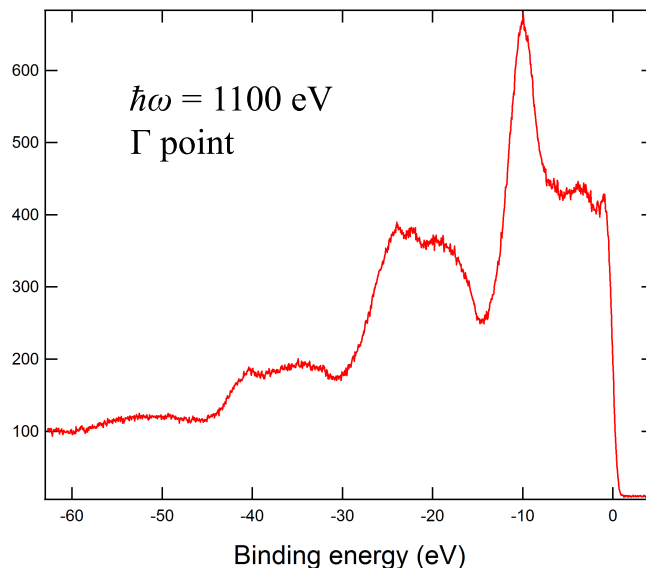


Figure 1.3: Angle resolved X-ray ($\hbar\omega = 1100\text{eV}$) photoemission experiment on aluminum, at the Γ point. Intensity (in linear scale) of the photoemitted electrons as a function of the binding energy, in eV. (from ref. [15]).

most prominent peak in fig. 1.2. In fact, together with their neutralizing ions, valence electrons generate a plasma-like medium in which quasiparticles (core and valence) propagate. This medium, which is quantized and originally in its ground state, can take part in the photoemission process by subtracting from the outgoing electron part of its energy, $\hbar\omega_p$. As the medium gets excited by one additional *plasmon*, the photoelectron is emitted with a lower kinetic energy, resulting in a smaller peak to the left of the quasiparticle, called *satellite* (see for example in fig. 1.2 the feature at around -20 eV). With lower probability, the medium can also take twice the energy it needs to get excited, $2\hbar\omega_p$: it thus goes to a higher excited state, consisting of *two* plasmons, and another satellite will show up in the photoemission spectrum, to the left of the previous one (the feature at ~ -35 eV in the aluminum spectrum). And so on and so forth with lower and lower probability.

These series of satellites, smaller and smaller as they depart from their quasiparticle, show up to the left of each prominent peak of the photoemission spectrum, in the valence as in the core region. They are not energy levels in the one-particle sense, but they are a clear benchmark of the *collective behaviour* of the electronic system [1], and they require a full many-body treatment to be theoretically reproduced.

Depending on the system, other mechanisms of energy-loss are possible [16], each resulting in other satellites in the photoemission spectrum.

Furthermore, in a photoemission experiment, other peaks can show up: they are the consequences of additional events like multiple scattering of the photoelectron before escaping the surface, or filling of the photohole left behind. Secondary processes like inelastically scattered electrons or results of “cascade” processes add up in the incoherent background which grows to the left (smaller kinetic energy of the photoelectron) of the most prominent features.

Finally, all spectroscopy techniques that involve electrons are highly *surface sensitive*. In particular, for kinetic energy of the photoelectron (which is determined by the photon energy and the binding energy range of interest) ranging from 10^0 to 10^3 eV, the corresponding electron inelastic mean free path λ_e is $4 \div 40 \text{ \AA}$ [17], a few lattice constants inside the material. Therefore, in general, the measured electrons stem from a region quite close to the surface. If one wants to probe the bulk, the surface must be as clean and as bulk-like as possible. Still, it will influence

the spectra. As an example, in fig. 1.3, the big shoulder at the right onset of the spectrum, at smaller binding energy than the quasiparticle, can indeed be interpreted as a non-dispersing surface contribution.

The qualitative picture I have just sketched shows how large is the possible number of effects that can occur in a photoemission experiment. To describe at least some of them, a reliable and efficient theory is needed.

1.1.1 The photoemission process

The standard approach to deal with the photoemission process from a many-body point of view simplifies the single photoemission event into the succession of three independent steps (*three-step model* [18]): an electron is excited by a photon in the solid, it propagates to the surface and it finally leaves the surface into the vacuum. Each of these steps contributes to the final photocurrent (detected electrons per unit time): an effective mean free path and a transmission probability through the surface take into account the last two steps [19], while the intrinsic photoexcitation of the electron can be described by the transition rate w_{fi} from the ground state of the N -electron system $|\Psi_0^{(N)}\rangle$ to an excited state $|\Psi_f^{(N)}\rangle$ – driven by a perturbing Hamiltonian \hat{H}_{int} . This is given, to first order in \hat{H}_{int} , by Fermi's golden rule [20, 21]:

$$w_{fi} = \frac{2\pi}{\hbar} \left| \langle \Psi_f^{(N)} | \hat{H}_{\text{int}} | \Psi_0^{(N)} \rangle \right|^2 \delta \left(E_f^{(N)} - E_0^{(N)} - \hbar\omega \right). \quad (1.1)$$

The perturbing Hamiltonian describes the interaction of the system with the electromagnetic field (ϕ, \mathbf{A}) . The scalar potential $\phi(\mathbf{r})$ can be set to zero by a gauge transformation. The vector potential is supposed to be small (linear response: $\mathbf{A} \cdot \mathbf{A} = 0$) and not varying with space (dipole approximation: $\nabla \cdot \mathbf{A} = 0$). With these assumptions, the perturbing Hamiltonian can be written as $\hat{H}_{\text{int}} = -i \frac{e\hbar}{mc} \mathbf{A} \cdot \nabla$ [17].

To evaluate the matrix element in eq. (1.1), a further simplification is usually made, called the *sudden approximation*²: the photoemitted electron is treated as completely decoupled from the sample; this allows one to factorize the final state $|\Psi_f^{(N)}\rangle$ into an antisymmetrized product of a photoelectron in the vacuum $\hat{c}_{\mathbf{k}}^\dagger |0\rangle$ and the $(N-1)$ electron system left behind in the excited state s , $|\Psi_s^{(N-1)}\rangle$. The photocurrent $\mathcal{I}_{\mathbf{k}}(\omega)$ is given by the total transition rate. It is the sum over all possible excited states s :

$$\mathcal{I}_{\mathbf{k}}(\omega) = \frac{2\pi}{\hbar} \sum_s \left| \langle \Psi_s^{(N-1)} | \hat{c}_{\mathbf{k}} \hat{H}_{\text{int}} | \Psi_0^{(N)} \rangle \right|^2 \delta \left(\varepsilon_{\mathbf{k}}^0 + E_s^{(N-1)} - E_0^{(N)} - \hbar\omega \right),$$

where the difference $E_0^{(N)} - E_s^{(N-1)}$ can be interpreted as the energy ε_s of an electron in the solid, measured from the Fermi energy μ , and $\varepsilon_{\mathbf{k}}^0$ is the energy of the free photoelectron in vacuum. The perturbing Hamiltonian can be expanded on a complete set of single-particle wavefunctions ϕ_l as $\hat{H}_{\text{int}} = \sum_{ll'} \hat{c}_l^\dagger \Delta_{ll'} \hat{c}_{l'}$, with³ $\Delta_{ll'} = \langle l | \hat{H}_{\text{int}} | l' \rangle$. Assuming that the ground state $|\Psi_0^{(N)}\rangle$ doesn't have any component along $|\mathbf{k}\rangle$, which is too high in energy⁴, one obtains:

$$\langle \Psi_s^{(N-1)} | \hat{c}_{\mathbf{k}} \hat{H}_{\text{int}} | \Psi_0^{(N)} \rangle = \sum_l \Delta_{\mathbf{k}l} \langle \Psi_s^{(N-1)} | \hat{c}_l | \Psi_0^{(N)} \rangle,$$

and the photocurrent becomes:

$$\mathcal{I}_{\mathbf{k}}(\omega) = \frac{2\pi}{\hbar} \sum_{ll'} \Delta_{\mathbf{k}l} \Delta_{\mathbf{k}l'}^* \left\{ \sum_s \langle \Psi_s^{(N-1)} | \hat{c}_l | \Psi_0^{(N)} \rangle \langle \Psi_0^{(N)} | \hat{c}_{l'}^\dagger | \Psi_s^{(N-1)} \rangle \delta \left(\varepsilon_{\mathbf{k}}^0 - \hbar\omega - \varepsilon_s \right) \right\}. \quad (1.2)$$

²The sudden approximation is justified when the kinetic energy of the photoemitted electron is large, which is the case for highly energetic impinging photons (see [22] to go beyond).

³In particular, for $\hat{H}_{\text{int}} = -i \frac{e\hbar}{mc} \mathbf{A} \cdot \nabla$ and constant \mathbf{A} , in the reciprocal space basis the representation is diagonal: $\hat{H}_{\text{int}} = \frac{e\hbar}{mc} \mathbf{A} \cdot \sum_{\mathbf{k}} \mathbf{k} \hat{c}_{\mathbf{k}}^\dagger \hat{c}_{\mathbf{k}}$ and $\Delta_{\mathbf{k}\mathbf{k}'} = \delta_{\mathbf{k}\mathbf{k}'} \frac{e\hbar}{mc} \mathbf{A} \cdot \mathbf{k}$.

⁴This assumption is justified for high energy photoelectrons in the three-step model.

While the first factors of the formula contain the radiation–matter interaction through the matrix elements Δ_{kl} , the part in curly brackets involves properties of the system only, from the excitation energies ε_s to the transition amplitudes $\langle \Psi_s^{(N-1)} | \hat{c}_l | \Psi_0^{(N)} \rangle$. Such a quantity, for reasons that will become clear later, is called *spectral function* and will be the main character of this thesis:

$$A_{ll'}(\omega) := \sum_s \langle \Psi_s^{(N-1)} | \hat{c}_l | \Psi_0^{(N)} \rangle \langle \Psi_0^{(N)} | \hat{c}_{l'}^\dagger | \Psi_s^{(N-1)} \rangle \delta\left(\omega - \frac{\varepsilon_s}{\hbar}\right). \quad (1.3)$$

With its help, the photocurrent becomes:

$$\mathcal{J}_{\mathbf{k}}(\omega) = \frac{2\pi}{\hbar^2} \sum_{ll'} \Delta_{kl} \Delta_{kl'}^* A_{ll'} \left(\frac{\varepsilon_{\mathbf{k}}^0}{\hbar} - \omega \right). \quad (1.4)$$

Finally, the matrix elements Δ_{kl} are evaluated in the basis l in which A is diagonal, and it is often assumed that $\Delta_{kl} = \text{const} := \Delta$. Thus one arrives at the final formula:

$$\boxed{\mathcal{J}_{\mathbf{k}}(\omega) = \frac{2\pi}{\hbar^2} |\Delta|^2 \sum_l A_{ll} \left(\frac{\varepsilon_{\mathbf{k}}^0}{\hbar} - \omega \right)} \quad (1.5)$$

namely the important result that the photocurrent is, to some multiplicative factors, the *trace of the spectral function* which, as it is well known, is independent of the particular basis $\{|l\rangle\}_l$.

Inverse photoemission (IPES) Strongly connected to photoemission is the specular process of *inverse photoemission*, which can be considered its time–inverted counterpart, as initial and final states swap their roles. Free electrons are sent on the sample, where they occupy empty levels; as a result, photons are ejected and collected by an analyser (see fig. 1.1).

The excitation energies are here defined as $\varepsilon_s = E_s^{(N+1)} - E_0^{(N)}$, and the conservation of energy states that $\varepsilon_{\mathbf{k}}^0 = \hbar\omega - \phi + \varepsilon_s$. By repeating the argument just above, the transition rate is still given by eq. (1.4) provided that the spectral function is defined as:

$$A_{ll'}(\omega) := \sum_s \langle \Psi_0^{(N)} | \hat{c}_l | \Psi_s^{(N+1)} \rangle \langle \Psi_s^{(N+1)} | \hat{c}_{l'}^\dagger | \Psi_0^{(N)} \rangle \delta\left(\omega - \frac{\varepsilon_s}{\hbar}\right). \quad (1.6)$$

Note that, besides being *specular* in time, IPES is also *complementary* to PES in the sense that, in a single–particle picture, it probes the empty levels of the system, while PES explores the occupied ones. The two approaches together give a full picture of the one–particle excitations of an electronic system.

Independent particles Neglecting the electron–electron interaction, the many–body system is equivalent to many one–body systems; the transition amplitudes in eq. (1.3) or (1.6) simplify to $\langle \Psi_s^{(N-1)} | \hat{c}_l | \Psi_0^{(N)} \rangle = \delta_{ls}$, and the spectral function becomes:

$$A_{ll'}^0(\omega) := \delta_{ll'} \delta\left(\omega - \frac{\varepsilon_l}{\hbar}\right) \quad (1.7)$$

with corresponding photocurrent:

$$\mathcal{J}_{\mathbf{k}}^0(\omega) = \frac{2\pi}{\hbar} |\Delta|^2 \sum_l \delta(\varepsilon_{\mathbf{k}}^0 - \varepsilon_l - \hbar\omega). \quad (1.8)$$

This is a series of delta peaks (see fig. 1.4 (b)) that can approximate at best the quasiparticle peaks; finite lifetime effects and collective excitations like plasmons are completely ruled out in such a picture. This is why, although very powerful for describing several properties of a many–electron system, effective one–particle approaches cannot in general catch the whole photoemission spectrum, and a truly many–body theory comes into play.

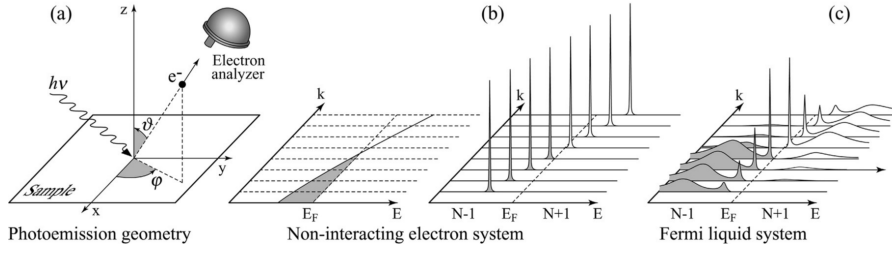


Figure 1.4: *Angle-resolved photoemission spectroscopy: (a) geometry of an ARPES experiment with specified emission direction (ϑ, φ); (b) momentum-resolved spectral function for a noninteracting electron system with a single energy band dispersing across μ ; (c) the same spectra for an interacting Fermi-liquid system (adapted from ref. [23]).*

1.1.2 Angle Resolved Photo Emission Spectroscopy (ARPES)

In the last decades, *Angle Resolved Photo Emission Spectroscopy* (ARPES) has become feasible: besides energy levels, also their dependence on the wavevector \mathbf{k} is experimentally accessible (see fig. 1.4). ARPES is an extremely useful technique for investigating the dispersion of valence states which, as already mentioned, present an important itinerant nature; in particular, for Fermi liquids, the position of the main quasiparticle peak as a function of \mathbf{k} is the *measured band structure*. Also the Fermi surface, as a mapping of the k -points with energy μ , is directly accessible by ARPES.

To interpret ARPES experiments, one has to relate the measured momentum (in vacuum) to the wave vector \mathbf{k} inside the solid: crossing the surface, the parallel (to the surface) component of the photoelectron momentum is conserved, while the perpendicular is not, and different approaches are used to determine it [19]. Besides the conservation of energy that we implemented above, also the *momentum conservation* in the solid must be taken into account: since the photon carries a negligible momentum in most cases, only *vertical* transitions are allowed, and the momentum of the electron in the material can be modified by reciprocal lattice vectors \mathbf{G} only. These vertical transitions between bands are determined by selection rules in the matrix elements. Finally, the photocurrent emitted in the direction \mathbf{k} is proportional to the *diagonal* of the spectral function in k space [17, 19]:

$$\mathcal{I}_{\mathbf{k}}(\omega) = \frac{2\pi}{\hbar^2} |\Delta_{\mathbf{k}\mathbf{k}}|^2 A\left(\mathbf{k}, \frac{\varepsilon_{\mathbf{k}}^0}{\hbar} - \omega\right), \quad (1.9)$$

where $A(\mathbf{k}, \omega) \equiv A_{\mathbf{k}\mathbf{k}}(\omega)$. As in eq. (1.5), the squared dipole matrix element $|\Delta_{\mathbf{k}\mathbf{k}}|^2 = |\langle \mathbf{k} | \hat{H}_{\text{int}} | \mathbf{k} \rangle|^2$ contains the radiation-matter interaction (in particular the dependence on the photon energy), while the whole many-body effects are accounted for by the spectral function, as it is clear from its definition:

$$A(\mathbf{k}, \omega) = \begin{cases} \sum_s \langle \Psi_s^{(N-1)} | \hat{c}_{\mathbf{k}} | \Psi_0^{(N)} \rangle \langle \Psi_0^{(N)} | \hat{c}_{\mathbf{k}}^\dagger | \Psi_s^{(N-1)} \rangle \delta(\omega - \varepsilon_s) & \text{if } \varepsilon_s = E_0^{(N)} - E_s^{(N-1)} \leq \mu \\ \sum_s \langle \Psi_0^{(N)} | \hat{c}_{\mathbf{k}} | \Psi_s^{(N+1)} \rangle \langle \Psi_s^{(N+1)} | \hat{c}_{\mathbf{k}}^\dagger | \Psi_0^{(N)} \rangle \delta(\omega - \varepsilon_s) & \text{if } \varepsilon_s = E_s^{(N+1)} - E_0^{(N)} \geq \mu \end{cases} \quad (1.10)$$

consistent with eq. (1.3) and (1.6). The main difference with angle-integrated photoemission is that ARPES selects a particular basis for the spectral function, while in photoemission only the trace of it is needed. This is why, if one wants to reproduce the outcome of ARPES experiments, the \mathbf{k} -resolved spectral function must be evaluated, while any basis is fine for integrated photoemission.

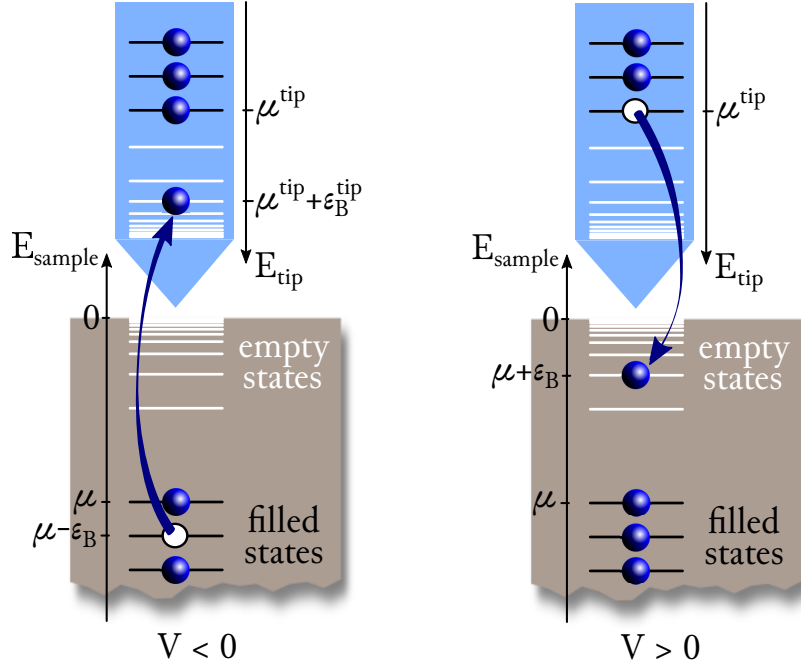


Figure 1.5: *Scanning Tunneling Spectroscopy schematically, in an independent particle picture, for negative (left) and positive (right) bias V . The grey box is the sample while the blue object is the probing tip. The process is analogous to the one of fig. 1.1. Alternatively occupied ($V < 0$) and empty states ($V > 0$) of the sample are explored.*

1.2 Scanning Tunneling Spectroscopy (STS)

A completely different experimental technique is *Scanning Tunnelling Spectroscopy* (STS), a purely *surface-sensitive* method based on the *tunnel effect*. The principle is very simple: a conducting probing tip is moved closer and closer to the surface of the sample, till the many-body wavefunctions of sample and tip overlap: in such a situation, if a suitable bias V is applied between tip and sample, tunnelling of electrons through the vacuum between the two becomes possible; thus, a *tunnelling current* $\mathcal{I}(V)$ can be measured.

As the tip moves around, by measuring the tunnelling current one can achieve a complete reconstruction and visualization of the surface with atomic resolution ($\sim 10^{-1} \div 10^0 \text{\AA}$), producing a real atomic microscope (STM: *scanning tunnelling microscope* [24]). Furthermore, besides visualization of single atoms [25], also the manipulation of them became feasible within this technique [26].

Although the physical principle on which they are based is different (tunnelling a barrier versus absorption of a photon), both in this technique and in photoemission electrons propagate and eventually are emitted (or absorbed) from the sample, see fig. 1.5. Therefore it is not surprising that, even though the *matrix elements* – that account for the experimental setups – are unrelated, both currents are proportional to the same *intrinsic* quantity, namely the spectral function. In particular, since here the tip probes *locally* the sample and only the least-bound electrons participate to the current, the *local* spectral function evaluated in a neighborhood of the chemical potential shows up [27, 28, 29, 30] (assuming for simplicity the same μ for both electrodes):

$$\mathcal{I}_{\mathbf{r}}(V) = \frac{4\pi e}{\hbar} \int_{\mu-eV}^{\mu} d\omega |T|^2 \rho_t(\omega + eV) A(\mathbf{r}, \mathbf{r}, \omega), \quad (1.11)$$

where $\rho_t(\omega)$ is the density of states of the tip and T is a matrix element depending, e.g., on the

geometry of the tip and the applied voltage V . It is not surprising that the densities of states of the two electrodes enter the formula, as electrons can jump between tip and sample only if the two can alternatively provide and accept electrons. In particular, depending on the sign of the voltage, empty ($V < 0$) or occupied states ($V > 0$) of the sample are probed, as the tip grants or gains electrons.

The sample enters eq. (1.11) through the spectral function in real space, defined as:

$$A(\mathbf{r}, \mathbf{r}', \omega) = \begin{cases} \sum_s \langle \Psi_s^{(N-1)} | \hat{\psi}(\mathbf{r}) | \Psi_0^{(N)} \rangle \langle \Psi_0^{(N)} | \hat{\psi}^\dagger(\mathbf{r}') | \Psi_s^{(N-1)} \rangle \delta(\omega - \varepsilon_s) & \text{if } \varepsilon_s = E_0^{(N)} - E_s^{(N-1)} \leq \mu \\ \sum_s \langle \Psi_0^{(N)} | \hat{\psi}(\mathbf{r}) | \Psi_s^{(N+1)} \rangle \langle \Psi_s^{(N+1)} | \hat{\psi}^\dagger(\mathbf{r}') | \Psi_0^{(N)} \rangle \delta(\omega - \varepsilon_s) & \text{if } \varepsilon_s = E_s^{(N+1)} - E_0^{(N)} \geq \mu \end{cases} \quad (1.12)$$

which can be derived from the generic $A_{ll'}(\omega)$ of eq. (1.3) and (1.6) via standard basis transformation.

In this chapter I have introduced an important object, the spectral function $A_{ll'}(\omega)$, which appears as a fundamental and recurrent quantity when considering different experimental techniques:

- 1) *its trace $\sum_l A_{ll}(\omega)$, that can be expressed in any basis, is needed to interpret photoemission and inverse photoemission experiments;*
- 2) *written in the reciprocal space basis, $A(\mathbf{k}, \omega)$ constitutes the intrinsic (in the sense of independent of the measurement procedure) part of ARPES spectra;*
- 3) *its diagonal in real space $A(\mathbf{r}, \mathbf{r}, \omega)$ is directly probed in scanning tunnelling spectroscopy.*

The spectral function contains essential information on the electronic structure of the sample, as can be seen from its definition, eq. (1.3) and (1.6). The challenge is therefore to derive it in the most efficient way from an ab-initio theory, in which just electrons and nuclei are present and no further parameters are used. I will show in the next chapter the state-of-the-art theory for obtaining the spectral function, while in the following I will develop a more efficient approach to the same goal.

The many-body problem

When Richard Feynman was asked which single knowledge had better survive a hypothetical fatal cataclysm, he replied with the *atomic theory* [31]: “*that all things are made of atoms – little particles that move around in perpetual motion, attracting each other when they are a little distance apart, but repelling upon being squeezed into one another*”.

The challenge was to transmit “the most information in the fewest words”, just one sentence to pass on to the next generation of (surviving) creatures. Had he been granted with more room, he would have probably specify that atoms – despite their name – were not the *fundamental* lego-bricks of nature.

Since the beginning of the century, indeed, scientists [32] have been aware that atoms are composed of big, heavy nuclei surrounded by light, tiny and fast electrons: their overall charge neutrality is the reason for the stability of atoms themselves, while the interplay between neighboring nuclei and electrons results in the attraction–repulsion dance that builds up the whole chemistry.

Well, not quite: it would be unfair to treat both nuclei and electrons with the same honours. The former, massive as they are, are pretty lazy compared to the far more active electrons. The latter move, scatter, lose and gain energy while, in many cases, one may consider that the nuclei stand by and watch, still approximately in their original state.

However, their only presence on stage is fundamental. Nuclei modify the properties of space around them, begging electrons for staying close. According to the configuration they assume, plenty of different materials come out, each one with its own characteristics.

Interacting electrons wandering in a lattice of nuclei will be the main character of the play described in this thesis.

2.1 The system

From a physical point of view, we can say that whenever two different time scales arise, a shorter one associated with electrons and a (much) longer one for the nuclear degrees of freedom, the nuclear motion can be considered as *adiabatically* frozen with respect to the electronic one; in this case, an *adiabatic* decoupling of their description is not only feasible but valuable.

That is something physicists quickly became aware of..

2.1.1 The Born–Oppenheimer decoupling

Indeed, soon after the birth of modern quantum mechanics [33, 34, 35], Born and Oppenheimer [36] showed how it was possible to deal with molecules by decoupling the slow nuclear motion from the fast electronic one. Assigning a wavefunction for independently describing each of them, Ψ for the electrons and Φ for the nuclei, the wavefunction of the coupled system can be, in some cases [37, 38], just the direct product of the two, $\Psi \cdot \Phi$.

Such a case occurs in particular in common solids, where massive¹ nuclei slightly move² and light electrons quickly adjust to the instantaneous configuration of the formers. Their “acclimatization” can be described by an electronic Schrödinger equation in which the nuclei enter only as a fixed set of parameters $\{\mathbf{R}_\alpha\}$:

$$\left[E_s^{\{\mathbf{R}_\alpha\}} - \hat{H}_e(\mathbf{r}_1, \dots, \mathbf{r}_N) - \sum_{i,\alpha} v_{eN}(|\mathbf{r}_i - \mathbf{R}_\alpha|) \right] \Psi_s^{\{\mathbf{R}_\alpha\}}(\mathbf{r}_1, \dots, \mathbf{r}_N) = 0, \quad (2.1)$$

where $\hat{H}_e(\mathbf{r}_1, \dots, \mathbf{r}_N)$ is the purely *electronic* Hamiltonian (see below) that depends only on the positions $\{\mathbf{r}_i\}_{i=1}^N$ of the N electrons, $v_{eN}(|\mathbf{r}_i - \mathbf{R}_\alpha|)$ is the Coulomb interaction between an electron in \mathbf{r}_i and a nucleus in \mathbf{R}_α and $\Psi_s^{\{\mathbf{R}_\alpha\}}(\mathbf{r}_1, \dots, \mathbf{r}_N)$ is the electronic wavefunction, describing electrons in $\mathbf{r}_1, \dots, \mathbf{r}_N$ when the nuclei are in $\{\mathbf{R}_\alpha\}$, with the multilabel s that specifies a complete set of quantum numbers for the electronic system.

The role of the eigenvalue $E_s^{\{\mathbf{R}_\alpha\}}$ is twofold: it is both the (output) total energy of the electron system and an (input) effective electronic energy that, on a longer time scale, contributes in determining the actual configuration of the nuclei. It is called (*adiabatic*) *potential energy surface*, and it is nothing but an electronic glue [39] that adds up to the nuclear Coulomb repulsion to set the dynamics of the lattice.

Indeed, the slower nuclear relaxation process can be described by the following *nuclear* Schrödinger equation, in which the electrons enter only through the potential $E_s^{\{\mathbf{R}_\alpha\}}$:

$$\left[\mathcal{E}_{\rho,s}^{tot} - \hat{H}_N(\{\mathbf{R}_\alpha\}) - E_s^{\{\mathbf{R}_\alpha\}} \right] \Phi_{\rho,s}(\{\mathbf{R}_\alpha\}) = 0, \quad (2.2)$$

where $\hat{H}_N(\{\mathbf{R}_\alpha\})$ is the purely *nuclear* Hamiltonian, $\Phi_{\rho,s}(\{\mathbf{R}_\alpha\})$ is the nuclear wavefunction and $\mathcal{E}_{\rho,s}^{tot}$ is the total energy of the electrons plus nuclei system, with ρ a set of quantum numbers for the nuclear Hamiltonian³.

Eq. (2.2) is a clear statement of adiabatic separation. It says that the nuclear motion does not modify the electronic state s , that enters as a parameter. In particular, electrons stay in their ground state $E_{s=0}^{\{\mathbf{R}_\alpha\}}$. The Born–Oppenheimer approximation breaks down when, on the

¹Even for the lightest atom, Hydrogen, the ratio between the mass of the electron and the nucleus is approximately 1/1836: the non-relativistic two-body problem can be separated into a center-of-mass that behaves like a free particle, of mass $M = m_p + m_e \sim m_p$, plus an orbiting particle of mass $\mu = \left(\frac{1}{m_e} + \frac{1}{m_p}\right)^{-1} \sim m_e$: eventually, in the center-of-mass reference system, a fixed “quasi-proton” and an orbiting “quasi-electron”.

²In a classical picture, the third Newton’s law states that the Coulomb force that an electron exerts on a proton is the same as the one that that proton exerts on the electron; as a consequence, their (change in) momentum is the same, hence their velocity is controlled by the ratio between their masses.

³A common approximation to $E_0^{\{\mathbf{R}_\alpha\}}$ is the *harmonic* one, where the adiabatic electronic potential is approximated by a quadratic function of the nuclear displacements, *i.e.*, $E_0^{\{\mathbf{R}_\alpha\}} \approx \sum_\alpha \frac{1}{2} M \omega^2 (\mathbf{R}_\alpha - \mathbf{R}_\alpha^{\text{eq}})^2$, with $\mathbf{R}_\alpha^{\text{eq}}$ the equilibrium position of the α -th nucleus: the Hamiltonian in eq. (2.2) results in a sum of independent harmonic oscillators, *i.e.*, free *phonons*; additional anharmonic contributions can be considered, resulting in *interacting* phonons.

A related approach, well suited in particular for molecules, is the separation of the nuclear dynamics into a rotational, vibrational and translational motion, pushing even forward the adiabatic separation idea by observing that different energy scales (*i.e.*, time scales) are involved in the three mentioned processes.

Finally, we mention the *Lennard–Jones* [40] and the *Morse* potential [41], used to parametrize the energy surface $E_{\{\mathbf{R}_\alpha\}}$.

contrary, there is an interplay between electronic states and lattice dynamics, that is when two different energy surfaces $E_s^{\{\mathbf{R}_\alpha\}}$ and $E_{s'}^{\{\mathbf{R}_\alpha\}}$ are so close to each other (eventually, they cross) that the slow nuclear dynamics induces transitions between different electronic states.

To conclude, eq. (2.2) states that it is possible to include the dynamics of the nuclei, and hence have access to the full many-body wavefunction in the Born–Oppenheimer approximation $\Psi_{\{\mathbf{R}_\alpha\}}(\mathbf{r}_1, \dots, \mathbf{r}_N) \cdot \Phi(\{\mathbf{R}_\alpha\})$, once the potential energy surface, and therefore the dynamics of the electrons, is at hand. The latter is controlled by eq. (2.1), the real bottleneck of the calculation. It is towards this very equation that we will now, and for the rest of the thesis, turn.

2.1.2 The electronic system

In atomic units⁴, which we will use for the rest of this thesis, the Hamiltonian that enters eq. (2.1) reads:

$$\hat{H} = \sum_{i=1}^N \left(\frac{\hat{p}_i^2}{2} + v^{\text{ext}}(\hat{\mathbf{r}}_i) \right) + \frac{1}{2} \sum_{i \neq j=1}^N \frac{1}{|\hat{\mathbf{r}}_i - \hat{\mathbf{r}}_j|} \quad (2.3)$$

where we have replaced the nucleus–electron interaction $v_{eN}(|\hat{\mathbf{r}}_i - \mathbf{R}_\alpha|)$ with a more generic external potential $v^{\text{ext}}(\hat{\mathbf{r}}_i)$. This is the most general Hamiltonian we will consider. It describes any realistic material in which 1) relativistic effects can be neglected, 2) spin–dependent interactions can be ignored and 3) the Born–Oppenheimer approximation holds.

These three requirements apply to a wide range of real physical systems, and we will focus in particular on *crystalline solids*, where the number of electrons is huge, of the order of the Avogadro number $N \sim 10^{23}$, and the arrangements of nuclei $\{\mathbf{R}_\alpha\}$ is regular, that is $\forall \alpha \exists (n_1, n_2, n_3) \in \mathbb{Z}^3 | \mathbf{R}_\alpha = n_1 \mathbf{a}_1 + n_2 \mathbf{a}_2 + n_3 \mathbf{a}_3$, with $\{\mathbf{a}_i\}_{i=1}^3$ primitive lattice vectors.

Furthermore, we will attach the innermost electrons, the *core electrons*, to their nuclei, freezing them together into a positively-charged *ion* structure. This is called the *frozen-core approximation*, and is motivated by the fact that only the *valence electrons* (the outermost ones) significantly contribute to the interatomic interaction. Hence N will be the number of valence electrons only, and $v^{\text{ext}}(\hat{\mathbf{r}}_i)$ the potential felt by an electron in \mathbf{r}_i due to the presence of the whole *ion* lattice. For the rest of the thesis, we will consider this lattice in a fixed configuration $\{\mathbf{R}_\alpha\}$, and we will drop the label $\{\mathbf{R}_\alpha\}$ from the formulas.

Finally, the Hamiltonian (2.3) completely defines the system, but we need the wavefunction Ψ to have access to its physical properties: the wavefunction obeys the Schrödinger equation, eq. (2.1), that reads⁵:

$$\hat{H}\Psi_s(\mathbf{r}_1, \dots, \mathbf{r}_N) = E_s \Psi_s(\mathbf{r}_1, \dots, \mathbf{r}_N) \quad (2.4)$$

Finally, with eq. (2.4) and eq. (2.3):

“The underlying physical laws necessary for the mathematical theory of a large part of physics and the whole of chemistry are thus completely known, ...”

2.2 The problem

“... and the difficulty is only that the exact application of these laws leads to equations much too complicated to be soluble.” [42]

⁴By definition, $m_e = e^2 = \hbar = 4\pi\epsilon_0 = 1$; as a consequence, the unit of length is the Bohr $a_0 = \frac{1}{\alpha} \frac{\hbar c}{m_e c^2} = 0.529 \text{ \AA}$, and the unit of energy is the Hartree $E_h = \alpha^2 m_e c^2 = 27.2114 \text{ eV}$.

⁵Since the Hamiltonian (2.3) does not couple spin and position variables, the total wavefunction will be factorized into the product of its spatial and spin components. The latter is not relevant for this thesis, and it will be not explicitly mentioned.

Believe it or not, despite the fact that the electronic many-body problem is completely and exactly defined, finding the wavefunction $\Psi_s(\mathbf{r}_1, \dots, \mathbf{r}_N)$ remains a formidable task. The reasons are mainly three:

1. *The number N of electrons in a solid is huge.* Take for instance the sample we used for the ARPES experiment that I mentioned in the previous chapter. It is a cylindrical sample of aluminum, 5 mm of diameter and 1.5 mm of height. It weighs less than 0.1 g, but it contains roughly $0.23 \cdot 10^{23}$ electrons.

Is this a large number? Walter Kohn [43] tried to answer this question from an optimistic perspective: if only we were to describe a molecule (or an atom!) of $N \sim 100$ electrons, by replacing each continuous coordinate $(\mathbf{r}^{(i)})_k \in (-\infty; \infty)$ in the wavefunction by just 3 parameters (a very rough trade!), the total numbers of these would be something like $\sim 10^{150}$, to obtain an accuracy in energy of $\sim 1\%$! No way to handle such a number, nor even to imagine it!

But let's stay positive and assume that some intelligent being whispers to us the solution. We start recording it, but still, needing at least two bits per parameter, we would quickly run out of *atoms* to store our $N = 100$ electrons solution, since the total number of atoms in the universe is estimated to be around 10^{80} (the situation is not always that drastic: in many cases, symmetries can help – see later with Bloch's theorem). This observation – that goes under the name of *van Vleck catastrophe* [44] – pushed Kohn to the following provocative statement [43]:

“In general the many-electron wave function $\Psi(\mathbf{r}_1, \dots, \mathbf{r}_N)$ for a system of N electrons is not a legitimate scientific concept, when $N \gtrsim 10^3$.”

2. The previous point would not be a big deal, if only electrons wouldn't interact. But *they do*, giving a job to thousands of physicists and, more importantly, life to billions of compounds, molecules and, eventually, human beings.

The interaction between electrons prevents the separation of \hat{H} into a direct sum of one-particle hamiltonians $\hat{h}(i)$. In general, one cannot even resort to a nearest neighbours model: the Coulomb interaction is long-range, meaning that each electron interacts, although sometimes weakly, with everyone else (in our 0.1 g Al sample, $\frac{1}{2}N(N-1)$ interactions means approximately 10^{44} couplings)!

3. The third reason why eq. (2.4) poses a *problem* is a conceptual issue: *having access to the wavefunction Ψ is not our final goal.*

The wavefunction is an *intermediate* object that completely describes (the knowledge we have of) a system. It contains *all* the information that can be extracted from it. In order to obtain in practice *a piece* of this information, one has to evaluate, from the wavefunction itself, some reduced, much reduced quantities with the properties of 1) being observables (in order to be compared with experiments) and 2) depending on just a few variables (in order to have a clear physical interpretation). The wavefunction itself is not one of these quantities, being a complex object whose interpretation is not even always unambiguous [45].

And struggling to build up a giant for finally picking up just a tiny pinch of it doesn't seem the most promising strategy.

Bearing these three arguments in mind – too many variables, an inseparable Hamiltonian and eventually an answer containing too much information – one had better give up on the quest for the full wavefunction Ψ , solution of eq. (2.4), and turn to what really matters.

2.3 Observables

What really matters is essentially just a bunch of operators – each one depending on a few degrees of freedom – whose expectation values are closely related to what is actually measured.

Being properties of the system, these expectation values are still functionals of the wavefunction but, containing (much) less information than Ψ_s , we expect them to describe the system from a *reduced* perspective only. On the other hand, their immediate meaning makes it easy(–ier) to speculate about their structure, and their relative small size makes them appealing quantities to work with.

The total energy The total energy of a system in the state s is formally defined by rearranging the Schrödinger equation (2.4) for the eigenvalue E_s , which becomes a *functional* $E_s = E_s[\Psi_s]$ of the wavefunction Ψ_s :

$$E_s = \int d^3r_1 \dots d^3r_N \Psi_s^*(\mathbf{r}_1, \dots, \mathbf{r}_N) \hat{H} \Psi_s(\mathbf{r}_1, \dots, \mathbf{r}_N). \quad (2.5)$$

In particular, the *ground state* total energy E_0 plays a crucial role. First, even at room temperature (~ 20 °C), most of common materials are in their ground state: take for instance our favourite Al sample ($r_s = 2.07 a_0$); its free Fermi energy (the valence band width) is $\epsilon_F^0 = 11.65$ eV, while $k_B T \sim 25$ meV; that makes a ratio of $k_B T / \epsilon_F^0 \sim 0.2\%$ thermally–excited electrons! Even perturbing the system, this is usually expected to finally relax to its ground state. Finally, in the Born Oppenheimer approximation, by minimizing $E_0 = E_0^{\{\mathbf{R}_\alpha\}}$ with respect to the lattice positions $\{\mathbf{R}_\alpha\}$, one can have access to many structural properties of the system itself (lattice constant, stress tensor, ...).

In conclusion, having the total energy of a many–body system means a lot. So much that, simply by inspecting E_s as a functional of the wavefunction, eq. (2.5), we will be able to introduce some very fundamental quantities, through which we will eventually reformulate the many–body problem.

The density Probably one of the simplest observables is the *electronic density* $n(\mathbf{r})$. It describes the distribution of electrons in space when the system is described by the wavefunction Ψ (that can either be the ground state Ψ_0 or an excited state Ψ_s). Density is defined as the number of electrons per unit volume, namely $n(\mathbf{r}) := \frac{dN}{d^3r} \Big|_{\mathbf{r}}$. It is directly related to the probability amplitude of finding an electron in \mathbf{r} , and its functional form in terms of the antisymmetric many–body wavefunction is:

$$n(\mathbf{r}) = N \int d^3r_2 \dots d^3r_N \Psi^*(\mathbf{r}, \mathbf{r}_2, \dots, \mathbf{r}_N) \Psi(\mathbf{r}, \mathbf{r}_2, \dots, \mathbf{r}_N), \quad (2.6)$$

which is the expectation value on the state Ψ of the *density operator* $\hat{n}(\mathbf{r}) := \sum_{i=1}^N \delta(\mathbf{r} - \hat{\mathbf{r}}_i)$ ⁶. This is quite a simple quantity, depending on just three continuous variables (and not $3N$ as the wavefunction), whose visualization is extremely human–friendly: everyone knows what “dense” means.

Besides being in itself a compact and clear object, the electronic density is also a fundamental ingredient for the expectation value of the many–body Hamiltonian (2.3). Indeed, the classical (self–)interaction energy of a cloud of charged electrons with density $n(\mathbf{r})$ is a simple *functional* of the density:

$$E_H = \frac{1}{2} \int d^3r d^3r' \frac{n(\mathbf{r})n(\mathbf{r}')}{|\mathbf{r} - \mathbf{r}'|}. \quad (2.7)$$

⁶The two definitions are completely equivalent provided the Pauli principle applies: if this is the case, summing over all but the first argument of $|\Psi|^2$ does not highlight this as a preferred variable. Otherwise, the proper definition would be $n(\mathbf{r}) = \sum_i \int d^3r_1 \dots d^3r_N \delta(\mathbf{r} - \mathbf{r}_i) \Psi^*(\mathbf{r}_1, \dots, \mathbf{r}_N) \Psi(\mathbf{r}_1, \dots, \mathbf{r}_N)$.

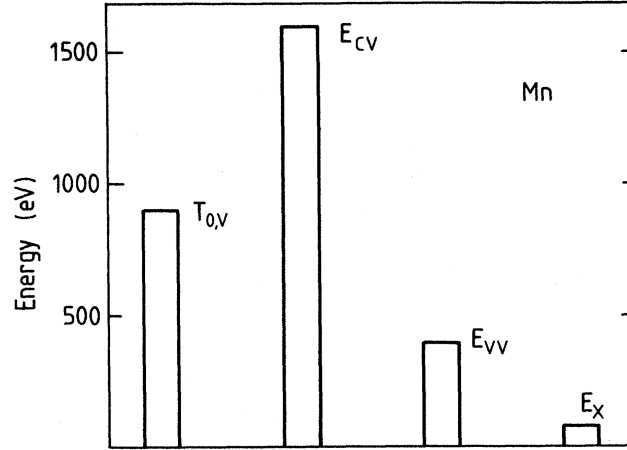


Figure 2.1: *Relative magnitudes of the different contributions to the total energy of Mn atoms (in eV), from ref. [46]. $T_{0,v}$ is the kinetic energy of the valence electrons, $E_{CV} = \int d^3r n(\mathbf{r}) v^{\text{ext}}(\mathbf{r})$ the interaction energy between the electrons and the ions, $E_{VV} = E_H$ the Hartree energy, eq. (2.7) and E_x the exchange contribution, eq. (2.9). The correlation term is even smaller, and is not represented.*

This is the famous *Hartree* contribution (see Appendix B), which often plays an important role (see figure 2.1) when evaluating the expectation value on the ground state of the electronic interaction term $\frac{1}{2} \sum_{i \neq j} \frac{1}{|\hat{\mathbf{r}}_i - \hat{\mathbf{r}}_j|}$.

On the other hand, one would never think that density alone is enough to have access to the *whole* ground state energy of the electronic system. The reason is simple: while density is a *local* quantity, both the kinetic and the Coulomb terms involve *non-local* interactions between particles. A new object pushes to be defined...

The density matrix A non-local generalization of density is the *one particle reduced density matrix* (1P-RDM), whose definition is the following:

$$\gamma(\mathbf{r}, \mathbf{r}') := N \int d^3r_2 \dots d^3r_N \Psi^*(\mathbf{r}', \mathbf{r}_2, \dots, \mathbf{r}_N) \Psi(\mathbf{r}, \mathbf{r}_2, \dots, \mathbf{r}_N). \quad (2.8)$$

This hermitian quantity, whose diagonal is the usual density, plays a twofold role in the ground state total energy.

First, electrons are *fermions*, and as such they obey the *Pauli exclusion principle*: no two electrons can occupy the same quantum level. In other words, the wavefunction Ψ is antisymmetric in its variables. This rule is powerful enough to go beyond the strictly classical Hartree term, eq. (2.7), even by still sticking to an *independent-particles* picture, that is by considering a factorized (but now also antisymmetrized) wavefunction: a *Slater determinant*. The corresponding energy contribution (derived in appendix B) is called the *exchange* or *Fock term*:

$$E_x = -\frac{1}{2} \int d^3r d^3r' \frac{\gamma(\mathbf{r}, \mathbf{r}') \gamma(\mathbf{r}', \mathbf{r})}{|\mathbf{r} - \mathbf{r}'|}. \quad (2.9)$$

This is the amount of energy that must be added to the classical Hartree term, for the reason that electrons, being fermions, tend to stay further apart from each other than their classical counterparts, and their Coulomb repulsion is therefore weaker (hence the minus sign [47]).

Not only does the density matrix enter the very first non-trivial (= non-classical) term in the interaction, but also the large (see figure 2.1) kinetic contribution to the total energy can be

exactly expressed in terms of it (see appendix B for a derivation):

$$T \equiv \langle \Psi | \sum_i \left(-\frac{\nabla_i^2}{2} \right) | \Psi \rangle = \int d^3 r \lim_{\mathbf{r}' \rightarrow \mathbf{r}} \left(-\frac{\nabla^2}{2} \right) \gamma(\mathbf{r}, \mathbf{r}'). \quad (2.10)$$

With these expressions, the total energy, so far, reads:

$$\int d^3 r d^3 r' \left\{ \delta(\mathbf{r}, \mathbf{r}') \left[\left(-\frac{\nabla_{\mathbf{r}}^2}{2} \right) + v^{\text{ext}}(\mathbf{r}) \right] \gamma(\mathbf{r}, \mathbf{r}') + \frac{1}{2} \frac{\gamma(\mathbf{r}, \mathbf{r})\gamma(\mathbf{r}', \mathbf{r}') - \gamma(\mathbf{r}, \mathbf{r}')\gamma(\mathbf{r}', \mathbf{r})}{|\mathbf{r} - \mathbf{r}'|} \right\}.$$

This is an explicit functional of $\gamma(\mathbf{r}, \mathbf{r}')$ only: “*the whole state [...] is completely described simply by this electric density [matrix]; it is not necessary to specify the individual three-dimensional wave functions that make up the total electric density. Thus one can deal with any number of electrons by working with just one matrix density function*”. [48]

Thus Spoke Dirac. End of story. Isn't it?

The pair density It is not. If the previous formula truly represented the total energy of Hamiltonian (2.3), nature would be very different from what we are used to, and definitely more boring. Indeed, while the first half of the formula is exact, the interaction contributions (2.7) and (2.9) have been derived under the assumption that the wavefunction could be represented by a *single* Slater determinant. That is usually not the case.

To catch what is missing, we introduce the *pair density*, proportional⁷ to the probability amplitude⁸ of finding *one* electron in \mathbf{r} and *another* in \mathbf{r}' :

$$n_2(\mathbf{r}, \mathbf{r}') := N(N-1) \int d^3 r_3 \dots d^3 r_N \Psi^*(\mathbf{r}, \mathbf{r}', \mathbf{r}_3, \dots, \mathbf{r}_N) \Psi(\mathbf{r}, \mathbf{r}', \mathbf{r}_3, \dots, \mathbf{r}_N). \quad (2.11)$$

Were Ψ a factorized wavefunction⁹, this quantity would reduce to $n(\mathbf{r})n(\mathbf{r}')$: the probability of finding an electron in \mathbf{r} *and* another in \mathbf{r}' would be given by the probability of finding an electron in \mathbf{r} *times* the probability of finding another electron in \mathbf{r}' : two uncorrelated events.

But this is clearly not the case, for the probability of finding an electron in \mathbf{r}' is *conditioned* by the presence of another electron in \mathbf{r} , since the two are interacting: the Pauli principle, on the one hand, struggles to keep spin-like electrons further apart (exchange effects), and the Coulomb interaction, on the other, does the same job for whatsoever electrons (strictly correlated contribution). Pictorially, the electron in \mathbf{r} digs a *probability hole* $n_{\text{xc}}(\mathbf{r}, \mathbf{r}')$ around itself, preventing the electron in \mathbf{r}' from further approaching:

$$n_2(\mathbf{r}, \mathbf{r}') = n(\mathbf{r})n(\mathbf{r}'|\mathbf{r}) = n(\mathbf{r})n(\mathbf{r}') + n(\mathbf{r})n_{\text{xc}}(\mathbf{r}, \mathbf{r}'), \quad (2.12)$$

where we have split the conditioned probability $n(\mathbf{r}'|\mathbf{r})$ in its uncorrelated part $n(\mathbf{r}')$ plus the *exchange-correlation hole* $n_{\text{xc}}(\mathbf{r}, \mathbf{r}')$. It is only by adding the exchange-correlation term that the full interaction energy can be *exactly* expressed as:

$$\langle \Psi | \frac{1}{2} \sum_{i \neq j} \frac{1}{|\hat{\mathbf{r}}_i - \hat{\mathbf{r}}_j|} | \Psi \rangle = \frac{1}{2} \int d^3 r d^3 r' \frac{n_2(\mathbf{r}, \mathbf{r}')}{|\mathbf{r} - \mathbf{r}'|} = E_{\text{H}} + \frac{1}{2} \int d^3 r d^3 r' \frac{n(\mathbf{r})n_{\text{xc}}(\mathbf{r}, \mathbf{r}')}{|\mathbf{r} - \mathbf{r}'|}, \quad (2.13)$$

⁷The pair density $n_2(\mathbf{r}, \mathbf{r}')$ is normalized to the number of electron pairs $N(N-1)$.

⁸The corresponding operator, of which eq. (2.11) is the expectation value on the antisymmetrized state $|\Psi\rangle$, is:

$$\hat{n}_2(\mathbf{r}, \mathbf{r}') := \sum_{i \neq j} \delta(\mathbf{r} - \hat{\mathbf{r}}_i) \delta(\mathbf{r}' - \hat{\mathbf{r}}_j) = \hat{n}(\mathbf{r})\hat{n}(\mathbf{r}') - \delta(\mathbf{r} - \mathbf{r}')\hat{n}(\mathbf{r})$$

⁹In the Hartree sense, see appendix B, and neglecting the self-interaction correction term.

where the last term is the *exchange–correlation energy* E_{xc} that, due to the particular form of the Coulomb interaction, can be written as:

$$E_{xc} = \frac{1}{2} \int d^3r n(\mathbf{r}) \int d^3u \frac{n_{xc}(\mathbf{r}, \mathbf{r} + \mathbf{u})}{|\mathbf{u}|}. \quad (2.14)$$

That is all, we are done. E_s is expressed as an exact functional of just two¹⁰ matrices, $\gamma^{(s)}(\mathbf{r}, \mathbf{r}')$ and $n_2^{(s)}(\mathbf{r}, \mathbf{r}')$, both obtained by integrating the information of the wavefunction Ψ_s :

$$E_s = \langle \Psi_s | \hat{H} | \Psi_s \rangle = \int d^3r d^3r' \left\{ \delta(\mathbf{r}, \mathbf{r}') \left[\left(-\frac{\nabla^2}{2} \right) + v^{\text{ext}}(\mathbf{r}) \right] \gamma^{(s)}(\mathbf{r}, \mathbf{r}') + \frac{1}{2} \frac{n_2^{(s)}(\mathbf{r}, \mathbf{r}')}{|\mathbf{r} - \mathbf{r}'|} \right\}. \quad (2.15)$$

This equation represents an exact reformulation of the Schrödinger equation (2.4), as far as the total energy is concerned.

The breakthrough with respect to eq. (2.5) is noteworthy: the total energy is no more a functional of the huge wavefunction, but of just two hermitian matrices I) whose size does not depend on the number N of electrons, making this procedure extremely appealing for studying extended systems, and 2) that are in principle observables, hence directly linked with experiments¹¹.

2.4 Reformulations of the problem: functionals

The observables introduced above are extremely useful to express in a concise way the total energy of a system, eq. (2.15). Moreover, they are light and clear objects one would rather handle over the wavefunction.

It turns out that some of these observables carry an important, fundamental reformulation of quantum mechanics, eq. (2.4). To see that, we will focus on the ground state.

2.4.1 The Rayleigh-Ritz principle

The ground state Ψ_0 stands out from the other states as it is associated to the *lowest* possible value of energy E_0 . With such an extremum property, the task of solving the eigenvalue problem of eq. (2.4) can be *exactly* recast, for $s = 0$ only, into the equivalent search for the minimum Ψ_0 of the functional $E_0[\Phi] := \int \Phi^* \hat{H} \Phi$ (where the integral is over all the degrees of freedom of Φ), with Φ N -electrons trial wavefunctions (normalized and antisymmetric):

$$E_0 = \min_{\Phi} E_0[\Phi] \quad \Longleftrightarrow \quad \left. \frac{\delta E_0[\Phi]}{\delta \Phi(\mathbf{r}_1, \dots, \mathbf{r}_N)} \right|_{\Phi=\Psi_0} = 0. \quad (2.16)$$

In practice, one considers trial wavefunctions Φ depending on some adjustable parameters $\{\alpha_i\}_i$, and determines the latter by searching for the minimum energy, eq. (2.16). This is the key principle of methods such as *configuration interaction* or *variational Monte Carlo*.

¹⁰Unfortunately, γ cannot be derived in a simple way from n_2 or viceversa: only the diagonal of γ , namely the usual density n , is $n(\mathbf{r}) = \gamma(\mathbf{r}, \mathbf{r}) = \frac{1}{N-1} \int d^3r' n_2(\mathbf{r}, \mathbf{r}')$; on the other hand, both can be derived from the *two-particles density matrix* $\Gamma^{(2)}(\mathbf{r}_1, \mathbf{r}_2; \mathbf{r}'_1, \mathbf{r}'_2) := N(N-1) \int d^3r_3 \dots d^3r_N \Psi^*(\mathbf{r}'_1, \mathbf{r}'_2, \mathbf{r}_3, \dots, \mathbf{r}_N) \Psi(\mathbf{r}_1, \mathbf{r}_2, \mathbf{r}_3, \dots, \mathbf{r}_N)$ [49]; then $n_2(\mathbf{r}, \mathbf{r}') = \Gamma^{(2)}(\mathbf{r}, \mathbf{r}'; \mathbf{r}, \mathbf{r}')$ and $\gamma(\mathbf{r}, \mathbf{r}') = \frac{1}{N-1} \int d^3r_2 \Gamma^{(2)}(\mathbf{r}, \mathbf{r}_2; \mathbf{r}', \mathbf{r}_2)$. Therefore, one can write the total energy as a functional of $\Gamma^{(2)}(\mathbf{r}, \mathbf{r}_2; \mathbf{r}', \mathbf{r}_2)$ alone, even if it is not yet clear which are the sufficient conditions $\Gamma^{(2)}$ has to fulfill to represent a true physical state, namely to correspond to an antisymmetric wavefunction (N -representability problem for $\Gamma^{(2)}$).

¹¹In particular, directly linked with experiments [50] is the *pair correlation function* $g(\mathbf{r}, \mathbf{r}')$, that describes the departure from an uncorrelated pair density through the relation $n_2(\mathbf{r}, \mathbf{r}') = n(\mathbf{r})g(\mathbf{r}, \mathbf{r}')n(\mathbf{r}')$; as a consequence, g is related to the exchange–correlation hole via the equation $g(\mathbf{r}, \mathbf{r}') = 1 + \frac{n_{xc}(\mathbf{r}, \mathbf{r}')}{n(\mathbf{r}')}$.

2.4.2 Hohenberg–Kohn Density Functional Theory (DFT)

What does the minimum principle (2.16) say in case the total energy is given by eq. (2.15)? Let us start by rearranging the latter in the following form, for $s = 0$:

$$\begin{aligned} E_0 &= \left\{ \int d^3 r \lim_{r' \rightarrow r} \left(-\frac{\nabla_r^2}{2} \right) \gamma(\mathbf{r}, \mathbf{r}') + \frac{1}{2} \int d^3 r d^3 r' \frac{n_2(\mathbf{r}, \mathbf{r}')}{|\mathbf{r} - \mathbf{r}'|} \right\} + \int d^3 r n(\mathbf{r}) v^{\text{ext}}(\mathbf{r}) = \\ &\equiv T[\gamma] + V_{\text{ee}}[n_2] + \int d^3 r n(\mathbf{r}) v^{\text{ext}}(\mathbf{r}), \end{aligned}$$

where, from now on, γ and n_2 are ground state $s = 0$ matrices. The external potential enters explicitly in E_0 only through the coupling with the density, and we can wonder whether or not two different external potentials, $v_1^{\text{ext}}(\mathbf{r})$ and $v_2^{\text{ext}}(\mathbf{r})$, differing by more than a constant, can yield the same density $n(\mathbf{r})$. Let us say so and see what happens.

The potential $v_1^{\text{ext}}(\mathbf{r})$ determines the Hamiltonian $\hat{H}^{(1)}$, whose ground state¹² is $\Psi_0^{(1)}$, from which we can build the matrices $\gamma^{(1)}(\mathbf{r}, \mathbf{r}')$ and $n_2^{(1)}(\mathbf{r}, \mathbf{r}')$. The same construction holds for the potential $v_2^{\text{ext}}(\mathbf{r})$, which yield the matrices $\gamma^{(2)}(\mathbf{r}, \mathbf{r}')$ and $n_2^{(2)}(\mathbf{r}, \mathbf{r}')$, different from the previous ones since $\Psi_0^{(1)} \neq e^{i\theta} \Psi_0^{(2)}$, by the hypothesis that the two potentials differ by more than a constant. Only the diagonal of the γ matrices, namely the density, is the same for the two potentials: $\gamma^{(1)}(\mathbf{r}, \mathbf{r}) = \gamma^{(2)}(\mathbf{r}, \mathbf{r}) = n(\mathbf{r})$.

Let us first consider the system $\hat{H}^{(1)}$; by the minimum principle (2.16) applied to a generic wavefunction $\Phi \neq e^{i\theta} \Psi_0^{(1)}$, we have $E_0^{(1)} \equiv E_0^{(1)}[\Psi_0^{(1)}] < E_0^{(1)}[\Phi]$. Take $\Phi = \Psi_0^{(2)}$; we have:

$$\begin{aligned} E_0^{(1)} &< E_0^{(1)}[\Psi_0^{(2)}] \equiv T[\gamma^{(2)}] + V_{\text{ee}}[n_2^{(2)}] + \int d^3 r n(\mathbf{r}) v_1^{\text{ext}}(\mathbf{r}) = \\ &= E_0^{(2)}[\Psi_0^{(2)}] + \int d^3 r n(\mathbf{r}) [v_1^{\text{ext}}(\mathbf{r}) - v_2^{\text{ext}}(\mathbf{r})] = \\ &\equiv E_0^{(2)} + \int d^3 r n(\mathbf{r}) [v_1^{\text{ext}}(\mathbf{r}) - v_2^{\text{ext}}(\mathbf{r})]. \end{aligned}$$

By repeating the same procedure for the system $\hat{H}^{(2)}$ and summing the resulting inequality to the one just above, one obtains the absurd conclusion that $E_0^{(1)} + E_0^{(2)} < E_0^{(2)} + E_0^{(1)}$.

The simplicity of this reasoning should not diminish the relevance of the result, that goes under the name of *first Hohenberg–Kohn theorem* [52]: “ $v^{\text{ext}}(\mathbf{r})$ is (to within a constant) a unique functional of $n(\mathbf{r})$ ”. Therefore, since the external potential fixes the Hamiltonian \hat{H} of eq. (2.3) and this determines all the spectrum, incredible as it may seem, *anything* is a functional of $n(\mathbf{r})$, from the ground state wavefunction $\Psi_0 = \Psi_0[n]$ to any excited state $\Psi_s = \Psi_s[n]$ to any of the observables introduced above.

From being huge functionals of the wavefunction Ψ , $\mathcal{O} = \mathcal{O}[\Psi]$, *everything* becomes a *functional* of the density: $\mathcal{O} = \mathcal{O}[\Psi] \equiv \mathcal{O}[\Psi[n]] = \mathcal{O}[n]$, hence the name *Density Functional Theory* (DFT) for this approach. Clearly, there is also a downside: while functionals of Ψ are generally explicit, see eq. (2.6) or (2.8), explicit functionals of density are most often unknown. All the difficulty of solving the many-body problem translates in the search for explicit expressions of the functionals. We will come back to this issue in the rest of the work.

As a particular case, the ground state total energy $E_0 = E_0[n]$ is a functional of n , too, and we can introduce a universal functional $F[n] := T[\gamma[n]] + V_{\text{ee}}[n_2[n]]$, independent of $v^{\text{ext}}(\mathbf{r})$, through which $E_0[n] = F[n] + \int d^3 r n(\mathbf{r}) v^{\text{ext}}(\mathbf{r})$. The actual ground state density is the one that minimizes the energy functional $E_0[\tilde{n}]$ (*second Hohenberg–Kohn theorem*), with \tilde{n} correspond-

¹²We assume that both $\Psi_0^{(1)}$ and $\Psi_0^{(2)}$ are non-degenerate ground states. In the degenerate situation, the conclusions still hold, as can be seen, *e.g.*, by the Levy and Lieb constrained-search method [51].

ing to an antisymmetric N -electrons wavefunction¹³:

$$E_0 = \min_{\tilde{n} \rightarrow N} E_0[\tilde{n}] \iff \left. \frac{\delta E_0[\tilde{n}]}{\delta \tilde{n}(\mathbf{r})} \right|_{\tilde{n}=n} = \left. \frac{\delta F[\tilde{n}]}{\delta \tilde{n}(\mathbf{r})} \right|_{\tilde{n}=n} + v^{\text{ext}}(\mathbf{r})[n] = 0, \quad (2.17)$$

which is exactly on the same footing of eq. (2.16), but requires a minimization with respect to a function of three (\tilde{n}) instead of $3N$ (Φ) variables! Still, “*the major part of the complexities of the many-electron problems are associated with the determination of the universal functional $F[n]$* ” [52].

2.4.3 One-body Reduced Density Matrix Functional Theory (RDMFT)

A clever strategy to bypass our ignorance of the functional $F[n]$ is choosing the density matrix as the fundamental quantity, working with a *Reduced Density Matrix Functional Theory* (RDMFT). The density matrix has indeed an additional degree of freedom (non-locality), through which more explicit information could be displayed.

Gilbert [53] has shown that there is a one-to-one correspondence between the ground state wavefunction and the ground-state density matrix. Moreover, we can extend the correspondence also to the local external potential $v^{\text{ext}}(\mathbf{r})$ that enters the Hamiltonian (2.3).

The reason for using $\gamma(\mathbf{r}, \mathbf{r}')$, which is a non-local object, instead of the local density $n(\mathbf{r})$, is simple: of the functional $F[n]$ introduced above, DFT knows exactly only the Hartree contribution E_H , eq. (2.7). Of the corresponding functional $\tilde{F}[\gamma] := T[\gamma] + V_{\text{ee}}[n_2[\gamma]]$ that can be analogously introduced here, RDMFT knows, at the exact level, the Hartree term, the exchange contribution E_x , eq. (2.9), and the kinetic contribution T , eq. (2.10), the three most often largest contributions to the total energy, see fig. 2.1. Only the purely correlation term $E_c[\gamma]$ is left behind, begging for an approximation:

$$\tilde{F}[\gamma] = T[\gamma] + E_H[\gamma] + E_x[\gamma] + E_c[\gamma].$$

Standard approximations to $E_c[\gamma]$ are, *e.g.*, the Müller-type functionals [54].

Both RDMFT [55, 56] and HK-DFT offer an appealing procedure to evaluate the diagonal of the spectral function, which is in principle an exact functional of density: $A(\mathbf{r}, \mathbf{r}, \omega) = A(\mathbf{r}, \mathbf{r}, \omega)[n]$. Building in practice this functional is a different matter: it is “notoriously difficult” [57] to express a frequency-dependent quantity from a static one, and we would really have a hard time in trying to directly do it. On the other hand, by adding to the density (or to the density matrix) additional degrees of freedom, expressing $A(\mathbf{r}, \omega)$ as a functional will be almost trivial, as it is shown in the next section.

2.5 Green's function (GF)

A fundamental quantity for this thesis, strongly related to the physics of photoemission experiments, is the time-ordered one-particle Green's function $G(\mathbf{r}t, \mathbf{r}'t')$ [3, 4, 58], defined (at zero temperature) as the probability amplitude to detect an additional electron in (\mathbf{r}, t) if it has been added to the N -electrons ground state $|\Psi_0\rangle$ in (\mathbf{r}', t') (or viceversa for a hole – PES):

$$iG(\mathbf{r}t, \mathbf{r}'t') := \langle \Psi_0 | \hat{\mathcal{T}} \hat{\psi}(\mathbf{r}, t) \hat{\psi}^\dagger(\mathbf{r}', t') | \Psi_0 \rangle, \quad (2.18)$$

¹³This is the N -representability problem for the density, which is solved by any reasonable non-negative function that integrates to N .

reduced quantity	associated theory	Energy functional	
		known part	unknown part
$n(\mathbf{r})$	DFT	$E_{\text{H}}[n]$	$F[n] = T[\gamma[n]] + V_{\text{ee}}[n_2[n]]$
$\gamma(\mathbf{r}, \mathbf{r}')$	RDMFT	$T[\gamma] + E_{\text{H}}[\gamma] + E_{\text{x}}[\gamma]$	$E_{\text{c}}[\gamma]$
$G(\mathbf{r}, \mathbf{r}', \omega)$	GF	$E_0[G]$	\emptyset

Table 2.1: *Energy functionals.*

where $\hat{\psi}$ and $\hat{\psi}^\dagger$ are Heisenberg field operators that destroy and create particles¹⁴, and $\hat{\mathcal{T}}$ is the time-ordering operator, that sets the operators to its right in chronological order, with a minus sign for each swap of operators.

The Green's function is a worth-studying quantity *per se*, as the expectation value of any one-particle operator $\hat{\mathcal{O}}^{(1)} = \int d^3r d^3r' \hat{\psi}^\dagger(\mathbf{r}, \mathbf{r}') \hat{\psi}(\mathbf{r}')$ is an *explicit functional* of the Green's function: $\langle \hat{\mathcal{O}}^{(1)} \rangle = -i \int d^3r d^3r' o(\mathbf{r}, \mathbf{r}') G(\mathbf{r}' t, \mathbf{r} t^+)$, with $t^+ \equiv t + \eta$, $\eta \rightarrow 0$. Two important examples are the density and the density matrix, that can be expressed through the Green's function as:

$$\begin{aligned} n(\mathbf{r}) &= -i G(\mathbf{r} t, \mathbf{r} t^+) \\ \gamma(\mathbf{r}, \mathbf{r}') &= -i G(\mathbf{r} t, \mathbf{r}' t^+). \end{aligned} \quad (2.19)$$

From the last of these relations, one can think to the Green's function as a *dynamical* generalization of the density matrix. This additional degree of freedom – time – contains the dynamics of the system set by the Hamiltonian, and allows one to express also the expectation value of \hat{H} – a *two-particles* operator – as an exact functional of G only, an unexpected result known as *Galitskii-Migdal theorem* [59]:

$$E_0 = -\frac{i}{2} \int d^3r \lim_{\mathbf{r}' \rightarrow \mathbf{r}} \lim_{t' \rightarrow t^+} \left[i \frac{\partial}{\partial t} + h_0(\mathbf{r}) \right] G(\mathbf{r} t, \mathbf{r}' t'), \quad (2.20)$$

with $h_0(\mathbf{r}) \equiv -\frac{\nabla^2}{2} + v^{\text{ext}}(\mathbf{r})$ the one-particle Hamiltonian. With such an equation, the journey that led us through different observables is now complete, as the whole total energy is an *explicit* functional of G : knowing the latter, the former would be at hand, too, with no additional effort. On the contrary, even if one knew the exact n or γ , one would still need the functional F or \tilde{F} to get the total energy.

This is an example of a general truth about functionals: the simpler the function, the more hidden the information; viceversa, the more degrees of freedom a function exhibits, the more explicit is usually the functional, see table 5.1. A clear example is the transition from DFT to RDMFT, and from that to Green's function theory, as we did above: the fundamental function that we use for the description of the system picks up additional degrees of freedom (from a *local* density to a *non-local* density matrix, and then to a *dynamical* non-local Green's function). As a consequence, most or the whole of the ground-state energy functional becomes explicitly known.

Viceversa, it is easier to express the conditions a quantity has to fulfill to be physical (the N -representability problem) for smaller quantities than for larger ones. Indeed, while these conditions are known for the density and the density matrix [49] and, they are still under debate for the Green's function [60].

¹⁴Field operators are in general spin-dependent, $\hat{\psi}_\sigma(\mathbf{r}, t)$, hence the Green's function, too, bears two spin-indices: $G_{\sigma\sigma'}$. On the other hand, since \hat{H} is spin-independent, the resulting Green's function is diagonal in spin space, $G_{\sigma\sigma'} = G \delta_{\sigma\sigma'}$. This last G is the one used throughout the text; spin shows up in some factors of $2 = \sum_{\sigma\sigma'} \delta_{\sigma\sigma'}$ that we omit for clarity.

2.5.1 Lehmann representation

Besides the interesting relations above, the main reason – for our purposes – of working with G becomes clear when realizing a particular feature of the many-body Hamiltonian (2.3), which can be recast into the following N -independent second-quantized form:

$$\hat{H} = \int d^3r \hat{\psi}^\dagger(\mathbf{r}) h_0(\mathbf{r}) \hat{\psi}(\mathbf{r}) + \frac{1}{2} \int d^3r d^3r' \hat{\psi}^\dagger(\mathbf{r}) \hat{\psi}^\dagger(\mathbf{r}') v_C(\mathbf{r}, \mathbf{r}') \hat{\psi}(\mathbf{r}') \hat{\psi}(\mathbf{r}), \quad (2.3a)$$

where $v_C(\mathbf{r}, \mathbf{r}') = 1/|\mathbf{r} - \mathbf{r}'|$ is the bare Coulomb interaction. The Hamiltonian does not depend on time, hence the time evolution of the field operators is $\hat{\psi}^\dagger(\mathbf{r}, t) = e^{i\hat{H}t} \hat{\psi}^\dagger(\mathbf{r}) e^{-i\hat{H}t}$ and analogously for $\hat{\psi}$. As a consequence, the Green's function (2.18) depends only on the difference $\tau = t - t'$ between its time arguments, as it is explicit from the following representation:

$$iG(\mathbf{r}, \mathbf{r}', \tau) = \theta(\tau) \langle \Psi_0 | \hat{\psi}(\mathbf{r}) e^{-i(\hat{H}-E_0)\tau} \hat{\psi}^\dagger(\mathbf{r}') | \Psi_0 \rangle - \theta(-\tau) \langle \Psi_0 | \hat{\psi}^\dagger(\mathbf{r}') e^{i(\hat{H}-E_0)\tau} \hat{\psi}(\mathbf{r}) | \Psi_0 \rangle. \quad (2.21)$$

We take advantage of this time translation symmetry by expressing the Green's function in the frequency domain. We get rid of the Hamiltonian operators by inserting two complete sets¹⁵ of energy eigenstates $|\Psi_s^{(N\pm 1)}\rangle$, with $\hat{H}|\Psi_s^{(N\pm 1)}\rangle = E_s^{(N\pm 1)}|\Psi_s^{(N\pm 1)}\rangle$, between the field operators. For a discrete system, the resulting expression is the *Lehmann representation* [61] of the Green's function:

$$G(\mathbf{r}, \mathbf{r}', \omega) = \sum_s \frac{f_s(\mathbf{r}) f_s^*(\mathbf{r}')}{\omega - \varepsilon_s + i\eta \text{sign}(\varepsilon_s - \mu)}, \quad (2.22)$$

with the *Lehmann amplitudes*, that form a complete but not orthogonal set, defined as:

$$f_s(\mathbf{r}) = \begin{cases} \langle \Psi_s^{(N-1)} | \hat{\psi}(\mathbf{r}) | \Psi_0^{(N)} \rangle & \text{if } \varepsilon_s < \mu \\ \langle \Psi_0^{(N)} | \hat{\psi}(\mathbf{r}) | \Psi_s^{(N+1)} \rangle & \text{if } \varepsilon_s > \mu, \end{cases} \quad (2.23)$$

and the *electron removal* and *addition* energies as:

$$\varepsilon_s = \begin{cases} E_0^{(N)} - E_s^{(N-1)} & \text{if } \varepsilon_s < \mu \\ E_s^{(N+1)} - E_0^{(N)} & \text{if } \varepsilon_s > \mu, \end{cases} \quad (2.24)$$

as measured in IPES and PES, see section 1.1.1. In particular, the highest removal energy ε_v is minus the *ionization potential*: $\varepsilon_v = -\text{IP} := E_0^{(N)} - E_0^{(N-1)}$, while the lowest addition energy ε_c is minus the *electron affinity*: $\varepsilon_c = -\text{EA} := E_0^{(N+1)} - E_0^{(N)}$ ¹⁶ (v and c stand for valence and conduction bands). In a non-metal, no poles are present between ε_v and ε_c , so that a gap in the energy spectrum (the *photoemission gap*) can be defined as:

$$E_g := \varepsilon_c - \varepsilon_v = (-\text{EA}) - (-\text{IP}) = E_0^{(N+1)} + E_0^{(N-1)} - 2E_0^{(N)}. \quad (2.25)$$

In such a case, the chemical potential μ lies somewhere inside the gap, and the system is an *insulator*. On the contrary, if the gap is zero, namely if $-\text{IP} = -\text{EA}$, then the system is *metallic* and $\mu = -\text{IP} = -\text{EA}$ coincides with the Fermi energy.

¹⁵The identity we consider is complete in Fock space $\mathcal{F}^{(-)}$, with all possible numbers N of particles: $\hat{1}_{\mathcal{F}^{(-)}} = \sum_{N=0}^{\infty} \hat{1}_{\mathcal{H}_N^{(-)}}$, where $\mathcal{H}_N^{(-)}$ is the Hilbert space of N electrons; of all these identities, only the ones relative to the $(N+1)$ and $(N-1)$ Hilbert space do survive, $\hat{1}_{\mathcal{H}_{N\pm 1}^{(-)}} = \sum_s |\Psi_s^{(N\pm 1)}\rangle \langle \Psi_s^{(N\pm 1)}|$, respectively for $\tau > 0$ and $\tau < 0$, which are the ones considered above.

¹⁶By using these concepts, the removal and addition energy can be re-expressed in terms of the purely excitations energies $\varepsilon_s^{(N\pm 1)}$ of the $(N\pm 1)$ -particle system:

$$\varepsilon_s = \begin{cases} [E_0^{(N)} - E_0^{(N-1)}] - [E_s^{(N-1)} - E_0^{(N-1)}] \equiv -\text{IP} - \varepsilon_s^{(N-1)} \leq -\text{IP} \leq \mu & \text{if } \varepsilon_s \leq \mu \\ [E_s^{(N+1)} - E_0^{(N+1)}] + [E_0^{(N+1)} - E_0^{(N)}] \equiv -\text{EA} + \varepsilon_s^{(N+1)} \geq -\text{EA} \geq \mu & \text{if } \varepsilon_s \geq \mu \end{cases}$$

2.5.2 Analytic properties of the Green's function: the spectral function

The representation (2.22) is of “limited value in actual calculations” [62], as it requires the exact solutions $\{E_s^{(N)}; |\Psi_s^{(N)}\rangle\}_s$ of the many-body Schrödinger equation (2.4) for deriving both the Lehmann amplitudes and the addition and removal energies. On the other hand, it is an extremely useful expression for investigating the analytical properties of the Green's function: indeed, without specifying any particular form for the Hamiltonian, the space and the frequency dependence of G are exactly decoupled, and frequency enters only the denominator of the Lehmann representation. Furthermore, the singularities of G – isolated *simple poles* – are precisely the additional and removal energies ε_s , with a tiny imaginary part just above or below the real axis. In the thermodynamic limit, these poles merge into a *branch cut* on certain regions of the real axis; in such a case it becomes useful to analytically continue the *physical* $G(\omega)$ in the complex plane $z \equiv \omega + i\xi$ (for $\xi \equiv \text{Im}[z] \neq 0$) via the following relations [63]:

$$G(\mathbf{r}, \mathbf{r}', \omega) = \lim_{\eta \rightarrow 0^+} \tilde{G}(\mathbf{r}, \mathbf{r}', \omega + i\eta \text{sign}(\omega - \mu)), \quad \tilde{G}(\mathbf{r}, \mathbf{r}', z) := \sum_s \frac{f_s(\mathbf{r}) f_s^*(\mathbf{r}')}{z - \varepsilon_s}, \quad (2.26)$$

from which eq. (2.22) is immediately recovered. \tilde{G} describes an analytic function of z for $\text{Im}[z] \neq 0$, with a branch cut in correspondence of the real axis $\text{Im}[z] = 0$. The discontinuity of \tilde{G} through the real axis [64] is called *spectral function* $A(\mathbf{r}, \mathbf{r}', \omega)$:

$$A(\mathbf{r}, \mathbf{r}', \omega) := \frac{1}{2\pi i} \lim_{\eta \rightarrow 0^+} \left[\tilde{G}(\mathbf{r}, \mathbf{r}', \omega - i\eta) - \tilde{G}(\mathbf{r}, \mathbf{r}', \omega + i\eta) \right] \quad (2.27)$$

$$= \sum_s f_s(\mathbf{r}) f_s^*(\mathbf{r}') \delta(\omega - \varepsilon_s), \quad (2.28)$$

where we applied the Sokhotski–Plemelj relation $\lim_{\eta \rightarrow 0^+} \frac{1}{x \pm i\eta} = \mathcal{P.V.} \frac{1}{x} \mp i\pi \delta(x)$ to \tilde{G} . From this expression and the anticommutation relation $[\hat{\psi}(\mathbf{r}), \hat{\psi}^\dagger(\mathbf{r}')]_+ = \delta(\mathbf{r} - \mathbf{r}')$, one can show that the spectral function is normalized to one, $\int_{-\infty}^{+\infty} d\omega A(\mathbf{r}, \mathbf{r}', \omega) = \sum_s f_s(\mathbf{r}) f_s^*(\mathbf{r}') = \delta(\mathbf{r} - \mathbf{r}')$. From eq. (2.28), the physical Green's function of eq. (2.22) can be recast into the following *spectral representation*:

$$G(\mathbf{r}, \mathbf{r}', \omega) = \int d\omega' \frac{A(\mathbf{r}, \mathbf{r}', \omega')}{\omega - \omega' + i\eta \text{sign}(\omega' - \mu)}. \quad (2.29)$$

Furthermore, whenever the product $f_s(\mathbf{r}) f_s^*(\mathbf{r}')$ is real (which is most of the times the case, *e.g.*, when it is symmetric under the interchange $\mathbf{r} \leftrightarrow \mathbf{r}'$ [63]), also the spectral function is real and it exhibits a straightforward connection with the physical Green's function:

$$A(\mathbf{r}, \mathbf{r}', \omega) = -\frac{1}{\pi} \text{sign}(\omega - \mu) \text{Im} G(\mathbf{r}, \mathbf{r}', \omega). \quad (2.30)$$

In such a situation, once the imaginary part of the Green's function – the spectral function – is at hand, its real part can be directly evaluated from it by an Hilbert transform:

$$\text{Re} G(\mathbf{r}, \mathbf{r}', \omega) = \mathcal{P.V.} \int d\omega' \frac{A(\mathbf{r}, \mathbf{r}', \omega')}{\omega - \omega'} = -\frac{1}{\pi} \mathcal{P.V.} \int d\omega' \frac{\text{Im} G(\mathbf{r}, \mathbf{r}', \omega') \text{sign}(\omega' - \mu)}{\omega - \omega'}, \quad (2.31)$$

which shows that the Green's function is not an analytic function [3] (for the presence of the sign operator at the very right, this differs from an usual Kramers–Kronig causal relation). Nonetheless, eq. (2.31) and more generally eq. (2.29) show that all the information of the Green's function is actually contained in the spectral function only (and in the position of the chemical potential μ , which the spectral function does not know). In particular, the density, the density

matrix (2.19) and the total energy (2.20) are exact functionals of the spectral function:

$$n(\mathbf{r}) = \int_{-\infty}^{\mu} d\omega A(\mathbf{r}, \mathbf{r}, \omega) \quad (2.32)$$

$$\gamma(\mathbf{r}, \mathbf{r}') = \int_{-\infty}^{\mu} d\omega A(\mathbf{r}, \mathbf{r}', \omega) \quad (2.33)$$

$$E_0 = \frac{1}{2} \int d^3r \lim_{\mathbf{r}' \rightarrow \mathbf{r}} \int_{-\infty}^{\mu} d\omega [\omega + h_0(\mathbf{r})] A(\mathbf{r}, \mathbf{r}', \omega) \quad (2.34)$$

Finally, swapping from real space to a discrete single-particle basis $\{|l\rangle\}_l$ via the relation $\hat{\psi}(\mathbf{r}) = \sum_l \phi_l(\mathbf{r}) \hat{c}_l$, with $\phi_l(\mathbf{r}) \equiv \langle \mathbf{r} | l \rangle$, the spectral function (2.28) can be expressed as $A(\mathbf{r}, \mathbf{r}', \omega) = \sum_{ll'} \phi_l(\mathbf{r}) A_{ll'}(\omega) \phi_{l'}^*(\mathbf{r}')$, with:

$$A_{ll'}(\omega) = \begin{cases} \sum_s \langle \Psi_s^{(N-1)} | \hat{c}_l | \Psi_0^{(N)} \rangle \langle \Psi_0^{(N)} | \hat{c}_{l'}^\dagger | \Psi_s^{(N-1)} \rangle \delta(\omega - \varepsilon_s) & \text{if } \varepsilon_s = E_0^{(N)} - E_s^{(N-1)} \leq \mu \\ \sum_s \langle \Psi_0^{(N)} | \hat{c}_l | \Psi_s^{(N+1)} \rangle \langle \Psi_s^{(N+1)} | \hat{c}_{l'}^\dagger | \Psi_0^{(N)} \rangle \delta(\omega - \varepsilon_s) & \text{if } \varepsilon_s = E_s^{(N+1)} - E_0^{(N)} \geq \mu \end{cases} \quad (2.35)$$

exactly the fundamental quantity that we introduced in eq. (1.3) and (1.6) to interpret photoemission and inverse photoemission experiments. In the previous chapter we focused on the experimental meaning of the spectral function, directly related to the probability of detecting photoelectrons with a particular energy. Here, on the other hand, we have shown the connection of the spectral function with the propagation of electrons and holes inside the material, described by the Green's function.

2.5.3 Standard route to the spectral function: the self energy

The standard way for evaluating the spectral function is through its definition in terms of the Green's function, eq. (2.30). Thus much time has been spent for calculating G , eq. (2.18). Most of the works rely on the equation of motion for G , which can be derived from the time-dependence of the field operators $\hat{\psi}$ and $\hat{\psi}^\dagger$ [4] and reads:

$$\left(i \frac{\partial}{\partial t} - h_0(\mathbf{r}) \right) G(\mathbf{r}t, \mathbf{r}'t') + i \int d^3\bar{r} v_C(\mathbf{r} - \bar{\mathbf{r}}) G_2(\mathbf{r}t, \bar{\mathbf{r}}t^+; \mathbf{r}'t', \bar{\mathbf{r}}t^{++}) = \delta(\mathbf{r} - \mathbf{r}') \delta(t - t'), \quad (2.36)$$

where G_2 is the *two*-particle Green's function – describing the coupled propagation of *two* particles (electrons or holes) – defined as $i^2 G_2(1, 2; 1', 2') \equiv \langle \Psi_0 | \hat{\mathcal{T}} \hat{\psi}(1) \hat{\psi}(2) \hat{\psi}^\dagger(2') \hat{\psi}^\dagger(1') | \Psi_0 \rangle$, with 1 a shorthand for (\mathbf{r}_1, t_1) and so on. The two-particle Green's function shows up as a consequence of the two-body Coulomb interaction; were it possible to turn off v_C , G_0 would be the solution of the simpler equation $\left(i \frac{\partial}{\partial t} - h_0(\mathbf{r}) \right) G_0(\mathbf{r}t, \mathbf{r}'t') = \delta(\mathbf{r} - \mathbf{r}') \delta(t - t')$, namely $G_0^{-1}(\mathbf{r}t, \mathbf{r}'t') = \delta(\mathbf{r} - \mathbf{r}') \delta(t - t') \left(i \frac{\partial}{\partial t} - h_0(\mathbf{r}) \right)$.

G_2 is as important for *neutral excitation experiments* (optical absorption, electron energy loss, ...) as G is for photoemission: from it one can derive the 4-points polarizability $L(1, 2; 1', 2')$, and hence the response function $\chi(1, 2)$, the dielectric constant ϵ_M and so on in a straightforward way [65]. However, one can avoid the detour in the two-particles realm if the interest is just in one-particle properties. Indeed, the previous equation can be *exactly* recast in the form¹⁷:

$$G^{-1}(1, 1') = G_0^{-1}(1, 1') + i \int d2d2' v_C(1, 2) G_2(1, 2^+; 2', 2^{++}) G^{-1}(2', 1').$$

If G only is needed, one does not have to evaluate the full $G_2(1, 1'; 2, 2')$, but just its reduced version integrated with v_C and G^{-1} , corresponding to the rightmost term of the previous relation.

¹⁷We define the instantaneous Coulomb interaction as $v_C(1, 2) := \delta(t_1 - t_2) v_C(\mathbf{r}_1, \mathbf{r}_2) \equiv \frac{\delta(t_1 - t_2)}{|\mathbf{r}_1 - \mathbf{r}_2|}$.

This suggests the introduction of a far simpler object than G_2 , depending on just two (and not four) space–time arguments, called the *self energy* $\Sigma(\mathbf{r}t, \mathbf{r}'t')$:

$$i\Sigma(1, 1') := \int d2d2' v_C(1, 2)G_2(1, 2^+; 2', 2^{++})G^{-1}(2', 1'). \quad (2.37)$$

The self energy contains less information than G_2 , but *all* that is needed for obtaining G . In this sense, it is a kind of generalized *effective potential*, a notion that will become more clear and more relevant in the following. By plugging the self energy in the equation of motion (2.36) in frequency space, the latter becomes:

$$\int d^3\bar{r} \left[\omega\delta(\mathbf{r} - \bar{\mathbf{r}}) - \left(\delta(\mathbf{r} - \bar{\mathbf{r}})h_0(\mathbf{r}) + \Sigma(\mathbf{r}, \bar{\mathbf{r}}, \omega) \right) \right] G(\bar{\mathbf{r}}, \mathbf{r}', \omega) = \delta(\mathbf{r} - \mathbf{r}'), \quad (2.38)$$

which has the same structure as the equation of motion for G_0 , but with the self energy that acts as an additional *non-local, complex and dynamical* effective potential on top of the one-particle Hamiltonian h_0 : this process generates an effective non-hermitian and frequency-dependent Hamiltonian $H_{\text{eff}}(\mathbf{r}, \mathbf{r}', \omega) = h_0(\mathbf{r}) + \Sigma(\mathbf{r}, \mathbf{r}', \omega)$ that, as far as the one-particle Green's function is concerned, contains the same amount of information as the many-body one, eq. (2.3).

Quasiparticles and satellites By continuing this Hamiltonian in the complex z plane, its left and right eigenfunctions $\Phi_\lambda^{(L)}(\mathbf{r}, z)$ and $\Phi_\lambda^{(R)}(\mathbf{r}, z)$, orthonormal in the sense that $\langle \Phi_\lambda^{(L)}(z) | \Phi_{\lambda'}^{(R)}(z) \rangle = \delta_{\lambda\lambda'}$, correspond to the same complex eigenvalue $\varepsilon_\lambda(z)$, and the solution to eq. (2.38) can be formally written as:

$$\tilde{G}(\mathbf{r}, \mathbf{r}', z) = \sum_\lambda \frac{\Phi_\lambda^{(R)}(\mathbf{r}, z)\Phi_\lambda^{(L)*}(\mathbf{r}', z)}{z - \varepsilon_\lambda(z)}, \quad (2.39)$$

as can be proved by plugging this ansatz in eq. (2.38) and by using the completeness relation $\sum_\lambda \Phi_\lambda^{(R)}(\mathbf{r}, z)\Phi_\lambda^{(L)*}(\mathbf{r}', z) = \delta(\mathbf{r} - \mathbf{r}')$.

This is another *exact* representation of the Green's function, alternative to the Lehmann one: while to obtain the latter one needs to solve the many-body Hamiltonian for three different numbers of particles, here only a diagonalization of the effective Hamiltonian $H_{\text{eff}}(\omega)$ is needed. In particular, an essential role is played by regions of the complex plane in which the denominator $z - \varepsilon_\lambda(z)$ approaches zero: if ε_λ is (one of) the complex solution(s) to the equation $z - \varepsilon_\lambda(z)|_{z=\varepsilon_\lambda} = 0$, one can evaluate the Hamiltonian H_{eff} in a neighborhood of ε_λ , obtaining an effective *single-particle* static Schrödinger equation:

$$h_0(\mathbf{r})\Phi_\lambda^{(R)}(\mathbf{r}, \varepsilon_\lambda) + \int d^3\bar{r} \Sigma(\mathbf{r}, \bar{\mathbf{r}}, \varepsilon_\lambda)\Phi_\lambda^{(R)}(\bar{\mathbf{r}}, \varepsilon_\lambda) = \varepsilon_\lambda\Phi_\lambda^{(R)}(\mathbf{r}, \varepsilon_\lambda), \quad (2.40)$$

which describes *collective* excitations $\Phi_\lambda^{(R)}(\mathbf{r}, \varepsilon_\lambda)$: many real Lehmann poles ε_s (particles) merge their amplitudes $f_s f_s^*$ together to form coherent structures that can alternatively be described by the *single* pole ε_λ in the complex plane. Note that, in general, the excitation ε_λ is a real particle ε_s when its imaginary part is zero, hence when the self energy is real, which is the case for independent particle propagation. As soon as particles interact in the thermodynamic limit, many transitions among almost-degenerate energy levels are allowed and the energy of the particle ε_s is spread into neighbouring energy levels. This is clear when considering the

spectral function, eq. (2.27), with G in the representation (2.39)¹⁸ :

$$\begin{aligned} A(\mathbf{r}, \mathbf{r}', \omega) &:= \frac{1}{2\pi i} \lim_{\eta \rightarrow 0^+} \left[\tilde{G}(\mathbf{r}, \mathbf{r}', \omega - i\eta) - \tilde{G}(\mathbf{r}, \mathbf{r}', \omega + i\eta) \right] \\ &= \frac{1}{\pi} \sum_{\lambda} \Phi_{\lambda}^{(R)}(\mathbf{r}, \omega - i\eta) \Phi_{\lambda}^{(L)*}(\mathbf{r}', \omega - i\eta) \operatorname{Im} \left[\frac{1}{\omega - \varepsilon_{\lambda}(\omega)} \right]. \end{aligned} \quad (2.41)$$

Assuming a prominent solution ε_{λ} of the equation $\varepsilon_{\lambda} - \varepsilon_{\lambda}(\varepsilon_{\lambda}) = 0$, this is called *quasiparticle* whenever it can be connected – via a hypothetical switching-on of the Coulomb interaction between particles – to a single particle excitation (a delta-peak) in an independent-particle picture. One can Taylor-expand the equation $\varepsilon_{\lambda} - \varepsilon_{\lambda}(\varepsilon_{\lambda}) = 0$ around the quasiparticle ε_{λ} , $z - \varepsilon_{\lambda}(z) \approx (z - \varepsilon_{\lambda}) \left(1 - \frac{\partial \varepsilon_{\lambda}(z)}{\partial z} \Big|_{z=\varepsilon_{\lambda}} \right)$, and obtain as a prominent feature in the spectral function the following contribution:

$$A_{QP}(\mathbf{r}, \mathbf{r}', \omega) = \Phi_{\lambda}^{(R)}(\mathbf{r}, \varepsilon_{\lambda}) \Phi_{\lambda}^{(L)*}(\mathbf{r}', \varepsilon_{\lambda}) Z_{\lambda} \frac{\frac{1}{\pi} \operatorname{Im} \varepsilon_{\lambda}}{(\omega - \operatorname{Re} \varepsilon_{\lambda})^2 + (\operatorname{Im} \varepsilon_{\lambda})^2}. \quad (2.42)$$

Apart from the space-dependent prefactors, this term represents a Lorentzian peak, rescaled by the *renormalization factor* $Z_{\lambda} = (1 - \partial \operatorname{Re} \varepsilon_{\lambda}(z) / \partial z|_{z=\varepsilon_{\lambda}})^{-1}$ [22]. It is centered on the energy $\operatorname{Re} \varepsilon_{\lambda}$, and it has a broadening $\operatorname{Im} \varepsilon_{\lambda}$, interpreted as the inverse of the lifetime of the collective excitation. Were the eigenvalue ε_{λ} real and static, we would be back to a delta-peak contribution with infinite lifetime.

If other local minima, or zeros, of $z - \varepsilon_{\lambda}(z)$ are present, which can be the case only if the self energy does depend on z , other coherent excitations will show up in the spectrum, with usually a smaller weight. They are called *satellites*, and they are a fingerprint of non-negligible correlation (in the sense of everything beyond Hartree-Fock) in the system.

As far as the quasiparticle dominates on the satellites, the many-body system can be regarded as a *Fermi liquid*. It is still a many-body system, in which particles are replaced by quasiparticles (which can be thought of as dressed particles) that weakly interact among themselves. The emergent behaviour is therefore very close to that of a Fermi gas of non-interacting particles with renormalized mass, in agreement with the phenomenology of most metals.

In the opposite situation, it becomes meaningless to identify a single prominent quasiparticle, as many satellites have considerable weight. These systems are known as strongly correlated, and they cannot be described as an almost free Fermi gas.

2.5.4 Dyson and Hedin equations

To build the quasiparticle Hamiltonian $H_{\text{eff}}(\omega)$, an expression for the self energy is needed. From its definition in terms of G_2 , eq. (2.37), one can extract the lower order terms of Σ – in a hypohetic e^2 expansion – by considering the independent-particle contributions to G_2 , namely its disconnected (in the sense of factorized) components:

$$G_2^{\text{indep}}(1, 2; 1', 2') = G(1, 1')G(2, 2') - G(1, 2')G(2, 1').$$

The resulting self energy expression is $\Sigma(\mathbf{r}, \mathbf{r}', \omega) = \delta(\mathbf{r} - \mathbf{r}') v_{\text{H}}(\mathbf{r}) + \Sigma_x(\mathbf{r}, \mathbf{r}')$, both real and static, with the local *Hartree potential* $v_{\text{H}}(\mathbf{r})$ and the Fock self energy $\Sigma_x(\mathbf{r}, \mathbf{r}')$ defined by:

$$v_{\text{H}}(\mathbf{r}) = \int d^3 \bar{\mathbf{r}} \frac{n(\bar{\mathbf{r}})}{|\mathbf{r} - \bar{\mathbf{r}}|} \quad (2.43)$$

$$\Sigma_x(\mathbf{r}, \mathbf{r}') = - \frac{\gamma(\mathbf{r}, \mathbf{r}')}{|\mathbf{r} - \mathbf{r}'|}, \quad (2.44)$$

¹⁸We use the properties $\Phi_{\lambda}^{(R)}(\mathbf{r}, z) = \Phi_{\lambda}^{(L)}(\mathbf{r}, z^*)$, $\varepsilon_{\lambda}(z^*) = \varepsilon_{\lambda}^*(z)$ that descend from the eigenvalue problem of the non-hermitian H_{eff} , and the symmetry of $\Phi_{\lambda}^{(R)}(\mathbf{r}, z) \Phi_{\lambda}^{(L)*}(\mathbf{r}', z)$ under the interchange $\mathbf{r} \leftrightarrow \mathbf{r}'$ (hence its reality for z real).

which are closely linked to the energy contributions (2.7) and (2.9). It is common to isolate the Hartree Hamiltonian $h_H(\mathbf{r}) := h_0(\mathbf{r}) + v_H(\mathbf{r})$ as the purely local contribution to H_{eff} , and redefine the self energy as its exchange–correlation part $\Sigma \rightarrow \Sigma - v_H(\mathbf{r})\delta(\mathbf{r} - \mathbf{r}')$, so that $H_{\text{eff}} = h_H + \Sigma$. To obtain this last term, Lars Hedin [66] proposed a closed set of equations, the *Hedin equations*, that involve, besides G and Σ , a *polarization* $\Pi(1, 2)$, a *screened interaction* $W(1, 2)$ and a *vertex function* $\Gamma(1, 2; 3)$. They read:

$$\begin{aligned}\Sigma(1, 2) &= iG(1, \bar{1})\Gamma(\bar{1}, 2; \bar{2})W(\bar{2}, 1^+) \\ W(1, 2) &= v_C(1, 2) + v_C(1, \bar{1})\Pi(\bar{1}, \bar{2})W(\bar{2}, 2) \\ \Pi(1, 2) &= -i\Gamma(\bar{1}, \bar{2}; 1)G(2, \bar{1})G(\bar{2}, 2) \\ \Gamma(1, 2; 3) &= \delta(1, 3)\delta(2, 3) + \Gamma(\bar{1}, \bar{2}; 3)G(\bar{3}, \bar{1})G(\bar{2}, \bar{4})\frac{\delta\Sigma(1, 2)}{\delta G(\bar{3}, \bar{4})},\end{aligned}\tag{2.45}$$

where barred indices are integrated over. These equations are formally closed by the equation of motion for G (2.38), that can be recast in the inspiring form:

$$G(1, 2) = G_0(1, 2) + G_0(1, \bar{1})[\nu_H(\bar{1})\delta(\bar{1} - \bar{2}) + \Sigma(\bar{1}, \bar{2})]G(\bar{2}, 2).\tag{2.46}$$

This equation goes under the name of Dyson equation. By solving the set of these five coupled equations, one has access to the exact Green's function G of the system. Unfortunately, such a solution seems unaccessible at the moment. Nevertheless, one can still truncate the Hedin equations at some low order in the interaction strength e^2 and look for an approximated form of Σ : plugging it in the Dyson equation, its effects are automatically spread to higher orders by the very form of the equation itself, as $G = G_0 + G_0\Sigma G_0 + G_0\Sigma G_0\Sigma G_0 + \dots$. One can then decide to take the resulting G and update the expression for the self energy until self consistency (*self consistent* calculation). Otherwise, one can stop at the first iteration, in which case the calculation is said to be *one shot*. In both cases, the spectral function A is finally obtained from G via equation (2.30), and can be analyzed as a sum of quasiparticles and satellites.

Approximative solutions to the Hedin equations Both the Hartree and the Hartree–Fock approaches can be considered as approximations to the exchange–correlation self energy. The former neglects it completely, while the latter – the Fock term – is:

$$\Sigma_x(1, 2) = i\nu_C(2, 1^+)G(1, 2),\tag{2.47}$$

which is nothing but eq. (2.44). Due to cancellation between exchange and correlation contributions [67], even the simple Hartree approximation is sometimes meaningful. The non–local Hartree–Fock self energy, which exactly treats the self–interaction problem, gives pretty good results for atoms, but also a zero density of states at the Fermi level for metals, and it generally overestimates the gap in semiconductors.

The state–of–the–art approximation for Σ is the *GW* one [66, 67, 5], where the vertex function Γ is set to its trivial delta contribution in both Σ and Π . The resulting self energy has the same structure as the Fock term (2.47), but with the screened dynamical interaction W in place of the bare Coulomb one ν_C , namely:

$$\Sigma_{\text{GW}}(1, 2) = iG(1, 2)W(2, 1^+).\tag{2.48}$$

The static $\omega = 0$ contribution to the *GW* self energy can be further decomposed into a screened–exchange (SEX) term plus a Coulomb–hole (COH) one, both Hermitian. The first is responsible for the static screening of the exchange interaction in the Fock term, while the second digs a correlation hole around each particle. Together, they form the COHSEX approximation, which

is simpler than GW because it is static, but calculations are still time-consuming due to its non-local nature.

The GW (or the simpler COHSEX) expression highlights some fundamental physical aspects of the propagation of a particle (electron or hole) in a medium. Indeed, as already mentioned, an exchange-correlation hole surrounds the propagating electron, creating shells of consecutive depletion and accumulation of charge (*Friedel oscillations* [68, 69]): the medium *polarizes* due to a non-zero polarization $\Pi_{\text{GW}}(1,2) = -iG(1,2)G(1,2)$, which in turns generates a non-trivial dielectric function $\epsilon := 1 - v_C\Pi$. As a consequence, the Coulomb interaction of the propagating electron with *all* the other electrons is *screened* by the charge shells around it, $W = \epsilon^{-1}v_C$; as it follows the particle which is moving, screening is dynamical in nature, hence the frequency dependence of W .

In this picture, the propagating electron together with its surrounding cloud of screening particles is detected as the *quasiparticle* of the system, while the charge density oscillations characteristic of the screening process will be interpreted as the satellites of the system, called *plasmons*. There is a non-trivial interplay between the two, as the polarized medium affects the propagation of the quasiparticle, which in turns alters the properties of the surrounding system: that is why G is a functional of Σ and viceversa.

Indeed, the set of Hedin equations should be solved self-consistently; on the other hand, it has been pointed out that lack of self-consistency in the GW approximation often balances the neglect of higher order corrections to the GW itself (vertex corrections, for instance) [67, 65]. That is why, to a large extent, one-shot or at least partially self-consistent calculations are still widely performed.

2.6 The Hubbard model

As already mentioned, the quasiparticle picture we have just presented is not universally valid. Indeed, whenever particle-like excitations are not robust enough to confront the adiabatic switching-on of the interaction, a one-particle picture ceases to be meaningful and the Fermi liquid theory breaks down.

In this regime, new phenomena appear, among which the well-known *Mott transition* [70, 71]: a strong electron-electron interaction reduces the itinerant nature of electrons, that therefore tend to localize; the system undergoes a metal-insulator transition which cannot be caught by standard Fermi liquid methods. This is the case when electrons are sufficiently far apart that their wavefunctions lightly overlap, and they are thus restrained from hopping between different locations: hence the resulting insulating character. At the same time, the Coulomb repulsion between electrons is enhanced by the long time spent in the localized state, hence the characterization of these electrons as *strongly correlated*.

These situations occur for many transition metal oxides, in which two electrons with opposite spin occupy the same narrow energy band (a half-filled d - or f -band) [72]. Describing these systems from a theoretical point of view is challenging, as independent-particle approaches (like Hartree-Fock) break down, and correlation between electrons, which is often treated as a small perturbation, is of primary importance. Moreover, methods based on Bloch's theorem highlight most often the wave-like nature of electrons, while in these systems the competition with real space localization is fundamental.

A promising strategy to face these problems is to employ simplified models, which highlight the physics of strong correlation. The most famous, and most studied, of such models is by far the Hubbard model, which catches from its very form the opposite tendency between itinerant (metals) and localized electrons (insulators).

The model The single-band Hubbard model [73, 74, 75] can be defined on a lattice as:

$$\hat{H} = -t \sum_{\langle i,j \rangle, \sigma} \hat{c}_{i\sigma}^\dagger \hat{c}_{j\sigma} + \sum_i \varepsilon_i \hat{n}_i + U \sum_i \hat{n}_{i\uparrow} \hat{n}_{i\downarrow}, \quad (2.49)$$

with i, j lattice sites, $\langle i, j \rangle$ nearest neighbours, $t, U > 0$ *hopping parameter* and *interaction strength*, and ε_i the on-site energies. The operators $\hat{c}_{i\sigma}^\dagger$ and $\hat{c}_{i\sigma}$ are fermionic creation and annihilation operators that act on the lattice site i with a certain spin σ , $\hat{n}_{i\sigma} = \hat{c}_{i\sigma}^\dagger \hat{c}_{i\sigma}$ is the spin-resolved density operator and finally $\hat{n}_i = \sum_\sigma \hat{n}_{i\sigma}$ is the usual density operator for the site i ; in the half-filling solution, $\langle \hat{n}_i \rangle = 1$: on average, there is one electron per site.

As for the interpretation of the lattice, one can refer to the original derivation of the model [75] from the many-body Hamiltonian (2.3a), in which case i is a band index (see appendix H). On the other hand, one can also view eq. (2.49) as a model by itself, in which the continuous space variable \mathbf{r} has been discretized into discrete lattice sites i ; this is the interpretation we will stick to for the following discussion: *local* quantities in space will depend on a single lattice site i , *bi-local* quantities on two sites i and j and so on...

The Hamiltonian (2.49) represents electrons that, by jumping from one site to the other, gain the amount of energy t . If a site i happens to be doubled occupied, U is the energy cost that has to be paid: it represents the Coulomb interaction between electrons on the same site, and it is the only interaction between electrons that is considered by the model (all the non-local terms are neglected [76]).

Note that the kinetic term in eq. (2.49) is diagonal in reciprocal space, where it can be expressed as $\sum_{\mathbf{k}} \varepsilon_{\mathbf{k}}^0 \hat{c}_{\mathbf{k}\sigma}^\dagger \hat{c}_{\mathbf{k}\sigma}$, while the interaction term is diagonal in real space. This is a result of the competition between itinerant and localized electrons that this model catches since its very form. It is also the reason why this model is so difficult to solve.

For large t , electrons tend to delocalize to lower their kinetic energy, no matter if they happen to occupy the same site twice. Eventually, when t is so large that U can be neglected, the Hubbard Hamiltonian becomes equivalent to a tight-binding Hamiltonian, and the resulting spectrum is the standard single-particle one, *e.g.*, for a one-dimensional chain, $\varepsilon_k^0 = -2t \cos k$: free electrons travelling from one site to the other, a metallic behaviour (at half filling, the chemical potential $\mu = 0$ lies inside the band).

On the contrary, in the limit of large U , double occupancy of the same site becomes unfavorable, and electrons prefer localizing on each lattice site. If U is much larger than t , electrons crystallize on their sites, with an additional excitation energy U if two electrons happen to be on the same site: in this limit, the system is a collection of independent two-levels sites.

The interesting physics – the Mott transition for example – is in between these two limits, where an analytic solution is missing. Although its apparent simplicity, indeed, the model is – so far [77] – analytically solvable only in one dimension (the celebrated *Bethe ansatz* solution [78]), and in infinite dimensions, where an exact application of DMFT (see pag. 52) solves numerically the model. Similarly to this last situation, also for the Bethe lattice with infinite coordination number the solution is at hand (it is the DMFT exact solution). We will consider explicitly this lattice in section 4.1.

The Green's function The Green's function for the Hubbard Hamiltonian (2.49) can be defined in the usual way, eq. (2.18), with the field operators in real space replaced by the corresponding ones in site space, $\hat{c}_{i\sigma}^\dagger$ and $\hat{c}_{i\sigma}$. At zero temperature, it reads:

$$iG_{ij,\sigma}(t, t') := \langle \Psi_0 | \hat{\mathcal{T}} \hat{c}_{i\sigma}(t) \hat{c}_{j\sigma}^\dagger(t') | \Psi_0 \rangle. \quad (2.50)$$

It is diagonal in spin, non-local in the sites and it depends only on the time difference $t - t'$, hence it can equivalently be expressed in frequency domain as $G_{ij,\sigma}(\omega)$.

As the non-interacting Hamiltonian is diagonal in reciprocal space, $\hat{H}^0 = \sum_{\mathbf{k}} \varepsilon_{\mathbf{k}}^0 \hat{c}_{\mathbf{k}\sigma}^\dagger \hat{c}_{\mathbf{k}\sigma}$, the non-interacting limit of the Green's function $G_{ij,\sigma}^0(\omega)$ reads:

$$G_{\mathbf{k}}^0(\omega) = \frac{1}{\omega - \varepsilon_{\mathbf{k}}^0 + i\eta \text{sign}(\omega - \mu)}, \quad (2.51)$$

with $\varepsilon_{\mathbf{k}}^0 = -2t \sum_{l=1}^3 \cos k_l$ for a three dimensional cubic lattice. Also the fully interacting Green's function is diagonal in reciprocal space, as the Hubbard Hamiltonian is translationally invariant. Therefore we can introduce the self energy via the Dyson equation $G_{\mathbf{k}}^{-1}(\omega) = G_{\mathbf{k}}^0{}^{-1}(\omega) - \Sigma_{\mathbf{k}}(\omega)$, so that the Green's function (2.50) reads:

$$G_{\mathbf{k}}(\omega) = \frac{1}{\omega - \varepsilon_{\mathbf{k}}^0 - \Sigma_{\mathbf{k}}(\omega)}. \quad (2.52)$$

I have presented a framework in which the many-body problem can be dealt with. In particular, for the description of photoemission and inverse photoemission experiments, the Green's function approach seems particularly suited, as it describes the many-body processes a system undergoes when an additional particle (hole or electron) is added to it. In this theory, a fundamental role is played by the self energy, which can be considered as a dynamical, non-local and non-hermitian effective potential felt (and generated) by the elementary excitations of the system, quasiparticles and satellites. However, the scope of this thesis is not to consider better approximations to the self energy, but to avoid it. This is the content of the next chapter.

Part II

Auxiliary systems

*Ils ne cherchent rien, ils sont bien installés
au cœur de la norme et ne questionnent jamais
la légitimité de ce qui est légal.¹*

MIGUEL BENASAYAG, Résister dans une époque obscure

*I tell you: one must still have chaos in one,
to give birth to a dancing star.
I tell you: ye have still chaos in you.*

[...]

*And even if one have all the virtues,
there is still one thing needful:
to send the virtues themselves to sleep
at the right time.*

FRIEDRICH NIETZSCHE, Thus Spake Zarathustra

¹They do not search for anything, they are comfortably installed at the heart of the norm, and never question the legitimacy of what is legal.

Auxiliary systems: an introduction

If one is interested in every single small detail of a quantum system, there is no way out: he/she must evaluate the wavefunction. Luckily, most of the times we are interested in other quantities than the wavefunction, which depend on less degrees of freedom and have a direct physical interpretation. In the previous chapter, I introduced some many-body approaches to evaluate these quantities, from independent-particle approximations like Hartree or Hartree-Fock, to reformulations like DFT or RDMFT, to the Green's function formalism. Within these approaches, the focus is moved from the wavefunction to a smaller quantity, and approximations are implemented in order to obtain that quantity.

An alternative path, that I will describe in this chapter, is represented by *auxiliary systems*. An auxiliary system is *another* system described by *another* set of equations. It exactly targets a specific quantity of interest p and it yields, in principle, the exact value of that quantity that one could have alternatively obtained in the *real system*. Since the auxiliary system is by definition simpler to solve with respect to the real system, one would rather work there in order to find p .

Actually, the *raison d'être* of the auxiliary system is precisely to yield the value of that quantity. There is no guarantee that the value of any other physical quantity, evaluated in the auxiliary system, should agree with the one evaluated in the real system. On the contrary, this is not usually the case: *an* auxiliary system is an apparatus specifically built for *one* quantity.

If solving the auxiliary system is usually easy (or easier), finding it (or, depending on the viewpoint, building it) is the real nightmare. The reason is simple: all the difficulties of the many-body problem, that were more or less explicit in the real system, are hidden in the quantities that define the auxiliary system: *there ain't no such thing as a free lunch*. In particular, while the Hamiltonian of the real system is exactly known, eq. (2.3), building an Hamiltonian for the auxiliary system is, in most cases, definitely not straightforward.

Thus, one is usually pushed to build *approximated* auxiliary systems. So, what is the gain in the end, if both methods eventually need approximations? The benefits are basically two: on the one hand, the auxiliary system is a conceptual tool that settles what can be achieved and what cannot, and the minimal form of the Hamiltonian which is able to yield the former. On the other, as the auxiliary system is suited to the particular quantity of interest p , it turns out that approximating the auxiliary system Hamiltonian is a better strategy than approximating the full many-body Hamiltonian, to finally obtain p .

Auxiliary systems are a very general tool that can be used whenever a quantity that carries less information than the wavefunction is considered. In particular, we here narrow our focus to quantities that can be derived from the one-particle Green's function via a self energy calculation, and that carry less information than the Green's function. The latter is what we will refer to as the *real system*.

3.1 Reduced quantities

In the previous chapter, we sketched the standard procedure to get the diagonal of the spectral function. The central quantity is the one-particle Green's function $G(\mathbf{r}, \mathbf{r}', \omega)$, from which the expectation value of any one-particle operator can be obtained as a different *functional*: the density $n(\mathbf{r})$ and the density matrix $\gamma(\mathbf{r}, \mathbf{r}')$, eq. (2.19), the total kinetic energy T [4], the on-site Green's function $G_{ll}(\omega)$, the current density, the spin density, ..., till the diagonal of the spectral function $A(\mathbf{r}, \mathbf{r}, \omega)$ itself through equation (2.30). Here I list again some of these quantities expressed as functionals of the Green's function:

$$\begin{aligned}
 n(\mathbf{r}) &= \int \frac{d\omega}{2\pi i} e^{i\omega\eta} G(\mathbf{r}, \mathbf{r}, \omega) \\
 \gamma(\mathbf{r}, \mathbf{r}') &= \int \frac{d\omega}{2\pi i} e^{i\omega\eta} G(\mathbf{r}, \mathbf{r}', \omega) \\
 T &= \int \frac{d\omega}{2\pi i} e^{i\omega\eta} \lim_{\mathbf{r}' \rightarrow \mathbf{r}} \left(-\frac{\nabla_{\mathbf{r}}^2}{2} \right) G(\mathbf{r}, \mathbf{r}', \omega) \\
 G_{ll}(\omega) &= \int d^3r d^3r' \varphi_l^*(\mathbf{r}) G(\mathbf{r}, \mathbf{r}', \omega) \varphi_l(\mathbf{r}') \\
 &\quad \dots \\
 A(\mathbf{r}, \mathbf{r}, \omega) &= -\frac{1}{\pi} \text{sign}(\omega - \mu) \text{Im} G(\mathbf{r}, \mathbf{r}, \omega) \quad .
 \end{aligned} \tag{3.1}$$

These formula can be condensed in (and generalized to) the more general expression:

$$p(\{\lambda_i\}) = \mathcal{P}_{\{\lambda_i\}}[G], \tag{3.2}$$

in which p is the observable that depends on some variables $\{\lambda_i\}$, and $\mathcal{P}_{\{\lambda_i\}}$ is the linear¹ functional that, when applied to the Green's function of the system, returns the quantity p evaluated at $\{\lambda_i\}$. For example, in the case of density, $p \equiv n$, $\{\lambda_i\} \equiv \mathbf{r}$ and $\mathcal{P}_{\{\lambda_i\}} \equiv \mathcal{P}_{n(\mathbf{r})}$, with $\mathcal{P}_{n(\mathbf{r})}[f] := \int \frac{d\omega}{2\pi i} e^{i\omega\eta} \delta(\mathbf{r} - \mathbf{r}_1) \delta(\mathbf{r} - \mathbf{r}_2) f(\mathbf{r}_1, \mathbf{r}_2, \omega)$ and $\mathcal{P}_{n(\mathbf{r})}[G] = n(\mathbf{r})$.

Two aspects are noteworthy: each of the quantities we displayed depend on a smaller set of variables than the Green's function, which is a complex-valued, frequency-dependent, non-local function: T is just a real number, $\gamma(\mathbf{r}, \mathbf{r}')$ depends on two space variables only, $A(\mathbf{r}, \mathbf{r}, \omega)$ is a real function of one space variable and one frequency, and so on. The application of the functional \mathcal{P} *reduces*, in general, the number of *degrees of freedom* of the Green's function.

Linked to this observation is the fact that each of the quantities p we presented contains a *reduced amount of explicit information* with respect to the full Green's function. In other words, some structure has been lost in passing from the Green's function to one of its functionals, and reverse engineering, namely going from a quantity $p(\{\lambda_i\})$ back to the full Green's function $G(\mathbf{r}, \mathbf{r}', \omega)$, is, in practice, not possible anymore.

These aspects define what we call *reduced quantities*, properties of the system that can be expressed as functionals of the Green's function, but reverse engineering is unfeasible. All the quantities of eq. (3.1) are in general reduced quantities, apart from particular situations in which, *e.g.*, symmetry makes reverse engineering possible (see the next chapter for some of these examples).

On the contrary, $G_{ll'}(\omega)$, obtained as $G_{ll}(\omega)$ in eq. (3.1) with two different l and l' , is not a reduced quantity, as $G(\mathbf{r}, \mathbf{r}', \omega)$ can be reconstructed from it. The same is true for $G_{nn'}(\mathbf{k}, \omega)$, which is the Green's function in the Bloch basis, or for any other Green's function in another basis.

¹The linearity of the functional \mathcal{P} will be important in the following, when G will be expressed via a Dyson equation; the property we need is $\mathcal{P}[\lambda_1 G_1 + \lambda_2 G_2] = \lambda_1 \mathcal{P}[G_1] + \lambda_2 \mathcal{P}[G_2]$.

...and how to find them To obtain the Green's function in standard many-body perturbation theory, one usually finds a form for the self energy, through an approximate implementation of the Hedin equations (2.45). Then, plugging the expression for the self energy into the Dyson equation (2.46), one obtains the Green's function.

This procedure is computationally demanding, as the self energy is a complex, frequency-dependent and non-local quantity, that has to be evaluated from scratch for each material. Moreover, once the self energy is at hand, one should in principle solve the Dyson equation $G^{-1} = G_0^{-1} - \Sigma$; this is a time-consuming procedure, even for simple approximations like Hartree-Fock, eq. (2.44), basically for the non-local nature of Σ .

We can regard the cost issue as a technical problem that is becoming less and less relevant with the progress of technology. Yet, the standard procedure is unsatisfying *in principle*, for the same two reasons as above: first, for studying properties of a *large number* of materials (material science), spending so much time in building up the self energy of each single system is definitely not an efficient procedure. A more attractive scheme would be to isolate some common (and computationally costly) properties of the self energy and evaluate them just once and for all, *e.g.*, in a model system. Then, one could refer to that single calculation each time a new material is considered, possibly correcting the model system self energy by some properties of the specific material. This is the content of chapter 5.

The second reason why this approach is unsatisfying is related to the use of the Green's function once it has been evaluated. The Green's function, as the many-body wavefunction, is most often just an *intermediate object*, which cannot directly be compared with experiments. On the contrary, the final target is usually one of the quantities in eq. (3.1), namely a *reduced quantity* $p(\{\lambda_i\})$, with a lower number of degrees of freedom than both the Green's function or the self energy.

The fact that the latter are well-studied, well-known objects, for which a perturbation expansion is at hand, should not obscure the fact that their evaluation constitutes a considerable double detour with respect to the calculation of p . The whole Green's function contains unneeded information for the knowledge of p , which nonetheless are included in the standard calculation. Also the complex, non-local and frequency-dependent self energy, employed to obtain the Green's function, is clearly too much to get the small $p(\{\lambda_i\})$.

A better strategy would be to directly target p , without passing through the full Green's function, and consequently without using the full self energy.

This is what auxiliary systems do.

3.2 How to build auxiliary systems

The possibility of building an *auxiliary system* rests on the concept of *reduced quantity*: the plan must not be to obtain the full information carried by G (in which case the auxiliary system discussed here would coincide with the real system itself), but just the reduced quantity $p = \mathcal{P}[G]$.

For such a purpose one can introduce *another* system, the *p-auxiliary system*, which can be described by *another* Green's function $G_p(\mathbf{r}, \mathbf{r}', \omega)$ that, however, yields *the same* quantity p for all the λ_i s:

$$\boxed{p(\{\lambda_i\}) = \mathcal{P}_{\{\lambda_i\}}[G_p] \quad \forall \lambda_i} \quad . \quad (3.3)$$

To be redundant and follow the notation in which the subscript p represents quantities of the p -auxiliary system, eq. (3.3) would actually be:

$$p_p(\{\lambda_i\}) := \mathcal{P}_{\{\lambda_i\}}[G_p] \stackrel{(3.3)}{=} \mathcal{P}_{\{\lambda_i\}}[G] = p(\{\lambda_i\}).$$

Note that the *same* functional $\mathcal{P}_{\{\lambda_i\}}$ has been employed in both the real and the auxiliary system. One could also design *another* auxiliary system described by \tilde{G}_p and say that $\tilde{p}_p(\{\lambda_i\}) := \mathcal{R}_{\{\lambda_i\}}[\tilde{G}_p]$ with $\tilde{p}_p(\{\lambda_i\}) = p(\{\lambda_i\})$. The functional \mathcal{R} can be completely different from the functional \mathcal{P} , but they return the same quantity p when applied to \tilde{G}_p and G respectively².

Having another system, besides the real one, that yields the same quantity p is not of particular benefit, unless the auxiliary system is simpler to solve and therefore one could completely avoid working in the real system. This is exactly the reasoning here, as we make the further assumption that the role of the self energy is played, in the p -auxiliary system, by a simpler p -effective potential $v_p(\{\mu_j\})$, that depends on some variables $\{\mu_j\}$ (for all practical purposes, we will see that $\{\mu_j\} \equiv \{\lambda_i\}$: the effective potential has the same degrees of freedom of p itself). Therefore, omitting variables and integrations, we can write the Dyson equation for G_p as:

$$G_p = G_0 + G_0 v_p G_p. \quad (3.4)$$

Eq. (3.3) and eq. (3.4) completely define the p -auxiliary system. If the ansatz we made were correct, namely if it were possible to obtain the quantity p from the effective potential $v_p(\{\mu_j\})$, and if we knew this potential, we would obtain the same quantity p *also* in the auxiliary system.

We call the first “if” the v_p -representability problem, summarized in the question: “which is the class of the p functions that can be obtained, through eq. (3.3) and eq. (3.4), via the p -effective potential $v_p(\{\mu_j\})$?”³ We will partly answer to this question in specific cases, by referring to some systems in which the p -potential is explicit. However, we will not consider this issue in general.

On the other hand, the second “if” represents the central question of this thesis: “can we actually find this potential?” A general answer is given in the following section.

3.2.1 The generalized Sham–Schlüter equation

An in principle exact way of finding the effective potential $v_p(\{\mu_j\})$ is based on a generalization of the Sham–Schlüter equation [11], obtained for the first time in [6]. This is based on a reformulation of eq. (3.3) using eq. (3.4) and the Dyson equation of the real system, eq. (2.46).

Indeed, as both G and G_p can be referred to the same⁴ G_0 , the latter can be excluded by writing a new Dyson equation that directly links G to G_p :

$$G = G_p + G_p [\Sigma - v_p] G.$$

If p is v_p -representable, we can implement eq. (3.3) by applying the linear functional \mathcal{P} to both sides of the previous equation, obtaining:

$$\mathcal{P}_{\{\lambda_i\}} \left[G_p [\Sigma - v_p] G \right] = 0. \quad (3.5)$$

²For example, take $p \rightarrow E$ the ground state energy of a system. Even if it is not a one-particle quantity, it can nevertheless be obtained as a linear functional of the Green’s function through the Galitskii–Migdal equation (2.20). The functional is $E = \frac{1}{2} \int d^3r \lim_{r' \rightarrow r} \int \frac{d\omega}{2\pi i} e^{i\omega\eta} [\omega + h_0(r)] G(r, r', \omega) := \mathcal{P}_E[G]$. We can introduce an E -auxiliary system described by G_E that returns the same value E when the functional \mathcal{P}_E is applied to G_E , namely $\mathcal{P}_E[G_E] = E_E = E$. We can also introduce another auxiliary system described by \tilde{G}_E that returns E only when the functional \mathcal{P}_T (kinetic energy), and not the functional \mathcal{P}_E , is applied: $\mathcal{P}_T[\tilde{G}_E] = T_{\tilde{E}} = E$: E is the total energy of the real system, the total energy of the auxiliary system described by G_E , but the kinetic energy of the system described by \tilde{G}_E ; the total energy of the system described by \tilde{G}_E is \tilde{E}_E and is different from E . This observation will be used in the discussion at page 89.

³Note that what we refer to as the v_p -representability problem is the generalization to p of the *non-interacting* v -representability problem of DFT, see below.

⁴Note that it is not fundamental that the real and the auxiliary systems *share* the same G_0 : the previous equation, indeed, would hold anyway with a shift of $\Sigma - v_p$.

having used that $\mathcal{P}_{\{\lambda_i\}}[G_p] = \mathcal{P}_{\{\lambda_i\}}[G] = p(\{\lambda_i\})$. This is the *generalized Sham–Schlüter equation*, that has been derived for the first time in [6, 79]. It is a highly non-linear equation for the unknown p -potential v_p , that enters the equation also in G_p via eq. (3.4): one can solve it iteratively, starting from a guess $v_p^{(k=0)}$ till, in principle, self-consistence.

The generalized Sham–Schlüter equation, which we will use throughout the thesis, is completely equivalent to eq. (3.3), with the aid of two Dyson equations. It explicitly displays the self energy and the degrees of freedom of the various quantities involved, hence it is of fundamental importance for discussing the existence of possible solutions.

3.2.2 What we have and what we have not

Consider an observable o , which is a functional \mathcal{O} of the function p , $o = \mathcal{O}[p]$. p is the quantity reproduced by the p -auxiliary system via the potential v_p ; if the latter is known, the quantity p_p evaluated in the p -auxiliary system coincides with p .

In the auxiliary system, everything gets a subscript p : the relation between o_p and p_p is fixed by the functional \mathcal{O}_p : $o_p = \mathcal{O}_p[p_p]$, which is often simpler than \mathcal{O} :

$$o = \mathcal{O}[p] \quad o_p = \mathcal{O}_p[p_p]. \quad (3.6)$$

An important point is that, even if the exact effective potential v_p were at hand, and thus the exact p were known, we would not, in general, get o from $\mathcal{O}_p[p_p = p]$:

$$o \neq \mathcal{O}_p[p].$$

In some cases, as o is a functional of p in the real system, a functional relation exists also in the auxiliary system. However, the functional is not \mathcal{O}_p , the analogous of \mathcal{O} in the auxiliary system, but a different one, $\tilde{\mathcal{O}}_p$:

$$o = \tilde{\mathcal{O}}_p[p].$$

We will use this observation in several part of this thesis.

Auxiliary systems as presented above are generalizations to generic quantities $p(\{\lambda_i\})$ of a particularly important auxiliary system, the prototype of all, the one relative to density.

It is the Kohn–Sham auxiliary system.

3.3 The Kohn–Sham system

The Kohn–Sham system is an auxiliary system we can build when the quantity of interest $p(\{\lambda_i\})$ is the local density $n(\mathbf{r})$, and the associated functional is $\mathcal{P}_{n(\mathbf{r})}[G] = \int \frac{d\omega}{2\pi i} e^{i\omega\eta} G(\mathbf{r}, \mathbf{r}, \omega)$.

Density is a reduced quantity, depending on just one space variable. It is nevertheless a fundamental quantity, as the Hohenberg–Kohn theorems of section 2.4.2 ensure that any property of the system is actually a density functional. The step forward represented by the paper of Kohn and Sham [7] lays in a concrete procedure for obtaining the density $n(\mathbf{r})$.

Their starting point is assuming (non-interacting⁵) $v_n(\mathbf{r})$ -representability for the density $n(\mathbf{r})$. In other words they suggest that the function $n(\mathbf{r})$ can be realized in a system in which the exchange–correlation part of the self energy is replaced by the real, local and static potential $v_n(\mathbf{r}) \equiv v_{xc}(\mathbf{r})$; therefore, the total potential felt by the electrons is the *Kohn–Sham potential* $v_{KS}(\mathbf{r})$:

$$v_{KS}(\mathbf{r}) = v^{\text{ext}}(\mathbf{r}) + v_H(\mathbf{r}) + v_{xc}(\mathbf{r}). \quad (3.7)$$

⁵A related concept, with which we will not deal, is the *N-representability problem*, which deals with the existence of a physical system whose ground state yields the density $n(\mathbf{r})$.

The idea rests on the observation that the Hohenberg–Kohn functional $F[n]$ introduced at page 25 can be separated into a free electron contribution $T_s[n]$ plus the Hartree term $E_H[n]$ of eq. (2.7), plus the rest $E_{xc}[n]$, called exchange–correlation contribution⁶. Thus, eq. (2.17) can be written:

$$\left. \frac{\delta T_s[\tilde{n}]}{\delta \tilde{n}(\mathbf{r})} \right|_{\tilde{n}=n} + (v^{\text{ext}}(\mathbf{r}) + v_H(\mathbf{r}) + v_{xc}(\mathbf{r})) = 0, \quad (3.8)$$

with $v_{xc}(\mathbf{r}) := \frac{\delta E_{xc}[n]}{\delta n(\mathbf{r})}$. The clever observation is that the equation above is “the same as one obtains [...] for a system of non–interacting electrons moving in the given potential” $v^{\text{ext}}(\mathbf{r}) + v_H(\mathbf{r}) + v_{xc}(\mathbf{r}) = v_{KS}(\mathbf{r})$ (provided that the same n is shared by both the real and the non–interacting auxiliary system).

Therefore, one can completely forget about the original definition of $v_{xc}(\mathbf{r})$ in terms of Coulomb interactions, and move to a system of non–interacting electrons (the Kohn–Sham system) which yields the same density as the real system as soon as the exact potential $v_{xc}(\mathbf{r})$ is known. Once the potential $v_{KS}(\mathbf{r})$ is at hand, the Kohn–Sham system is relatively easy to solve, as the equations of motion for the electrons are single–particle Schrödinger equations with an external potential $v_{KS}(\mathbf{r})$:

$$\left[-\frac{\nabla^2}{2} + v_{KS}(\mathbf{r}) \right] \varphi_l^{\text{KS}}(\mathbf{r}) = \varepsilon_l^{\text{KS}} \varphi_l^{\text{KS}}(\mathbf{r}), \quad (3.9)$$

with $\varepsilon_l^{\text{KS}}$ and $\varphi_l^{\text{KS}}(\mathbf{r})$ eigenvalues and eigenfunctions. The expression for the density, too, is easy in this framework, much easier than eq. (2.6):

$$n^{\text{KS}}(\mathbf{r}) = \sum_l \theta(\mu^{\text{KS}} - \varepsilon_l^{\text{KS}}) |\varphi_l^{\text{KS}}(\mathbf{r})|^2 = n(\mathbf{r}), \quad (3.10)$$

with μ^{KS} the highest occupied level of the Kohn–Sham system. To solve the system, one usually starts with a guess for $v_{KS}(\mathbf{r})$, solves the Kohn–Sham equations (3.9), finds the density through eq. (3.10) and with this new density updates the potential $v_{KS}(\mathbf{r})$, till self–consistency.

Note that the Kohn–Sham system yields also the exact value E_0 of the ground state total energy of the real system, but not through the functional E_0^{KS} ; indeed, the ground state total energy of the Kohn–Sham system is nothing but:

$$E_0^{\text{KS}} = \sum_l \theta(\mu^{\text{KS}} - \varepsilon_l^{\text{KS}}) \varepsilon_l^{\text{KS}}, \quad (3.11)$$

while the total energy of the real system can be found as⁷:

$$E_0 = E_0^{\text{KS}} - E_H + E_{xc} - \int d^3r n(\mathbf{r}) v_{xc}(\mathbf{r}). \quad (3.12)$$

This is an application of the general discussion of section 3.2.2: in the same auxiliary system, density stems from the standard functional while the total energy stems from *another* functional.

⁶Although the name is the same, this “xc” has not the same physical meaning as the “xc” introduced in the previous chapter: the latter represents all the contributions to the electronic interaction energy beyond the Hartree–Fock approximation; the former considers also the correction in the kinetic energy that results from taking only the independent–particle contribution in $F_s[n]$.

⁷Here is the proof:

$$\begin{aligned} E_0 &= F + \int d^3r n(\mathbf{r}) v^{\text{ext}}(\mathbf{r}) = T_s + E_H + E_{xc} + \int d^3r n(\mathbf{r}) v^{\text{ext}}(\mathbf{r}) = \\ &= \left(T_s + \int d^3r n(\mathbf{r}) v_{KS}(\mathbf{r}) \right) + E_H + E_{xc} - \int d^3r n(\mathbf{r}) v^{\text{KS}}(\mathbf{r}) + \int d^3r n(\mathbf{r}) v^{\text{ext}}(\mathbf{r}) = \\ &= E_0^{\text{KS}} - E_H + E_{xc} - \int d^3r n(\mathbf{r}) v^{\text{xc}}(\mathbf{r}) \end{aligned}$$

The same observation holds for the fundamental gap E_g . In the real system, this is given by eq. (2.25), $E_g = \varepsilon_c - \varepsilon_v = E_g[n]$, with ε_c and ε_v defined in eq. (2.24) for s the ground state. Because of the Hohenberg–Kohn theorems, the gap is a functional of the density n . In the Kohn–Sham system, the analogous functional is expressed as a difference of the Kohn–Sham levels: $E_g^{\text{KS}} = \varepsilon_c^{\text{KS}} - \varepsilon_v^{\text{KS}} = E_g^{\text{KS}}[n^{\text{KS}}]$, which is still a functional of n^{KS} . If we knew the exact Kohn–Sham potential v^{KS} , we would have the exact density: $n^{\text{KS}} = n$; by contrast, it is well known that, even with the exact density, $E_g^{\text{KS}}[n^{\text{KS}} = n] \neq E_g[n]$ (indeed, KS usually underestimates the gap). To have in principle the correct value of the gap, we must introduce another functional, which is $E_g^{\text{KS}}[n^{\text{KS}}] + \Delta^{\text{KS}}[n^{\text{KS}}]$, [80, 81, 11] through which:

$$E_g^{\text{KS}}[n] + \Delta^{\text{KS}}[n] = E_g[n].$$

This observation, together with the fact that the total energy of the real system cannot be expressed as the sum of $\varepsilon_l^{\text{KS}}$, clarifies that the role of the Kohn–Sham states $\varphi_l^{\text{KS}}(\mathbf{r})$ is purely *ancillary*: they are intermediate objects, useful to introduce in order to easily get the density and the total energy; but they have no direct physical meaning. In particular the Kohn–Sham eigenvalues cannot be interpreted as addition and removal excitation energies.

A general feature of auxiliary systems is the following: if on the one hand the equations of motion are usually simpler (compare eq. (3.9) to eq. (2.4) or eq. (2.38)), on the other hand the effective potential is more difficult to find. Indeed, all the difficulties of the many–body problem are hidden in the form of the potential itself.

An exact way of obtaining the potential is the Sham–Schlüter equation (3.5), which was actually developed – in its original form – precisely for the density [11, 82].

3.3.1 The Sham–Schlüter equation

The information contained in the Kohn–Sham eigenvalues and eigenfunctions $\varepsilon_l^{\text{KS}}$ and $\varphi_l^{\text{KS}}(\mathbf{r})$ can be recast into a Green’s function $G_n := G^{\text{KS}}$ associated with the Kohn–Sham Hamiltonian $\hat{h}^{\text{KS}}(\mathbf{r}) = -\frac{\nabla^2}{2} + v_{\text{KS}}(\mathbf{r})$. Since particles are non–interacting, the Lehmann amplitudes (2.23) in the basis $\{l\}$ that diagonalizes $\hat{h}^{\text{KS}}(\mathbf{r})$ are the eigenfunctions $\varphi_l^{\text{KS}}(\mathbf{r})$ themselves, and the excitation energies are the eigenvalues $\varepsilon_l^{\text{KS}}$. Therefore, the Kohn–Sham Green’s function reads:

$$G^{\text{KS}}(\mathbf{r}, \mathbf{r}', \omega) = \sum_l \frac{\varphi_l^{\text{KS}}(\mathbf{r})\varphi_l^{\text{KS}*}(\mathbf{r}')}{\omega - \varepsilon_l^{\text{KS}} + i\eta \text{sign}(\varepsilon_l^{\text{KS}} - \mu^{\text{KS}})}, \quad (3.13)$$

with the sum over both occupied and empty Kohn–Sham orbitals⁸.

⁸Both the density and the ground state total energy can be recast into standard functionals of G^{KS} :

$$\begin{aligned} n^{\text{KS}}(\mathbf{r}) &\equiv \mathcal{D}_{n(\mathbf{r})}[G^{\text{KS}}] = \int \frac{d\omega}{2\pi i} e^{i\omega\eta} G^{\text{KS}}(\mathbf{r}, \mathbf{r}, \omega) = \sum_l |\varphi_l^{\text{KS}}(\mathbf{r})|^2 \int \frac{d\omega}{2\pi i} \frac{e^{i\omega\eta}}{\omega - \varepsilon_l^{\text{KS}} + i\eta \text{sign}(\varepsilon_l^{\text{KS}} - \mu^{\text{KS}})} = \\ &= \sum_l |\varphi_l^{\text{KS}}(\mathbf{r})|^2 \theta(\mu^{\text{KS}} - \varepsilon_l^{\text{KS}}) \\ E_0^{\text{KS}} &\equiv \mathcal{D}_E[G^{\text{KS}}] = \frac{1}{2} \int d^3r \lim_{\mathbf{r}' \rightarrow \mathbf{r}} \int \frac{d\omega}{2\pi i} e^{i\omega\eta} [\omega + h_0(\mathbf{r})] G^{\text{KS}}(\mathbf{r}, \mathbf{r}', \omega) = \frac{1}{2} \sum_l \int d^3r |\varphi_l^{\text{KS}}(\mathbf{r})|^2 \\ &\cdot \int \frac{d\omega}{2\pi i} \frac{(\omega + \varepsilon_l^{\text{KS}}) e^{i\omega\eta}}{\omega - \varepsilon_l^{\text{KS}} + i\eta \text{sign}(\varepsilon_l^{\text{KS}} - \mu^{\text{KS}})} = \frac{1}{2} \sum_l \int d^3r |\varphi_l^{\text{KS}}(\mathbf{r})|^2 2\varepsilon_l^{\text{KS}} \theta(\mu^{\text{KS}} - \varepsilon_l^{\text{KS}}) = \sum_l \varepsilon_l^{\text{KS}} \theta(\mu^{\text{KS}} - \varepsilon_l^{\text{KS}}) \end{aligned}$$

as in eq. (3.10) and (3.11). On the contrary, as already stated, $E_0 \neq \mathcal{D}_E[G^{\text{KS}}]$, but it is *another* functional of G^{KS} : $E_0 = \mathcal{D}_E[G^{\text{KS}}]$, with \mathcal{D} given by eq. (3.12) with everything expressed as a functional of G^{KS} .

Using the Green's function, one can implement the Sham–Schlüter equation for the density; indeed, from the request that both G and G^{KS} yield the same density $n(\mathbf{r})$, eq. (3.5) reads:

$$\mathcal{P}_{n(\mathbf{r})} \left[G^{\text{KS}} [\Sigma - v_{\text{xc}}] G \right] = 0, \quad (3.14)$$

or, writing explicitly the functional $\mathcal{P}_{n(\mathbf{r})}[f]$ and the integration variables, and using the fact that $v_{\text{xc}}(\mathbf{r})$ is a local and static potential:

$$\int d^3 r_1 d^3 r_2 \int \frac{d\omega}{2\pi i} e^{i\omega\eta} G^{\text{KS}}(\mathbf{r}, \mathbf{r}_1, \omega) \left[\Sigma(\mathbf{r}_1, \mathbf{r}_2, \omega) - v_{\text{xc}}(\mathbf{r}_1) \delta(\mathbf{r}_1 - \mathbf{r}_2) \right] G(\mathbf{r}_2, \mathbf{r}, \omega) = 0. \quad (3.15)$$

Introducing the quantity $\zeta_{\text{KS}}(\mathbf{r}, \mathbf{r}') := \int \frac{d\omega}{2\pi i} e^{i\omega\eta} G^{\text{KS}}(\mathbf{r}, \mathbf{r}', \omega) G(\mathbf{r}', \mathbf{r}, \omega)$, a formal solution of the previous equation exists if $\zeta_{\text{KS}}(\mathbf{r}, \mathbf{r}')$ is invertible:

$$v_{\text{xc}}(\mathbf{r}) = \int d^3 r_1 \zeta_{\text{KS}}^{-1}(\mathbf{r}, \mathbf{r}_1) \int d^3 r_2 d^3 r_3 \int \frac{d\omega}{2\pi i} e^{i\omega\eta} G^{\text{KS}}(\mathbf{r}_1, \mathbf{r}_2, \omega) \Sigma(\mathbf{r}_2, \mathbf{r}_3, \omega) G(\mathbf{r}_3, \mathbf{r}_1, \omega).$$

The full Green's function G is often replaced by G^{KS} (also in the structure of the self energy), obtaining the *linear–response* Sham–Schlüter equation [83]:

$$\int d^3 r_1 d^3 r_2 \int \frac{d\omega}{2\pi i} e^{i\omega\eta} G^{\text{KS}}(\mathbf{r}, \mathbf{r}_1, \omega) \left[\Sigma(\mathbf{r}_1, \mathbf{r}_2, \omega) [G^{\text{KS}}] - v_{\text{xc}}(\mathbf{r}_1) \delta(\mathbf{r}_1 - \mathbf{r}_2) \right] G^{\text{KS}}(\mathbf{r}_2, \mathbf{r}, \omega) = 0. \quad (3.16)$$

This equation does not rest anymore on the idea that the real and the auxiliary systems share the same density; therefore, its solution $v_{\text{xc}}(\mathbf{r})$ is in general just an approximate version of the exact $v_{\text{xc}}(\mathbf{r})$. Nevertheless, eq. (3.16) is important in itself, as it coincides with the equation for the *optimized effective potential* $v_{\text{xc}}^{\text{OEP}}(\mathbf{r})$ introduced in [84, 85]. This is the variationally best local potential that extremizes the energy evaluated through Σ ; in particular, if $\Sigma = \Sigma_x$, eq. (2.44), the potential is known as the “exact exchange” approximation to $v_{\text{xc}}(\mathbf{r})$, and it represents the best (as far as the total energy is concerned) local approximation to the non–local Σ_x [84, 85, 86].

As pointed out in [83], “attempts to improve on $v_{\text{xc}}^{\text{OEP}}(\mathbf{r})$ as an approximation to $\Sigma(\mathbf{r}, \mathbf{r}', \omega)$ [as far as the total energy is considered] should involve non–locality either in space or in time”. The two possibilities are investigated below: the first involves the density matrix, while the second is linked to the diagonal of the spectral function.

3.4 An auxiliary system for the density matrix

As Kohn–Sham systems exist for the density, one could wonder if analogous auxiliary systems exist for the density matrix $\gamma(\mathbf{r}, \mathbf{r}')$. This amounts to a non–local generalization $v_\gamma(\mathbf{r}, \mathbf{r}')$ of the Kohn–Sham potential as an effective potential in a Kohn–Sham–like auxiliary system of non–interacting particles.

Requiring that the potential $v_\gamma(\mathbf{r}, \mathbf{r}')$ exactly reproduces the density matrix of the real system, eq. (2.8), one would come out with the Sham–Schlüter equation (3.5) generalized to the density matrix:

$$\int d^3 r_1 d^3 r_2 \int \frac{d\omega}{2\pi i} e^{i\omega\eta} G_\gamma(\mathbf{r}, \mathbf{r}_1, \omega) \left[\Sigma(\mathbf{r}_1, \mathbf{r}_2, \omega) - v_{\text{xc}}^\gamma(\mathbf{r}_1, \mathbf{r}_2) \right] G(\mathbf{r}_2, \mathbf{r}', \omega) = 0, \quad (3.17)$$

with the auxiliary system Green's function $G_\gamma(\mathbf{r}_1, \mathbf{r}_2, \omega)$ defined in terms of the γ –effective potential $v_{\text{xc}}^\gamma(\mathbf{r}_1, \mathbf{r}_2)$ via the Dyson equation $G_\gamma^{-1}(\mathbf{r}_1, \mathbf{r}_2, \omega) = G_{\text{H}}^{-1}(\mathbf{r}_1, \mathbf{r}_2, \omega) - v_{\text{xc}}^\gamma(\mathbf{r}_1, \mathbf{r}_2)$.

Although eq. (3.17) looks a legitimate equation, it does not have any solution when Σ is frequency dependent. Two examples of this statement are shown in appendix E, for two systems

that we will consider in the next chapter, the Hubbard dimer and the homogeneous electron gas.

Indeed, the fundamental question is: are density matrices ν_γ -representable? The general answer is no: while the same density function $n(\mathbf{r})$ can be most often realized both in an interacting and a non-interacting system, usually the same density matrix can not (at zero temperature). This is a consequence of the structure of the density matrix. Indeed, being hermitian, it can be diagonalized and expressed as:

$$\gamma(\mathbf{r}, \mathbf{r}') = \sum_{\alpha} n_{\alpha} \phi_{\alpha}(\mathbf{r}) \phi_{\alpha}^{*}(\mathbf{r}'), \quad (3.18)$$

with n_{α} eigenvalues, $0 \leq n_{\alpha} \leq 1$ and $\sum_{\alpha} n_{\alpha} = N$ (they can be interpreted as a probability distribution), called *occupation numbers*, and $\phi_{\alpha}(\mathbf{r})$ the eigenvectors of γ , called *natural orbitals*.

A fractional occupation $0 < n_{\alpha} < 1$ is the fingerprint of correlation, as any system of independent particles displays only integer occupation numbers, $n_{\alpha} = 1$ if the one-particle state described by $|\alpha\rangle$ is occupied, and $n_{\alpha} = 0$ otherwise.

One can express the same concept by considering the squared density matrix $\gamma^2(\mathbf{r}, \mathbf{r}') := \int d^3 r_1 \gamma(\mathbf{r}, \mathbf{r}_1) \gamma(\mathbf{r}_1, \mathbf{r}') = \sum_{\alpha} n_{\alpha}^2 \phi_{\alpha}(\mathbf{r}) \phi_{\alpha}^{*}(\mathbf{r}')$, having used the property that the natural orbitals are orthogonal and normalized. For a system of independent particles, as $n_{\alpha} = \{0; 1\}$, $n_{\alpha}^2 = n_{\alpha}$ and therefore $\gamma_0^2 = \gamma_0$. By contrast, for a correlated system, $n_{\alpha}^2 < n_{\alpha}$ and in general $\gamma^2 \neq \gamma$. Even the reverse is true: if $\gamma^2 = \gamma$, then the occupation numbers are integers and γ describes a system of independent particles.

Therefore, a density matrix γ_0 corresponding to a non-interacting system will in general be different from a real system density matrix, in which correlation is always present. This blocks any attempt to build an independent-particle auxiliary system that reproduces γ .

In other words, eq. (3.17) has no solutions when Σ is frequency dependent. By contrast, the linearized version of (3.17), in which G is replaced by G_{γ} everywhere, does have sometimes a solution [83].

3.5 The spectral potential

The fundamental quantity of this work is $A(\mathbf{r}, \mathbf{r}, \omega)$, the diagonal of the spectral function in real space. It is a reduced quantity, as it contains less information than the full Green's function: the density $n(\mathbf{r})$, the interacting density of states $\text{DOS}(\omega)$, the diagonal of the Green's function $G(\mathbf{r}, \mathbf{r}, \omega)$ can all be derived from $A(\mathbf{r}, \mathbf{r}, \omega)$, while the full Green's function, and consequently the on-site Green's function $G_{II}(\omega)$ of DMFT (see below), the \mathbf{k} -resolved Green's function $G(\mathbf{k}, \omega)$, the density matrix $\gamma(\mathbf{r}, \mathbf{r}')$, the total energy E_0, \dots , cannot.

As the information content is reduced, one does not need the full self energy to obtain $A(\mathbf{r}, \mathbf{r}, \omega)$, but just a part of the information carried by it. This is where the idea of an auxiliary system for the diagonal of the spectral function arises. In particular, as for reproducing the density $n(\mathbf{r})$ we need a local potential $\nu_{\text{KS}}(\mathbf{r})$ (KS-DFT), and for reproducing the on-site Green's function $G_{II}(\omega)$ we need an on-site self energy $\Sigma_{II}(\omega)$ (DMFT, see below), here we make the ansatz that a *local, real and frequency-dependent* potential, the *spectral potential* $\nu_{\text{SF}}(\mathbf{r}, \omega)$, can reproduce the diagonal of the spectral function, which is indeed local, real and frequency-dependent.

Therefore, we introduce an auxiliary system described by the Green's function $G_{\text{SF}}(\mathbf{r}, \mathbf{r}', \omega)$, defined by the following inverted Dyson equation:

$$G_{\text{SF}}^{-1}(\mathbf{r}, \mathbf{r}', \omega) = G_0^{-1}(\mathbf{r}, \mathbf{r}', \omega) - \nu_{\text{SF}}(\mathbf{r}, \omega) \delta(\mathbf{r} - \mathbf{r}'). \quad (3.19)$$

To such a Green's function, a spectral function is associated in the usual way, see eq. (2.30):

$$A_{\text{SF}}(\mathbf{r}, \mathbf{r}', \omega) = -\frac{1}{\pi} \text{sign}(\omega - \mu) \text{Im} G_{\text{SF}}(\mathbf{r}, \mathbf{r}', \omega). \quad (3.20)$$

Finally, the spectral potential is fixed by the requirement, analogous to eq. (3.3):

$$\boxed{A_{\text{SF}}(\mathbf{r}, \mathbf{r}, \omega) = A(\mathbf{r}, \mathbf{r}, \omega)} \quad (3.21)$$

Note that, if the previous equation holds, so does the equation $n_{\text{SF}}(\mathbf{r}) = n(\mathbf{r})$: not only the diagonal of the spectral function, but also the density is reproduced by this new auxiliary system, that can therefore be considered as a dynamical generalization of the Kohn–Sham system. The excitation energies of the latter cannot be directly compared to the one–electron excitation spectrum, while with this auxiliary system the spectrum is exact by definition, eq. (3.21). Moreover, the spectrum is quickly obtained via a local and real potential, computationally lighter than the non–local and complex–valued self energy.

Generalized Sham–Schlüter equation The ansatz represented by the three equations above is supported by the structure of the generalized Sham–Schlüter equation (3.5) applied to the spectral function $A(\mathbf{r}, \mathbf{r}, \omega)$; it reads:

$$\mathcal{P}_{A(\mathbf{r}, \mathbf{r}, \omega)} \left[G_{\text{SF}}[\Sigma - v_{\text{xc}}^{\text{SF}}] G \right] = 0, \quad (3.22)$$

with $\mathcal{P}_{A(\mathbf{r}, \mathbf{r}, \omega)}[f] := -\frac{1}{\pi} \text{sign}(\omega - \mu) \text{Im} f(\mathbf{r}, \mathbf{r}, \omega)$. The exchange–correlation part of the spectral potential $v_{\text{xc}}^{\text{SF}}(\mathbf{r}, \omega)$ is introduced in the usual way as the non–classical part of the full potential: $v_{\text{SF}}(\mathbf{r}, \omega) = v^{\text{ext}}(\mathbf{r}) + v_{\text{H}}(\mathbf{r}) + v_{\text{xc}}^{\text{SF}}(\mathbf{r}, \omega)$. Explicitly, the previous equation reads:

$$\int d^3 r_1 d^3 r_2 \text{Im} [G_{\text{SF}}(\mathbf{r}, \mathbf{r}_1, \omega) \Sigma(\mathbf{r}_1, \mathbf{r}_2, \omega) G(\mathbf{r}_2, \mathbf{r}, \omega)] = \int d^3 r_1 v_{\text{xc}}^{\text{SF}}(\mathbf{r}_1, \omega) \text{Im} [G_{\text{SF}}(\mathbf{r}, \mathbf{r}_1, \omega) G(\mathbf{r}_1, \mathbf{r}, \omega)] \quad (3.23)$$

which is a non–linear equation for the real potential $v_{\text{xc}}^{\text{SF}}(\mathbf{r}, \omega)$ [6, 79].

By looking at the structure of eq. (3.23), it is clear that a static but non–local potential $v_{\text{xc}}^{\text{SF}}(\mathbf{r}_1, \mathbf{r}_2)$, in place of $v_{\text{xc}}^{\text{SF}}(\mathbf{r}, \omega)$, could not do the job. Indeed, the self energy will in general add a non–trivial frequency dependence to the product of the two Green's function on the left–hand–side, hence a frequency–dependent potential is needed on the right–hand–side. By the same reasoning, also a local and static potential $v_{\text{xc}}^{\text{SF}}(\mathbf{r})$, like the Kohn–Sham one, is ruled out. Indeed, as it is well known and as we mentioned already, Kohn–Sham spectra are a by–product of the auxiliary system construction, and they are not related in any simple way to the spectra of the corresponding real system [81]. Finally, a purely frequency–dependent potential $v_{\text{xc}}^{\text{SF}}(\omega)$ would not catch the space dependence of the self energy, while a complex spectral potential looks superfluous, as the quantity to reproduce, $A(\mathbf{r}, \mathbf{r}, \omega)$, is real–valued.

Clearly, were the self energy real and local, the spectral potential would coincide with the self energy itself. On the contrary, as soon as the self energy becomes complex or/and non–local, eq. (3.23) becomes non–trivial: to get $A(\mathbf{r}, \mathbf{r}, \omega)$, the spectral potential condensates the essential information carried by the self energy into just two degrees of freedom, locality and frequency.

A formal solution of eq. (3.23) is possible. As in the Kohn–Sham case, we introduce the quantity $\zeta_{\text{SF}}(\mathbf{r}, \mathbf{r}', \omega) := \text{Im} [G_{\text{SF}}(\mathbf{r}, \mathbf{r}', \omega) G(\mathbf{r}', \mathbf{r}, \omega)]$. If this is invertible, namely if $\zeta_{\text{SF}}^{-1}(\mathbf{r}, \mathbf{r}', \omega)$ exists, the formal solution to the previous equation reads:

$$\boxed{v_{\text{xc}}^{\text{SF}}(\mathbf{r}, \omega) = \int d^3 r_1 \zeta_{\text{SF}}^{-1}(\mathbf{r}, \mathbf{r}_1, \omega) \int d^3 r_2 d^3 r_3 \text{Im} [G_{\text{SF}}(\mathbf{r}_1, \mathbf{r}_2, \omega) \Sigma(\mathbf{r}_2, \mathbf{r}_3, \omega) G(\mathbf{r}_3, \mathbf{r}_1, \omega)]} \quad (3.24)$$

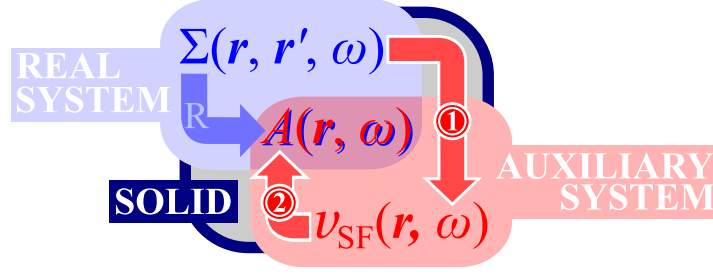


Figure 3.1: A scheme of the auxiliary system approach for the spectral function: the blue box represents the real system, in which the local part of the spectral function $A(\mathbf{r}, \omega) \equiv A(\mathbf{r}, \mathbf{r}, \omega)$ stems from the non-local self energy $\Sigma(\mathbf{r}, \mathbf{r}', \omega)$ (reference calculation, arrow R). In the auxiliary system (red box), the role of the self energy is played by the spectral potential $v_{\text{SF}}(\mathbf{r}, \omega)$. To obtain it, one solves the generalized Sham–Schlüter equation (3.24), arrow (1). Once the spectral potential is at hand, one evaluates the spectral function, arrow (2), which turns out to be exactly the same of the real system.

As $v_{\text{xc}}^{\text{SF}}(\mathbf{r}, \omega)$ enters also the Green's function $G_{\text{SF}}(\mathbf{r}_1, \mathbf{r}_2, \omega)$ on the right hand side, one usually has to solve eq. (3.24) iteratively in the spectral potential, till, in principle, self-consistency.

Note that, as in the Kohn–Sham case, also eq. (3.23) can be linearized by setting $G = \tilde{G}_{\text{SF}}$ everywhere (also in the functional expression of the self energy in terms of G : $\tilde{\Sigma} = \Sigma[\tilde{G}_{\text{SF}}]$):

$$\int_{\mathbf{r}_1, \mathbf{r}_2} \text{Im}[\tilde{G}_{\text{SF}}(\mathbf{r}, \mathbf{r}_1, \omega) \tilde{\Sigma}(\mathbf{r}_1, \mathbf{r}_2, \omega) G(\mathbf{r}_2, \mathbf{r}, \omega)] = \int_{\mathbf{r}_1} \tilde{v}_{\text{xc}}^{\text{SF}}(\mathbf{r}_1, \omega) \text{Im}[\tilde{G}_{\text{SF}}(\mathbf{r}, \mathbf{r}_1, \omega) \tilde{G}(\mathbf{r}_1, \mathbf{r}, \omega)]. \quad (3.25)$$

The system that results from such an equation, described by \tilde{G}_{SF} , does not share any more the diagonal of the spectral function with the real system. It rests on the weaker condition that the linear response of the spectral function to the perturbation converting the auxiliary system into the real system is zero [83], and it can be derived from a minimization condition on the total energy [87]. The solution – if any – of this equation, $\tilde{v}_{\text{xc}}^{\text{SF}}(\mathbf{r}, \omega)$, can therefore be interpreted as the *variationally best* [83] local, real and frequency-dependent potential that *approximates* the self energy for the evaluation of the total energy. Nothing to do with our approach, whose focus is on the exact $A(\mathbf{r}, \mathbf{r}, \omega)$ rather than an approximated total energy.

Biorthonormal representation Eq. (3.23) holds for each single value of ω , independently of all other frequencies. Therefore, one can treat frequency as an external parameter (a label) attached to each quantity [79]. The auxiliary system itself can be viewed as a collection of Kohn–Sham–like auxiliary systems, each labeled by a value of frequency: each of them reproduces the local density $n(\mathbf{r})$, and together they yield the local spectral function $A(\mathbf{r}, \mathbf{r}, \omega)$. In particular, the spectral potential, real and local, can be viewed as a dynamical generalization of the Kohn–Sham potential.

Therefore, for a discrete system, one can easily generalize eq. (3.13) by expressing the Green's function of the auxiliary system, eq. (3.19), as:

$$G_{\text{SF}}(\mathbf{r}, \mathbf{r}', \omega) = \sum_l \frac{\phi_l^{\text{SF}}(\mathbf{r}, \omega) \phi_l^{\text{SF}*}(\mathbf{r}', \omega)}{\omega - \varepsilon_l^{\text{SF}}(\omega) + i\eta \text{sign}(\varepsilon_l^{\text{SF}}(\omega) - \mu^{\text{SF}})}, \quad (3.26)$$

with the frequency-dependent (or frequency-labelled) eigenvalues and eigenfunctions $\varepsilon_l^{\text{SF}}(\omega)$ and $\phi_l^{\text{SF}}(\mathbf{r}, \omega)$ that satisfy the following Schrödinger-like equation:

$$\left[-\frac{\nabla^2}{2} + v_{\text{SF}}(\mathbf{r}, \omega) \right] \phi_l^{\text{SF}}(\mathbf{r}, \omega) = \varepsilon_l^{\text{SF}}(\omega) \phi_l^{\text{SF}}(\mathbf{r}, \omega). \quad (3.27)$$

This equation of motion is in between eq. (3.9) and eq. (2.38), in the same way as the representation (3.26) is a compromise between the Lehmann representation of eq. (2.22), which exactly applies to the Kohn–Sham Green’s function, eq. (3.13), and the biorthonormal representation of eq. (2.39).

Not that, as the spectral potential is real, the one–particle effective Hamiltonian $h_{\text{eff}}^{\text{SF}}(\mathbf{r}, \omega) := \left[-\frac{\nabla^2}{2} + v_{\text{SF}}(\mathbf{r}, \omega) \right] \equiv h_0(\mathbf{r}) + v_{\text{xc}}^{\text{SF}}(\mathbf{r}, \omega)$ is hermitian. As a consequence, its eigenvalues $\varepsilon_l^{\text{SF}}(\omega)$ are real and its eigenfunctions are orthonormal. Therefore, even if the representation (3.26) is extremely similar to eq. (2.39), its mathematical properties are – frequency by frequency – similar to the Kohn–Sham Lehmann representation. The difference with the latter is the frequency–dependence that enters both the eigenvalues and the eigenfunctions.

From eq. (3.26), an explicit expression for the diagonal of the spectral function is:

$$A_{\text{SF}}(\mathbf{r}, \mathbf{r}, \omega) = \sum_l |\phi_l^{\text{SF}}(\mathbf{r}, \omega)|^2 \delta(\omega - \varepsilon_l^{\text{SF}}(\omega)). \quad (3.28)$$

As the spectral potential is frequency–dependent, the equation $\omega - \varepsilon_l^{\text{SF}}(\omega) = 0$ has in general more than one solution $\varepsilon_l^{\text{SF}}$. Therefore, the single delta function of above can be expressed as a sum over several delta functions, each centered on one of the solutions $\varepsilon_l^{\text{SF}}$:

$$\delta(\omega - \varepsilon_l^{\text{SF}}(\omega)) = \sum_{\varepsilon_l^{\text{SF}}} Z_{\varepsilon_l^{\text{SF}}}^{\text{SF}} \delta(\omega - \varepsilon_l^{\text{SF}}),$$

with $Z_{\varepsilon_l^{\text{SF}}}^{\text{SF}-1} := (1 - \partial \varepsilon_l^{\text{SF}}(\omega) / \partial \omega)_{\omega = \varepsilon_l^{\text{SF}}}$ an analogous of the renormalization factor which is different from one even for static self energies. Therefore, the diagonal of the spectral function in the auxiliary system becomes:

$$A_{\text{SF}}(\mathbf{r}, \mathbf{r}, \omega) = \sum_l \sum_{\varepsilon_l^{\text{SF}}} Z_{\varepsilon_l^{\text{SF}}}^{\text{SF}} |\phi_l^{\text{SF}}(\mathbf{r}, \varepsilon_l^{\text{SF}})|^2 \delta(\omega - \varepsilon_l^{\text{SF}}), \quad (3.29)$$

namely a sum of weighted simple delta peaks. This quantity has to be compared to the real system $A(\mathbf{r}, \mathbf{r}, \omega)$ given by:

$$A(\mathbf{r}, \mathbf{r}, \omega) = \sum_s |f_s(\mathbf{r})|^2 \delta(\omega - \varepsilon_s). \quad (2.28)$$

The two are equal by construction, $A_{\text{SF}}(\mathbf{r}, \mathbf{r}, \omega) = A(\mathbf{r}, \mathbf{r}, \omega)$. On the contrary, the single delta peaks need not, in principle, to match: if, for a certain ω , there exists a quantum number s such that $\omega = \varepsilon_s$, and therefore $A(\mathbf{r}, \mathbf{r}, \omega) \neq 0$, there must be also (at least) a quantum number l such that $\omega = \varepsilon_l^{\text{SF}}$, with l not necessarily equal to s (if they are in the same basis)⁹. For example, if the spectral functions are represented on the Bloch basis, not necessarily $\varepsilon_{n\mathbf{k}}^{\text{SF}} = \varepsilon_{n\mathbf{k}}$: the *band structure* is, in general, not reproduced.

Not only the peak position, but also their amplitudes must be the same at each frequency; assuming, for simplicity, that the delta peak in the real system at $\omega = \varepsilon_s$ is reproduced by another single delta peak in the auxiliary system at $\omega = \varepsilon_l^{\text{SF}}$, the following relation must hold:

$$\boxed{|f_s(\mathbf{r})|_{s=s_0(\omega)}^2 = Z_{\omega}^{\text{SF}} |\phi_{l_0^{\text{SF}}(\omega)}^{\text{SF}}(\mathbf{r}, \omega)|^2} \quad (3.30)$$

with $s_0(\omega)$ the solution to the equation $\omega - \varepsilon_s = 0$ and $l_0^{\text{SF}}(\omega)$ the solution of $\omega - \varepsilon_l^{\text{SF}} = 0$. This is an exact relation, equivalent to eq. (3.21), that can be solved for $v^{\text{SF}}(\mathbf{r}, \omega)$.

⁹Note also that a single peak $\delta(\omega - \varepsilon_s)$ can be reproduced by the sum of several delta peaks, corresponding to the same quantum number l or to several ones.

Lehmann representation In general, a Lehmann representation in the auxiliary system does not hold. The Lehmann representation of a time-ordered Green's function is linked to causality, which in turn rests on the symmetric treatment of electrons and holes. This is possible if, whenever the self energy is frequency-dependent, it is also complex-valued.

Clearly, this is not the case in the auxiliary system, where the role of the self energy is played by a real, yet frequency-dependent, spectral potential. Causality breaks down, as the Kramers-Kronig relation that relates the real to the imaginary part of the self energy

$$\operatorname{Re}\Sigma(\mathbf{r}, \mathbf{r}', \omega) = -\frac{1}{\pi} \mathcal{P.V.} \int d\omega' \operatorname{sign}(\omega' - \mu) \frac{\operatorname{Im}\Sigma(\mathbf{r}, \mathbf{r}', \omega')}{\omega - \omega'} \quad (3.31)$$

does not hold any more for $\Sigma(\mathbf{r}, \mathbf{r}', \omega) \rightarrow v_{\text{SF}}(\mathbf{r}, \omega)$. Therefore, the corresponding Kramers-Kronig relation for the Green's function,

$$\operatorname{Re}G(\mathbf{r}, \mathbf{r}', \omega) = -\frac{1}{\pi} \mathcal{P.V.} \int d\omega' \operatorname{sign}(\omega' - \mu) \frac{\operatorname{Im}G(\mathbf{r}, \mathbf{r}', \omega')}{\omega - \omega'}, \quad (3.32)$$

is not fulfilled either when $G = G_{\text{SF}}$. By adding to both sides of the previous equation the imaginary part of G , it becomes evident that eq. (3.32) is completely equivalent to eq. (2.29); this, in turn, is equivalent to the Lehmann representation. We conclude, therefore, that, in general, a Lehmann representation does not hold in the auxiliary system.

Another way of seeing the same thing is the following: from the bi-orthonormal representation (3.26), the real part of the diagonal of the Green's function reads:

$$\operatorname{Re}G_{\text{SF}}(\mathbf{r}, \mathbf{r}, \omega) = \sum_l \frac{|\phi_l^{\text{SF}}(\mathbf{r}, \omega)|^2}{\omega - \varepsilon_l^{\text{SF}}(\omega)}, \quad (3.33)$$

which is a consequence of the reality of the spectral potential. On the other hand, if the Lehmann representation holds, $\operatorname{Re}G_{\text{SF}}^{\text{Leh}}(\mathbf{r}, \mathbf{r}, \omega)$ would be given by eq. (2.29), with $A_{\text{SF}}(\mathbf{r}, \mathbf{r}, \omega)$ from eq. (3.28):

$$\operatorname{Re}G_{\text{SF}}^{\text{Leh}}(\mathbf{r}, \mathbf{r}, \omega) = \mathcal{P.V.} \int d\omega' \frac{A_{\text{SF}}(\mathbf{r}, \mathbf{r}, \omega')}{\omega - \omega'} = \sum_l \mathcal{P.V.} \int d\omega' \frac{|\phi_l^{\text{SF}}(\mathbf{r}, \omega')|^2}{\omega - \omega'} \delta(\omega' - \varepsilon_l^{\text{SF}}(\omega')).$$

Writing the last delta function as a sum over the contributions from the peaks $\varepsilon_l^{\text{SF}}$, the Hilbert transform of $A_{\text{SF}}(\mathbf{r}, \mathbf{r}, \omega)$ reads:

$$\operatorname{Re}G_{\text{SF}}^{\text{Leh}}(\mathbf{r}, \mathbf{r}, \omega) = \sum_l \sum_{\varepsilon_l^{\text{SF}}} Z_{\varepsilon_l^{\text{SF}}}^{\text{SF}} \frac{|\phi_l^{\text{SF}}(\mathbf{r}, \varepsilon_l^{\text{SF}})|^2}{\omega - \varepsilon_l^{\text{SF}}}, \quad (3.34)$$

which has a different frequency-dependence than the one in eq. (3.33). The Lehmann representation, in general, yields an expression for $\operatorname{Re}G_{\text{SF}}(\mathbf{r}, \mathbf{r}, \omega)$, that is $\operatorname{Re}G_{\text{SF}}^{\text{Leh}}(\mathbf{r}, \mathbf{r}, \omega)$, which is not the expected one, $\operatorname{Re}G_{\text{SF}}(\mathbf{r}, \mathbf{r}, \omega)$.

The same conclusion can be analyzed from the other way round: as $A_{\text{SF}}(\mathbf{r}, \mathbf{r}, \omega) = A(\mathbf{r}, \mathbf{r}, \omega)$, also $\operatorname{Re}G_{\text{SF}}^{\text{Leh}}(\mathbf{r}, \mathbf{r}, \omega)$ obtained from the Lehmann representation, eq. (3.34), is the real system one, $\operatorname{Re}G(\mathbf{r}, \mathbf{r}, \omega)$. Therefore, the auxiliary system exhibits a $\operatorname{Re}G_{\text{SF}}(\mathbf{r}, \mathbf{r}, \omega)$, eq. (3.33), which is not the one of the real system: the diagonal of the Green's function is reproduced by the auxiliary system only in its imaginary part (the spectral function), but not in its real part.

On the other hand, if one wants to have access also to $\operatorname{Re}G(\mathbf{r}, \mathbf{r}, \omega)$, one can find it from the Kramers-Kronig relation (3.32): as the imaginary part of G is exact by definition, also the real part is the exact one. However, it is important to remark that one has used a relation, eq. (3.32), that *does not* hold in the auxiliary system or, equivalently, one has employed *another* functional (see section 3.2.2 for a general discussion).

Of course, one could wonder whether a function that does not fulfill the Lehmann representation could be considered a Green's function. Equivalently, one could be puzzled by having a real and frequency-dependent function (the spectral potential) that replaces the self energy.

These objections are certainly pertinent. The simplest answer is that, in its basics, the auxiliary system is just a mathematical construction that yields the correct value of the reduced quantity of interest, nothing less, nothing (in general) more.

3.6 DMFT and spectralDFT

Also *dynamical mean field theory* (DMFT) [88, 9, 89] in the *spectral density functional theory* formulation [8] can be considered in the framework of auxiliary systems. DMFT is a powerful theory to handle strongly correlated materials, whose focus is on the *local* (on-site) Green's function.

The real system, in this case, is the Hubbard model of eq. (2.49) and the one-particle properties of it are contained in the Green's function (2.50), which is non-local in the site basis. To obtain $G_{ij}(\omega)$, the standard route is to introduce the non-local self energy $\Sigma_{ij}(\omega)$, evaluate it and then solve the Dyson equation.

DMFT is an alternative to this procedure when the interest is just in a smaller quantity. That quantity is the on-site Green's function $G_{ii}(\omega)$, which does not depend on the site i if the lattice is regular: $G_{ii}(\omega) \equiv G_{\text{loc}}(\omega)$. This is a reduced quantity, as it does not contain the information on the off-diagonal elements of the Green's function. DMFT is a method to evaluate $G_{\text{loc}}(\omega)$.

A way to view DMFT is the following [8]: one considers, besides the real system (the Hubbard model), an *auxiliary system* in which the self energy is local, and hence, for a regular lattice, site-independent; we call it $\Sigma_{G_{\text{loc}}}(\omega)$ as it is – in the notations we used above – the G_{loc} -effective potential that one needs to reproduce $G_{\text{loc}}(\omega)$. If this effective self energy were known, the value of $G_{\text{loc}}(\omega)$ would be exactly reproduced in the auxiliary system.

Note that it is tacitly assumed that $G_{\text{loc}}(\omega)$ be $\Sigma_{G_{\text{loc}}}(\omega)$ -representable, namely that, in principle, $G_{\text{loc}}(\omega)$ can be derived from a local – as opposed to a non-local – self energy. This assumption – and consequently DMFT – is exact in two very important limits: the first one is the non interacting limit, in which the self energy of the real system, and hence also of the auxiliary system, is zero. The second one is the limit of infinite dimensions or infinite number of nearest neighbours: it can be shown that in this case the self energy of the real system becomes local, hence the auxiliary system self energy coincides with it [72].

Finding in practice the effective potential, namely the local self energy, is the big challenge of DMFT. The solution is similar to the one proposed in this thesis for the spectral potential, namely building a model system and importing its value from it. We will discuss this method in chapter 5.

Spectral DFT Spectral density functional theory (SDFT) can be considered as a generalization of DMFT to real systems described by the fully *ab-initio* many-body Hamiltonian, eq. (2.3a). The Green's function is therefore given by eq. (2.18) and the self energy by eq. (2.37).

As in DMFT, the interesting quantity is the *local* Green's function, where the meaning of the adjective “local” is broad: indeed, for every point \mathbf{r} , a region $\Omega_{\mathbf{r}}$ around \mathbf{r} is defined such that $\theta_{\Omega_{\mathbf{r}}}(\mathbf{r}') = 0$ or 1 if, respectively, \mathbf{r}' belongs or not to $\Omega_{\mathbf{r}}$. The local Green's function is defined as $G_{\text{loc}}(\mathbf{r}, \mathbf{r}', \omega) := G(\mathbf{r}, \mathbf{r}', \omega)\theta_{\Omega_{\mathbf{r}}}(\mathbf{r}')$. In particular, if $\Omega_{\mathbf{r}}$ is shrunk to the point \mathbf{r} itself, the quantity of interest becomes $G(\mathbf{r}, \mathbf{r}, \omega)$, which can be viewed as the continuous generalization of $G_{ii}(\omega)$, hence the relation to DMFT.

To obtain the quantity of interest $G_{\text{loc}}(\mathbf{r}, \mathbf{r}', \omega)$, an auxiliary system is built, in which the role of the full self energy $\Sigma(\mathbf{r}, \mathbf{r}, \omega)$ is played by a local self energy $\Sigma_{\text{loc}}(\mathbf{r}, \mathbf{r}', \omega)$, which is clearly not

simply $\Sigma(\mathbf{r}, \mathbf{r}, \omega)\theta_{\Omega_{\mathbf{r}}}(\mathbf{r}')$. Again, if we restrict ourselves to $\Omega_{\mathbf{r}} = \{\mathbf{r}\}$, then the effective potential $\Sigma_{\text{loc}}(\mathbf{r}, \mathbf{r}', \omega)$ is truly diagonal in real space, and can be written as $\Sigma^{\text{SDFT}}(\mathbf{r}, \omega)$: a complex, local and frequency-dependent effective potential.

Note that, in the purely local situation $\Omega_{\mathbf{r}} = \{\mathbf{r}\}$, $G(\mathbf{r}, \mathbf{r}, \omega)$ is very close to the quantity we focus on in this thesis, $A(\mathbf{r}, \mathbf{r}, \omega)$. Actually, the two bear the same amount of information, and hence the two descriptions are completely equivalent, whenever the Kramers–Kronig relations hold. If that is the case, one can pass from A to G without any problem.

Does this mean that our approach is actually SDFT? The answer is no, exactly because the Kramers–Kronig relations, as shown above, do not hold. Indeed, to reproduce the local Green's function, which is complex, a local self energy is needed, complex as well. On the contrary, if one wants to reproduce only the spectral function, which is real, a real spectral potential is enough. Clearly, being real, this potential does not fulfill the Kramers–Kronig relations, hence the link from A to G is broken. Therefore, our approach can be viewed as a further restriction of SDFT when only the spectral function is needed.

I have presented the effective framework in which I will move for the rest of the thesis. It consists of an auxiliary system designed for targeting the diagonal of the spectral function of the real system exactly. To do so, a real, local and frequency-dependent potential – the spectral potential – is introduced. It contains the minimal information required for reproducing the diagonal of the spectral function, and it is computationally lighter than the self energy. Exact relations have been given throughout the chapter, but can we actually find this potential in practice? In the next chapter, I will show three exactly solvable models in which the answer to that question is yes.

Auxiliary systems: explicit examples

The chapter of truth is here: for a given self energy, does a corresponding auxiliary system actually exist? Can we really solve the generalized Sham–Schlüter equation for some system? Is it feasible to write down and look at one of these spectral potentials? Do they have any physical meaning?

I will answer these question by explicitly considering some systems for which the analytic solution is at hand. I will show that for the three cases I will study, non trivial and very different among themselves, auxiliary systems exist and the corresponding spectral potentials can be explicitly evaluated. This shows that the set of ν_{SF} -representable spectral functions is not completely empty: it contains, at least, three elements!

I will first consider the *Hubbard model* on the *Bethe lattice* with infinite number of nearest neighbours: the self energy is local and frequency dependent, but *complex-valued*; the non-trivial duty of the auxiliary system will be to enfold the information enclosed in the imaginary part of the self energy into additional frequency dependence of the spectral potential.

A step forward is represented by the Hubbard model on two sites (a *dimer*): the self energy is here not only complex, but also *non-local*; the efforts sustained by the auxiliary system are therefore intensified, as also the information encoded in the non-locality of the self energy must be transferred into the frequency dependence of the spectral potential.

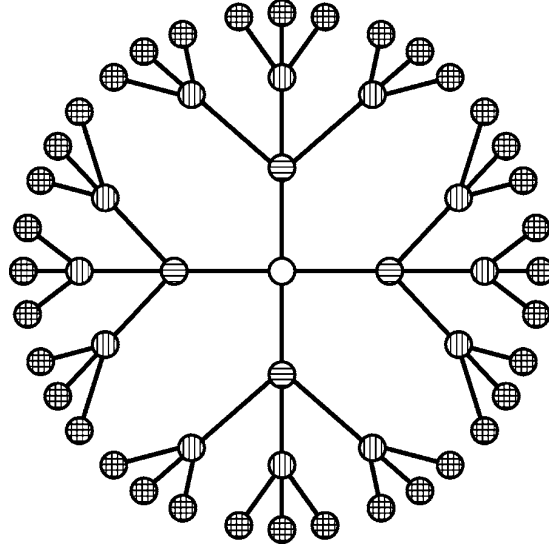
Finally, the third example will be the *homogeneous electron gas* with a purely non-local self energy: in contrast to the previous cases, there is no frequency dependence yet in the self energy, and the generalized Sham–Schlüter equation’s challenge will be to completely erase the non-locality of the standard self energy approach in favour of a newly born frequency dependence in the spectral potential. Moreover, the homogeneous electron gas will allow us to clarify some aspects concerning the relation between discrete (Hubbard) and continuous systems.

4.1 The Hubbard model on the Bethe lattice

A Bethe lattice is an infinite graph with no cycles (a *tree*), in which every site has the same number of neighbours z [90]. Apart from the simplest case $z = 2$, which describes a one-dimensional chain, the Bethe lattice is not a crystal lattice, as there is no translational symmetry; an example with $z = 4$ is represented in fig. 4.1.

Here we will define the Hubbard Hamiltonian on a Bethe lattice as eq. (2.49) with i and j sites of the lattice. We will take the on-site energies $\varepsilon_i = 0$, so that all sites are equivalent and any local function f_i becomes site-independent: $f_i = f$.

We will further consider the infinite connectivity limit $z \rightarrow \infty$, an extremely important limit in which the self energy $\Sigma_{ij}(\omega)$ associated with the Hubbard Hamiltonian becomes *local* (al-

Figure 4.1: Part of the Bethe lattice with $z = 4$, from ref. [92].

though still complex) and site-independent [91, 76]: $\Sigma_{ij}(\omega) \xrightarrow{z \rightarrow \infty} \delta_{ij} \Sigma(\omega)$.

In the $z \rightarrow \infty$ limit, the scaling $t \rightarrow t/\sqrt{z}$ yields a *finite* free density of states, defined¹ as $A_0(\omega) = -\frac{1}{\pi} \text{Im} G_0(\omega)$, with $G_0(\omega) \equiv G_{0ii}(\omega)$ the on-site Green's function at $U = 0$; this can be evaluated by using non-Bloch based methods, as it is done in [93]; the result reads $G_0(\omega) = \frac{2}{\omega + \sqrt{\omega^2 - D^2}}$, from which [91, 76] $A_0(\omega) = \theta(D - |\omega|) \frac{2}{\pi D} \sqrt{1 - \left(\frac{\omega}{D}\right)^2}$. This is a semielliptical density of states, of half-bandwidth $D = 2t$, which closely resembles the gaussian density of states of a hypercubic lattice [94].

We solve the fully interacting model in appendix C, at half-filling ($\mu = 0$), within the *coherent potential approximation* (CPA). The result is summarized by the following two relations:

$$G(\omega) = \frac{1}{2} \left(\frac{1}{\mathcal{G}_0^{-1}(\omega) + \frac{U}{2}} + \frac{1}{\mathcal{G}_0^{-1}(\omega) - \frac{U}{2}} \right) \quad (4.1)$$

$$\mathcal{G}_0^{-1}(\omega) = \omega - \frac{D^2}{4} G(\omega). \quad (4.2)$$

The first of these is equivalent to a Dyson equation $G^{-1}(\omega) = \mathcal{G}_0^{-1}(\omega) - \Sigma(\omega)$ supplied with the definition of the self energy $\Sigma(\omega) = \frac{U^2}{4} \mathcal{G}_0(\omega)$. The second is the self consistent relation of the DMFT loop [72]; it links $G(\omega)$ to $\mathcal{G}_0(\omega)$; this is the impurity Green's function², which can be considered, for our purposes, as an auxiliary function. It permits to write down a closed equation for $G(\omega)$:

$$\left(\frac{D^2}{4}\right)^2 [G(\omega)]^3 - \frac{D^2}{2} \omega [G(\omega)]^2 + \left(\frac{D^2}{4} - \frac{U^2}{4} + \omega^2\right) G(\omega) - \omega = 0 \quad (4.3)$$

This is a third order equation that can be solved by standard methods, see appendix C. From the solution $G(\omega)$, the corresponding spectral function is:

$$A(\omega) = -\frac{1}{\pi} \text{Im} G(\omega) \quad (4.4)$$

which is positive and even, and it is evaluated numerically for different values of U in figure 4.2: for $U = 0$, we recover the free density of states we started from, $A_0(\omega) = \theta(D - |\omega|) \frac{2}{\pi D} \sqrt{1 - \left(\frac{\omega}{D}\right)^2}$:

¹For this section I use the retarded formalism, instead of the time-ordered one, as it is often done in DMFT.

² $\mathcal{G}_0(\omega)$ already contains part of the interaction; specifically, the on-site interaction evaluated in the Anderson Impurity Model.

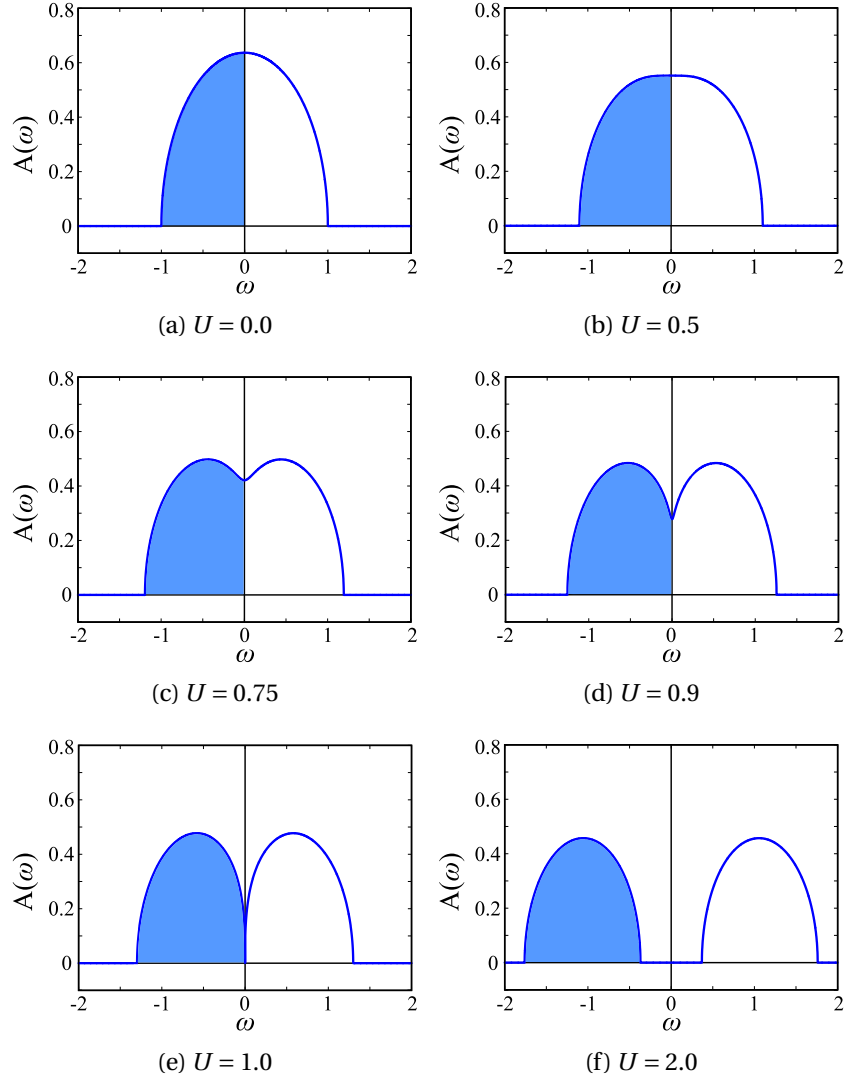


Figure 4.2: Spectral function $A(\omega)$ as a function of ω , in units of D , for different values of U , as indicated. The coloured area represents the occupied band: for $U < D$ we have a metal, then a transition at $U = D$ and finally an insulator for $U > D$.

it represents a single band centered on $\omega = \mu = 0$; that is the *quasi particle* of the system, which is in this stage a metal (no gap between occupied and unoccupied states).

For increasing U , the quasi particle band splits into two symmetric features that get further and further away. Eventually, at $U = D$, the two features separate and, for $U > D$, they form two different Hubbard bands, separated by a gap of the order of U : the system becomes an insulator, and the critical point $U = D$ models the Mott metal–insulator transition.

At the critical point $U = D$, the Green's function at $\omega = 0$ (where the gap opens) is zero, as well as, through eq. (4.2), $\mathcal{G}_0^{-1}(\omega = 0)$. Therefore, from its definition in terms of $\mathcal{G}_0(\omega)$, the self energy blows up:

$$\Sigma(\omega = 0) \xrightarrow{U \rightarrow D} \infty \quad (4.5)$$

both in its real as well as in its imaginary parts. Note that this is the opposite of what happens in Fermi liquid systems, where the self energy at the Fermi level is zero.

The challenge is therefore to reproduce the opening of the gap with a spectral potential that, being real by definition, has always a zero imaginary part.

4.1.1 The auxiliary system

The auxiliary system's job is to provide the exact value of the spectral function, eq. (4.4), with a real and local potential. Therefore, to build the auxiliary system, we replace the complex-valued self energy $\Sigma(\omega)$ with the spectral potential $\nu_{\text{SF}}(\omega)$; both are local in the infinite coordination limit; therefore, we expect the frequency dependence of the potential to account for both the dynamics of the self energy and for the refolding of its real and imaginary part into a single real number.

The definition of the auxiliary system Green's function follows its counterpart in the real system:

$$G_{\text{SF}}^{-1}(\omega) = \mathcal{G}_0^{-1}(\omega) - \nu_{\text{SF}}(\omega) \quad (4.6)$$

with $\mathcal{G}_0^{-1}(\omega)$ given by eq. (4.2). To such a Green's function, it is associated the following spectral function:

$$\begin{aligned} A_{\text{SF}}(\omega) &= -\frac{1}{\pi} \text{Im} G_{\text{SF}}(\omega) = \frac{1}{\pi} \frac{\text{Im} G_{\text{SF}}^{-1}(\omega)}{[\text{Re} G_{\text{SF}}^{-1}(\omega)]^2 + [\text{Im} G_{\text{SF}}^{-1}(\omega)]^2} = \\ &= \frac{\frac{D^2}{4} A(\omega)}{\left[\omega - \nu_{\text{SF}}(\omega) - \frac{D^2}{4} \text{Re} G(\omega)\right]^2 + \left[\frac{\pi D^2}{4} A(\omega)\right]^2} \end{aligned}$$

The spectral potential We now implement the generalized Sham–Schlüter equation in the form $A_{\text{SF}}(\omega) = A(\omega)$; hence, wherever the spectral function is non-zero, the spectral potential is given by:

$$\nu_{\text{SF}}(\omega) = \omega - \frac{D^2}{4} \text{Re} G(\omega) \mp \frac{D}{2} \sqrt{1 - \left(\frac{\pi D}{2} A(\omega)\right)^2} \quad (4.7)$$

To assure that, like the self energy, $\nu_{\text{SF}}(\omega)$ goes to zero as $U \rightarrow 0$, we choose the upper sign for $\omega \geq 0$ and the lower otherwise. As a consequence, $\nu_{\text{SF}}(\omega)$ is not an analytic function of ω .

When the spectral function in the real system $A(\omega)$ is zero, the spectral function in the auxiliary system is automatically zero, too, under the only condition that $\nu_{\text{SF}}(\omega) \neq \omega - \frac{D^2}{4} \text{Re} G(\omega)$; that leaves us a lot of freedom for defining the spectral potential in this region: we choose to remove from $\nu_{\text{SF}}(\omega)$ its $U = 0$ contribution, so that the potential is zero in the non-interacting limit, like the self energy.

We have evaluated numerically eq. (4.7) for different values of U , at $D = 1$; the results are presented in fig. 4.3: the potential – meaningful only where the spectral function is non-zero – interpolates somehow the real and the imaginary part of the self energy. As both the real as well as the imaginary part of the Green's function in the real system are bounded, also the spectral function $\nu_{\text{SF}}(\omega)$ never blows up. This is not the case for the self energy, whose real and imaginary parts diverge at $\omega = 0$ for $U \geq D$ and for $U = D$ respectively.

Note also that, at the critical point $U = D$, the spectral potential is finite, and its value is:

$$\lim_{\omega \rightarrow 0^\pm} \nu_{\text{SF}}(\omega) = \mp \frac{U}{2}.$$

On the other hand its first derivative is singular at $\omega = 0$:

$$\lim_{\omega \rightarrow 0^\pm} \frac{d\nu_{\text{SF}}(\omega)}{d\omega} = \mp \infty.$$

Therefore, as the critical point $U = D$ is the singularity in which $\text{Im}\Sigma(\omega) \rightarrow \infty$ in the real system, in the auxiliary system the same singularity is reproduced and identified by $\frac{d\nu_{\text{SF}}(\omega)}{d\omega} \rightarrow \infty$.

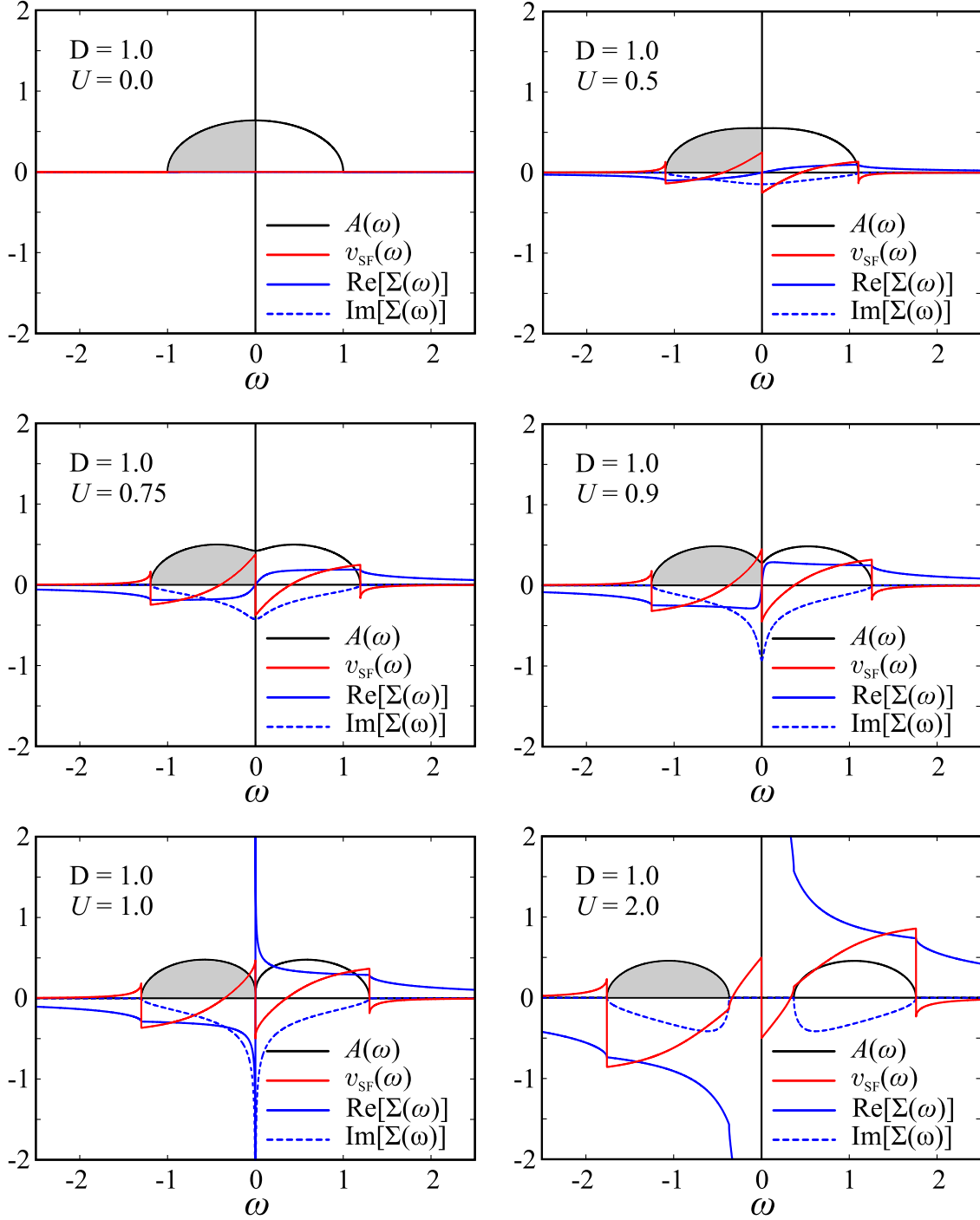


Figure 4.3: Spectral function, in black, for $U = 0.0$, $U = 0.5$, $U = 0.75$, $U = 0.9$, $U = 1.0$ and $U = 2.0$, with $D = 1.0$. In blue the selfenergy, real (full) and imaginary part (dashed line), in red the spectral potential $v_{\text{SF}}(\omega)$ of eq. (4.7). I stress here that the spectral potential is meaningful only where the spectral function is non zero.

The real part of the Green's function As it is often the case with auxiliary systems, the spectral potential yields what it is supposed to yield, but no more. In particular, the real part of the real system Green's function is not reproduced for any value of U larger than $U = 0$, as it is shown in fig. (4.4).

The fact that the real part of the Green's function $\text{Re}G(\omega)$ is not reproduced is not surprising: a *real* spectral potential in general may not yield the full Green's function, or it would be a

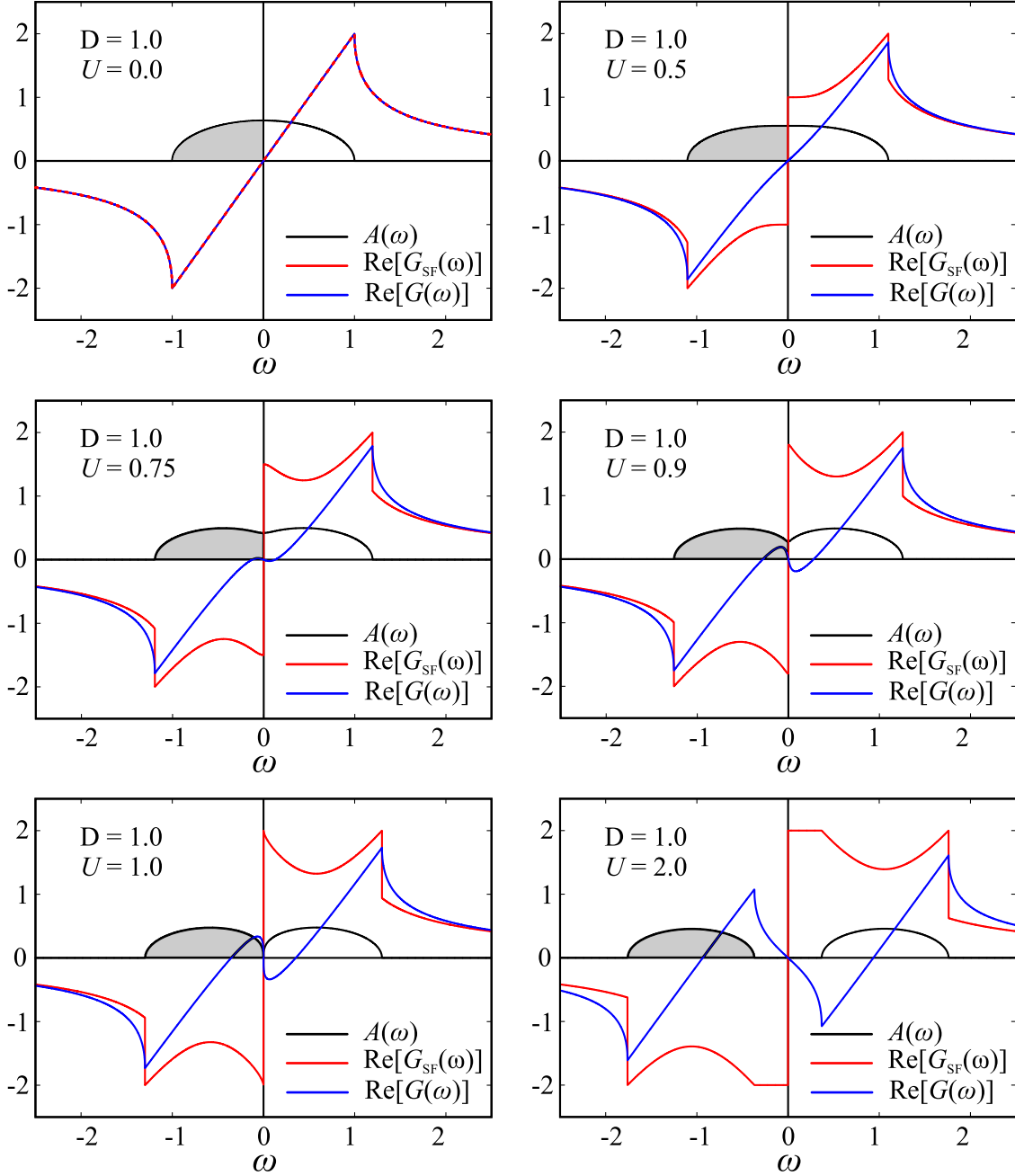


Figure 4.4: Green's functions for different values of U , with $D = 1.0$. In black the spectral function, in blue the real part of the real system Green's function and in red the real part of the auxiliary system Green's function.

complex self energy. On the other hand, since the spectral function is exactly reproduced, one can use *another* prescription – namely another *functional* – to obtain the exact real part of the Green's function, in the auxiliary system. This prescription is clearly the Hilbert transform, eq. (2.29), which does not hold in the auxiliary system but can be implemented as a functional found out of a hat:

$$\hat{\text{HT}}[f](\omega) = \int d\omega' \frac{f(\omega')}{\omega - \omega' + i\eta \text{sign}(\omega')} \quad (4.8)$$

Since in the real system the Kramers–Kronig relations eq. (2.31) hold, $\hat{\text{HT}}[A](\omega) = G(\omega)$ and,

using the fact that $A_{\text{SF}}(\omega) = A(\omega)$, we also have:

$$\hat{\text{HT}}[A_{\text{SF}}](\omega) = \hat{\text{HT}}[A](\omega) = G(\omega) \quad (4.9)$$

Therefore, in the auxiliary system, we can obtain *also* the real part of the real system Green's function by using the functional $[\text{Re}G(\omega)]_{\text{SF}} = \text{Re} \hat{\text{HT}}[A_{\text{SF}}](\omega)$ and, by construction, $[\text{Re}G(\omega)]_{\text{SF}} = G(\omega)$. We stress that this new functional does not yield an auxiliary system Green's function G_{SF} whose real part is equal to $\text{Re}G$. On the contrary, it gives a function, $\text{Re}[\hat{\text{HT}}[A_{\text{SF}}](\omega)]$, which is numerically equal to $\text{Re}G(\omega)$ but, in the auxiliary system, does not have any direct physical meaning (see paragraph 3.2.2 for a general discussion of this topic).

To conclude, we finally obtained what we wanted: the spectral function is *always* reproduced by a real spectral potential. In particular, we reproduce the Mott metal–insulator transition, hallmark of strong correlation identified by the divergence of $\text{Im}\Sigma(\omega)$, by a finite real potential.

Yet, this system cannot display the full power of the spectral potential: as far as the diagonal of the spectral function is concerned, $\nu_{\text{SF}}(\omega)$ is able to absorb not only the imaginary part of the self energy, but also its non–locality. To explicitly show it, a non–local self energy is needed: that is why we now move to the Hubbard dimer.

4.2 The symmetric Hubbard dimer

Let us consider a simplification of the Hubbard model that still exhibits a non–trivial competition between localization and delocalization behaviour. Indeed, if the lattice consists of just *two* sites, both at the same energy ε_0 , the Hamiltonian (2.49) describes what is known as a *symmetric Hubbard dimer*:

$$\hat{H} = -t \sum_{\sigma} \left(\hat{c}_{1\sigma}^{\dagger} \hat{c}_{2\sigma} + \hat{c}_{2\sigma}^{\dagger} \hat{c}_{1\sigma} \right) + \varepsilon_0 \sum_i \hat{n}_i + U \sum_i \hat{n}_{i\uparrow} \hat{n}_{i\downarrow} \quad (4.10)$$

Such a model [95] is not only of academic interest, as some real systems calculations exhibit a dimer behaviour, *e.g.*, the simple hydrogen molecules H_2 or H_2^+ . For our purposes, the interest in this model lays in the fact that it can be solved analytically, resulting in a self energy which is complex, dynamical and *non–local*, too, as I show in the next section.

One–fourth filling solution We here consider the one–fourth filling case, in which there is only $N = 1$ electron. In the site basis, defined and ordered as $\{|\uparrow, 0\rangle, |0, \uparrow\rangle, |\downarrow, 0\rangle, |0, \downarrow\rangle\}$, where $|\sigma, 0\rangle$ represents an electron with spin σ (measured on the z axis, with $S_z(\sigma = \uparrow) = \frac{1}{2}$ and $S_z(\sigma = \downarrow) = -\frac{1}{2}$) in the first site and zero electrons on the second site and so on, the Hamiltonian is block–diagonal in spin–sectors:

$$\hat{H} \longrightarrow H_{(i,\sigma),(j,\sigma')} \equiv \langle i, \sigma | \hat{H} | j, \sigma' \rangle = \begin{pmatrix} \varepsilon_0 & -t & 0 & 0 \\ -t & \varepsilon_0 & 0 & 0 \\ 0 & 0 & \varepsilon_0 & -t \\ 0 & 0 & -t & \varepsilon_0 \end{pmatrix} \quad (4.11)$$

This Hamiltonian has spin–independent eigenvalues $\varepsilon_{\pm} = \varepsilon_0 \pm t$, corresponding to the eigenstates:

$$|\pm, \sigma\rangle = \frac{1}{\sqrt{2}} \left[|\sigma, 0\rangle \mp |0, \sigma\rangle \right] \quad (4.12)$$

ordered as follows: $\{|-, \uparrow\rangle, |+, \uparrow\rangle, |-, \downarrow\rangle, |+, \downarrow\rangle\}$ (henceforth called *bonding–antibonding basis*³). We break the spin–symmetry by considering a ground state consisting of a spin–up electron in the *bonding* state $|GS\rangle \equiv |-, \uparrow\rangle$; therefore, the chemical potential is $\mu = \varepsilon_- = \varepsilon_0 - t$ and the excited state (*antibonding orbital*) is well separated with energy $\varepsilon_+ = \varepsilon_0 + t$.

Non-interacting Green's function In the bonding–antibonding basis, where the operator $\hat{c}_\alpha^\dagger = \sum_{i,\sigma} \langle i, \sigma | \alpha \rangle \hat{c}_i^\dagger$ creates a particle in the state $|\alpha\rangle$ (α runs over the four possible states $\{|\pm, \sigma\rangle\}$ ordered as above), it is simple to express the non-interacting Green's function $G_{\alpha\beta}^0(t, t') := -i \langle GS | \hat{T} \hat{c}_\alpha(t) \hat{c}_\beta^\dagger(t') | GS \rangle \equiv \delta_{\alpha\beta} G_\alpha^0(t - t')$; indeed, $\hat{c}_\alpha(t) \equiv e^{i\hat{H}_0 t} \hat{c}_\alpha e^{-i\hat{H}_0 t} = e^{-i\varepsilon_\alpha t} \hat{c}_\alpha$, with $\varepsilon_\alpha = \varepsilon_0 \pm t$, from which:

$$G_\alpha^0(\omega) = \left\{ \frac{\delta_{\alpha, |-, \uparrow\rangle}}{\omega - \varepsilon_- - i\eta} + \frac{1 - \delta_{\alpha, |-, \uparrow\rangle}}{\omega - \varepsilon_+ + i\eta} \right\} \rightarrow \begin{pmatrix} \frac{1}{\omega - \varepsilon_- - i\eta} & 0 & 0 & 0 \\ 0 & \frac{1}{\omega - \varepsilon_+ + i\eta} & 0 & 0 \\ 0 & 0 & \frac{1}{\omega - \varepsilon_- + i\eta} & 0 \\ 0 & 0 & 0 & \frac{1}{\omega - \varepsilon_+ + i\eta} \end{pmatrix}$$

Back to the site basis via the relation $G_{ij,\sigma}^0(\omega) = \sum_\alpha \langle i, \sigma | \alpha \rangle G_\alpha^0(\omega) \langle \alpha | j, \sigma \rangle$, the non-interacting Green's function is:

$$G_{ij,\sigma}^0(\omega) = \frac{1}{2} \left\{ \frac{1}{\omega - \varepsilon_- - i\eta \text{sign}\sigma} + \frac{(-1)^{i-j}}{\omega - \varepsilon_+ + i\eta} \right\} \quad (4.13)$$

with sign $\sigma = + (-)$ for $\sigma = \uparrow (\downarrow)$. Its interpretation goes as follows: we can remove $(-i\eta)$ a spin-up electron ($\sigma = \uparrow$) from the ground state ε_- or add it $(+i\eta)$ to the excited state ε_+ ; besides, we can add $(+i\eta)$ a spin-down electron ($\sigma = \downarrow$) to both the ground and the excited state. The prefactor $\frac{1}{2}$ assures the normalization of the associated spectral function.

The Green's function The full Green's function $G_{ij,\sigma}(t, t') := -i \langle GS | \hat{T} \hat{c}_{i\sigma}(t) \hat{c}_{j\sigma}^\dagger(t') | GS \rangle$ can be derived from the exact diagonalization of the $N = 0$ (trivial), $N = 1$, eq. (4.12), and $N = 2$ electron Hamiltonians, shown in appendix D, eq. (D.1), via the Lehmann representation (2.22); the task is simplified in the bonding–antibonding basis, where the Green's function $G_{\alpha\beta}(t, t') := -i \langle GS | \hat{T} \hat{c}_\alpha(t) \hat{c}_\beta^\dagger(t') | GS \rangle \equiv \delta_{\alpha\beta} G_\alpha(t - t')$ is diagonal because the two sites $i = 1$ and $i = 2$ have the same on-site energy ε_0 .

The result for the spin–up case is trivial:

$$G_{-, \uparrow}(\omega) = \frac{1}{\omega - \varepsilon_- - i\eta} \quad G_{+, \uparrow}(\omega) = \frac{1}{\omega - \varepsilon_+ + i\eta} \quad (4.14)$$

These expressions state that a spin–up electron in the state $|-, \uparrow\rangle$ can only be removed from the system $(-i\eta)$ while it can be added $(+i\eta)$ if it goes to the antibonding orbital (ε_+). No other possibility is allowed by the Pauli principle. In the site basis the spin–up Green's function reads:

$$G_{ij, \uparrow}(\omega) = \frac{1}{2} \left\{ \frac{1}{\omega - \varepsilon_- - i\eta} + \frac{(-1)^{i-j}}{\omega - \varepsilon_+ + i\eta} \right\} \quad (4.15)$$

which coincides with its non-interacting $U \rightarrow 0$ limit, eq. (4.13); indeed, having already a spin–up electron in the bonding orbital, an additional $(+i\eta)$ spin–up electron can only sit on the antibonding orbital, where it doesn't interact with the former.

³The transformation from the site basis $\{|i, \sigma\rangle\} \equiv \{|1, 0\rangle, |0, \uparrow\rangle, |1, 0\rangle, |0, \downarrow\rangle\}$ to the bonding–antibonding basis $\{|\alpha\rangle\} = \{|\pm, \sigma\rangle\} \equiv \{|-, \uparrow\rangle, |+, \uparrow\rangle, |-, \downarrow\rangle, |+, \downarrow\rangle\}$ is $f_{\alpha\beta} = \sum_{i,j,\sigma,\sigma'} \langle \alpha | i, \sigma \rangle f_{i\sigma, j\sigma'} \langle j, \sigma' | \beta \rangle$, with the change of basis matrix

$$\langle \alpha | i, \sigma \rangle \text{ given by } \frac{1}{\sqrt{2}} \begin{pmatrix} 1 & 1 & 0 & 0 \\ 1 & -1 & 0 & 0 \\ 0 & 0 & 1 & 1 \\ 0 & 0 & 1 & -1 \end{pmatrix}.$$

	<i>peak position</i>	<i>peak amplitude</i>
1st pole	$\omega_1 = \varepsilon_0 + t + \frac{1}{2}(U - c)$	$Z_1 = \frac{1}{2} + \frac{2t}{c}$
2nd pole	$\omega_2 = \varepsilon_0 + t$	$Z_2 = \frac{1}{2}$
3rd pole	$\omega_3 = \varepsilon_0 + t + U$	$Z_3 = \frac{1}{2}$
4th pole	$\omega_4 = \varepsilon_0 + t + \frac{1}{2}(U + c)$	$Z_4 = \frac{1}{2} - \frac{2t}{c}$

Table 4.1: Peaks positions ω_s and amplitudes Z_s .

The spin-down Green's function is far more interesting: it doesn't show any removal energy, as no spin-down electron is present in the system, but there are many addition *channels* describing the different processes an incoming spin-down electron can undergo:

$$\begin{aligned}
 G_{-, \downarrow}(\omega) &= \left(\frac{1}{2} + \frac{2t}{c}\right) \frac{1}{\omega - \omega_1 + i\eta} + \left(\frac{1}{2} - \frac{2t}{c}\right) \frac{1}{\omega - \omega_4 + i\eta} = \sum_{s=1,4} \frac{Z_s}{\omega - \omega_s + i\eta} \\
 G_{+, \downarrow}(\omega) &= \frac{1}{2} \left\{ \frac{1}{\omega - \omega_2 + i\eta} + \frac{1}{\omega - \omega_3 + i\eta} \right\} = \sum_{s=2,3} \frac{Z_s}{\omega - \omega_s + i\eta}
 \end{aligned} \tag{4.16}$$

or, in the site basis:

$$\begin{aligned}
 G_{ij, \downarrow}(\omega) &= \left(\frac{1}{4} + \frac{t}{c}\right) \frac{1}{\omega - \omega_1 + i\eta} + \frac{(-1)^{i-j}}{4} \left\{ \frac{1}{\omega - \omega_2 + i\eta} + \frac{1}{\omega - \omega_3 + i\eta} \right\} + \left(\frac{1}{4} - \frac{t}{c}\right) \frac{1}{\omega - \omega_4 + i\eta} = \\
 &= \frac{(-1)^{i-j}}{2} \sum_{s=1}^4 \frac{Z_s}{\omega - \omega_s + i\eta}
 \end{aligned} \tag{4.17}$$

with the poles ω_s and the amplitudes Z_s defined in table 4.1.

The peaks ω_s are excitation energies relative to the addition of a spin-down electron: $\omega_s = \varepsilon_s^{(N=2)} - \varepsilon_-^{(N=1)}$, with $\varepsilon_s^{(N=2)}$ the eigenenergies of the $N = 2$ system (appendix D), and $\varepsilon_-^{(N=1)} = \varepsilon_0 - t$ the ground state energy of the $N = 1$ system. In particular, the first and the fourth poles are associated to an additional spin-down electron in the bonding state, and the second and the third to an antibonding state, in agreement with eq. (4.16).

We can characterize these peaks in a one-particle picture, by referring to the eigenstates $\varepsilon_s^{(N=2)} = \omega_s + \varepsilon_-$ displayed in appendix D, depending on the site and on the orbital the additional spin-down electron goes:

- The pole ω_1 represents the addition of a spin-down electron to the already-occupied bonding orbital ($E = 2(\varepsilon_0 - t)$): then, since they are on the same orbital, electrons interact with an effective interaction⁴ $\tilde{U}_{--} = 2t + \frac{1}{2}(U - c)$. Hence $\varepsilon_{s=1}^{(N=2)} = 2(\varepsilon_0 - t) + \tilde{U}_{--} = 2\varepsilon_0 + \frac{1}{2}(U - c)$ and $\omega_1 = \varepsilon_0 + t + \frac{1}{2}(U - c)$.
- The pole ω_2 describes two electrons sitting on two different sites and occupying two different orbitals (therefore, no interaction), namely a bonding ($\varepsilon = \varepsilon_0 - t$) and an antibonding ($\varepsilon = \varepsilon_0 + t$) orbital, giving a total energy $\varepsilon_{s=2}^{(N=2)} = (\varepsilon_0 - t) + (\varepsilon_0 + t) = 2\varepsilon_0$, and $\omega_2 = \varepsilon_0 + t$.
- The pole ω_3 is associated with two electrons occupying the same site (bare interaction: U) but in two different orbitals; the total energy is therefore $\varepsilon_{s=3}^{(N=2)} = (\varepsilon_0 - t) + (\varepsilon_0 + t) + U = 2\varepsilon_0 + U$, and the position of the pole is $\omega_3 = \varepsilon_0 + t + U$.

⁴ U is the interaction term for two electrons on the same site, \tilde{U} is the interaction for two electrons on the same orbital: sites and orbitals are just two different *basis*, and if the electrons aren't interacting in a basis, they are not even in the other basis: for this reason, \tilde{U} always goes to zero in the limit of zero bare interaction, and this is actually the way in which the electrons are assigned to the bonding or to the antibonding orbitals in the picture given above.

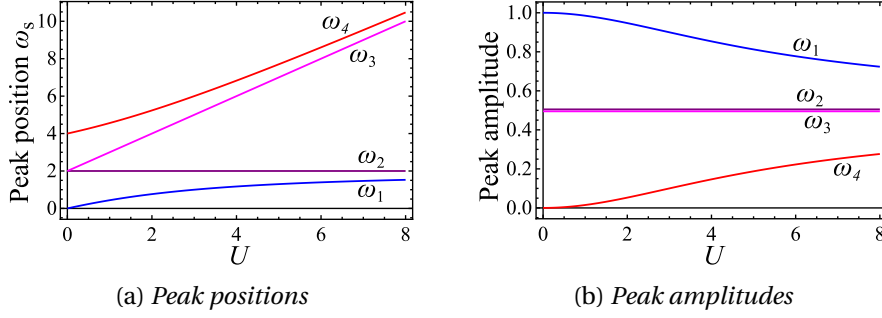


Figure 4.5: Peak positions and amplitudes of the spectral function (4.21) as a function of U , in units of t ; in the left panel, the chemical potential $\mu = \varepsilon_0 - t$ is set to zero. See also table 4.1.

- Finally, the pole ω_4 represents two electrons occupying the same antibonding orbital ($E = 2(\varepsilon_0 + t)$) with an effective interaction $\tilde{U}_{++} = -2t + \frac{1}{2}(U + c)$: a spin-down electron enters the system in the bonding orbital, where a spin-up electron was already sitting; the former excites ($+4t$) the latter, and both end up in an excited state, the antibonding state, where they interact via \tilde{U}_{++} . This process results in a total energy of the two-electron state equals to $\varepsilon_{s=4}^{(N=2)} = 2(\varepsilon_0 - t) + 4t + \tilde{U}_{++} = 2\varepsilon_0 + \frac{1}{2}(U + c)$; the pole is $\omega_4 = \varepsilon_0 + t + \frac{1}{2}(U + c)$.

The effective interaction we just introduced is summarized as follows:

$$\tilde{U}_{\alpha\beta} = \begin{cases} 0 & \text{if } \langle \hat{n}_{i,\uparrow} \hat{n}_{i,\downarrow} \rangle = 0 \\ \begin{pmatrix} \tilde{U}_{--} & \tilde{U}_{-+} \\ \tilde{U}_{+-} & \tilde{U}_{++} \end{pmatrix} = \begin{pmatrix} 2t + \frac{U-c}{2} & U \\ U & -2t + \frac{U+c}{2} \end{pmatrix} & \text{if } \langle \hat{n}_{i,\uparrow} \hat{n}_{i,\downarrow} \rangle \neq 0 \end{cases} \quad (4.18)$$

where the first line corresponds to electrons occupying certainly different sites, while the second line is for electrons with a non-zero probability of laying on the same site.

In the non-interacting limit $U \rightarrow 0$, where both eq. (4.15) and (4.17) tend to eq. (4.13), ω_2 and ω_3 merge to the antibonding pole $\varepsilon_0 + t$, while ω_1 accounts for the bonding state. The fourth pole goes to $\varepsilon_0 + 3t$: two electrons excited ($+4t$) from the bonding $2(\varepsilon_0 - t)$ to the antibonding $2(\varepsilon_0 + t)$ orbital, which now do not interact. This process, not present in the non-interacting Green's function, is indeed suppressed by the amplitude of the associated peak, $Z_4 = \frac{1}{2} - \frac{2t}{c}$, which goes to zero like $(\frac{U}{8t})^2$ as $U \rightarrow 0$, as expected. The positions and the amplitudes of these poles as a function of U is shown in fig. 4.5.

The spectral function Since the Lehmann amplitudes are real, the definition (2.30) for the spectral function applies in the form $A_{ij,\sigma}(\omega) = -\frac{1}{\pi} \text{sign}(\omega - \mu) \text{Im} G_{ij,\sigma}(\omega)$; from equations (4.15) and (4.17) we get:

$$\begin{aligned} A_{ij,\uparrow}(\omega) &= \frac{1}{2} \delta(\omega - \varepsilon_-) + \frac{(-1)^{i-j}}{2} \delta(\omega - \varepsilon_+) \\ A_{ij,\downarrow}(\omega) &= \left(\frac{1}{4} + \frac{t}{c} \right) \delta(\omega - \omega_1) + \frac{(-1)^{i-j}}{4} \left[\delta(\omega - \omega_2) + \delta(\omega - \omega_3) \right] + \left(\frac{1}{4} - \frac{t}{c} \right) \delta(\omega - \omega_4) \end{aligned} \quad (4.19)$$

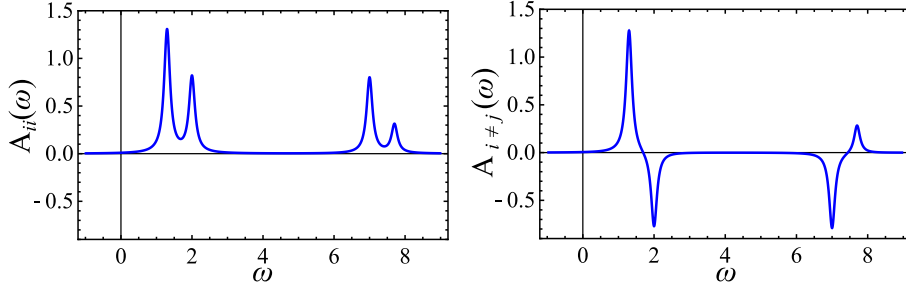


Figure 4.6: *Diagonal (left) and off-diagonal (right) elements of the spectral function, $A_{ii,\downarrow}(\omega)$ and $A_{i\neq j,\downarrow}(\omega)$, as a function of ω for $\mu = 0$, in units of t , for $U = 5$. A broadening $\eta = 0.1$ is added for clarity reasons.*

or, in the bonding–antibonding basis:

$$\begin{aligned}
 A_{-,\uparrow}(\omega) &= \delta(\omega - \varepsilon_-) \\
 A_{+,\uparrow}(\omega) &= \delta(\omega - \varepsilon_+) \\
 A_{-,\downarrow}(\omega) &= \left(\frac{1}{2} + \frac{2t}{c}\right)\delta(\omega - \omega_1) + \left(\frac{1}{2} - \frac{2t}{c}\right)\delta(\omega - \omega_4) \\
 A_{+,\downarrow}(\omega) &= \frac{1}{2} \left[\delta(\omega - \omega_2) + \delta(\omega - \omega_3) \right]
 \end{aligned} \tag{4.20}$$

Since both sites are equal, the Green’s function is symmetric under exchange of the site indices; in particular, the diagonal elements of the spectral function are the same and equal to:

$$A_{ii,\downarrow}(\omega) = \left(\frac{1}{4} + \frac{1}{c}\right)\delta(\omega - \omega_1) + \frac{1}{4} \left[\delta(\omega - \omega_2) + \delta(\omega - \omega_3) \right] + \left(\frac{1}{4} - \frac{1}{c}\right)\delta(\omega - \omega_4) \tag{4.21}$$

Note that, while the previous quantity is non–negative, this is not the case for the off–diagonal elements of the spectral function, in accordance with the Lehmann decomposition (2.22), see fig. 4.6:

$$A_{i\neq j,\downarrow}(\omega) = \left(\frac{1}{4} + \frac{1}{c}\right)\delta(\omega - \omega_1) - \frac{1}{4} \left[\delta(\omega - \omega_2) + \delta(\omega - \omega_3) \right] + \left(\frac{1}{4} - \frac{1}{c}\right)\delta(\omega - \omega_4) \tag{4.22}$$

The behaviour of the spectral function for different values of U is presented in fig. 4.7: for small U , there is a prominent peak at ω_1 and two smaller peaks at ω_2 and ω_3 , while the peak at ω_4 is negligible. Increasing U , the peak in ω_1 loses weight as the one in ω_4 rises up; eventually, merging with the two peaks in ω_2 and ω_3 , they tend to a strong correlation regime $U \gg t$ in which two Hubbard bands emerge, separated by a distance of the order of U .

The self energy The spin–down self energy (the spin–up one is zero, as an additional spin–up electron cannot interact) can be obtained from the inverted Dyson equation $\Sigma_\alpha(\omega) = G_{0\alpha}^{-1}(\omega) - G_\alpha^{-1}(\omega)$, with $G_{0\alpha}^{-1}(\omega) = \omega - \varepsilon_\alpha$ and $G_\alpha^{-1}(\omega) = 1/G_\alpha(\omega)$. It reads:

$$\begin{aligned}
 \Sigma_{-,\downarrow}(\omega) &= \frac{U}{2} + \frac{\frac{U^2}{4}}{\omega - (\varepsilon_0 + 3t + \frac{U}{2}) + i\eta} \\
 \Sigma_{+,\downarrow}(\omega) &= \frac{U}{2} + \frac{\frac{U^2}{4}}{\omega - (\varepsilon_0 + t + \frac{U}{2}) + i\eta}
 \end{aligned} \tag{4.23}$$

or, in the site basis:

$$\Sigma_{ij,\downarrow}(\omega) = \frac{U}{2}\delta_{ij} + \frac{U^2}{8} \left[\frac{(-1)^{i-j}}{\omega - (\varepsilon_0 + t + \frac{U}{2}) + i\eta} + \frac{1}{\omega - (\varepsilon_0 + 3t + \frac{U}{2}) + i\eta} \right] \tag{4.24}$$

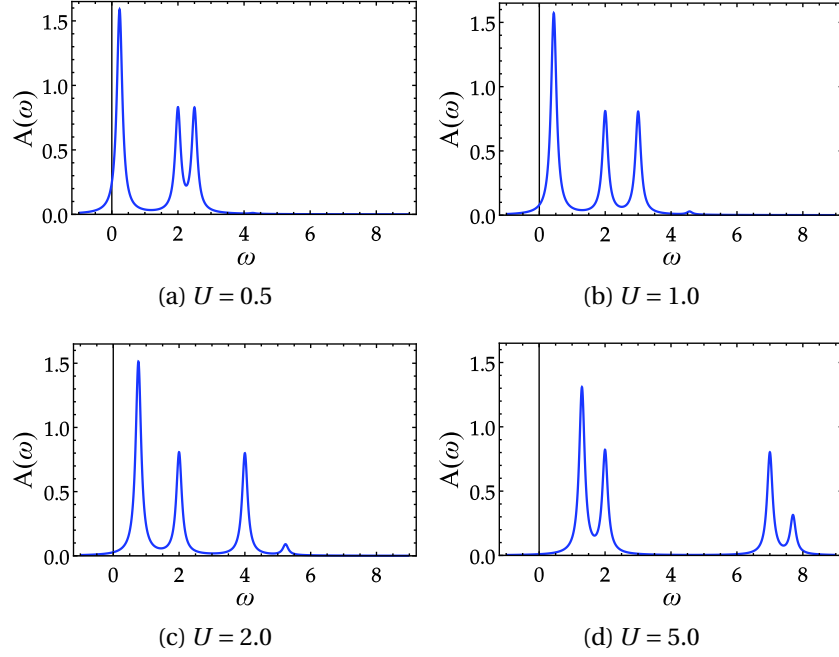


Figure 4.7: *Diagonal of the spectral function $A_{i,i,1}(\omega)$ as a function of ω for $\mu = 0$, in units of t , for different values of U , as indicated. A broadening $\eta = 0.1$ is added for clarity reasons.*

which, as expected, goes to zero in the limit of $U \rightarrow 0$ almost everywhere, namely apart from $\Sigma_{-,1}(\omega_4) \xrightarrow{U \rightarrow 0} 4t$, which is the energy needed to excite the system to the pole ω_4 , a process which is suppressed for $U = 0$ but is nonetheless present for small interaction U^5 . Note that this is a truly *non-local* self energy in the site basis, with an imaginary part given by the sum of two delta peaks:

$$\text{Im} \Sigma_{i,j,1}(\omega) = -\frac{\pi U^2}{8} \left\{ (-1)^{i-j} \delta\left(\omega - \left(\varepsilon_0 + t + \frac{U}{2}\right)\right) + \delta\left(\omega - \left(\varepsilon_0 + 3t + \frac{U}{2}\right)\right) \right\} \quad (4.25)$$

The poles ω_s can be arranged as quasiparticles and satellites of the system, determined by the real part of the self energy. Indeed, from the relation $\omega - \varepsilon_\alpha - \text{Re} \Sigma_\alpha(\omega) = 0$ one obtains ω_1 and ω_4 when considering the bonding state, and ω_2 and ω_3 when considering the antibonding. The renormalization factors $Z_s^{-1} := 1 - \partial \text{Re} \Sigma_{\alpha(s)}(\omega) / \partial \omega|_{\omega_s}$ are nothing but the amplitudes of the Green's function in eq. (4.16) which, being diagonal, has positive amplitudes. They are:

$$Z_1 := 1 - \left. \frac{\partial \text{Re} \Sigma_\alpha(\omega)}{\partial \omega} \right|_{\omega_1} = \frac{1}{2} + \frac{2t}{c} \quad Z_2 = Z_3 = \frac{1}{2} \quad Z_4 = \frac{1}{2} - \frac{2t}{c} \quad (4.26)$$

From the fact that, in the non-interacting limit, all the weight of the bonding peaks is in ω_1 and nothing in ω_4 , the pole ω_1 can be considered as the quasiparticle, while the one at ω_4 its satellite: if the quasiparticle dominates at small interaction, for large U (strong correlation) both ω_1 and ω_4 have the same weight $\frac{1}{2}$.

In the next section, we will reproduce the diagonal of the spectral function by replacing the non-local and complex-valued self energy (4.24) with a *real* and *local* (in the site basis) potential.

⁵Taking the limit is a continuous operation from positive values of U to $U = 0$; since the process described by the pole ω_4 is actually suppressed for $U = 0$, one could decide to redefine “by hand” $\Sigma_{-,1}(\omega_4)|_{U=0} := 0$ and nothing would change. As a result, also $\nu_{\text{SF}}(\omega_4)$ – see below – would be redefined at $U = 0$ as $\nu_{\text{SF}}(\omega_4)|_{U=0} := 0$.

4.2.1 The auxiliary system

The auxiliary system is requested to provide the same local spectral function as the real system one, eq. (4.19). Since the spin-symmetry is broken by the choice of a spin-up ground state, we will furthermore consider a spin-dependent spectral potential; for reproducing the spin-up spectral function, a zero spectral potential will trivially do the job, as $\Sigma_{ij,\uparrow}(\omega) = 0$, too.

We will henceforth focus on the spin-down sector, dropping the \downarrow notation. The auxiliary system is defined by the following inverted Dyson equation:

$$G_{\text{SF}ij}^{-1}(\omega) = G_{0ij}^{-1}(\omega) - \nu_{\text{SF}i}(\omega)\delta_{ij} \quad (4.27)$$

having introduced the *local* spectral potential $\nu_{\text{SF}i}(\omega)$; since the two sites are equivalent, the potential takes the same value $\nu_{\text{SF}}(\omega)$ on both sites, and the previous equation can be written as $G_{\text{SF}ij}^{-1}(\omega) = G_{0ij}^{-1}(\omega - \nu_{\text{SF}}(\omega))$ or, using eq. (4.13), in the following form:

$$G_{\text{SF}ij}(\omega) = \frac{\frac{1}{2}}{\omega - (\varepsilon_0 - t + \nu_{\text{SF}}(\omega)) + i\eta} + \frac{(-1)^{(i-j)\frac{1}{2}}}{\omega - (\varepsilon_0 + t + \nu_{\text{SF}}(\omega)) + i\eta} \quad (4.28)$$

Instead of working in the site basis, we can move to the bonding-antibonding basis $\{\pm\} \equiv \{|-, \downarrow\rangle, |+, \downarrow\rangle\}$ where, by virtue of the symmetry of the problem, everything is diagonal. Moreover, in the bonding-antibonding basis the value of the potential is the same⁶, as $\nu_{\text{SF}}(\omega)$ can be considered as a frequency-dependent energy shift, no matter the basis. Therefore, the bonding-antibonding character is settled by the non-interacting Green's function $G_{0\pm}^{-1}(\omega) = \omega - \varepsilon_{\pm}$ only, and the inverted Green's function in the bonding-antibonding basis simply reads:

$$G_{\text{SF}\pm}^{-1}(\omega) = \omega - \varepsilon_{\pm} - \nu_{\text{SF}}(\omega) \quad (4.29)$$

By definition the Green's function in the site basis, eq. (4.28), must have the same local spectral function as its real system counterpart, eq. (4.17):

$$-\frac{1}{\pi} \text{Im} G_{\text{SF}ii}(\omega) \equiv A_{\text{SF}ii}(\omega) \stackrel{!}{=} A_{ii}(\omega) \quad (4.30)$$

Since we are in a discrete system, this equation means that both the positions and the amplitudes of the peaks must be reproduced by the auxiliary system.

Position of the peaks Since their position does not depend on the basis (see eq. (2.22)), and we are in a discrete system, the poles of $G_{\text{SF}\pm}(\omega)$ and $G_{\pm}(\omega)$ must be the same, namely:

$$\omega - \varepsilon_{\pm} - \nu_{\text{SF}}(\omega)|_{\omega=\omega_s} = 0 \quad (4.31)$$

with ω_s the four poles of table 4.1, no more, no less. For small interaction $U/t \ll 1$, the effect of the potential will be to *slightly* move the poles from their $U = 0$ position, see fig. 4.5; we assume that, since its effects are small, the spectral potential be small, too, in this regime, like the self energy. It is therefore natural to assume that the *nature* of the poles be unchanged, namely that (anti)bonding poles of the real system be reproduced by (anti)bonding poles of the auxiliary system (to exchange their nature, a finite energy of the order of t should be needed at vanishing

⁶Indeed, considering a local potential ν_i , we have:

$$\begin{pmatrix} \nu_{--} & \nu_{-+} \\ \nu_{+-} & \nu_{++} \end{pmatrix} = \frac{1}{2} \begin{pmatrix} 1 & 1 \\ 1 & -1 \end{pmatrix} \begin{pmatrix} \nu_1 & 0 \\ 0 & \nu_2 \end{pmatrix} \begin{pmatrix} 1 & 1 \\ 1 & -1 \end{pmatrix} = \frac{1}{2} \begin{pmatrix} \nu_1 + \nu_2 & \nu_1 - \nu_2 \\ \nu_1 - \nu_2 & \nu_1 + \nu_2 \end{pmatrix} = \begin{pmatrix} \nu & 0 \\ 0 & \nu \end{pmatrix}$$

where in the last equality we implemented the site-symmetry property $\nu_1 = \nu_2 := \nu$; therefore, the mixed terms are zero and both the bonding ν_{--} and antibonding ν_{++} potentials are equal to ν , too.

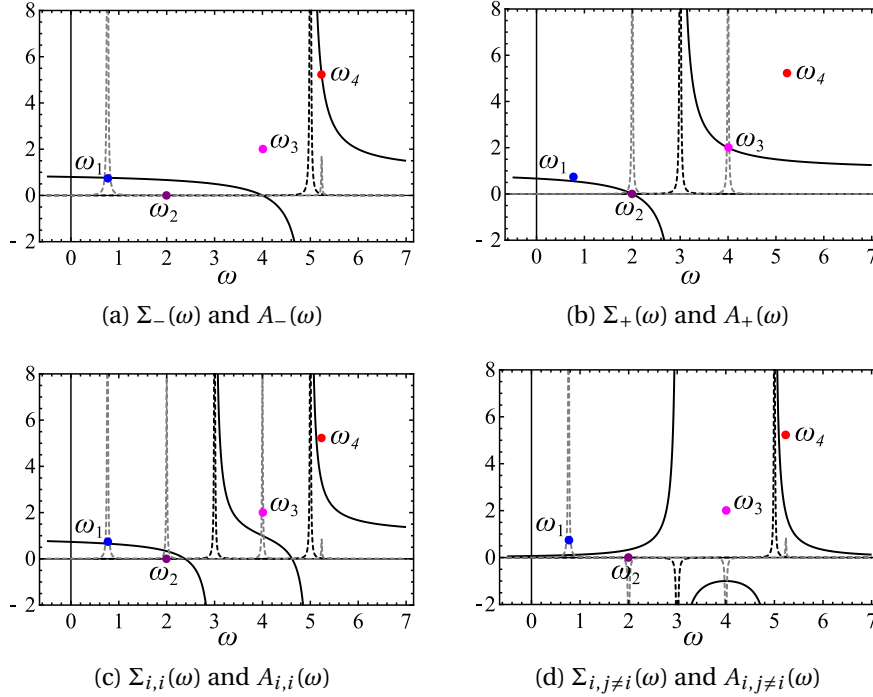


Figure 4.8: *Selfenergy, in black, real (thick) and imaginary part (dashed line) and spectral function (gray dashed line) in different basis, as a function of ω , aligned with $\mu = 0$ for $U = 2$, with $\eta = 0.01$, in units of t ; the coloured dots represent the values of the spectral potential at the poles: it is clear that, while $v_{\text{SF}}(\omega_s) = \Sigma_{\pm}(\omega_s)$ depending if ω_s is a bonding or an antibonding pole, the same is no more true in the site basis, where $v_{\text{SF}}(\omega_s) \neq \Sigma_{ii}(\omega_s)$.*

U). This assumption can be also written as $\omega_s^{\text{SF}} = \omega_s$, and it means that the “band structure”, namely the dependence of the energy ω_s on the state s , is automatically reproduced. Therefore, the previous relation could be split into the following two:

$$\begin{aligned} \omega - \varepsilon_- - v_{\text{SF}}(\omega)|_{\omega=\omega_1, \omega_4} &= 0 \\ \omega - \varepsilon_+ - v_{\text{SF}}(\omega)|_{\omega=\omega_2, \omega_3} &= 0 \end{aligned} \quad (4.32)$$

from which the value of $v_{\text{SF}}(\omega)$ at the poles is:

$$\begin{aligned} v_{\text{SF}}(\omega_1) &= 2t + \frac{U-c}{2} \\ v_{\text{SF}}(\omega_2) &= 0 \\ v_{\text{SF}}(\omega_3) &= U \\ v_{\text{SF}}(\omega_4) &= 2t + \frac{U+c}{2} \end{aligned} \quad (4.33)$$

which are shown in fig. 4.9a. Note that two equations analogous to eq. (4.32) hold in the real system with $\Sigma_{\pm}(\omega)$ in place of $v_{\text{SF}}(\omega)$:

$$\begin{aligned} \omega - \varepsilon_- - \Sigma_-(\omega)|_{\omega=\omega_1, \omega_4} &= 0 \\ \omega - \varepsilon_+ - \Sigma_+(\omega)|_{\omega=\omega_2, \omega_3} &= 0 \end{aligned} \quad (4.34)$$

Indeed, for a discrete system (not in the thermodynamic limit), the self energy is real at the poles [63], see eq. (4.25), and in particular the spectral potential is nothing but the self energy

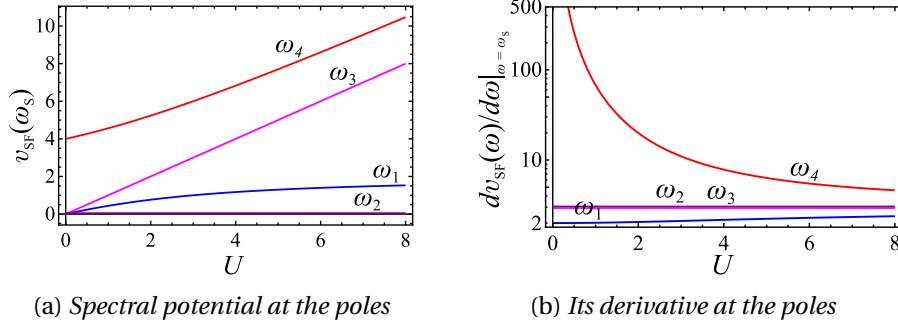


Figure 4.9: Value of the spectral potential $v_{\text{SF}}(\omega)$ and its first derivative (in logarithmic scale) $dv_{\text{SF}}(\omega)/d\omega$ at the poles ω_s .

at the poles:

$$v_{\text{SF}}(\omega_s) = \begin{cases} \Sigma_-(\omega_s) & \text{if } \omega_s = \omega_1, \omega_4 \\ \Sigma_+(\omega_s) & \text{if } \omega_s = \omega_2, \omega_3 \end{cases} \quad (4.35)$$

as can be explicitly checked and as shown in fig. 4.8. On the contrary, $v_{\text{SF}}(\omega) \neq \text{Re}\Sigma_{ii}(\omega)$, as one could naively guess, because in the site basis the self energy is non local.

From these relations or directly from eq. (4.33), the spectral potential can be interpreted as the additional energy which the auxiliary system needs to mimic the behaviour of the real one. In particular, $v_{\text{SF}}(\omega_s)$ is related to the effective interactions we introduced in eq (4.18):

$$\begin{aligned} v_{\text{SF}}(\omega_1) &= \tilde{U}_{--} \langle \hat{n}_{i,1} \hat{n}_{i,1} \rangle \neq 0 \\ v_{\text{SF}}(\omega_2) &= \tilde{U}_{\alpha\beta} \langle \hat{n}_{i,1} \hat{n}_{i,1} \rangle = 0 \\ v_{\text{SF}}(\omega_3) &= \tilde{U}_{+-} \langle \hat{n}_{i,1} \hat{n}_{i,1} \rangle \neq 0 \\ v_{\text{SF}}(\omega_4) &= 4t + \tilde{U}_{++} \langle \hat{n}_{i,1} \hat{n}_{i,1} \rangle \neq 0 \end{aligned} \quad (4.36)$$

Only $v_{\text{SF}}(\omega_4)$ differs from the corresponding effective interaction \tilde{U}_{++} by $4t$: indeed, $4t$ is the energy that must be provided to both electrons to go from the bonding to the antibonding state, where they are then free to interact with an energy \tilde{U}_{++} ; the spectral potential, like the self energy, provides the system with both the activation energy $4t$ and the interaction \tilde{U}_{++} , so that $v_{\text{SF}}(\omega_4) = \Sigma_-(\omega_4) = 4t + \tilde{U}_{++}$.

Amplitude of the peaks Eq. (4.35) holds whenever the system is discrete and the self energy is diagonal. It could remind of the general observation that, whenever the self energy is local and real (and it is, in the bonding–antibonding basis at the poles), the spectral potential *is* the self energy. However, to write such a sentence, we still should prove that $v_{\text{SF}}(\omega)$ reproduces *also* the spectral function, peak positions and *amplitudes*, in the bonding–antibonding basis.

Indeed, not only $G_{\text{SF}}(\omega)$ must have four poles in the four positions ω_s , but also the positive ($A_{\text{SF}ii}(\omega)$ is a *diagonal* spectral function, hence its peak amplitudes are non–negative) amplitudes of the corresponding peaks must match the real system ones (4.21); for the symmetric dimer, the Lehmann weights $|f_s(i)f_s^*(j)| = 2Z_s$ are independent of i and j , see eq. (4.19), and also, modulus $\frac{1}{2}$, even independent of the particular basis, compare eq. (4.19) and (4.20). Therefore, we can simply match, in the bonding–antibonding basis, the positive weights $|f_s(\pm)f_s^*(\pm)| = Z_s$ of eq. (4.26) with the corresponding ones of the auxiliary system, defined by $\left|1 - \frac{\partial v_{\text{SF}}(\omega)}{\partial \omega}\right|_{\omega=\omega_s} = 1/Z_s^{\text{SF}}$; thus, besides a condition on $v_{\text{SF}}(\omega_s)$, we obtain four constraints on

the derivatives of $\nu_{\text{SF}}(\omega)$ evaluated at ω_s , namely $\left|1 - \frac{\partial \nu_{\text{SF}}(\omega)}{\partial \omega}\right|_{\omega=\omega_s} = \frac{1}{Z_s^{\text{SF}}} = \frac{1}{Z_s}$:

$$\frac{\partial \nu_{\text{SF}}(\omega)}{\partial \omega}\bigg|_{\omega=\omega_s} = \begin{cases} \frac{\frac{2t}{c} + (\frac{1}{2} \pm 1)}{\frac{2t}{c} + \frac{1}{2}} & \text{if } \omega_s = \omega_1 \\ -1 \vee +3 & \text{if } \omega_s = \omega_2 \\ -1 \vee +3 & \text{if } \omega_s = \omega_3 \\ \frac{\frac{2t}{c} - (\frac{1}{2} \pm 1)}{\frac{2t}{c} - \frac{1}{2}} & \text{if } \omega_s = \omega_4 \end{cases} \quad (4.37)$$

where the double possibility for each pole reminds of the fact that Z_s is just an absolute value; the positive alternative is shown in fig. 4.9b.

Note that the requirement that eq. (4.31) do not have any other solutions than $\omega = \omega_s$ can be relaxed: indeed, other poles $\tilde{\omega}_s$ can show up as additional crossings of the two lines $\omega - \varepsilon_{\pm}$ with the function $\nu_{\text{SF}}(\omega)$, provided that their weight $\tilde{Z}_s = \left|1 - \frac{\partial \nu_{\text{SF}}(\omega)}{\partial \omega}\right|_{\omega=\tilde{\omega}_s}^{-1}$ be zero, namely that $\frac{\partial \nu_{\text{SF}}(\omega)}{\partial \omega}\bigg|_{\omega=\tilde{\omega}_s}$ diverge. Therefore, the potential – univocally fixed with its derivative by eq. (4.33) and (4.37) wherever the spectral function is non-zero – can be arbitrarily defined also where $A_{ii}(\omega) = 0$ provided that, if it crosses the lines $\omega - \varepsilon_{\pm}$, its tangent be vertical.

With eq. (4.33) and eq. (4.37) the problem is solved: indeed, if eq. (4.32) do not have any further solutions apart from the indicated ones and if the derivatives of the potential are fixed to the values of eq. (4.37), the auxiliary system spectral function in the bonding–antibonding basis is given by:

$$\begin{aligned} A_{\text{SF}-}(\omega) &= -\frac{1}{\pi} \text{Im} G_{\text{SF}-}(\omega) \stackrel{(4.29)}{=} -\frac{1}{\pi} \text{Im} \frac{1}{\omega - (\varepsilon_0 - t) - \nu_{\text{SF}}(\omega) + i\eta} = \\ &= \delta\left[\omega - (\varepsilon_0 - t + \nu_{\text{SF}}(\omega))\right] \stackrel{(4.32)}{=} \sum_{\omega_s=\{\omega_1, \omega_4\}} \frac{\delta(\omega - \omega_s)}{\left|1 - \frac{\partial \nu_{\text{SF}}(\omega)}{\partial \omega}\right|_{\omega=\omega_s}} = \\ &\stackrel{(4.37)}{=} \sum_{\omega_s=\{\omega_1, \omega_4\}} Z_s \delta(\omega - \omega_s) \stackrel{(4.20)}{=} A_{-}(\omega) \\ A_{\text{SF}+}(\omega) &= \dots = \sum_{\omega_s=\{\omega_2, \omega_3\}} Z_s \delta(\omega - \omega_s) \stackrel{(4.20)}{=} A_{+}(\omega) \end{aligned} \quad (4.38)$$

By transforming to the site basis, the spectral function can be expressed as:

$$\begin{aligned} [A_{\text{SF}ij}(\omega)]_{i,j} &= \frac{1}{2} \begin{pmatrix} 1 & 1 \\ 1 & -1 \end{pmatrix} \begin{pmatrix} A_{\text{SF}-}(\omega) & 0 \\ 0 & A_{\text{SF}+}(\omega) \end{pmatrix} \begin{pmatrix} 1 & 1 \\ 1 & -1 \end{pmatrix} = \\ &= \begin{pmatrix} A_{\text{SF}-}(\omega) + A_{\text{SF}+}(\omega) & A_{\text{SF}-}(\omega) - A_{\text{SF}+}(\omega) \\ A_{\text{SF}-}(\omega) - A_{\text{SF}+}(\omega) & A_{\text{SF}-}(\omega) + A_{\text{SF}+}(\omega) \end{pmatrix} = \\ &\stackrel{(4.38)}{=} \begin{pmatrix} A_{-}(\omega) + A_{+}(\omega) & A_{-}(\omega) - A_{+}(\omega) \\ A_{-}(\omega) - A_{+}(\omega) & A_{-}(\omega) + A_{+}(\omega) \end{pmatrix} = \\ &\stackrel{(4.19)}{=} [A_{ij}(\omega)]_{i,j} \end{aligned} \quad (4.39)$$

Note that, in particular, the spectral function is reproduced in the *non-interacting limit* $U = 0$ (trivial), and also in the *atomic limit* $t \rightarrow 0$. In this latter case, the potential assumes the values $\nu_{\text{SF}}(\omega) = 0$ in ω_1 and ω_2 , and $\nu_{\text{SF}}(\omega) = U$ in ω_3 and ω_4 , yielding the two separated Hubbard bands exactly, something that not only DFT, but not even the GW approximation is able to do [96].

Summarizing, with the choice of eq. (4.33) and eq. (4.37), we obtain the following *more-than-welcome* results:

$$A_{\text{SF}\pm}(\omega) = A_{\pm}(\omega) \quad A_{\text{SF}ij}(\omega) = A_{ij}(\omega) \quad (4.40)$$

More than expected? Eq. (4.40) contains far more than what we expected: the spectral potential $\nu_{\text{SF}}(\omega)$, indeed, has the duty of reproducing only the diagonal of the spectral function in the site basis, namely $A_{\text{SF } ii}(\omega) = A_{ii}(\omega)$, and that's it. The reason we actually get also the off-diagonal elements (and we could not avoid them) is due to the fact that the matrix of change of basis is fixed; therefore, since the spectral function is reproduced in a basis (the bonding–antibonding one, eq. (4.38)), it will be fully reproduced also in the other, diagonal and off-diagonal elements.

One question remains: why is the bonding–antibonding spectral function fully reproduced? The reasons are three: 1) for the symmetry of the problem (two equivalent sites), $\nu_{\text{SF}}(\omega)$ is just a frequency–dependent number in any basis, and in particular in the bonding–antibonding basis; 2) in a discrete system the number of poles is discrete and their position is independent of the basis; their assignment to the correct bonding or antibonding character is done on the basis of continuity with the $U = 0$ case; 3) in the bonding–antibonding basis the spectral function is diagonal and, in particular, positive, as diagonal and positive is the $A_{ii}(\omega)$ we aim at reproducing; the difference in their weights (the $\frac{1}{2}$ factor) is completely accounted for by the change of basis matrix.

As a consequence, in a discrete system in which $\nu_{\text{SF}}(\omega)$ is homogeneous (not site–dependent), the whole spectral function in any diagonal basis (if any) is fully reproduced; therefore, not only the diagonal but even the off–diagonal elements of the site–basis spectral function are exactly reproduced.

In other words, it's all a matter of symmetry and of a discrete number of poles. This is why our effective theory yields more quantities than expected: just ask $\nu_{\text{SF}}(\omega)$ to reproduce the diagonal of the spectral function in a certain basis, and it will automatically reproduce the whole spectral function in any basis.

Lehmann representation and Kramers–Kronig relations As the spectral function is completely reproduced, both the peak positions and weights, one would be very tempted to assume a Lehmann representation for G_{SF} and conclude that, as $A_{\text{SF } ij}(\omega) = A_{ij}(\omega)$, also $G_{\text{SF } ij}(\omega) = G_{ij}(\omega)$. This is actually not the case as the Lehmann representation is equivalent to the Kramers–Kronig relations, which do not hold with a real spectral potential. Indeed, should one try to impose a Lehmann decomposition for the Green's function of eq. (4.28), with four simple poles fixed to the position of the peaks of the spectral function and their amplitudes determined by their weight, one would obtain the following splitting:

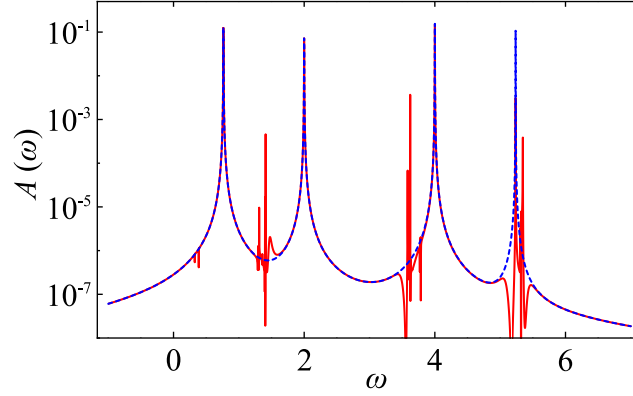
$$\frac{\frac{1}{2}}{\omega - (\varepsilon_- - \nu_{\text{SF}}(\omega)) + i\eta} \stackrel{!}{=} \sum_{s=1,4} \frac{Z_s}{\omega - \omega_s + i\eta}$$

$$\frac{\frac{1}{2}}{\omega - (\varepsilon_+ - \nu_{\text{SF}}(\omega)) + i\eta} \stackrel{!}{=} \sum_{s=2,3} \frac{Z_s}{\omega - \omega_s + i\eta},$$

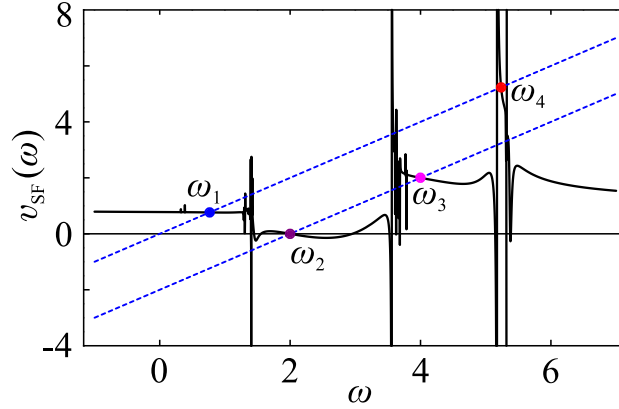
and it is possible to show that these equations have no solutions if $\nu_{\text{SF}}(\omega) \in \mathbb{R}$; indeed, the only solution of these equations is the complex–valued self energy itself. This, besides proving that the Green's function is not reproduced although the whole spectral function is, also explicitly shows that a Lehmann decomposition does not hold in the auxiliary system, and therefore the spectral potential is not a simple function of ω , as it will become evident in the next section.

4.2.2 Sham–Schlüter equation approach

The proceeding above has the merit of showing step by step the construction of the spectral potential, providing a clear picture of its meaning and role. On the other hand, not always one can afford to pursue this path, and in general a true solution of the generalized Sham–Schlüter



(a) The spectral function resulting from $v_{\text{SF}}^{(k=3)}(\omega)$, in red, versus the real system spectral function, in blue, in logarithmic scale.



(b) The spectral potential $v_{\text{SF}}^{(k=3)}(\omega)$, in black; in blue, the two lines $\omega - \varepsilon_{\pm} = 0$; the coloured dots are the expected values of the potential at the poles, eq. (4.33).

Figure 4.10: The result of the generalized Sham–Schlüter equation (4.42) at the fourth iteration, using the prescription $G_{\text{SF}ii}(\omega)[v_{\text{SF}}^{(k)}] = \text{Re}[G_{\text{SF}ii}(\omega)[v_{\text{SF}}^{(k)}] - i\pi A_{ii}(\omega)]$ (third column of fig. 4.13 and 4.12) for $U = 2$, $t = 1$, $\eta = 10^{-6}$ and $\mu = 0$.

equation (3.5) is needed; this equation is on the same footing of eq. (4.30), and can be written as:

$$v_{\text{SF}}(\omega) \sum_j \text{Im} [G_{\text{SF}ij}(\omega) G_{ji}(\omega)] = \sum_{jl} \text{Im} [G_{\text{SF}ij}(\omega) \Sigma_{jl}(\omega) G_{li}(\omega)] \quad (4.41)$$

The Sham–Schlüter equation can be solved iteratively, starting from an input $v_{\text{SF}}^{(k)}(\omega)$, with $k = 0$, and evaluating the output $v_{\text{SF}}^{(k+1)}(\omega)$, till – in principle – self-consistency, according to the following prescription⁷:

$$v_{\text{SF}}^{(k+1)}(\omega) = \frac{\text{Tr} \left[\text{Im} \left(G_{\text{SF}}(\omega) [v_{\text{SF}}^{(k)}] \Sigma(\omega) G(\omega) \right) \right]}{\text{Tr} \left[\text{Im} \left(G_{\text{SF}}(\omega) [v_{\text{SF}}^{(k)}] G(\omega) \right) \right]} \quad (4.42)$$

The real system Green's function and self energy are given by eq. (4.17) and (4.24) respectively. They are exact, since we solved analytically the model. In most situation this is not the

⁷This is only one possible choice among others: one can decide to update the spectral potential in one of the auxiliary system Green's functions and treat the explicit spectral potential as an input, and so on...

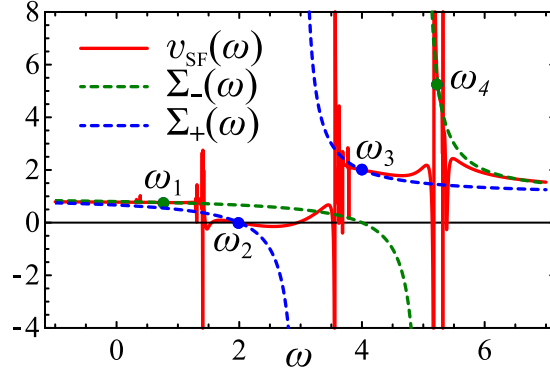


Figure 4.11: Same as figure 4.10b, but with the real part of the bonding (in green) and antibonding (blue) self energies. Since the self energy is diagonal in the bonding–antibonding basis, the potential coincides with the self energy at the poles, both in its value (exactly) and in its first derivative (exactly at ω_1 and ω_4 , almost at ω_3 and not yet at ω_2 ; as mentioned in the text, the reason for this disagreement are instabilities of the amplitudes for small values of η .)

case, hence the linearized version of the Sham–Schlüter equation, eq. (3.25), is considered.

As for the auxiliary system Green’s function $G_{SF ij}(\omega)[v_{SF}^{(k)}]$, given by eq. (4.28), only the imaginary part of its diagonal can be considered as known; one can directly implement this knowledge, substituting $\text{Im} G_{SF ii}(\omega)[v_{SF}^{(k)}]$ with $-\pi A_{ii}(\omega)$ wherever found (let us call this approach “C”), or leave also the imaginary part of the diagonal as a functional of $v_{SF}^{(k)}(\omega)$ (approach “B”). The latter seems a more egalitarian prescription, as every component is a functional of the same spectral potential, while the former, in which any component is a functional of $v_{SF}^{(k)}$ but $\text{Im} G_{SF ii}$, which is exact and can be considered as a functional of $v_{SF}^{(k \rightarrow \infty)}$, could be a quicker approach. In a third implementation (approach “A”) we suppose (wrongly) that also the real part of the diagonal of the Green’s function is reproduced, namely we use that $G_{SF ii}(\omega)[v_{SF}^{(k)}] = \text{Re}[G_{ii}(\omega) - i\pi A_{ii}(\omega)]$, with the spectral potential that doesn’t enter at all the diagonal of G_{SF} . Here is a summary of the three approaches:

$$G_{SF ii}(\omega)[v_{SF}^{(k)}] = \begin{cases} \text{Re}[G_{ii}(\omega) - i\pi A_{ii}(\omega)] & \text{1st column (Ak)} \\ \text{Re}[G_{SF ii}(\omega)[v_{SF}^{(k)}] + i\text{Im}[G_{SF ii}(\omega)[v_{SF}^{(k)}]] & \text{2nd column (Bk)} \\ \text{Re}[G_{SF ii}(\omega)[v_{SF}^{(k)}] - i\pi A_{ii}(\omega) & \text{3rd column (Ck)} \end{cases}$$

I stress that, at self-consistency, only the second and the third choice are correct, while the first is not from the beginning (it reproduces too much).

We implemented the three techniques in `mathematica 10.1`, starting from a zero spectral potential $v_{SF}^{(k=0)}(\omega) = 0$ (the Kohn–Sham potential, actually) and updating till the fourth interaction $k = 4$. The output potentials at each iteration and the relative spectral function are presented in fig. 4.12 and fig. 4.13: the first column for the approach A, the second for B and the third for C.

The final result at the fourth iteration – almost converged – in the approach C is presented in fig. 4.10. We first notice that the potential $v_{SF}(\omega)$ is defined on the whole frequency axis, and not just at the poles. This is not a contradiction with our analytic results: numerically, the spectral function, too, is defined on the whole axis, see fig. 4.10a, because η is small but non zero. Therefore, also the spectral potential is univocally fixed for every frequency. This is an important point: the numerical implementation is different from the analytical model I discussed above. The former gets closer and closer to the latter the smaller the value of η . On

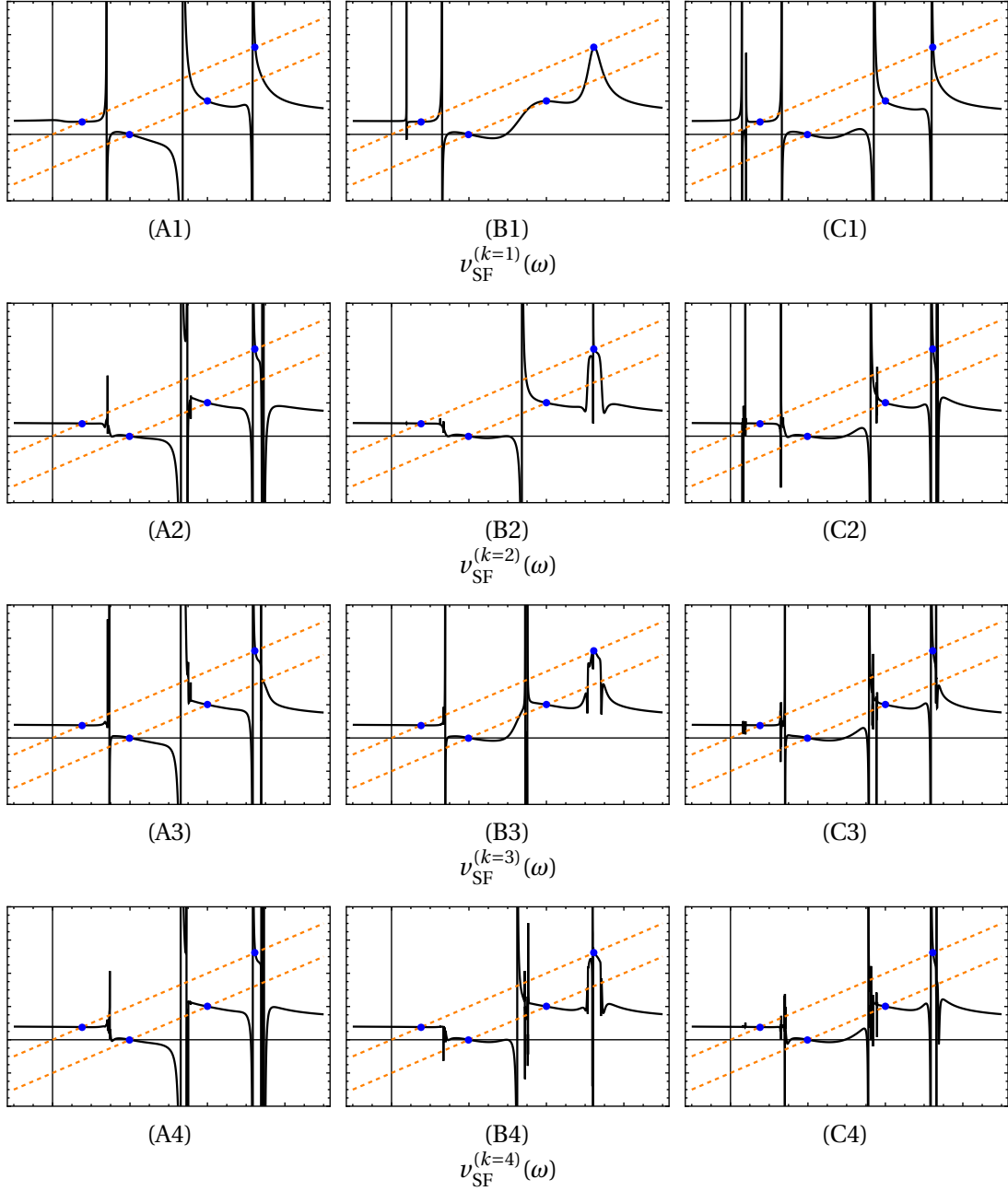


Figure 4.12: Solution $v_{\text{SF}}^{(k)}(\omega)$ at the k -th iteration of the generalized Sham–Schlüter equation (4.42), for $U = 2$, $t = 1$, $\eta = 10^{-6}$ and $\mu = 0$. The scale is the same as in fig. 4.10b.

the other hand (see below) too small values of η generate numerical instabilities. Therefore, a compromise was chosen with $\eta = 10^{-6}t$.

An essential confirmation of the theory is that peaks in the spectral function arise wherever the two lines $\omega - \varepsilon_{\pm} = 0$ cross the potential $v_{\text{SF}}(\omega)$, the amplitude being larger the smaller the derivative of the potential at the crossing. The potential of fig. 4.10b has indeed the expected values at the four pole position ω_s , eq. (4.33). Moreover, it crosses the two lines $\omega - \varepsilon_{\pm} = 0$ with a derivative which is close to the expected one, eq. (4.37). Indeed, the generalized Sham–Schlüter equation must be solved for a value of η very close to zero, in order to display delta peaks and be as close as possible to the analytic model; with tiny values of η , the amplitudes become numerically unstable, as can be seen also from the exact spectral function, that presents two different amplitudes for the peaks at ω_2 and ω_3 , which should instead be the same. Therefore,

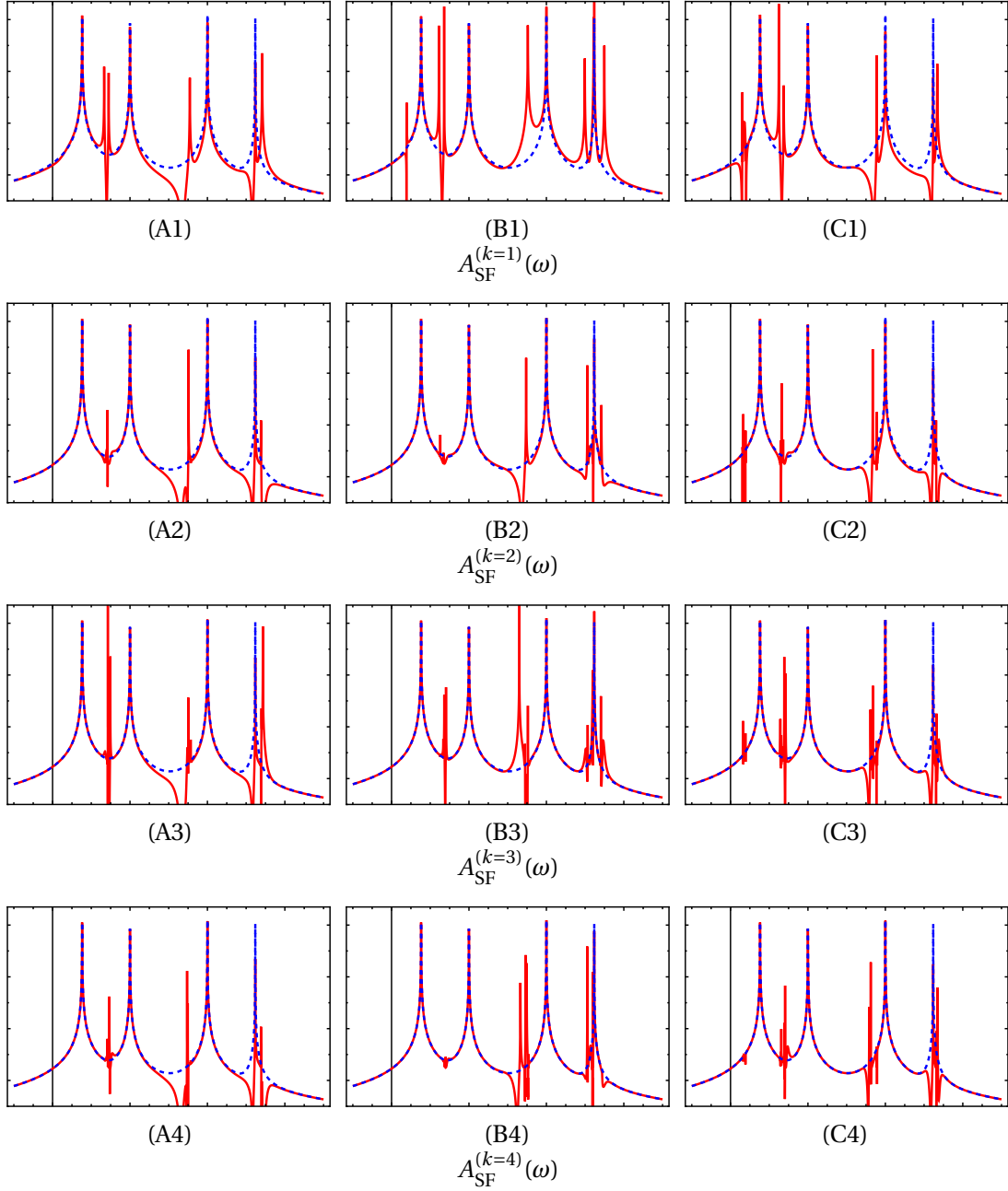


Figure 4.13: *Spectral functions evaluated with the potentials of fig. 4.12, in red, and the real system result, in blue. The scale is the same as in fig. 4.10a.*

we cannot say much about the derivative of the potential at the poles from these plots.

Besides the four expected poles, there are other crossings between the lines $\omega - \varepsilon_{\pm} = 0$ and the potential $v_{\text{SF}}(\omega)$. In general, iterating the equation (see figure 4.12), the potential function gets more and more vertical at these spurious crossings, and the spurious peaks in fig. 4.13 become less and less important. This is a confirmation of the fact that the auxiliary system can display additional poles (crossings) provided that their weight is zero (vertical tangent).

By comparing the spectral functions at different iterations, we can conclude that the procedure is converging to the expected result both in the second (B) and the third column (C), but not, as expected, for the first one (A): for $\omega \sim 3$, between the second and the third peak, and for $\omega \sim 5$, between the third and the fourth peak, the auxiliary system spectral function of the first column does not match its real system counterpart, and the mismatch does not reduce with

the iterations. On the contrary, for the other two schemes, in the same regions, the agreement improves.

As for the corresponding spectral potentials, more and more features appear by increasing the number of iterations, but they are mostly harmless as they are far from the poles and with vertical tangent.

We have thus confirmed the general finding of above. Furthermore, we have shown that even for a very small system (two sites), even when the real system Green's function and self energy are exactly known, solving the Sham–Schlüter equation is far from trivial. That is why more efficient approaches, like the one developed in chapter 5, constitute appealing alternatives.

4.3 The homogeneous electron gas

The homogeneous electron gas (HEG, for brevity) is a model whose importance cannot be overestimated [47]. Besides giving an approximated picture of metals and plasmas [4], exhibiting real phenomena like screening, Friedel oscillations and occurrence of plasmons, it is a test for many theoretical approaches that take into account the electron–electron interaction, as the further complication of inhomogeneity due to the lattice is lifted.

Indeed, the homogeneous electron gas consists of N interacting electrons in a volume V in the thermodynamic limit $N, V \rightarrow \infty$, whose finite density $n = N/V$ is a *constant* that completely characterizes the model; a uniform positively charged background of density n , too, which mimics the inert and lifeless ions of the Born–Oppenheimer approximation, ensures the overall neutrality of the system. An additional simplification due to homogeneity is the rotational and translational symmetry of the whole system.

For such a model the Hamiltonian (2.3a) in reciprocal space, in the thermodynamic limit, reads [4]:

$$\hat{H}_{\text{HEG}} = \sum_{\mathbf{k}} \frac{k^2}{2} \hat{c}_{\mathbf{k}}^\dagger \hat{c}_{\mathbf{k}} + \frac{1}{2V} \sum_{\mathbf{k}, \mathbf{k}'} \sum_{\mathbf{q} \neq \mathbf{0}} \hat{c}_{\mathbf{k}+\mathbf{q}}^\dagger \hat{c}_{\mathbf{k}'-\mathbf{q}}^\dagger \frac{4\pi}{|\mathbf{q}|^2} \hat{c}_{\mathbf{k}'} \hat{c}_{\mathbf{k}} \quad (4.43)$$

where the zero transferred momentum $\mathbf{q} = \mathbf{0}$ is exactly balanced by the interaction of the electrons with the neutralizing background (and the self energy of the background, too): as a result, the external and the Hartree potential sum to zero, plus a constant interaction energy of the background with itself.

It is useful to introduce a quantity, the *Wigner–Seitz radius* r_s , defined (in atomic units) as the radius of a sphere containing exactly one electron: $\frac{4}{3}\pi r_s^3 = \frac{1}{n}$: the denser the system, the smaller r_s and viceversa.

As the Fermi surface remains a sphere (for symmetry reasons) enclosing the same volume both for non–interacting as well as for interacting electrons (*Luttinger theorem*), it is easy to express the Fermi wave vector as a function of r_s : $k_F = \left(\frac{9\pi}{4}\right)^{\frac{1}{3}} \frac{1}{r_s} = \frac{1.9192}{r_s}$; also the plasma frequency, $\omega_P = \sqrt{4\pi n}$, is $\omega_P = \frac{3^{1/2}}{r_s^{3/2}} = \frac{1.7320}{r_s^{3/2}}$.

As r_s represents the average distance between electrons, it sets the behaviour of both the kinetic and the Coulomb energy of the Hamiltonian (4.43): if the latter goes as $1/r_s$, the former scales as $1/r_s^2$ (or as k_F^2); thus the system will be close to a free–electron gas in the high density limit, $r_s \ll 1$ whereas it will exhibit particle–like behaviour in the low density regime $r_s \gg 1$ till, eventually, a crystallization of the electrons at fixed positions, the Wigner crystal [97] (strong correlation regime).

Thus, in the high–density limit $r_s \rightarrow 0$, the electron–electron interaction can be considered as a small perturbation of the kinetic term, although “the potential is not weak nor short range” [4]; the ground state energy is therefore $E_0 \stackrel{r_s \rightarrow 0}{=} \frac{3}{5} N \epsilon_F \left(1 - \left(\frac{125}{18\pi^4}\right)^{\frac{1}{3}} r_s + \mathcal{O}(r_s^2 \ln r_s)\right)$ [98], where

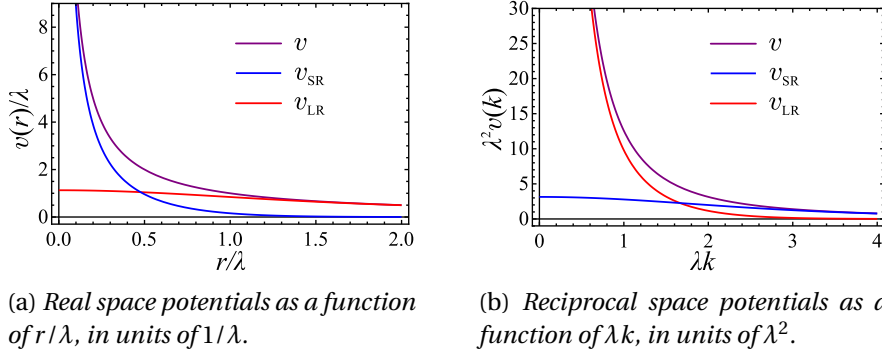


Figure 4.14: Full (purple), short range (blue) and long range (red) Coulomb potential in real and reciprocal space; the full potential is the sum of its short and long range components, and it asymptotically approaches them (in real space) in the limits $r \ll \lambda$ and $r \gg \lambda$ respectively.

$E_0^{(0)} = \frac{3}{5} N \varepsilon_F = \frac{3}{10} \left(\frac{9\pi}{4} \right)^{\frac{2}{3}} \frac{N}{r_s^2}$ is the ground state energy of a free Fermi gas (of purely kinetic origin), while the second term is the *exchange energy* $E_x = -N \frac{3}{4} \left(\frac{3}{\pi} \right)^{\frac{1}{3}} n^{\frac{1}{3}}$, and it is exact [99, 100].

On the opposite side, in the strongly-correlated regime $r_s \gg 1$, the ground state total energy has the asymptotic behaviour describing a Wigner crystal: $E_0 \xrightarrow{r_s \rightarrow \infty} \frac{N}{2} \left(-\frac{1.79}{r_s} + \frac{2.66}{r_s^{3/2}} + \dots \right)$, which is lower than the $E_0^{r_s \rightarrow 0}$ one: localization of electrons is favoured over their spreading.

In the intermediate situation, which is of the most relevance as the average densities of most metals correspond to $1.8 < r_s < 6$ [101], one can resort to interpolating techniques [102], perturbation expansions or Monte-Carlo simulations [103]: the ground state total energy expressed as a functional of the density (or of r_s) is, for the homogeneous electron gas, finally at hand.

The situation is not the same for the excited states...

4.3.1 Real system viewpoint: HSE06 solution

Despite the enormous simplification represented by eq. (4.43) with respect to eq. (2.3a), namely a homogeneous system with no ions instead of a true ion-driven inhomogeneous one, a full exact solution of \hat{H}_{HEG} is still out of reach. In particular, the exact spectral function that corresponds to \hat{H}_{HEG} , as well as the exact Green's function and self energy, are unknown.

To test the spectral potential approach, we must resort to approximate forms of Σ . We will consider the HSE06 self energy [104, 12], as 1) it is *non-local*, hence it will provide a true challenge to our approach; 2) it is *real* and *static*, meaning all the frequency-dependence of the corresponding $\nu_{\text{SF}}(\mathbf{r}, \omega)$ will be just a consequence of non-locality and 3) it is a *realistic* self energy, widely employed for studying real materials [105], from phonons [106] to impurities [107].

The HSE06 functional stems from the observation that density functional theory and the Hartree-Fock approximation usually depart from experiments in opposite directions: in DFT, LDA and PBE [108] underestimate gap and bandwidth, while Hartree-Fock overestimates them; LDA has overbinding tendencies, while Hartree-Fock favours dissociation and localization. Moreover, from a theoretical viewpoint, most of DFT functionals suffer from a self-interaction issue, but they include correlation to a certain extent; on the other hand, Hartree-Fock is self-interaction free but does not include correlation.

These observations encouraged to compensate the opposite drawbacks of both approaches by building *hybrids* of the two, from the simplest “half-and-half” one [109] to a more elaborate semiempirical mixture (B3PW91 [110], B3LYP) to the PBE0 functional [111], which takes the

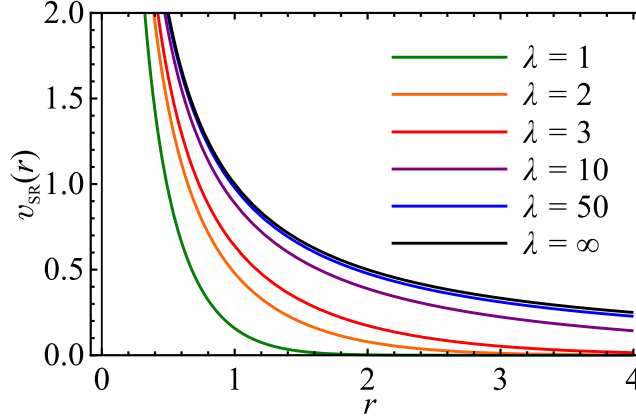


Figure 4.15: Short range Coulomb potential as a function of r , for different screening length λ : when there is no screening, $\lambda \rightarrow \infty$, we are back to the full Coulomb result.

correlation contribution from the PBE functional of DFT [108], $E_c^{\text{PBE0}} = E_c^{\text{DFT}} \equiv E_c^{\text{PBE}}$, while it splits the exchange part E_x^{PBE0} into:

$$E_x^{\text{PBE0}} = \alpha E_x^{\text{HF}} + (1 - \alpha) E_x^{\text{PBE}} \quad (4.44)$$

with E_x^{HF} the one of eq. (2.9), and the mixing parameter α set to $\frac{1}{4}$ by perturbation theory⁸.

The HSE06 functional [104] is based on the further consideration that the Coulomb interaction in solids is actually screened, a phenomenon that – among other things – prevents divergences or unphysical behaviour in the exchange contribution. To take advantage of screening in the simplest possible way, the Coulomb potential is separated into a short (SR) and a long range (LR) parts via the introduction of a screening length λ ⁹:

$$\frac{1}{r} = \underbrace{\frac{\text{erfc}\left(\frac{r}{\lambda}\right)}{r}}_{v_{\text{SR}}(r)} + \underbrace{\frac{\text{erf}\left(\frac{r}{\lambda}\right)}{r}}_{v_{\text{LR}}(r)} \quad (4.45)$$

This separation is exact, as $\text{erfc}(x) \equiv 1 - \text{erf}(x)$, with the error function defined as $\text{erf}(x) := \frac{2}{\sqrt{\pi}} \int_0^x dt e^{-t^2}$; the behaviour of the short and long range components of the Coulomb potential is shown in fig. 4.14.

The proposal of [104] is to apply the range separation (4.45) [113] to the exchange part of the PBE0 functional E_x^{PBE0} ; as the long range parts of the PBE and the Fock exchange functionals are small and tend to cancel each other, the exchange and correlation energy of eq. (4.44) becomes:

$$E_{\text{xc}}^{\text{HSE06}} = E_{\text{xc}}^{\text{PBE}} + \alpha \left(E_x^{\text{HF,SR}} - E_x^{\text{PBE,SR}} \right) \quad (4.46)$$

where the superscript ^{SR} means that only the short range part of the Coulomb potential must be considered. Eq. (4.46) represents a hybrid functional in which only the short-range component of exchange is affected by the Fock term. In the long screening-length limit, the short range part dominates and tends to the full Coulomb potential, and $E_{\text{xc}}^{\text{HSE06}} \xrightarrow{\lambda \gg 1} E_{\text{xc}}^{\text{PBE0}}$; on the opposite side, for large screening (small screening length), the long range component dominates and the short range one goes to zero, so that we recover the usual PBE: $E_{\text{xc}}^{\text{HSE06}} \xrightarrow{\lambda \ll 1} E_{\text{xc}}^{\text{PBE}}$. Here,

⁸Note that α itself can be interpreted as a screening of the Fock exchange term [112].

⁹The parameter λ is the inverse of ω , the symbol often used in literature; we prefer not to use the latter to avoid confusion with frequency.

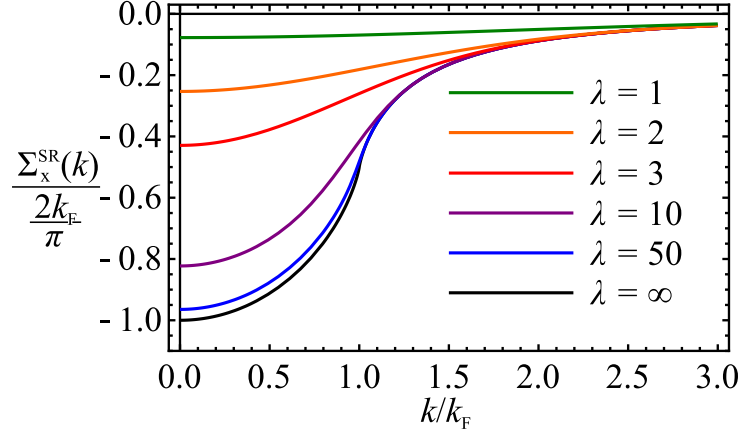


Figure 4.16: Short range Fock self energy (4.50) in units of $\frac{2k_F}{\pi}$ (the Hartree–Fock value at $k = 0$), as a function of k/k_F , for different screening length λ : when there is no screening, $\lambda \rightarrow \infty$, we are back to the Hartree Fock result, which exhibits a vertical tangent for $k = k_F$.

we consider an intermediate value $\lambda = 9.0909\text{\AA}$, chosen from a fit to semiconductor results [12, 114].

The energy functional (4.46) corresponds to the following exchange–correlation self energy (or generalized Kohn–Sham potential):

$$\Sigma_{xc}^{\text{HSE06}}(\mathbf{r}, \mathbf{r}') = \left[v_{xc}^{\text{PBE}}(\mathbf{r}) - \alpha v_x^{\text{PBE,SR}}(\mathbf{r}) \right] \delta(\mathbf{r} - \mathbf{r}') + \alpha \Sigma_x^{\text{SR}}(\mathbf{r}, \mathbf{r}'), \quad (4.47)$$

which is real and static. Of all its ingredients, only the last term is a true non–local self energy, from which all the frequency dependence of the spectral potential will stem.

In the homogeneous electron gas, the local contributions to $\Sigma_{xc}^{\text{HSE06}}$ are just numbers, and it is useful to move to reciprocal space, where the self energy reads:

$$\Sigma_{xc}^{\text{HSE06}}(k) = \left[v_{xc}^{\text{PBE}} - \alpha v_x^{\text{PBE,SR}} \right] + \alpha \Sigma_x^{\text{SR}}(k). \quad (4.48)$$

For simplifying the notation, we call $h_{xc}^{\text{loc}} := v_{xc}^{\text{PBE}} - \alpha v_x^{\text{PBE,SR}}$ the local (hence constant) part of $\Sigma_{xc}^{\text{HSE06}}$. The short range part of the Fock self energy $\Sigma_x^{\text{SR}}(k)$ is defined from an analogous of eq. (2.47), with $v_{\text{SR}}(\mathbf{r})$ in place of $v_C(\mathbf{r})$:

$$\Sigma_x^{\text{SR}}(k) = i \int \frac{d^3q}{(2\pi)^3} \frac{d\omega'}{2\pi} e^{i\omega'\eta} G(|\mathbf{k} + \mathbf{q}|, \omega + \omega') v_{\text{SR}}(q) = - \int \frac{d^3q}{(2\pi)^3} v_{\text{SR}}(q) n_{|\mathbf{k} + \mathbf{q}|}, \quad (4.49)$$

with the occupation number $n_{\mathbf{q}}$ defined as $n_{\mathbf{q}} = \int \frac{d\omega}{2\pi} e^{i\omega\eta} G(\mathbf{q}, \omega)$. The integral in eq. (4.49) can be evaluated analytically, as we have done in appendix (F). The result is:

$$\begin{aligned} \Sigma_x^{\text{SR}}(k) = & -\frac{k_F}{\pi} \left[1 - \frac{k^2 - k_F^2}{2k_F k} \ln \left| \frac{k_F + k}{k_F - k} \right| \right] + \\ & + \frac{1}{\pi \lambda^2 k} \left\{ e^{-\frac{\lambda^2}{4}(k+k_F)^2} - e^{-\frac{\lambda^2}{4}(k-k_F)^2} + \sqrt{\pi} \lambda k \left[\text{erf} \left(\frac{\lambda(k+k_F)}{2} \right) - \text{erf} \left(\frac{\lambda(k-k_F)}{2} \right) \right] \right. \\ & \left. + \frac{\lambda^2}{4} (k^2 - k_F^2) \left[\text{Ei} \left(-\frac{\lambda^2}{4} (k-k_F)^2 \right) - \text{Ei} \left(-\frac{\lambda^2}{4} (k+k_F)^2 \right) \right] \right\}. \quad (4.50) \end{aligned}$$

where the first line is the usual Hartree–Fock self energy, while the rest is $-\Sigma_x^{\text{LR}}(k)$; the exponential integral is defined as $\text{Ei}(x) := -\int_{-x}^{+\infty} dt \frac{e^{-t}}{t}$. As it is clear from fig. (4.16), $\Sigma_x^{\text{SR}}(k)$ removes

the divergence in the derivative of the Hartree–Fock self energy at $k = k_F$, which is at the origin of many unphysical behaviours like a zero density of states at the Fermi level.

Putting back $\Sigma_x^{\text{SR}}(k)$ in eq. (4.48), one can evaluate the Green's function $G(k, \omega)$ and therefore the \mathbf{k} -resolved spectral function $A(k, \omega)$, which is:

$$A(k, \omega) = -\frac{1}{\pi} \text{sign}(\omega - \mu) \text{Im}G(k, \omega) = \delta \left[\omega - \left(\varepsilon_k^0 + h_{\text{xc}}^{\text{loc}} + \alpha \Sigma_x^{\text{SR}}(k) \right) \right], \quad (4.51)$$

namely a single delta function centered on the single-particle energy $\varepsilon_k = \varepsilon_k^0 + h_{\text{xc}}^{\text{loc}} + \alpha \Sigma_x^{\text{SR}}(k)$; the latter equation defines the band structure, in which an energy $\omega = \varepsilon_k$ is associated to each \mathbf{k} . Since, in the homogeneous electron gas with static self energy, the correspondence $k \leftrightarrow \varepsilon_k = \omega$ is one to one, we can invert the relation $\omega = \varepsilon_k$ and get the *inverse band structure* $k = k_0(\omega)$ (in the most general case, other solutions $k_1(\omega)$, $k_2(\omega)$, ..., show up, corresponding to satellites). Note that $k_0(\omega)$ exists whenever $\omega \geq \mu - W$, with the expression of the bandwidth W given in eq. (F.7).

The full spectral function in real space is:

$$A(\mathbf{r}, \mathbf{r}', \omega) = \int \frac{d^3k}{(2\pi)^3} e^{i\mathbf{k} \cdot (\mathbf{r} - \mathbf{r}')} A(k, \omega). \quad (4.52)$$

This integral can be evaluated analytically, see appendix F, and the result is:

$$A(\mathbf{r}, \mathbf{r}', \omega) = \frac{\theta(\omega - \mu + W)}{\pi^2} \left| \frac{\frac{k^2}{2}}{k + \alpha \frac{d\Sigma_x^{\text{SR}}(k)}{dk}} \right| \frac{\sin(k|\mathbf{r} - \mathbf{r}'|)}{(k|\mathbf{r} - \mathbf{r}'|)} \Big|_{k=k_0(\omega)}. \quad (4.53)$$

The spectral function can also be expressed as:

$$A(\mathbf{r}, \mathbf{r}', \omega) = A(\mathbf{r}, \mathbf{r}, \omega) \left\{ \frac{\sin(k|\mathbf{r} - \mathbf{r}'|)}{(k|\mathbf{r} - \mathbf{r}'|)} \Big|_{k=k_0(\omega)} \right\}, \quad (4.54)$$

which has not, in general, a definite sign. By contrast, its diagonal:

$$A(\mathbf{r}, \mathbf{r}, \omega) = \frac{\theta(\omega - \mu + W)}{\pi^2} \left| \frac{\frac{k^2}{2}}{k + \alpha \frac{d\Sigma_x^{\text{SR}}(k)}{dk}} \right|_{k=k_0(\omega)} \quad (4.55)$$

is positive, and has the behaviour shown in fig. 4.17. Note that the correspondence between ω and $A(\mathbf{r}, \mathbf{r}, \omega)$ is one-to-one as far as $A(\mathbf{r}, \mathbf{r}, \omega)$ is monotonically increasing, namely as far as there is no ω for which the derivative of $A(\mathbf{r}, \mathbf{r}, \omega)$ is zero; this condition can be further formalized by saying that for no ω the corresponding $k = k_0(\omega)$ fulfills the equation $\frac{1}{\alpha} = \Sigma''(k) - \frac{2}{k} \Sigma'(k)$; for our scopes, the limit $\lambda \lesssim 65$ (with $k_F = 1$) is enough, as we will work with $\lambda k_F \sim 3 \div 10$.

Relation between diagonal and off-diagonal elements An important consideration about eq. (4.54) is the following: the knowledge of the diagonal of the spectral function is not enough – at first sight – to obtain the full spectral function; also the additional term $\frac{\sin(k|\mathbf{r} - \mathbf{r}'|)}{(k|\mathbf{r} - \mathbf{r}'|)}$ is needed, that only apparently is a property of space only, independent of the form of the self energy; the latter, indeed, enters the definition of $k = k_0(\omega)$, and the relation $k = k_0(\omega)$, namely the *inverse band structure*, must be at hand in order to obtain the additional factor. One would conclude that, as expected, even if we knew $A(\mathbf{r}, \mathbf{r}, \omega)$, we would still need the band structure $k_0(\omega)$ to get to $A(\mathbf{r}, \mathbf{r}', \omega)$.

This conclusion, that should hold in general, is not true in this case, in which there is a one-to-one correspondence both between $k_0(\omega)$ and ω and between ω and $A(\mathbf{r}, \mathbf{r}, \omega)$, at least for the λ we consider. Therefore one can express the band structure $k_0(\omega)$ as a functional of

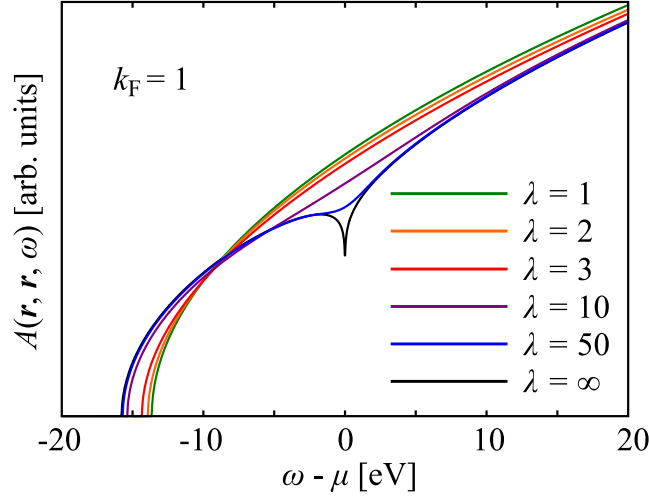


Figure 4.17: *Diagonal of the spectral function (4.54), in arbitrary units, for different values of λ , as a function of frequency with $\mu = 0$, for $k_F = 1$. In the unscreened situation, we recover the Hartree–Fock density of states, and the free behaviour $\sim \sqrt{\omega}$ for $\lambda \leq 1$.*

$A(\mathbf{r}, \mathbf{r}, \omega)$, by inverting eq. (4.55), and get the *whole* spectral function from eq. (4.54): *as soon as the interaction is sufficiently screened, for a large class of static self-energies, the knowledge of the diagonal of the spectral function completely defines the system.*

On the opposite side, were we in the Hartree–Fock limit $\lambda \rightarrow \infty$, the knowledge of $A(\mathbf{r}, \mathbf{r}, \omega)$ would not be equivalent to the one of $k_0(\omega)$, as the band structure $\omega \leftrightarrow k_0(\omega)$ would still be one-to-one, but the same value of $A(\mathbf{r}, \mathbf{r}, \omega)$ could correspond to up to three different frequencies: more generally, *dips (or peaks) in $A(\mathbf{r}, \mathbf{r}, \omega)$ are regions in which a true knowledge of the band structure is needed, if one wants to reproduce also the off-diagonal elements: there, the diagonal of the spectral function does not offer a complete description of the spectral properties; we will come back to this observation when we will consider real materials.*

Note also that the situation is analogous to the dimer of eq. (4.19): even there, we could have written:

$$A_{ij}(\omega) = A_{ii}(\omega) \left\{ \delta_{\omega_s, ab} (-1)^{(i-j)} \right\},$$

which is on the same footing of eq. (4.54): it says that, whenever a peak ω_s is associated to an antibonding peak, the relative weight changes sign: that is the “band structure”, the knowledge of the character of the peaks, namely if they are bonding or antibonding peaks.

Two simplifications happen in the dimer: first, since the poles are discrete, we can read them from $A_{ii}(\omega)$: in the “band structure” analogy, we know the energy $\omega(k)$ without knowing yet to which k it corresponds; but since the poles are well-separated, we can follow their behaviour from $U = 0$ to increasing U , *adiabatically connecting* the poles of the interacting dimer to the ones of the non-interacting one; this trick allows us to infer the *state dependence*, namely to connect each ω_s to a bonding or an antibonding $U = 0$ peak (analogously, the band structure: connect $\omega(k)$ to k), hence to know the factor $\delta_{\omega_s, ab}$.

Furthermore, once we know whether we have to use it or not, the multiplicative factor $(-1)^{(i-j)}$ is completely independent of the approximation used for the self energy, and it is just a property of space; hence, we would not even need the knowledge of the band structure here.

The situation would be analogous to a hypothetical *discrete* homogeneous electron gas, with a discrete set of k -points: there, assuming the validity of eq. (4.54), we could read the poles from $A(\mathbf{r}, \mathbf{r}, \omega)$ and infer their position from an adiabatic switching-on of the interaction; that would be enough to know the band structure, and the full spectral function $A(\mathbf{r}, \mathbf{r}', \omega)$ could be

at hand.

4.3.2 The auxiliary system

We now aim at reproducing the diagonal of the spectral function, eq. (4.55), with a local spectral potential which, in the homogeneous electron gas, does not depend on space: $v_{\text{SF}}(\omega)$; as the exchange–correlation self energy (4.47) is composed of a local and a non–local part, $\Sigma_{\text{xc}}(k) = h_{\text{xc}}^{\text{loc}} + \alpha \Sigma_{\text{x}}^{\text{SR}}(k)$, the truly frequency–dependent part of the spectral potential is the one corresponding to the non–local part of the self energy; therefore we can write $v_{\text{SF}}(\omega) = h_{\text{xc}}^{\text{loc}} + \alpha v_{\text{x}}^{\text{SR}}(\omega)$, maintaining the symmetry of the two formulations.

Let us now build the system corresponding to a real, local and frequency dependent potential $v_{\text{SF}}(\omega)$.

The auxiliary system The auxiliary system differs from the real one in the fact that the role of the exchange correlation self energy is played by a real, local and frequency dependent potential $v_{\text{SF}}(\omega)$. Therefore, the inverse Green’s function of it is, in reciprocal space:

$$G_{\text{SF}}^{-1}(k, \omega) = G_0^{-1}(k, \omega) - v_{\text{SF}}(\omega) \quad (4.56)$$

with $G_0^{-1}(k, \omega) = \omega - \varepsilon_k^0$. The associated spectral function is:

$$A_{\text{SF}}(k, \omega) = \delta(\omega - \varepsilon_k^0 - v_{\text{SF}}(\omega)) \quad (4.57)$$

This is nothing but $A_0(k, \omega - v_{\text{SF}}(\omega))$, with $A_0(k, \omega) = \delta(\omega - \varepsilon_k^0)$ the non–interacting spectral function associated to G_0 . From this observation, the auxiliary system full spectral function $A_{\text{SF}}(\mathbf{r}, \mathbf{r}', \omega)$ will be the analogous of eq. (4.53), with $\Sigma_{\text{xc}} = 0$ and shifted frequency argument:

$$A_{\text{SF}}(\mathbf{r}, \mathbf{r}', \omega) = \frac{\theta(\omega - v_{\text{SF}}(\omega))}{\pi^2} \left| \frac{k^2}{k} \right| \frac{\sin(k|\mathbf{r} - \mathbf{r}'|)}{(k|\mathbf{r} - \mathbf{r}'|)} \Big|_{k=k_0^0(\omega - v_{\text{SF}}(\omega))}$$

as $\mu^0 - W^0 = 0$. In the free case, the inverted band structure $k_0^0(\omega)$ is trivial, as $k_0^0(\omega)$ is the positive solution to the simple equation $\omega = \varepsilon_k^0$, namely $k_0^0(\omega) = \sqrt{2\omega}$; therefore, the previous expression becomes:

$$A_{\text{SF}}(\mathbf{r}, \mathbf{r}', \omega) = A_{\text{SF}}(\mathbf{r}, \mathbf{r}, \omega) \frac{\sin(k|\mathbf{r} - \mathbf{r}'|)}{(k|\mathbf{r} - \mathbf{r}'|)} \Big|_{k=\sqrt{2[\omega - v_{\text{SF}}(\omega)]}} \quad (4.58)$$

with:

$$A_{\text{SF}}(\mathbf{r}, \mathbf{r}, \omega) = \frac{\theta(\omega - v_{\text{SF}}(\omega))}{2\pi^2} \sqrt{2[\omega - v_{\text{SF}}(\omega)]} \quad (4.59)$$

These expressions are quite general, as we have not specified yet the form of the potential, nor we have characterized in any way the auxiliary system, but for the fact that its self energy is real and local; nevertheless, an important consequence of this last assumption already shows up: we can explicitly notice that the knowledge of the diagonal of the spectral function only is enough to reconstruct the off–diagonal terms, too:

$$A_{\text{SF}}(\mathbf{r}, \mathbf{r}', \omega) = \frac{\sin\left[2\pi^2|\mathbf{r} - \mathbf{r}'|A_{\text{SF}}(\mathbf{r}, \mathbf{r}, \omega)\right]}{2\pi^2|\mathbf{r} - \mathbf{r}'|} \quad (4.60)$$

Note that in this case there is no condition on the form of the potential, or, which is the same, on the magnitude of λ : that is a hint that the two formulations somehow differ.

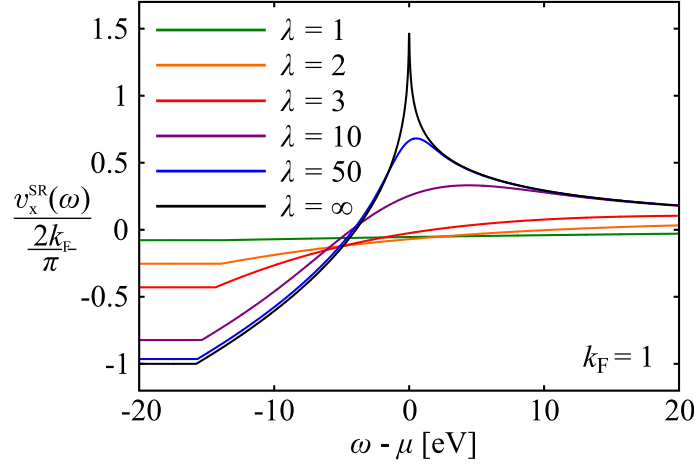


Figure 4.18: The purely frequency–dependent part of the spectral potential $v_x^{\text{SR}}(\omega)$ as a function of frequency with $\mu = 0$, in units of $\frac{2k_F}{\pi}$ for $k_F = 1$, for different values of λ . This figure has to be compared to fig. 4.16.

The generalized Sham–Schlüter equation The auxiliary system is defined once we implement the generalized Sham–Schlüter equation in the simple form $A_{\text{SF}}(\mathbf{r}, \mathbf{r}, \omega) = A(\mathbf{r}, \mathbf{r}, \omega)$, with the real and the auxiliary system spectral functions given by eq. (4.55) and eq. (4.59) respectively:

$$A(\mathbf{r}, \mathbf{r}, \omega) = \frac{\theta(\omega - \mu + W)}{\pi^2} \left| \frac{\frac{k^2}{2}}{k + \alpha \frac{d\Sigma_x^{\text{SR}}(k)}{dk}} \right|_{k=k_0(\omega)} = \frac{\theta(\omega - v_{\text{SF}}(\omega))}{2\pi^2} \sqrt{2[\omega - v_{\text{SF}}(\omega)]} \quad (4.61)$$

When $\omega \leq \mu - W$, the spectral function is zero, and it is enough that $v_{\text{SF}}(\omega) \geq \omega$ to make the auxiliary system spectral function zero as well. On the other hand, when $\omega \geq \mu - W$, a non trivial relation links the spectral potential to the diagonal of the real system spectral function, namely:

$$v_{\text{SF}}(\omega) = \omega - \frac{1}{2} \left[2\pi^2 A(\mathbf{r}, \mathbf{r}, \omega) \right]^2 \quad (4.62)$$

which can be analytically continued also in the region where $A(\mathbf{r}, \mathbf{r}, \omega) = 0$ by $v_{\text{SF}}(\omega) = \omega$; we will choose, instead, in agreement with [79], the alternative continuation $v_{\text{SF}}(\omega) = \mu - W$, namely a constant potential equals to its value at the bottom band; in this way, $v_{\text{SF}}(\omega \leq \mu - W) = \Sigma_{\text{xc}}^{\text{HSE06}}(k=0)$, as can be seen by comparing fig. 4.18 with fig. 4.16. Finally, the spectral potential results in:

$$v_{\text{SF}}(\omega) = \begin{cases} \text{const} = \mu - W & \text{if } \omega \leq \mu - W \\ \omega - 2 \left| \frac{\frac{k^2}{2}}{k + \alpha \frac{d\Sigma_x^{\text{SR}}(k)}{dk}} \right|_{k=k_0(\omega)}^2 & \text{if } \omega \geq \mu - W \end{cases} \quad (4.63)$$

represented, for different values of λ , in fig. 4.19. Comparing the spectral potential of fig. 4.18 with the self energy of fig. 4.16, we can appreciate the transformation of non–locality into frequency dependence [6] that we obtained: the more the self energy is non–local, namely the more it varies with k , the stronger the dependence on frequency of the spectral potential (in this case, for large values of λ).

Off–diagonal elements With such a potential, the diagonal of the spectral function is exact by construction; since, by eq. (4.54) and the discussion that follows, $A(\mathbf{r}, \mathbf{r}', \omega)$ is linked to $A(\mathbf{r}, \mathbf{r}, \omega)$, one could expect that also the off–diagonal elements are exactly reproduced by $v_{\text{SF}}(\omega)$: that is the content of eq. (4.60), which is even simpler than eq. (4.54).

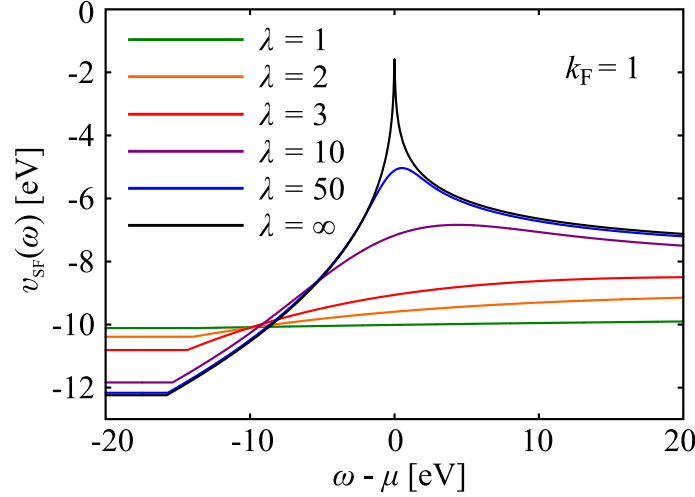


Figure 4.19: Same as fig. 4.19 but for the full spectral potential $v_{\text{SF}}(\omega) = h_{\text{xc}}^{\text{loc}} + \alpha v_{\text{x}}^{\text{SR}}(\omega)$, this time in eV.

However, this is not the case: as discussed in paragraph 3.2.2, functionals in the real and the auxiliary system usually differ, and the same function (the exact $A(\mathbf{r}, \mathbf{r}', \omega)$), plugged in the two expressions, yields different results. This is what happens here, and the full spectral function is given, in the real and the auxiliary system, respectively by eq. (4.54) and eq. (4.60), that can both be expressed in terms of $k = k_0(\omega)$ in the following way:

$$\begin{aligned}
 A(\mathbf{r}, \mathbf{r}', \omega) &= \frac{\theta(\omega - \mu + W)}{2\pi^2} \frac{k^2}{k + \alpha \frac{d\Sigma_{\text{x}}^{\text{SR}}(k)}{dk}} \frac{\sin(k|\mathbf{r} - \mathbf{r}'|)}{(k|\mathbf{r} - \mathbf{r}'|)} \\
 A_{\text{SF}}(\mathbf{r}, \mathbf{r}', \omega) &= \frac{\theta(\omega - \mu + W)}{2\pi^2} \frac{k^2}{k + \alpha \frac{d\Sigma_{\text{x}}^{\text{SR}}(k)}{dk}} \frac{\sin\left(\frac{k|\mathbf{r} - \mathbf{r}'|}{1 + \frac{\alpha}{k} \frac{d\Sigma_{\text{x}}^{\text{SR}}(k)}{dk}}\right)}{\left(\frac{k|\mathbf{r} - \mathbf{r}'|}{1 + \frac{\alpha}{k} \frac{d\Sigma_{\text{x}}^{\text{SR}}(k)}{dk}}\right)}
 \end{aligned} \tag{4.64}$$

Clearly, if $\mathbf{r} \neq \mathbf{r}'$, the two expressions usually differ; they yield the same result only for $d\Sigma_{\text{x}}^{\text{SR}}/dk = 0$, that is for $k_0(\omega) = 0$ and $k_0(\omega) \rightarrow \infty$; this corresponds to $\omega = \mu - W$ and $\omega \rightarrow \infty$.

The fact that the off-diagonal elements of the spectral function are non reproduced by the auxiliary system pushes us to investigate the behaviour of the spectral function in \mathbf{k} -space.

\mathbf{k} -resolved spectral function Like the off-diagonal elements, also the \mathbf{k} -resolved spectral function is not a quantity we expect to be reproduced in the auxiliary system; indeed, the two are just linked by a Fourier transform, eq. (4.52).

The \mathbf{k} -resolved spectral function in the real system is given by eq. (4.51), namely a delta function centered on the excitation energy ε_k :

$$\varepsilon_k = \varepsilon_k^0 + h_{\text{xc}}^{\text{loc}} + \alpha \Sigma_{\text{x}}^{\text{SR}}(k). \tag{4.65}$$

In the auxiliary system, the inverse Fourier transform of the full real space spectral function, eq. (4.60), yields:

$$A_{\text{SF}}(k, \omega) = \delta[\omega - (\varepsilon_k^0 + v_{\text{SF}}(\omega))], \tag{4.66}$$

which can be a single delta function as well as, in principle, a more complicated object. That depends on the number of solutions of the equation $\omega = \varepsilon_k^0 + v_{\text{SF}}(\omega)$, namely on the number of

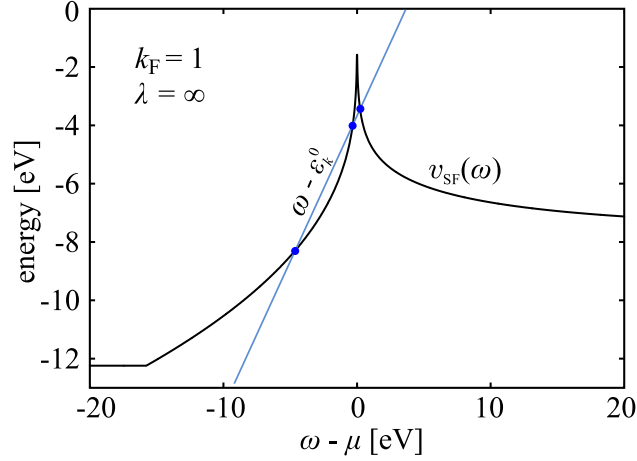


Figure 4.20: Same as fig. 4.18, only the $\lambda \rightarrow \infty$ spectral potential $v_{\text{SF}}(\omega)$, in eV. Also the line $\omega - \varepsilon_k^0$ is shown, for a particular value of k . It crosses the potential for three values of frequencies, yielding three peaks in the spectral function.

crossings of the potential $v_{\text{SF}}(\omega)$ with the line $\omega - \varepsilon_k^0$; these can be more than one, as the spectral potential depends non-trivially on frequency.

In the limit $\lambda \rightarrow \infty$, for instance, there are values of \mathbf{k} for which *three* crossings are present, see fig. 4.20: for one of the smallest of such \mathbf{k} s, $A_{\text{SF}}(k, \omega)$ is composed of three peaks: a more intense one associated with the usual quasi particle, and two smaller ones around the Fermi energy, that can be interpreted as satellites associated with the cusp of the potential; for increasing k , some weight is transferred from the quasi particle to the satellites, until, finally, the higher energy satellite acquires all the spectral weight and becomes the quasi particle itself.

For the screening that we consider, such a situation never occurs, and the crossing between the potential $v_{\text{SF}}(\omega)$ and $\omega - \varepsilon_k^0$ is always unique: to any k there corresponds a single delta function centered on the energy:

$$\varepsilon_k^{\text{SF}} = \varepsilon_k^0 + v_{\text{SF}}(\varepsilon_k^{\text{SF}}) \equiv \varepsilon_k^0 + h_{\text{xc}}^{\text{loc}} + \alpha v_{\text{x}}^{\text{SR}}(\varepsilon_k^{\text{SF}}). \quad (4.67)$$

As the correspondence is always one-to-one, the map $k \rightarrow \varepsilon_k^{\text{SF}}$ constitutes the *band structure* of the auxiliary system, as well as the map $k \rightarrow \varepsilon_k$, eq. (4.65), is the band structure of the real system. The natural question is the connection between the two.

The band structure in the auxiliary system can be found by fixing the wavenumber \mathbf{k} , and then solving the equation $\omega - \varepsilon_k^0 = v_{\text{SF}}(\omega)|_{\omega=\varepsilon_k^{\text{SF}}}$ with the spectral potential given by eq. (4.63). The result is:

$$\frac{k_0(\varepsilon_{\mathbf{k}}^{\text{SF}})}{|\mathbf{k}|} = 1 + \frac{\alpha}{k_0(\varepsilon_{\mathbf{k}}^{\text{SF}})} \left. \frac{d\Sigma_{\text{x}}^{\text{SR}}(k)}{dk} \right|_{k=k_0(\varepsilon_{\mathbf{k}}^{\text{SF}})} \quad (4.68)$$

which is an implicit equation that links the excitation energy $\varepsilon_{\mathbf{k}}^{\text{SF}}$ to the wave vector \mathbf{k} , by passing through the intermediate object k_0 . In particular, from the fact that no quantity in the previous equation is negative, we can directly affirm that $k_0(\varepsilon_{\mathbf{k}}^{\text{SF}}) \geq |\mathbf{k}|$ for all \mathbf{k} and, since $k_0(\omega)$ is an increasing function of ω , we can conclude that:

$$\varepsilon_{\mathbf{k}}^{\text{SF}} \geq \varepsilon_{\mathbf{k}} \quad \forall \mathbf{k} \quad (4.69)$$

with the equality holding when $d\Sigma_{\text{x}}^{\text{SR}}(k)/dk = 0$, namely for $\mathbf{k} = \mathbf{0}$ and $|\mathbf{k}| \rightarrow \infty$. Eq. (4.68) can be solved numerically and the result is shown in fig. 4.21, left panel: the red curve, which represents the auxiliary system dispersion $\varepsilon_{\mathbf{k}}^{\text{SF}}$, is always at higher energy than the blue curve,

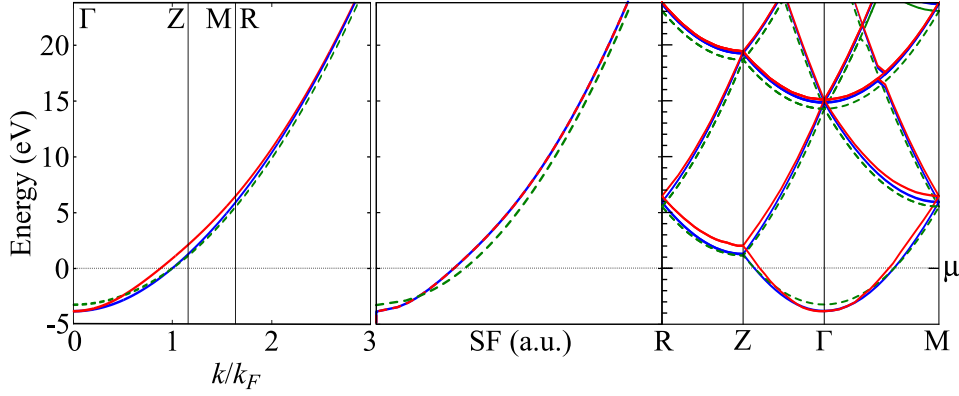


Figure 4.21: HEG ($r_s = 3.9315a_0$, Na average value) dispersion (left), spectral function (middle) and band structure (right). The blue curve has been calculated using the self energy, while the red one is the auxiliary system approach (as a comparison, the green-dashed curve for Kohn–Sham in the LDA approximation). The high symmetry points in the band structure refer to a simple cubic unit cell: $R = (0, \frac{1}{2}, \frac{1}{2})$, $Z = (0, 0, \frac{1}{2})$, $\Gamma = (0, 0, 0)$ and $M = (\frac{1}{2}, \frac{1}{2}, 0)$.

the standard dispersion $\varepsilon_{\mathbf{k}}$. We call the difference between the two $\Delta_{\mathbf{k}}$:

$$\begin{aligned} \Delta_{\mathbf{k}} &:= \varepsilon_{\mathbf{k}}^{\text{SF}} - \varepsilon_{\mathbf{k}} = \nu_{\text{SF}}(\varepsilon_{\mathbf{k}}^{\text{SF}}) - \Sigma_{\text{xc}}(|\mathbf{k}|) = \\ &= \alpha \left[\nu_{\text{x}}^{\text{SR}}(\varepsilon_{\mathbf{k}}^{\text{SF}}) - \Sigma_{\text{x}}^{\text{SR}}(|\mathbf{k}|) \right] \end{aligned} \quad (4.70)$$

This difference goes to zero as $\mathbf{k} = \mathbf{0}$ or $|\mathbf{k}| \rightarrow \infty$, as expected.

The two different band structures $\varepsilon_{\mathbf{k}}^{\text{SF}}$ and $\varepsilon_{\mathbf{k}}$ yield two different spectral functions, eq. (4.64), as one would expect. What is more surprising is that $\varepsilon_{\mathbf{k}}^{\text{SF}}$ and $\varepsilon_{\mathbf{k}}$, on the other hand, give rise to the *same* diagonal of the spectral function, $A_{\text{SF}}(\mathbf{r}, \mathbf{r}, \omega) = A(\mathbf{r}, \mathbf{r}, \omega)$.

The reason why this is possible is that we are in a *continuous* system, the homogeneous electron gas in the thermodynamic limit; in such a limit, the poles of the Green's function merge into a branch cut on the real axis [63], and their position becomes less relevant as far as the amplitude is reproduced. This is shown in more details in the next paragraph.

Discrete and continuous systems Let us consider, indeed, the diagonal of the spectral function in real space as a sum over the band structure of the different peaks, both in the real and in the auxiliary system, eq. (4.52); integrating out the angular coordinates, we have:

$$\begin{aligned} A(\mathbf{r}, \mathbf{r}, \omega) &= \frac{1}{2\pi^2} \int_0^{+\infty} dk k^2 \delta(\omega - \varepsilon_k) \\ A_{\text{SF}}(\mathbf{r}, \mathbf{r}, \omega) &= \frac{1}{2\pi^2} \int_0^{+\infty} dk_{\text{SF}} k_{\text{SF}}^2 \delta(\omega - \varepsilon_{k_{\text{SF}}}^{\text{SF}}(\omega)) \end{aligned} \quad (4.71)$$

with k_{SF} a dummy integration variable. Evaluating also the radial integrals in k and k_{SF} would result in eq. (4.55) and eq. (4.59). These integrals say that the diagonal of the spectral function in real space is made up of many delta peaks, each centered on a one-particle energy, ε_k or $\varepsilon_{k_{\text{SF}}}^{\text{SF}}$, where the latter is the solution of $\omega - \varepsilon_{k_{\text{SF}}}^{\text{SF}}(\omega) = 0$, with a weight given by k^2 or k_{SF}^2 .

Were we in a *discrete system*, integrals would be sums and, to have $A(\mathbf{r}, \mathbf{r}, \omega) = A_{\text{SF}}(\mathbf{r}, \mathbf{r}, \omega)$, we could simply match the pole positions, $\varepsilon_{k_{\text{SF}}}^{\text{SF}} = \varepsilon_k$, and their weights, $k_{\text{SF}}^2 = k^2$. In one single move, we would obtain both the spectral function and the band structure, and the off-diagonal elements $A(\mathbf{r}, \mathbf{r}', \omega)$ as well. This is exactly the procedure we followed in the homogeneous

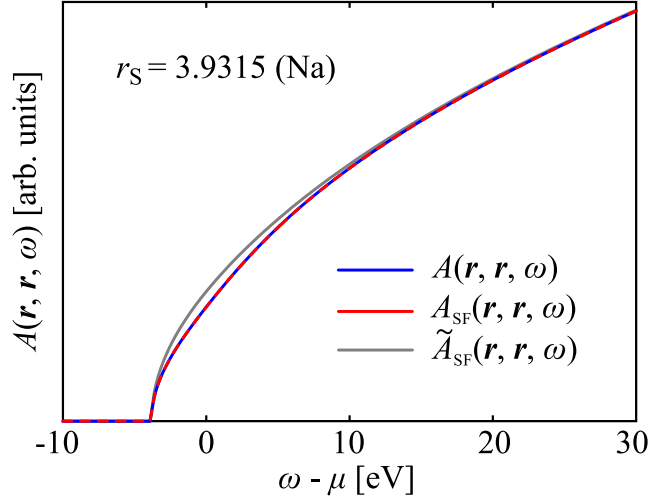


Figure 4.22: The diagonal of the auxiliary system spectral functions $A_{\text{SF}}(\mathbf{r}, \mathbf{r}, \omega)$ obtained with the spectral potential $v_{\text{SF}}(\omega)$, in red, and $\tilde{A}_{\text{SF}}(\mathbf{r}, \mathbf{r}, \omega)$ corresponding to $\tilde{v}_{\text{SF}}(\omega)$, in gray, as a function of frequency with $\mu = 0$ ($r_s = 3.9315a_0, \lambda = 9.0909\text{\AA}$). In blue, the reference spectral function $A(\mathbf{r}, \mathbf{r}, \omega)$.

dimer (indeed, a discrete system), and the quantities we obtained were analogous (the spectral function in the bonding–antibonding basis and hence the full spectral function in the site basis).

Moreover, in a discrete system, the spectral potential would be meaningful only where the spectral function is non-zero, namely at the poles. From the conditions $\varepsilon_{k_{\text{SF}}}^{\text{SF}} = \varepsilon_k$ and $k_{\text{SF}} = k$, that is $\varepsilon_k^{\text{SF}} = \varepsilon_k$, we would obtain the following discrete spectral potential $\tilde{v}_{\text{SF}}(\varepsilon_k)$:

$$\tilde{v}_{\text{SF}}(\varepsilon_k) = \Sigma_{\text{xc}}(k) \quad (4.72)$$

which is on the same footing of the dimer potential, eq. (4.35). Clearly, such a potential will reproduce the band structure, and hence, in the discrete, the full spectral function.

Let us now move to the *continuum* $N, V \rightarrow \infty$ with $n = N/V$ finite. In this limit, the sum over k and the one over k_{SF} span the same whole positive axis, and only the amplitude of each delta peak becomes relevant; in the real system, the factor k^2 , which comes from the integration volume $d^3k = 4\pi k^2 dk$, is supplied by the additional factor $\frac{1}{k + \alpha \frac{d\Sigma_{\text{SR}}^{\text{SR}}(k)}{dk}}$, that comes from the expression of the Dirac delta in k -space; the derivative of the self energy is well defined as k is a continuum variable. The total weight becomes $\frac{k^2}{k + \alpha \frac{d\Sigma_{\text{SR}}^{\text{SR}}(k)}{dk}}$, and the real system $A(\mathbf{r}, \mathbf{r}, \omega)$ reads:

$$A(\mathbf{r}, \mathbf{r}, \omega) = \frac{1}{2\pi^2} \int_0^{+\infty} dk \frac{k^2}{k + \alpha \frac{d\Sigma_{\text{SR}}^{\text{SR}}(k)}{dk}} \delta(k - k_0(\omega))$$

On the contrary, as the spectral potential $v_{\text{SF}}(\omega)$ does not depend on k , the additional factor to the weight k^2 is simply $\frac{1}{k}$, and the auxiliary system spectral function becomes:

$$A_{\text{SF}}(\mathbf{r}, \mathbf{r}, \omega) = \frac{1}{2\pi^2} \int_0^{+\infty} dk \frac{k^2}{k} \delta(k - k_0^{\text{SF}}(\omega))$$

with $k_0^{\text{SF}}(\omega) \equiv k_0^0(\omega - v_{\text{SF}}(\omega)) = \sqrt{2(\omega - v_{\text{SF}}(\omega))}$. As already mentioned, the position of the peaks is irrelevant as far as the weights of two of them coincide for a determined value of ω ; therefore,

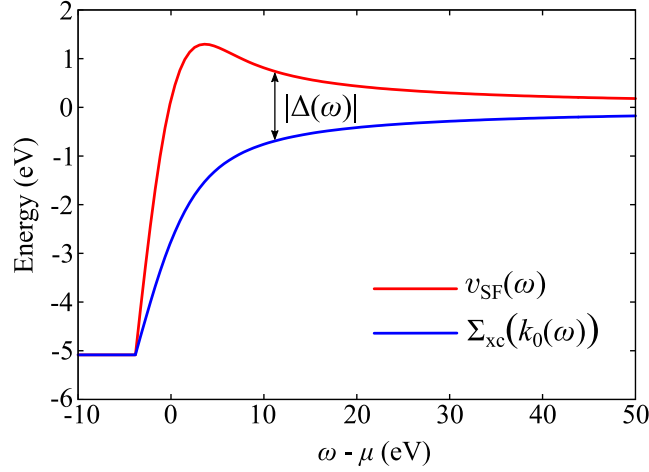


Figure 4.23: The $\Delta(\omega)$ term introduced in eq. (4.76), as a function of frequency for $\mu = 0$, in eV ($r_s = 3.9315a_0$, $\lambda = 9.0909\text{\AA}$).

for a given frequency ω , we can match the weights of the two peaks $\delta(k - k_0^{\text{SF}}(\omega))$ and $\delta(k - k_0(\omega))$, and obtain the following relation:

$$k_0^{\text{SF}}(\omega) = \frac{k^2}{k + \alpha \frac{d\Sigma_x^{\text{SR}}(k)}{dk}} \Bigg|_{k=k_0(\omega)} \quad \forall \omega$$

which is exactly the definition of the spectral potential and, as shown in eq. (4.68), states that, in general, $k_0^{\text{SF}}(\omega) \neq k_0(\omega)$. In the continuum limit, one cannot reproduce both the peak positions (the band structure) and amplitudes (the diagonal of the spectral function) at the same time.

An exactification of the band structure in the continuum As the quantities they yield are different, it is clear that the continuum limit of $\tilde{v}_{\text{SF}}(\varepsilon_k)$ is not $v_{\text{SF}}(\omega)$ evaluated at $\omega = \varepsilon_k$, but another potential, associated with another auxiliary system, that we call $\tilde{v}_{\text{SF}}(\omega)$:

$$\tilde{v}_{\text{SF}}(\omega) = \lim_{\substack{N, V \rightarrow \infty \\ N/V = n}} \tilde{v}_{\text{SF}}(\varepsilon_k) \Big|_{\omega = \varepsilon_k} \quad (4.73)$$

From eq. (4.72), this potential is nothing but the self energy at $k_0(\omega)$:

$$\tilde{v}_{\text{SF}}(\omega) = \Sigma_{\text{xc}}(k_0(\omega)), \quad (4.74)$$

which can also be expressed in terms of the spectral potential as:

$$\tilde{v}_{\text{SF}}(\omega) = v_{\text{SF}}(\omega) - \Delta(\omega), \quad (4.75)$$

with:

$$\Delta(\omega) := v_{\text{SF}}(\omega) - \Sigma_{\text{xc}}(k_0(\omega)) \quad (4.76)$$

In contrast to the spectral potential, $\tilde{v}_{\text{SF}}(\omega)$ reproduces the band structure but not the spectral function, as I will now show.

The band structure is the zero of the equation $\omega - \tilde{\varepsilon}_k^{\text{SF}}(\omega) = 0$, with $\tilde{\varepsilon}_k^{\text{SF}}(\omega)$ the energy associated to the potential $\tilde{v}_{\text{SF}}(\omega)$, namely $\tilde{\varepsilon}_k^{\text{SF}}(\omega) = \varepsilon_k^0 + \tilde{v}_{\text{SF}}(\omega)$. Using eq. (4.74) and the definition of $k_0(\omega)$, the equation $\omega - \tilde{\varepsilon}_k^{\text{SF}}(\omega) = 0$ becomes:

$$\varepsilon_{k_0(\omega)}^0 - \varepsilon_k^0 = 0,$$

<i>effective potential</i>	<i>quasi particle equation</i>	<i>band structure</i>	<i>spectral function</i>
$\Sigma_{\text{xc}}(k)$	$\omega - \varepsilon_k^0 - \Sigma_{\text{xc}}(k) = 0$	$\varepsilon_k = \varepsilon_k^0 + \Sigma_{\text{xc}}(k)$	$A(\mathbf{r}, \mathbf{r}, \omega) = \frac{1}{2\pi^2} \int dk k^2 \delta(\omega - \varepsilon_k)$
$v_{\text{SF}}(\omega)$	$\omega - \varepsilon_k^{\text{SF}}(\omega) = 0$	$\varepsilon_k^{\text{SF}} = \varepsilon_k^{\text{SF}}(\varepsilon_k^{\text{SF}})$	$A_{\text{SF}}(\mathbf{r}, \mathbf{r}, \omega) = \frac{1}{2\pi^2} \int dk k^2 \delta(\omega - \varepsilon_k^{\text{SF}}(\omega))$
$\tilde{v}_{\text{SF}}(\omega)$	$\omega - \tilde{\varepsilon}_k^{\text{SF}}(\omega) = 0$	$\tilde{\varepsilon}_k^{\text{SF}} = \tilde{\varepsilon}_k^{\text{SF}}(\tilde{\varepsilon}_k^{\text{SF}}) = \varepsilon_k$	$\tilde{A}_{\text{SF}}(\mathbf{r}, \mathbf{r}, \omega) = \frac{1}{2\pi^2} \int dk k^2 \delta(\omega - \tilde{\varepsilon}_k^{\text{SF}}(\omega))$

Table 4.2: *Band structure and diagonal of the spectral function for the real system and the two auxiliary systems defined by $v_{\text{SF}}(\omega)$ and $\tilde{v}_{\text{SF}}(\omega)$.*

with the only solution $k = k_0(\omega)$, namely the band structure of the real system.

As for the diagonal of the spectral function, it reads:

$$\tilde{A}_{\text{SF}}(\mathbf{r}, \mathbf{r}, \omega) = \frac{1}{2\pi^2} \int_0^{+\infty} dk k^2 \delta(\omega - \tilde{\varepsilon}_k^{\text{SF}}(\omega)) = \frac{1}{2\pi^2} \int_0^{+\infty} dk k^2 \delta(\varepsilon_{k_0(\omega)}^0 - \varepsilon_k^0) = \frac{1}{2\pi^2} k_0(\omega), \quad (4.77)$$

which is the analogous of eq. (4.59) with $k_0(\omega)$ in place of $k_0^{\text{SF}}(\omega) = \sqrt{2(\omega - v_{\text{SF}}(\omega))}$; as the two k_0 s are different (apart from $\omega = \mu - W$ and $\omega \rightarrow \infty$, see eq. (4.64) or eq. (4.68)), also $\tilde{A}_{\text{SF}}(\mathbf{r}, \mathbf{r}, \omega)$ differs from $A_{\text{SF}}(\mathbf{r}, \mathbf{r}, \omega)$, and so from the real $A(\mathbf{r}, \mathbf{r}, \omega)$, too, as it is shown in fig. (4.22).

To conclude, if with $v_{\text{SF}}(\omega)$ we reproduce the exact $A(\mathbf{r}, \mathbf{r}, \omega)$ but the wrong band structure, with $\tilde{v}_{\text{SF}}(\omega)$ the band structure is exact but the spectral function is not, see also table 4.2. Thus $\tilde{v}_{\text{SF}}(\omega)$ is not a spectral potential, in accordance with the fact that the solution (4.63) of the generalized Sham–Schlüter equation (4.61) is unique.

A trick to have both A natural question arises at this point: is there a way to have, in the continuum limit, both the band structure and the spectral function by using a real and frequency-dependent local potential?

The answer is no, if we stick to the standard procedure of above; it is yes, if we change prescription: we first employ $\tilde{v}_{\text{SF}}(\omega)$ to get the correct band structure $\tilde{\varepsilon}_k^{\text{SF}}(\tilde{\varepsilon}_k^{\text{SF}}) = \varepsilon_k$, and then, from this, we evaluate the spectral function as a sum over delta peaks centered on ε_k :

$$\tilde{\tilde{A}}_{\text{SF}}(\mathbf{r}, \mathbf{r}, \omega) := \frac{1}{2\pi^2} \int_0^{+\infty} dk k^2 \delta(\omega - \tilde{\varepsilon}_k^{\text{SF}}), \quad (4.78)$$

which is equal to $A(\mathbf{r}, \mathbf{r}, \omega)$ as $\tilde{\varepsilon}_k^{\text{SF}} = \varepsilon_k$. Note that this prescription differs from the usual one that we used in eq. (4.77): there, $\tilde{\varepsilon}_k^{\text{SF}}(\omega)$ was a function of ω , while here $\tilde{\varepsilon}_k^{\text{SF}}$ is a k -dependent number, found from solving the equation $\omega - \tilde{\varepsilon}_k^{\text{SF}}(\omega) = 0$.

Eq. (4.78) can alternatively be viewed as the functional that yields the exact diagonal of the spectral function $A(\mathbf{r}, \mathbf{r}, \omega)$ in the system defined by $\tilde{v}_{\text{SF}}(\omega)$. That is a special case of what we discussed in paragraph 3.2.2. As in DFT there exists a functional of the density that yields the correct gap, but it is not the gap of the Kohn–Sham system, here we have a functional of the band structure, eq. (4.78), that yields the correct spectral function, even if it is not the spectral function we would evaluate from $\tilde{v}_{\text{SF}}(\omega)$.

To summarize, in the homogeneous electron gas the spectral potential $v_{\text{SF}}(\omega)$ can be explicitly found, and it does exactly what it is requested to do: it reproduces the diagonal of the spectral function of the real system, no more and no less; in particular, it does not reproduce the off diagonal elements of the spectral function, nor the band structure. If one wanted to have the latter, another potential must be introduced, which differs from the spectral potential by the additional term $\Delta(\omega)$; with such a potential the band structure is exactly reproduced,

but clearly not the spectral function. To have *also* the latter, another functional must be considered, the one of eq. (4.78), that yields the exact spectral function whenever the band structure is reproduced.

In this chapter, I have shown the capabilities (and the limits) of the spectral potential for three very different systems: an infinitely extended discrete system, the Hubbard model on the Bethe lattice, a finite and discrete system, the Hubbard dimer, and finally an infinite continuous system, the homogeneous electron gas. These systems are characterized by a non-trivial expression for the self energy: a complex-valued dynamical self energy in the first case, a fully complex, dynamical and non-local one for the dimer and a purely non-local self energy in the homogeneous electron gas. For each of these situations, the spectral potential, real, local and frequency dependent, can be explicitly found, and it can be used to replace the self energy for obtaining the diagonal of the spectral function. In some cases, symmetry plays a fundamental role and more quantities than expected are reproduced in the auxiliary system; this is the case for the dimer, where any element of the spectral function is reproduced, or the discrete homogeneous electron gas, whose auxiliary system displays both the exact spectral function as well as the exact band structure.

Still, the procedure employed here for obtaining the spectral potential always requires the full knowledge of the self energy; this approach is not efficient as soon as we abandon academic interest and we want an efficient way to study real materials. This is the issue of the next chapters.

Part III

The connector and dynLCA

*La spéculation est un luxe,
tandis que l'action est une nécessité.¹*

HENRY-LOUIS BERGSON, L'évolution créatrice

*What to do? Mon dieu, quoi faire?
Improvize, you idiot.*

PAUL GOLDING, The Abomination

¹Speculation is a luxury, whilst action is a necessity.

The connector

An approach based on an exact solution of the generalized Sham–Schlüter equation (3.24) (or its variants) is very interesting from the point of view of principle, but not efficient at all in practice. Aside from the technical problem of actually solving the equation, which is in general a non-linear integral matrix equation, an in principle dissatisfaction remains. Indeed, in that framework, one has first to evaluate both the exact Green’s function G and the full self energy Σ to feed the Sham–Schlüter equation, solve the equation self-consistently, find the spectral potential ν_{SF} , and finally evaluate the spectral function from ν_{SF} . A much more convenient strategy, if Σ and G are already at hand, is to directly calculate the spectral function from them, without the detour in the auxiliary system.

Indeed, the auxiliary system approach is useful whenever it offers a *true alternative* to the calculation in the real system. If, to evaluate the effective potential, we still have to pass through Σ and G , there is no much practical gain.

Therefore, if we want to construct an efficient strategy, we must get the effective potential somewhere else. A promising scheme, employed both in DFT and in DMFT, is represented by the introduction of a *model system* and a *connector*. The model system is a system in which we can afford to carry out the demanding calculation of the effective potential. Then, the effective potential in the auxiliary system is the one evaluated in the model, adapted by the connector. In other words, the connector is the prescription of how to import the effective potential in the auxiliary system.

To clarify what all of this means, let us have a look at the prototypical example of this approach: the local density approximation for density functional theory.

5.1 The connector idea: Local Density Approximation (LDA)

In the Kohn–Sham approach to density functional theory, too, we face the problem of how to find the Kohn–Sham potential $\nu_{\text{KS}}^{\text{xc}}(\mathbf{r})$. The very first solution to this issue, already presented in the same paper in which the general theory was developed [7], is to build a model system and take the potential from it.

The procedure focuses on the exchange–correlation part of the total energy $E_{\text{xc}}[n] = F[n] - T_s[n] - E_{\text{H}}[n]$, introduced at page 44. For an extended system, it is assumed that $E_{\text{xc}}[n]$ can be expressed as a sum of local contributions, each of which weighted by the local density, $E_{\text{xc}}[n] = \int d^3r n(\mathbf{r})\varepsilon_{\text{xc}}(\mathbf{r})$, see eq. (2.14).

One way to evaluate the purely Coulomb part of $\varepsilon_{\text{xc}}(\mathbf{r})$ is furnished by its exact expression

in terms of the exchange–correlation hole, eq. (2.14):

$$\varepsilon_{\text{xc}}^{(\text{C})}(\mathbf{r}) = \frac{1}{2} \int d^3 r' \frac{n_{\text{xc}}(\mathbf{r}, \mathbf{r}')}{|\mathbf{r} - \mathbf{r}'|}. \quad (5.1)$$

An analogous expression holds true here, where $E_{\text{xc}}[n]$ contains also the kinetic contribution $T[n] - T_{\text{s}}[n]$, which is absent from the expression in eq. (2.14). To account also for this additional term, n_{xc} is not given by eq. (2.12), but by an integration of $n_{\text{xc}}^{(\lambda)}$ over the coupling constant λ [115, 116], with $n_{\text{xc}}^{(\lambda)}$ obtained from eq. (2.12) in the case in which the bare Coulomb interaction is $\frac{\lambda}{|\mathbf{r} - \mathbf{r}'|}$ and the local density is fixed to $n(\mathbf{r})$:

$$\varepsilon_{\text{xc}}(\mathbf{r}) = \frac{1}{2} \int d^3 r' \int_0^1 d\lambda \frac{n_{\text{xc}}^{(\lambda)}(\mathbf{r}, \mathbf{r}')}{|\mathbf{r} - \mathbf{r}'|}. \quad (5.2)$$

By the Hohenberg–Kohn theorem, $n_{\text{xc}}^{(\lambda)}(\mathbf{r}, \mathbf{r}')$ is a functional of the density. However, it contains all the non-trivial many-body effects of the Coulomb interaction as well as the difference between $T[n]$ and $T_{\text{s}}[n]$, and an explicit form for it is hard to find.

On the other hand, $\varepsilon_{\text{xc}}(\mathbf{r})$ is a *local* quantity, to which a very important concept, the *near-sightedness principle* [117, 118, 43], applies. In simple words, it states that local quantities mostly depend on local properties of the system, like the local density, or the local external potential: each electron, in most of the cases, cannot see beyond its first neighbouring shells. Therefore, at least for slowly varying density, it seems reasonable to substitute each element of volume $d^3 r$ around \mathbf{r} with a *homogeneous system* having the same local density $n(\mathbf{r})$. This is clearly an approximation, but it is motivated by physical insight and it avoids evaluating the many-body quantity $n_{\text{xc}}(\mathbf{r}, \mathbf{r}')$. Indeed, in this approach, $\varepsilon_{\text{xc}}(\mathbf{r})$ is given by its value in a homogeneous system with density $n^h = n(\mathbf{r})$:

$$\varepsilon_{\text{xc}}^{\text{LDA}}(\mathbf{r}) = \varepsilon_{\text{xc}}^h(n^h = n(\mathbf{r})), \quad (5.3)$$

which is a much simpler quantity than (5.2). Moreover, from being a *functional* of the density function, eq. (5.2), $\varepsilon_{\text{xc}}(\mathbf{r})$ becomes a *function* of the local density $n(\mathbf{r})$. Therefore, the exchange–correlation energy reads:

$$E_{\text{xc}}^{\text{LDA}}[n] = \int d^3 r n(\mathbf{r}) \varepsilon_{\text{xc}}^h(n^h = n(\mathbf{r})). \quad (5.4)$$

So far, Hohenberg and Kohn [52]. How does this translate in the Kohn–Sham formalism [7]? There, an auxiliary system is introduced, in which particles interact with an external potential, the Kohn–Sham potential $v_{\text{KS}}(\mathbf{r})$. Its exchange–correlation part $v_{\text{KS}}^{\text{xc}}(\mathbf{r})$ is given by $v_{\text{xc}}(\mathbf{r}) := \frac{\delta E_{\text{xc}}[n]}{\delta n(\mathbf{r})}$. Using expression (5.4) for the exchange–correlation energy, the exchange–correlation potential in the LDA approximation reads:

$$\begin{aligned} v_{\text{LDA}}^{\text{xc}}(\mathbf{r}) &= \frac{\delta E_{\text{xc}}^{\text{LDA}}[n]}{\delta n(\mathbf{r})} = \varepsilon_{\text{xc}}^h(n^h = n(\mathbf{r})) + \int d^3 r' n(\mathbf{r}') \frac{\delta \varepsilon_{\text{xc}}^h(n^h = n(\mathbf{r}'))}{\delta n(\mathbf{r})} = \\ &= \varepsilon_{\text{xc}}^h(n^h = n(\mathbf{r})) + \left. \frac{d\varepsilon_{\text{xc}}^h(n^h)}{dn^h} \right|_{n^h = n(\mathbf{r})} = v_{\text{KS}}^{\text{xc}h}(n^h = n(\mathbf{r})), \end{aligned} \quad (5.5)$$

being $v_{\text{KS}}^{\text{xc}h}(n^h) = \frac{1}{V} \frac{dE_{\text{xc}}^h(n^h)}{dn^h}$ and $E_{\text{xc}}^h(n^h) = V n^h \varepsilon_{\text{xc}}^h(n^h)$. We thus obtain a very important result, which descends from eq. (5.3):

$$v_{\text{LDA}}^{\text{xc}}(\mathbf{r}) = v_{\text{KS}}^{\text{xc}h}(n^h = n(\mathbf{r})). \quad (5.6)$$

This equation can be interpreted as a practical prescription to obtain the Kohn–Sham potential: for each point \mathbf{r} we consider a *model system*, the homogeneous electron gas that has density

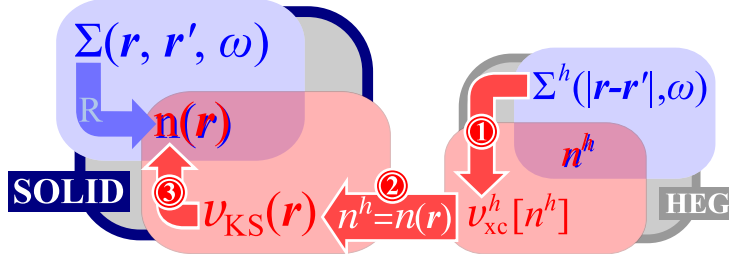


Figure 5.1: A schematic representation of LDA: to the left, the solid, with the real system (blue box) in which the density $n(\mathbf{r})$ is obtained from the self-energy, and the auxiliary system (red box), in which the same density is obtained from the Kohn–Sham potential. 1) To find the Kohn–Sham potential, we build a model system, the HEG, to the right. There we obtain v_{xc}^h , for example from the self energy Σ^h ; both yield the same density n^h . 2) The LDA prescription is to set n^h to the local density of the solid, $n(\mathbf{r})$. In this way, the HEG potential v_{xc}^h can be imported in the auxiliary system, where it becomes $v_{KS}(\mathbf{r})$. 3) Finally, from it, the density in the solid is evaluated.

n^h equal to the local density $n(\mathbf{r})$; assuming we know the exchange–correlation potential in the HEG for the density $n^h = n(\mathbf{r})$, $v_{KS}^{xc h}(n^h = n(\mathbf{r}))$, we take this as the local value of the potential in the auxiliary system, $v_{KS}^{xc}(\mathbf{r})$.

The approach can be generalized in the following way: we first decide that we will import $v_{KS}^{xc}(\mathbf{r})$ from a model system. We then choose the homogeneous electron gas as the model system, where the potential $v_{KS}^{xc h}(n^h)$ is at hand. Some questions naturally arise: how do we choose the density n^h of the HEG? How can we obtain a local quantity, $v_{KS}^{xc}(\mathbf{r})$, out of one that does not depend on \mathbf{r} , namely $v_{KS}^{xc h}(n^h)$? The answer dwells in the *connector*, that is the prescription that tells us how to use the potential obtained in the model system to represent the potential of the auxiliary system. The connector suggested by LDA is the local density, $n^h = n(\mathbf{r})$, see fig. 5.1.

Other connectors are possible. The average density \bar{n} corresponds to the *mean density approximation* (MDA): $v_{MDA}^{xc}(\mathbf{r}) = v_{KS}^{xc h}(n^h = \bar{n})$. A locally weighted density $\bar{n}(\mathbf{r})$ yields the *weighted density approximation* (WDA): $v_{WDA}^{xc}(\mathbf{r}) = v_{KS}^{xc h}(n^h = \bar{n}(\mathbf{r}))$. And so on.

In principle, we can even go beyond and introduce the concept of *exact connector*. It is a prescription (a machine) that to every point \mathbf{r} associates a homogeneous electron gas of density $n^h = \mathcal{E}(\mathbf{r})[n]$ such that the *exact* exchange–correlation potential in the auxiliary system is the exchange–correlation potential of the model system:

$$\forall \mathbf{r} \exists n^h = \mathcal{E}(\mathbf{r})[n] \quad | \quad v_{KS}^{xc}(\mathbf{r}) = v_{KS}^{xc h}(n^h). \quad (5.7)$$

This equation holds true if the range spanned by the potential in the auxiliary system is a subset of the range spanned by the potential of the model system. LDA, MDA and WDA can be viewed as approximations to the exact functional $\mathcal{E}(\mathbf{r})[n]$. For example, we recover LDA if we set $\mathcal{E}(\mathbf{r})[n] = n(\mathbf{r})$.

The LDA success The physical arguments that led to the LDA prescription, eq. (5.3), are reasonable and valid in the limit of slowly varying density [52, 7]. However, the success of LDA goes beyond this limit, and it is usually a very good approximation for a vast class of materials. The reason for this success has been explained by an important exact constraint that the LDA functional fulfills.

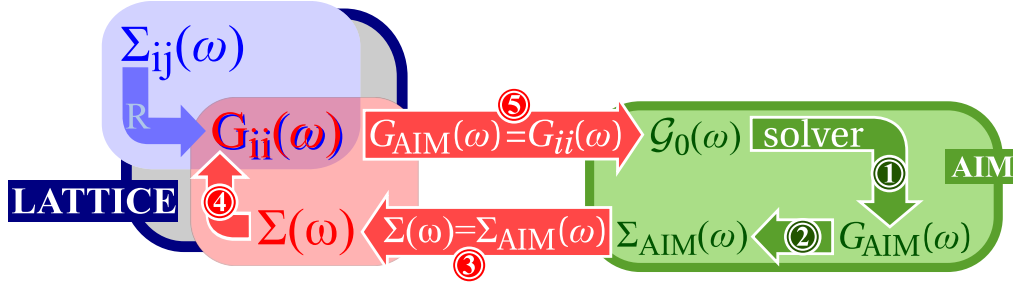


Figure 5.2: A schematic view of DMFT, explained in the text; the blue box represents the real system, the Hubbard model on the lattice. The red box is the auxiliary system, in which the self energy is local. The green box is the Anderson Impurity Model, the model system.

Indeed, due to the isotropic nature of the Coulomb interaction [46], eq. (5.1) reads:

$$\varepsilon_{xc}(\mathbf{r}) = \frac{1}{2} \int_0^{+\infty} d\rho \rho \int_{4\pi} d\Omega_\rho n_{xc}(\mathbf{r}, \mathbf{r} - \boldsymbol{\rho}), \quad (5.8)$$

with $n_{xc} = \int_0^1 d\lambda n_{xc}^{(\lambda)}$. From this equation it is clear that only the spherical average of $n_{xc}^{(\lambda)}$ is relevant to ε_{xc} , which is the quantity we import from the model. Although the exchange–correlation hole $n_{xc}^{(\lambda)}(\mathbf{r}, \mathbf{r}')$ in the LDA approximation can be very different from the expected one, it has been shown that LDA yields, in general, a good spherical average of it [119].

The LDA database A more practical reason for the success of the LDA approximation is represented by the fact that the model system it refers to, the homogeneous electron gas, is *one* system. It certainly depends on the value of the density n^h , but that can be considered as a parameter that can easily be tuned to the desired value.

This is a great advantage, as the LDA prescription does not require to solve a truly different model system for any different material under study. On the contrary, for every material, it always requires the solution of the same model for different parameters n^h .

One can indeed just refer to a database, with entries $(n, v_{KS}^{xc h}(n^h = n))$, that can be evaluated, with a certain accuracy, just once and for all [103]. The information stored in the database can be further compressed by a fitting [120] of the potential $v_{KS}^{xc h}(n^h)$ as a function of n^h ; a list of some proposed fittings is displayed in [102].

To conclude, LDA rests on three ingredients: the choice of the quantity to import (the exchange correlation density of energy, or the exchange correlation potential), the choice of a model system (the homogeneous electron gas), and finally the choice of the connector (the local density).

Other approaches, that rest on the same viewpoint, are possible.

5.2 Dynamical Mean Field Theory (DMFT)

Dynamical mean field theory, too, fits this framework: I left halfway the discussion on DMFT in section 3.6: an auxiliary system with a local self energy $\Sigma_{G_{loc}}(\omega) \equiv \Sigma(\omega)$ was introduced to reproduce the local part of the Green's function $G_{loc}(\omega) \equiv G_{ii}(\omega)$.

How to find the effective potential $\Sigma(\omega)$ is the big issue. The DMFT strategy is to import it from a model system, the Anderson Impurity model (AIM), which is a single site system embedded in a bath, described by the Green's function $G_{AIM}(\omega)$. As the HEG was determined by the

parameter n^h , also the AIM is fixed by its non-interacting properties, namely the energy levels of the bath and the coupling between the bath and the site; these define the non-interacting Green's function of the AIM, $\mathcal{G}_0^{-1}(\omega) := \omega - \Delta(\omega)$, with $\Delta(\omega)$ hybridization function, which is of fundamental importance for DMFT.

Once the hybridization function is at hand, one employs a solver to solve the model and obtain the fully interacting Green's function of the model, $G_{\text{AIM}}(\omega)$ (step 1 in fig. 5.2). From the Dyson equation, then, the self energy of the model is $\Sigma_{\text{AIM}}(\omega) = \mathcal{G}_0^{-1}(\omega) - G_{\text{AIM}}^{-1}(\omega)$ (step 2).

This is then imported in the auxiliary system as the effective potential $\Sigma(\omega) = \Sigma_{\text{AIM}}(\omega)$ (step 3), and it is used to evaluate the local Green's function $G_{ii}(\omega)$ (step 4).

But a question remains: which AIM should one use in the beginning? The answer dwells in the connector, which has not – so far – been fixed. The DMFT approach is to use the Green's function itself as a connector: the AIM Green's function $G_{\text{AIM}}(\omega)$ must be equal to the local Green's function of the auxiliary system $G_{ii}(\omega)$ (step 5). This generates a loop, represented by the following equations (with l number of the iteration):

1. $\mathcal{G}_0^{(l)}(\omega) \xrightarrow{\text{solver}} G_{\text{AIM}}^{(l)}(\omega)$
2. $\Sigma_{\text{AIM}}^{(l)}(\omega) = \mathcal{G}_0^{(l)-1}(\omega) - G_{\text{AIM}}^{(l)-1}(\omega)$
3. $\Sigma^{(l)}(\omega) = \Sigma_{\text{AIM}}^{(l)}(\omega)$
4. $\Sigma^{(l)}(\omega) \longrightarrow G_{ii}^{(l)}(\omega)$
5. Update: $G_{\text{AIM}}^{(l+1)}(\omega) = G_{ii}^{(l)}(\omega)$
 $\mathcal{G}_0^{(l+1)-1}(\omega) = G_{\text{AIM}}^{(l+1)-1}(\omega) + \Sigma_{\text{AIM}}^{(l)}(\omega)$,

(5.9)

that can be iterated until self consistency.

This way of viewing DMFT highlights the interplaying roles of the real system, the auxiliary system and the model system, in pretty much the same way as LDA: the quantity to import is different, the model system is different and the connector, too, is different, but the idea is the same.

However, there is a more fundamental contrast between DMFT and LDA, which resides in a difference between the model systems they employ, AIM and HEG. The latter, indeed, can be solved for a wide range of densities even before a real material is considered: one has just to fix a density n^h and solve the system (as we did in section 4.3). The same procedure is not pursued in the AIM: the hybridization factor $\Delta(\omega)$, that defines the non-interacting part of the AIM, depends on the particular real system under consideration, and the solver generates a truly different solution for every different $\Delta(\omega)$. Therefore, no database is available, and one has to solve the model system from scratch, at each iteration step, every time a new system is studied.

This is clearly not efficient if the aim is to have a reliable but quick way of obtaining the spectral function.

5.3 A generalization

These two paradigmatic examples, LDA and DMFT, show how one can obtain the effective potential of the auxiliary system from a model system. In the LDA case, the effective potential is the exchange–correlation part of the Kohn–Sham potential; in DMFT, it is the local self energy.

We can generalize this approach to generic auxiliary systems, like the ones introduced in section 3.2. There we focused on the observable $p(\{\lambda_i\})$, whose value can alternatively be obtained in the real system, through the self energy Σ , and in the auxiliary system, through the effective potential $v_p(\{\mu_j\})$.

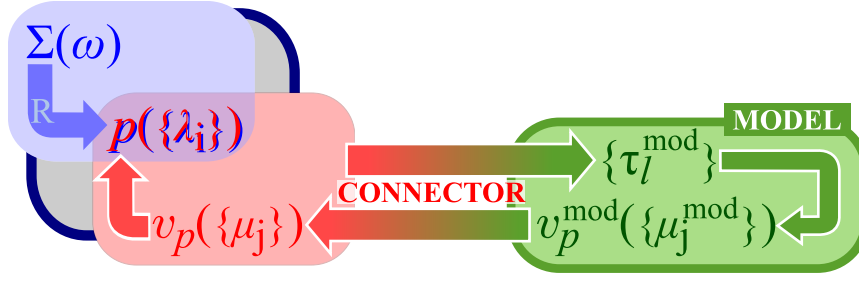


Figure 5.3: A general model system approach to find the effective potential of the auxiliary system.

The generalized Sham–Schlüter approach, eq. (3.5), is in principle exact way of finding the value of $v_p(\{\mu_j\})$. However, it is not efficient as it requires the knowledge of both Green's function and self energy of the real system.

The model An alternative strategy is followed by LDA and DMFT. It amounts to building another system, the *model system*, with just two characteristics: 1) It must be solvable (even approximately); 2) It must provide some quantity which we can identify as the analogous of $v_p(\{\mu_j\})$, which we call $v_p^{\text{mod}}(\{\mu_j^{\text{mod}}\})$. A third characteristic is desirable, but not mandatory: 3) The model system, and therefore the quantity $v_p^{\text{mod}}(\{\mu_j^{\text{mod}}\})$, should possess some tunable parameters $\{\tau_l^{\text{mod}}\}$ which we can change in order to be as close as possible to the auxiliary system. A model system with no tunable parameters is still an acceptable model, but it is likely to be too rigid to provide a good source for the effective potential in the auxiliary system (see next chapter on the asymmetric Hubbard dimer).

In DMFT, the model system is the Anderson Impurity Model. Its non-interacting part is described by the hybridization function $\Delta(\omega)$, which plays the role of the tunable parameter. Clearly, a tunable *function* means a huge amount of freedom to define the system; on the one hand, this allows to be as close as possible to the auxiliary system; on the other, it makes more difficult to find an *a priori* solution that could be saved and stored. However, once the tunable parameter $\Delta(\omega)$ is fixed, the model is solvable, via a solver. Finally, the self energy of the model is considered as the analogous of the self energy of the auxiliary system, and therefore imported there.

LDA is similar: the model system is the homogeneous electron gas. It has a single tunable parameter, its density n^h that, for instance, can be tuned to the local density, and it is solvable, approximately or numerically [103]. LDA replicates the scheme real/auxiliary system also in the model system (see fig. 5.1), hence the natural analogous of $v_{\text{KS}}^{\text{xc}}(\mathbf{r})$ is $v_{\text{KS}}^{\text{xc}h}$, and this is indeed the quantity LDA imports.

The connector Set up and solved the model for $v_p^{\text{mod}}(\{\mu_j^{\text{mod}}\})$, the question is how to use this quantity in the auxiliary system: which is the *prescription* to transform $v_p^{\text{mod}}(\{\mu_j^{\text{mod}}\})$, which depends on the choice of the model through $\{\tau_l^{\text{mod}}\}$, into the effective potential $v_p(\{\mu_j\})$ of the auxiliary system?

The answer is the *connector*. It is a prescription that states how to import the potential of the model system into the auxiliary system. Such a prescription is extremely general: it can consist of tuning the parameters of the model system, $\{\tau_l^{\text{mod}}\}$, as well as in a relation between the degrees of freedom $\{\mu_j^{\text{mod}}\}$ of the potential of the model system and the corresponding ones in the auxiliary system, $\{\mu_j\}$.

Does the exact connector exist? As we already discussed in the case of LDA, if the range

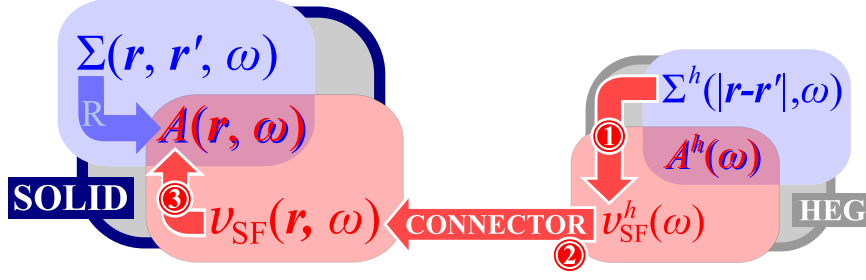


Figure 5.4: A schematic view of dynLCA; the blue box represents the real system, the red one the auxiliary system. To the left the solid and to the right the model.

spanned by the potential we want to find, $v_p(\{\mu_j\})$, is a subset of the range spanned by the potential of the model system, $v_p^{\text{mod}}(\{\mu_j^{\text{mod}}\})$, even changing the model system, namely tuning the parameters $\{\tau_l^{\text{mod}}\}$, then, in principle, an exact connector (a machine) does exist. In formulas, there exists a functional \mathcal{C} that, for every $v_p(\{\mu_j\})$ in the auxiliary system associates the corresponding potential in the model system: $v_p^{\text{mod}}(\{\mu_j^{\text{mod}}\}) = \mathcal{C}_{\{\tau_l^{\text{mod}}\}}[v_p(\{\mu_j\})]$.

Clearly, finding the exact connector in practice is another story. Indeed, the model system is usually a simplified version of the real one, with less degrees of freedom. The exact connector, therefore, must be able to bring back in v_p the degrees of freedom needed for the evaluation of p .

For example, in LDA, the model system, the HEG, does not account for the inhomogeneities of the real system; the connector $n^h = n(\mathbf{r})$ reestablishes a dependence on \mathbf{r} ; however, the possible dependence of $v_{\text{KS}}^{\text{xc}}(\mathbf{r})$ on densities other than $n(\mathbf{r})$ is not accounted for by this connector. That is why attempts to go beyond LDA are, for instance, the GGA functionals, in which also the derivative of the density is taken into account by the connector.

Note that, eventually, if one had exactly solved the model system for $v_p^{\text{mod}}(\{\mu_j^{\text{mod}}\})$ and knew the exact connector, the exact quantity $p(\{\lambda_i\})$ would be available, without passing through the real system. The amount of information carried by the self energy in the real system is exactly equivalent to the information carried by the potential in the model system plus the information carried by the connector.

To which extent one can disentangle the whole self energy information into a model potential plus a connector is an interesting issue. For example, if in DFT we choose to take the Kohn–Sham potential from the homogeneous electron gas, it is clear that all the inhomogeneities are lost there; if one wants the exact Kohn–Sham potential, these inhomogeneities must be restored by the connector.

5.4 The dynamical local connector approximation (dynLCA)

Having introduced a general scheme to find the effective potential in a model system, it is time to turn to the spectral function and its auxiliary system. In section 3.5, we have shown that the diagonal of the spectral function in the real system, $A(\mathbf{r}, \mathbf{r}, \omega)$, can be obtained in an auxiliary system in which particles interact via a local, real, and frequency–dependent potential, the spectral potential $v_{\text{SF}}(\mathbf{r}, \omega)$.

One way to find this potential is solving the generalized Sham–Schlüter equation (3.23). As already said, this method is not efficient, as it requires the knowledge of both Green’s function and self energy in the real system, which we do not want to evaluate.

The strategy we want to follow, instead, is the same employed by LDA and DMFT: build a

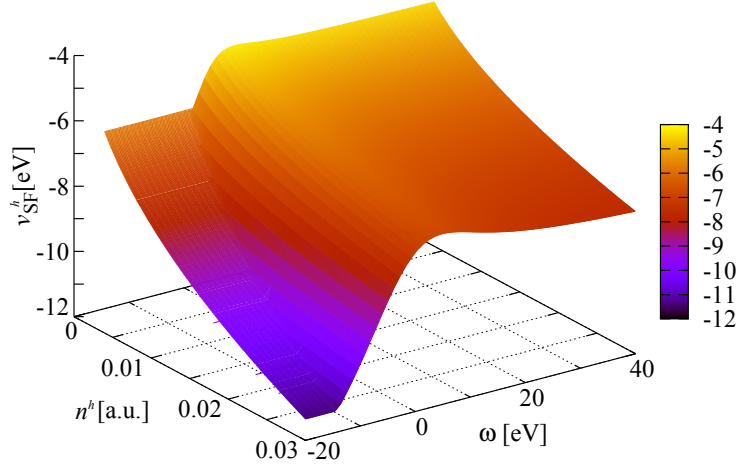


Figure 5.5: HSE06 spectral potential $v_{SF}^h(\omega)$ (in eV) in the HEG as a function of frequency (in eV), for different values of densities (in a_0^{-3}), ranging from $n^h = 3.93 \cdot 10^{-3} a_0^{-3}$ ($r_s = 3.93 a_0$, corresponding to sodium) to $n^h = 3.26 \cdot 10^{-2} a_0^{-3}$ ($r_s = 1.94 a_0$, argon).

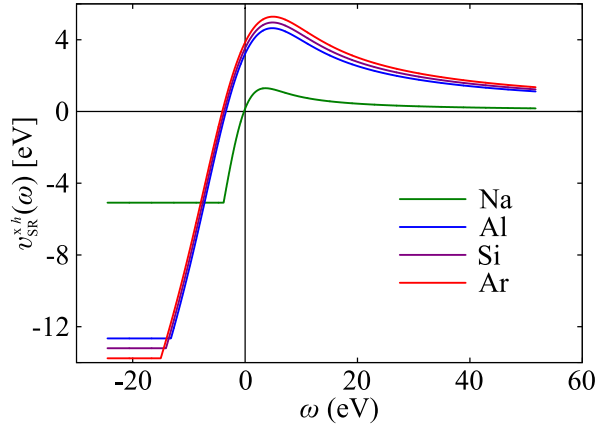


Figure 5.6: The purely frequency-dependent part $v_{SR}^{xh}(\omega)$ of the spectral potential of fig. 5.5 as a function of frequency, in eV, for the average densities of the four materials that we will consider.

model system and import the effective potential from it.

The model system The first natural question is: which model system do we choose?

There is no one single exact response to this problem, but just different possible strategies. The one we follow here is to stick to the LDA choice and use, as a model system, the homogeneous electron gas. The reasons are different: first, it is a sufficiently simple system, for which one can find the spectral function corresponding to some approximation to the self energy [121, 122, 123, 124], and therefore the spectral potential, as we did in section 4.3 for the hybrids approximation.

Second, the model is determined by one simple tunable parameter n^h , its density, nothing more; therefore, one could consider of solving the model for a wide range of densities and store the resulting spectral potentials, without need of solving the model each time a new system is considered, like in DMFT.

Third, the homogeneous electron gas is already a good approximation for systems of slowly varying density.

	LDA	DMFT	dynLCA
$p(\{\lambda_i\})$	$n(\mathbf{r})$	$G_{ii}(\omega)$	$A(\mathbf{r}, \mathbf{r}, \omega)$
$v_p(\{\mu_j\})$	$v_{\text{KS}}^{\text{xc}}(\mathbf{r})$	$\Sigma(\omega)$	$v_{\text{SF}}(\mathbf{r}, \omega)$
<i>model system</i>	HEG	AIM	HEG
$v_p^{\text{mod}}(\{\mu_j^{\text{mod}}\})$	$v_{\text{KS}}^{\text{xc}h}$	$\Sigma_{\text{AIM}}(\omega)$	$v_{\text{SF}}^h(\omega)$
$\{\tau_l^{\text{mod}}\}$	n^h	$\Delta(\omega)$	n^h
<i>connector</i>	$n^h = n(\mathbf{r})$	$G_{\text{AIM}}(\omega) = G_{ii}(\omega)$	$A^h(\omega - c) = A(\mathbf{r}, \mathbf{r}, \omega)$
<i>prescription</i>	$v_{\text{KS}}^{\text{xc}}(\mathbf{r}) =$ $= v_{\text{KS}}^{\text{xc}h} n^h = n(\mathbf{r})$	$\Sigma_{\text{AIM}}(\omega) =$ $= \Sigma(\omega)_{G_{\text{AIM}}(\omega) = G_{ii}(\omega)}$	$v_{\text{SF}}(\mathbf{r}, \omega) =$ $= v_{\text{SF}}^h n^h = \dots(\omega + \dots)$

Table 5.1: Auxiliary and model systems for LDA, DMFT and dynLCA: the quantity of interest $p(\{\lambda_i\})$, the effective potential in the auxiliary system $v_p(\{\mu_j\})$, model system potential and parameters and finally the connector.

Fourth, in most of the cases we can consider a system as locally similar to a homogeneous electron gas at the local density (nearsightedness principle).

For these reasons, the homogeneous electron gas will be our model system. There, both the real system and the auxiliary system are easier to solve. In particular, for the HSE06 approximation to the self energy, I showed in section 4.3 that the spectral function in the real system is even analytical, eq. (4.53). From it, a closed expression for the spectral potential can be easily obtained, eq. (4.63). The procedure $\Sigma^h \rightarrow A^h \rightarrow v_{\text{SF}}^h$ is in principle equivalent to a solution of the generalized Sham–Schlüter equation in the HEG, which is represented by the arrow (1) in figure 5.4.

Once the spectral potential $v_{\text{SF}}^h(\omega)[n^h]$ has been obtained for a value of n^h , one should carry out the same calculation for several values of n^h , obtaining plenty of these potentials. Eventually one stores all of these data in a file. This file will be ready to be read whenever the potential of the model for a particular density and at a particular frequency is needed in the auxiliary system.

Note that, even if the evaluation of the spectral potential in the model system would be time-consuming, it would be nonetheless worthwhile. Indeed, the model system we have chosen must be solved just one time. In principle, *every* real material will refer to that same calculation. Therefore, a little effort is not a waste.

The result of this procedure for the HSE06 self energy of section 4.3 is shown in fig. 5.5: the frequency-dependent spectral potential $v_{\text{SF}}^h(\omega)$ for densities ranging from $n^h = 3.93 \cdot 10^{-3} a_0^{-3}$ (average density of sodium) to $n^h = 3.26 \cdot 10^{-2} a_0^{-3}$ (average density of argon). The data needed to plot that picture are freely available on the ETSF website, <https://etsf.polytechnique.fr/research/connector/dynLCA>. They can be downloaded and used by anyone who would like to do a HSE06 calculation on whatever material.

Finally, note that the spectral potential, both as a function of frequency and of n^h , is pretty smooth¹. Therefore, one can think, in a second time, about fitting the dependence of v_{SF}^h on ω and n^h , obtaining an even lighter (hence more efficient) method for carrying the model system data.

¹I remind that, below the bottom of the occupied band, many definitions of the potential are possible, that can make the potential smooth even in the region around the bottom of the band itself (see section 4.3).

5.5 The connector

Once the potential is at hand, it must be imported in the auxiliary system. This is the most difficult part of the method, as we would like a universal connector, namely a single prescription that, for any real material (a metal or an insulator), tells us how to modify the spectral potential of the HEG in order to exactly reproduce the diagonal in space of its spectral function.

The connector must depend on simple quantities of the auxiliary system, like the Kohn–Sham potential or the local density. Through these, it must be able to bring back some dependence on \mathbf{r} in the model system potential $v_{\text{SF}}^h(\omega)$, which is clearly completely absent in the HEG.

5.5.1 General structure of the connector

An equation that relates the diagonal of spectral function of the solid, $A_{\text{SF}}(\mathbf{r}, \mathbf{r}, \omega)$, with the one of the model (the homogeneous electron gas), $A_{\text{SF}|n^h}^h(\omega)$, both seen in their corresponding auxiliary system and both evaluated with the same expression for the self energy, is not straightforward. The reason is that the two spectral functions are usually very different: for instance, the homogeneous electron gas is always a well-behaved metal, while the real system can present gaps, spikes, isolated non-dispersive bands, and so on.

This is where the connector idea comes into play. For each point \mathbf{r} and each frequency ω , $A_{\text{SF}}(\mathbf{r}, \mathbf{r}, \omega)$ is just a real positive number. This number belongs for sure to the range of $A_{\text{SF}|n^h}^h(\omega)$, which is $[0, +\infty)$ in most cases (see fig. 4.17).

Naively, one could introduce a function $\mathcal{F}(\mathbf{r}, \omega)$, which, by the Hohenberg–Kohn theorem, is a functional of density, through which:

$$A_{\text{SF}}(\mathbf{r}, \mathbf{r}, \omega) = A_{\text{SF}|n^h=\mathcal{F}(\mathbf{r}, \omega)[n]}^h(\omega - \mu + \mu_{n^h=\mathcal{F}(\mathbf{r}, \omega)[n]}^h). \quad (5.10)$$

In this formula the chemical potential of the solid μ has been aligned with the one of the model system $\mu_{n^h}^h$ in order to define energy in the two systems. In this way, one fixes the frequency argument of the model spectral function, and just selects a particular density n^h of the model system, taking advantage of the fact that, by tuning that parameter, $A_{\text{SF}|n^h}^h(\omega - \mu + \mu^h)$ can assume whatever positive number. However, this equation cannot hold in general. In particular, problems arise in the unoccupied region. There, the smallest possible value for $A_{\text{SF}|n^h}^h(\omega - \mu + \mu^h)$ is $A_{\text{SF}|n^h=0}^h(\omega - \mu + \mu_{n^h=0}^h)$, namely the spectral function of the homogeneous electron gas with no electrons at all. If, for some \mathbf{r} , $A_{\text{SF}}(\mathbf{r}, \mathbf{r}, \omega - \mu)$ is smaller than $A_{\text{SF}|n^h=0}^h(\omega - \mu_{n^h=0}^h)$ (for instance, a gap in the unoccupied band, where $A_{\text{SF}}(\mathbf{r}, \mathbf{r}, \omega) = 0$), it cannot be represented by eq. (5.10). This is shown in figure 5.7.

The reason of the failure suggests also the way to overcome the problem. Indeed, as can be seen from fig. 5.7 one just needs to shift the chemical potential of the model system to be able to catch also the part of the spectrum in the shaded area. This new approach amounts to a shift of the frequency argument, independent of the chemical potential $\mu_{n^h}^h$, that allows small values of $A_{\text{SF}|n^h}^h(\omega)$ also in the empty part of the spectrum of the solid. Therefore, we introduce a non-trivial *correction* $c(\mathbf{r}, \omega)$ in the frequency argument of $A_{\text{SF}|n^h}^h(\omega)$, which in principle allows for a complete reshaping of the spectral function of the model system:

$$A_{\text{SF}}(\mathbf{r}, \mathbf{r}, \omega) = A_{\text{SF}|n^h=\mathcal{F}(\mathbf{r}, \omega)[n]}^h(\omega - c(\mathbf{r}, \omega)). \quad (5.11)$$

With such a general c , we can restrict \mathcal{F} to a simpler functional of the density, the local density. Of course, different choices are possible, like an average density or a weighted density, or leave

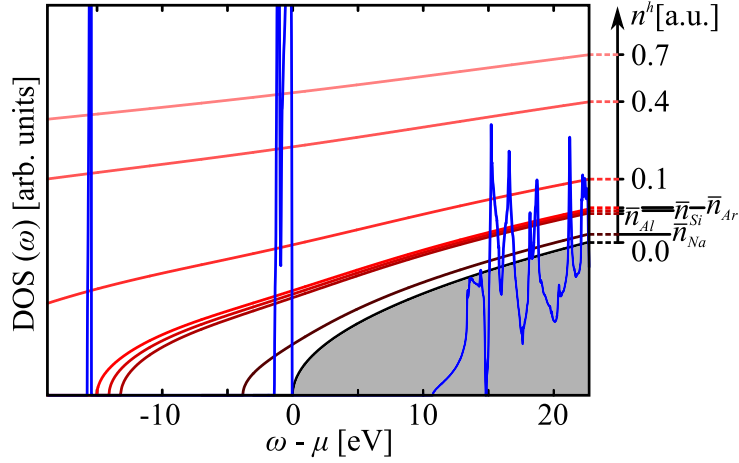


Figure 5.7: Schematic representation of the discussion at pag. 102. In blue, $A_{\text{SF}}(\mathbf{r}, \mathbf{r}, \omega)$ (the DOS of Argon obtained with the hybrids self energy), while in different shades of red some $A_{\text{SF}|n^h}^h(\omega)$ corresponding to different densities n^h (the curves corresponding to homogeneous electron gases with the average densities of sodium, aluminum, silicon and argon are included). All spectra are aligned with their Fermi energies at $\omega = 0$. If the blue spectrum lays in the shaded area, no homogeneous electron gas exists which is able to reproduce it.

a more general functional $\mathcal{F}[n(\mathbf{r})]$. It can be shown that the final results do not depend too much on this choice. The important point is that we remove the frequency dependence from the choice of the homogeneous electron gas (which n^h) to use. Thus, we assume the following ansatz:

$$A_{\text{SF}}(\mathbf{r}, \mathbf{r}, \omega) = A_{\text{SF}|n^h=n(\mathbf{r})}^h(\omega - c(\mathbf{r}, \omega)). \quad (5.12)$$

Sham–Schlüter approach If eq. (5.12) holds, a Sham–Schlüter equation can be set up. The auxiliary system Green’s functions for the solid and for the model are G_{SF} and G_{SF}^h respectively, where we drop the subscript $n^h = n(\mathbf{r})$, which is implied. They can be derived from the same non–interacting Green’s function G_0 via the following inverted Dyson equations:

$$\begin{aligned} G_{\text{SF}}^{-1}(\mathbf{r}, \mathbf{r}', \omega) &= G_0^{-1}(\mathbf{r}, \mathbf{r}', \omega) - \left[v^{\text{ext}}(\mathbf{r}) + v_{\text{H}}(\mathbf{r}) + v_{\text{SF}}^{\text{xc}}(\mathbf{r}, \omega) \right] \delta(\mathbf{r} - \mathbf{r}') \\ G_{\text{SF}}^{h-1}(\mathbf{r}, \mathbf{r}', \omega) &= G_0^{-1}(\mathbf{r}, \mathbf{r}', \omega) - v_{\text{SF}}^h(\omega) \delta(\mathbf{r} - \mathbf{r}') \end{aligned} \quad (5.13)$$

with $G_0^{-1}(\mathbf{r}, \mathbf{r}', \omega) = \delta(\mathbf{r} - \mathbf{r}') \left[\omega - \left(-\frac{\nabla^2}{2} \right) \right]$ for both systems. In the framework of auxiliary systems, these relations are in principle exact. By shifting the frequency argument of $c(\mathbf{r}, \omega)$, from the second of eq. (5.13), $G_{\text{SF}}^{h-1}(\mathbf{r}, \mathbf{r}', \omega - c(\mathbf{r}, \omega))$ is equal to:

$$G_{\text{SF}}^{h-1}(\mathbf{r}, \mathbf{r}', \omega - c(\mathbf{r}, \omega)) = G_0^{-1}(\mathbf{r}, \mathbf{r}', \omega) - \left[v_{\text{SF}}^h(\omega - c(\mathbf{r}, \omega)) + c(\mathbf{r}, \omega) \right] \delta(\mathbf{r} - \mathbf{r}') \quad (5.14)$$

This equation is exact in the homogeneous electron gas, and we implement it in the solid by localizing $c(\omega)$ in the spirit of LDA. Thus, one can bypass G_0^{-1} and directly relate $G_{\text{SF}}^{-1}(\mathbf{r}, \mathbf{r}', \omega)$ to $G_{\text{SF}}^{h-1}(\mathbf{r}, \mathbf{r}', \omega - c(\mathbf{r}, \omega))$:

$$\begin{aligned} G_{\text{SF}}^{-1}(\mathbf{r}, \mathbf{r}', \omega) &= G_{\text{SF}}^{h-1}(\mathbf{r}, \mathbf{r}', \omega - c(\mathbf{r}, \omega)) + \\ &\quad - \left\{ v^{\text{ext}}(\mathbf{r}) + v_{\text{H}}(\mathbf{r}) + v_{\text{SF}}^{\text{xc}}(\mathbf{r}, \omega) - c(\mathbf{r}, \omega) - v_{\text{SF}}^h(\omega - c(\mathbf{r}, \omega)) \right\} \delta(\mathbf{r} - \mathbf{r}'). \end{aligned}$$

Inverting this equation, we obtain a Dyson-like equation between G_{SF} and G_{SF}^h :

$$G_{\text{SF}}(\mathbf{r}, \mathbf{r}', \omega) = G_{\text{SF}}^h(\mathbf{r}, \mathbf{r}', \omega - c(\mathbf{r}, \omega)) + \int d\bar{\mathbf{r}} G_{\text{SF}}^h(\mathbf{r}, \bar{\mathbf{r}}, \omega - c(\mathbf{r}, \omega)) \left\{ v_{\text{SF}}^{\text{xc}}(\bar{\mathbf{r}}, \omega) - v_{\text{SF}}^h(\omega - c(\bar{\mathbf{r}}, \omega)) - c(\bar{\mathbf{r}}, \omega) + v^{\text{ext}}(\bar{\mathbf{r}}) + v_{\text{H}}(\bar{\mathbf{r}}) \right\} G_{\text{SF}}(\bar{\mathbf{r}}, \mathbf{r}', \omega).$$

To this expression one can now apply eq. (5.12), and obtain:

$$0 = \int d\bar{\mathbf{r}} \left\{ v_{\text{SF}}^{\text{xc}}(\bar{\mathbf{r}}, \omega) - v_{\text{SF}}^h(\omega - c(\bar{\mathbf{r}}, \omega)) - c(\bar{\mathbf{r}}, \omega) + v^{\text{ext}}(\bar{\mathbf{r}}) + v_{\text{H}}(\bar{\mathbf{r}}) \right\} \times \text{Im} \left[G_{\text{SF}}^h(\mathbf{r}, \bar{\mathbf{r}}, \omega - c(\mathbf{r}, \omega)) G_{\text{SF}}(\bar{\mathbf{r}}, \mathbf{r}, \omega) \right],$$

which can be solved by setting to zero the kernel in curly brackets. This yields the desired relation between the potentials:

$$\boxed{v_{\text{SF}}^{\text{xc}}(\mathbf{r}, \omega) = v_{\text{SF}|n^h=n(\mathbf{r})}^h(\omega - c(\mathbf{r}, \omega)) + c(\mathbf{r}, \omega) - v^{\text{ext}}(\mathbf{r}) - v_{\text{H}}(\mathbf{r})} \quad (5.15)$$

or, adding the external and the Hartree potentials to the exchange–correlation part of the spectral potential:

$$v_{\text{SF}}(\mathbf{r}, \omega) = v_{\text{SF}|n^h=n(\mathbf{r})}^h(\omega - c(\mathbf{r}, \omega)) + c(\mathbf{r}, \omega). \quad (5.16)$$

Homogeneous systems If the system under consideration is the homogeneous electron gas itself, in which $v^{\text{ext}} + v_{\text{H}} = 0$, the previous equation must be equivalent to the identity $v_{\text{SF}}^{\text{xc}}(\mathbf{r}, \omega) = v_{\text{SF}|n^h=n^h}^h(\omega)$; this is the case if $c^h(\omega) = 0$. More interesting is a homogeneous system in which $v^{\text{ext}} + v_{\text{H}} \neq 0$. In such a case, the resulting spectrum is just a rigid shift (by $v^{\text{ext}} + v_{\text{H}}$) of the spectrum of the homogeneous electron gas, hence, from eq. (5.12), $c(\omega) = v^{\text{ext}} + v_{\text{H}}$, and eq. (5.15) reads:

$$v_{\text{SF}}^{\text{xc}}(\mathbf{r}, \omega) = v_{\text{SF}|n^h=n}^h(\omega - v^{\text{ext}} - v_{\text{H}}) \quad \text{if } n(\mathbf{r}) = n$$

For such a system, the chemical potential is $\mu = \frac{k_F^2}{2} + v^{\text{ext}} + v_{\text{H}} + \Sigma^h(k_F)$, with $k_F = (3\pi^2 n)^{1/3}$. For the homogeneous electron gas with density $n^h = n$, the chemical potential is $\mu^h = \frac{k_F^2}{2} + \Sigma^h(k_F)$, with the same k_F , which is determined by the density only. It follows that $v^{\text{ext}} + v_{\text{H}} = \mu - \mu^h$, and the previous equation becomes:

$$v_{\text{SF}}^{\text{xc}}(\mathbf{r}, \omega) = v_{\text{SF}|n^h=n}^h(\omega - \mu + \mu^h) \quad \text{if } n(\mathbf{r}) = n \quad (5.17)$$

This is the connector we will start from to treat real system in the next chapter. We will finally realize that a more powerful prescription is needed, in the spirit of eq. (5.15), with a non-trivial choice of $c(\mathbf{r}, \omega)$.

5.5.2 Perturbation expansion

The structure of eq. (5.15) is confirmed by a first order perturbation expansion in the external potential. Indeed, one can assume the existence of the spectral potential $v_{\text{SF}}^h(\omega)$ in the homogeneous model system, where $v^{\text{ext}} + v_{\text{H}} = 0$, and then turn on a small perturbation $\delta v^{\text{ext}}(\mathbf{r})$. The analysis is carried out in appendix G, eq. (G.5); the resulting exchange–correlation part of the spectral potential reads:

$$v_{\text{SF}}^{\text{xc}}(\mathbf{r}, \omega) = v_{\text{SF}}^h(\omega) + \int_{\mathbf{x}, \mathbf{y}, \mathbf{z}} \tilde{\zeta}_{\text{SF}}^{h-1}(\mathbf{r}, \mathbf{x}, \omega) \text{Im} \left[G^h(\mathbf{x}, \mathbf{y}, \omega) \left[(\delta v^{\text{ext}}(\mathbf{y}) + \delta v_{\text{H}}(\mathbf{y})) \delta(\mathbf{y} - \mathbf{z}) + \delta \Sigma(\mathbf{y}, \mathbf{z}, \omega) \right] G^h(\mathbf{z}, \mathbf{x}, \omega) \right] - (\delta v^{\text{ext}}(\mathbf{r}) + \delta v_{\text{H}}(\mathbf{r})), \quad (5.18)$$

with, at the right hand side, the first order changes in the Hartree potential $\delta v_H(\mathbf{r})$ and in the self energy $\delta\Sigma(\mathbf{y}, \mathbf{z}, \omega)$, stemming from the small inhomogeneity driven by $\delta v^{\text{ext}}(\mathbf{r})$. These quantities, pertaining to the real system, are handled by Green's functions of the homogeneous system only, which we can in principle evaluate just once and for all, no matter $\delta v^{\text{ext}}(\mathbf{r})$. These are the Green's function $G^h(\mathbf{r}, \mathbf{r}', \omega)$, its auxiliary system counterpart $G_{\text{SF}}^h(\mathbf{r}, \mathbf{r}', \omega)$, and the quantity $\tilde{\zeta}_{\text{SF}}^h(\mathbf{r}, \mathbf{r}', \omega) := \text{Im} [G_{\text{SF}}^h(\mathbf{r}, \mathbf{r}', \omega) G_{\text{SF}}^h(\mathbf{r}', \mathbf{r}, \omega)]$.

A further decomposition is useful for the discussion (compare with eq. (G.7) of appendix G): we can gather the terms involving the external and the Hartree potential on the one hand, and the term involving the self energy on the other. The result is:

$$\begin{aligned} v_{\text{SF}}^{\text{xc}}(\mathbf{r}, \omega) = & \left\{ v_{\text{SF}}^h(\omega) + \int_{\mathbf{x}, \mathbf{y}, \mathbf{z}} \tilde{\zeta}_{\text{SF}}^{h-1}(\mathbf{r}, \mathbf{x}, \omega) \text{Im} \left[G^h(\mathbf{x}, \mathbf{y}, \omega) \delta\Sigma(\mathbf{y}, \mathbf{z}, \omega) G^h(\mathbf{z}, \mathbf{x}, \omega) \right] \right\} + \\ & + \int_{\mathbf{y}} \left[\int_{\mathbf{x}} \tilde{\zeta}_{\text{SF}}^{h-1}(\mathbf{r}, \mathbf{x}, \omega) \tilde{\zeta}^h(\mathbf{x}, \mathbf{y}, \omega) - \delta(\mathbf{r} - \mathbf{y}) \right] (\delta v^{\text{ext}}(\mathbf{y}) + \delta v_H(\mathbf{y})), \end{aligned} \quad (5.19)$$

with $\tilde{\zeta}^h(\mathbf{r}, \mathbf{r}', \omega) := \text{Im} [G^h(\mathbf{r}, \mathbf{r}', \omega) G^h(\mathbf{r}', \mathbf{r}, \omega)]$, the corresponding of $\tilde{\zeta}_{\text{SF}}^h(\mathbf{r}, \mathbf{r}', \omega)$ in the real system. This formula separates quantities related to the exchange–correlation part of the interaction (first line) from quantities related to the lattice ($v^{\text{ext}}(\mathbf{r})$) and the classical interaction energy $v_H(\mathbf{r})$. In particular this last contribution is zero if $\tilde{\zeta}^h = \tilde{\zeta}_{\text{SF}}^h$, which is not the case as the Green's function G^h and G_{SF}^h are usually different (only the diagonal of their imaginary parts is the same by definition).

Therefore, the last term measures both the departure of the auxiliary system Green's function from its real system counterpart, through the factor $[\tilde{\zeta}_{\text{SF}}^{h-1} \tilde{\zeta}^h - 1]$, and the inhomogeneity of the system, via the explicit factors $\delta v^{\text{ext}}(\mathbf{r})$ and $\delta v_H(\mathbf{r})$. We call it $\mathcal{C} [\delta v^{\text{ext}}(\mathbf{r}) + \delta v_H(\mathbf{r})] - (\delta v^{\text{ext}}(\mathbf{r}) + \delta v_H(\mathbf{r}))$.

The terms in curly brackets, on the contrary, are non zero even if $\tilde{\zeta}^h = \tilde{\zeta}_{\text{SF}}^h$. They are both due to the exchange–correlation part of the interaction, which is completely accounted for by $v_{\text{SF}}^h(\omega)$ in the homogeneous system. In the real system, the inhomogeneity correction $\delta\Sigma$ is localized by the product of different Green's function, all pertaining to the homogeneous electron gas. The connector idea is based on this observation: if the triple integral in eq. (5.18) is small, since the physics it contains is analogous to the one in $v_{\text{SF}}^h(\omega)$, one can assume the existence of a small *corrector* $\delta c(\mathbf{r}, \omega)$ such that the triple integral contribution can be absorbed by the frequency dependence of $v_{\text{SF}}^h(\omega)$ through a shift of it by $\delta c(\mathbf{r}, \omega)$. In formulas:

$$v_{\text{SF}}^h(\omega) + \int_{\mathbf{x}, \mathbf{y}, \mathbf{z}} \tilde{\zeta}_{\text{SF}}^{h-1}(\mathbf{r}, \mathbf{x}, \omega) \text{Im} \left[G^h(\mathbf{x}, \mathbf{y}, \omega) \delta\Sigma(\mathbf{y}, \mathbf{z}, \omega) G^h(\mathbf{z}, \mathbf{x}, \omega) \right] = v_{\text{SF}}^h(\omega - \delta c(\mathbf{r}, \omega)), \quad (5.20)$$

with $\delta c(\mathbf{r}, \omega)$ defined through a Taylor expansion of $v_{\text{SF}}^h(\omega - \delta c(\mathbf{r}, \omega))$ around $v_{\text{SF}}^h(\omega)$:

$$-\delta c(\mathbf{r}, \omega) \frac{dv_{\text{SF}}^h(\omega)}{d\omega} = \int_{\mathbf{x}, \mathbf{y}, \mathbf{z}} \tilde{\zeta}_{\text{SF}}^{h-1}(\mathbf{r}, \mathbf{x}, \omega) \text{Im} \left[G^h(\mathbf{x}, \mathbf{y}, \omega) \delta\Sigma(\mathbf{y}, \mathbf{z}, \omega) G^h(\mathbf{z}, \mathbf{x}, \omega) \right]. \quad (5.21)$$

If these assumptions are correct, eq. (5.19) reads:

$$v_{\text{SF}}^{\text{xc}}(\mathbf{r}, \omega) = v_{\text{SF}}^h(\omega - \delta c(\mathbf{r}, \omega)) + \mathcal{C} [\delta v^{\text{ext}}(\mathbf{r}) + \delta v_H(\mathbf{r})] - (\delta v^{\text{ext}}(\mathbf{r}) + \delta v_H(\mathbf{r})), \quad (5.22)$$

which is exactly² eq. (5.15) once we identify the function $c(\mathbf{r}, \omega)$ with the functional $\mathcal{C} [v^{\text{ext}} + v_H]_{\mathbf{r}} \equiv \int_{\mathbf{y}, \mathbf{x}} \tilde{\zeta}_{\text{SF}}^{h-1}(\mathbf{r}, \mathbf{x}, \omega) \tilde{\zeta}^h(\mathbf{x}, \mathbf{y}, \omega) (v^{\text{ext}}(\mathbf{y}) + v_H(\mathbf{y}))$, both with the same homogeneous limit $v^{\text{ext}} + v_H$.

²A slight difference with the previous derivation is that here the model system, the homogeneous electron gas, is fixed to a certain predetermined value of density.

5.6 Model systems without auxiliary systems

Three systems, the real one, the auxiliary one and the model one, are a lot. One could wonder if the auxiliary system is needed at all.

Indeed, sometimes its introduction is completely avoided, and one uses the model system and a connector to directly approximate the real system. This is the case for the Thomas–Fermi approximation in DFT, DMFT as it is usually seen and the Sham–Kohn quasiparticle local density approximation.

Thomas–Fermi The Thomas–Fermi approach [125, 126] is a way to *approximate* the kinetic energy density $t(\mathbf{r})$ of the real system, defined by $T = \int d^3r n(\mathbf{r}) t(\mathbf{r})$. It follows exactly the same line of thinking of LDA, just there is no Kohn–Sham system and the quantity to approximate is $t(\mathbf{r})$ instead of $v_{\text{KS}}^{\text{xc}}(\mathbf{r})$. The idea is to import $t(\mathbf{r})$ from a model system, the non-interacting homogeneous electron gas, with the local density as a connector, $n^h = n(\mathbf{r})$.

The kinetic energy density in the non-interacting HEG is given by $t^h = \frac{3}{10}(3\pi^2)^{2/3} n^{h2/3}$. Therefore, in the real system, using the local connector $n^h = n(\mathbf{r})$, the kinetic energy reads:

$$T^{\text{TF}} = \int d^3r n(\mathbf{r}) t_{n^h(\mathbf{r})}^h = \frac{3}{10}(3\pi^2)^{2/3} \int d^3r [n(\mathbf{r})]^{5/3}.$$

This is an explicit density functional. Together with the external and the Hartree term, it can be used to describe physical systems. However, its performances are limited [127], and the reason is mainly to be searched in the poor description of the kinetic term, which often plays a dominant role in the energy contributions, see fig. 2.1. Viceversa, the auxiliary system approach of Kohn–Sham yields most often a very good description of the ground state, also because of the exact, although non-interacting, treatment of the kinetic energy term.

DMFT (standard point of view) In DMFT, one can also think not to introduce the auxiliary system in which the self energy is local. Simply, by referring to fig. 5.2, line 3, the self energy of the model system Σ_{AIM} is directly imported as the self energy of the real system. One therefore makes the assumption that $\Sigma_{ij}(\omega) \approx \delta_{ij} \Sigma(\omega) = \delta_{ij} \Sigma_{\text{AIM}}(\omega)$. Only the local diagrams of the self energy are retained to evaluate the local Green’s function. This is clearly an approximation, as the non-local diagrams, which in the real system should be considered, are disregarded.

On the other hand, if one introduces the auxiliary system, there are no non-local diagrams for the self energy. In the auxiliary system, the local Green’s function is obtained exactly from a local self energy, which can be found from a model system (the AIM in this case).

5.6.1 Sham–Kohn Quasi Particle LDA

An approach very close to dynLCA, which nevertheless does not rely on any auxiliary system, is the local density approximation introduced by Sham and Kohn in the least known of their three papers of 1965 [128]. Their idea is to *approximate* the self energy with a *local* expression, and then use this form to evaluate approximate excitation energies. Indeed, they consider a system of almost constant density, $n(\mathbf{r}) = n_0 + n_1(\mathbf{r})$, where n_1 is small and has zero spatial average. They show that:

$$\Sigma(\mathbf{r}, \mathbf{r}', \omega) = \Sigma^h(\mathbf{r} - \mathbf{r}', \omega - v^{\text{ext}}(\mathbf{r}_0) - v_{\text{H}}(\mathbf{r}_0)) + \int d^3s n_1(\mathbf{s}) \Sigma^{(1)}(\mathbf{r}, \mathbf{r}'; \mathbf{r}_0 - \mathbf{s}, \omega - v^{\text{ext}}(\mathbf{r}_0) - v_{\text{H}}(\mathbf{r}_0))$$

with $\Sigma^{(1)}$ a short-range function of $\mathbf{r}_0 - \mathbf{s}$, and \mathbf{r}_0 the average position $\frac{\mathbf{r} + \mathbf{r}'}{2}$. Therefore, for slowly varying densities, to a first approximation one can neglect the additional term on the right hand

side, and simply take the non-local self energy $\Sigma(\mathbf{r}, \mathbf{r}', \omega)$ from the model system. To set the HEG, they use for a connector the density of the real system evaluated at \mathbf{r}_0 :

$$\Sigma(\mathbf{r}, \mathbf{r}', \omega) \approx \Sigma_{n^h=n(\mathbf{r}_0)}^h(\mathbf{r} - \mathbf{r}', \omega - \nu^{\text{ext}}(\mathbf{r}_0) - \nu_H(\mathbf{r}_0)). \quad (5.23)$$

This equation is very similar to the DMFT relation $\Sigma_{ij}(\omega) \approx \delta_{ij} \Sigma_{\text{AIM}}(\omega)$. Note by contrast that the connector acts also on the frequency argument, shifting it by the same local alignment of the Fermi energies we will use also in our theory, see eq. (7.14). That shift is needed to reproduce the limit of slowly varying density, [129, 128], where we expect the approximation to well describe the system. It allows the model system to take into account both the external and Hartree potentials, which sum to zero in the HEG. With such a choice for the frequency argument, “the functional form of the self energy is independent of any uniform shift of the electrostatic potential” [128]: indeed, the Schrödinger equation for the effective Hamiltonian, $\left[-\frac{\nabla^2}{2} + \nu^{\text{ext}} + \nu_H + \Sigma^h(\omega - \nu^{\text{ext}} - \nu_H)\right] \phi = \omega \phi$, can be also written as $\left[-\frac{\nabla^2}{2} + \Sigma^h(\omega - \nu^{\text{ext}} + \nu_H)\right] \phi = (\omega - \nu^{\text{ext}} + \nu_H) \phi$. If the density is constant, it reads $\left[-\frac{\nabla^2}{2} + \Sigma^h(\omega)\right] \phi = \omega \phi$, which is the expected result.

Subsequently, they approximate the non-local operator (5.23) by a local one, with a WKB-like argument; to this aim, consider the quasi particle equation (2.40):

$$h_H(\mathbf{r}) \phi_n(\mathbf{r}) + \int d^3 r' \Sigma(\mathbf{r}, \mathbf{r}', \varepsilon_n) \phi_n(\mathbf{r}') = \varepsilon_n \phi_n(\mathbf{r}), \quad (5.24)$$

and, in the same limit of slowly varying density, restrict the set of eigenstates to plane waves $\varphi_{\mathbf{k}(\mathbf{r})}(\mathbf{r})$, labelled by a *local* momentum $\mathbf{k}(\mathbf{r})$.

When the self energy (5.23) operates on $\varphi_{\mathbf{k}(\mathbf{r})}(\mathbf{r}) \sim e^{i\mathbf{k}(\mathbf{r}) \cdot \mathbf{r}}$, since these are the eigenstates of the HEG, we can substitute it with its eigenvalue (mathematically, a Fourier transform does the job; the \mathbf{r} -dependence of \mathbf{k} is neglected):

$$\int d^3 r' \Sigma^h(\mathbf{r} - \mathbf{r}', \varepsilon_k) \varphi_{\mathbf{k}}(\mathbf{r}') = \Sigma_{n^h=n(\mathbf{r})}^h(\mathbf{k}(\mathbf{r}), \varepsilon_k) \varphi_{\mathbf{k}}(\mathbf{r}).$$

The idea is to use the local operator $\Sigma_{n^h=n(\mathbf{r})}^h(\mathbf{k}(\mathbf{r}), \omega - \nu^{\text{ext}}(\mathbf{r}) - \nu_H(\mathbf{r}))$ instead of the non-local self energy, no matter if the eigenstate is not a plane wave. A third step is the Thomas–Fermi approximation, $\mu = \mu_{n^h=n(\mathbf{r})}^h + \nu^{\text{ext}}(\mathbf{r}) + \nu_H(\mathbf{r})$, which allows one to remove the explicit spatial dependence from eq. (5.24), that becomes:

$$\omega - \varepsilon_k^0 - \Sigma_{n^h=n(\mathbf{r})}^h(\mathbf{k}, \omega - \mu + \mu_{n^h=n(\mathbf{r})}^h) = \mu - \mu_{n^h=n(\mathbf{r})}^h. \quad (5.25)$$

a relation that defines the local wavevector $k = k(\mathbf{r}, \omega)$; this choice guarantees that $k = k_F$ when $\varepsilon_k = \mu$ (Fermi surface). The self energy is thus replaced by the following local operator:

$$\nu_{\text{SK}}(\mathbf{r}, \omega) = \Sigma_{n^h=n(\mathbf{r})}^h\left(\mathbf{k}(\mathbf{r}, \omega), \omega - \mu + \mu_{n^h=n(\mathbf{r})}^h\right). \quad (5.26)$$

with $k = k(\mathbf{r}, \omega)$ the solution of eq. (5.25). Note that this potential is in principle an *approximation* to the self energy, local and in general not real. It is not designed to have the exact, e.g., spectral function. This approximation, called *Quasi Particle Local Density Approximation* (QPLDA) has been first used in real materials by Pickett and Wang, to describe the spectra of insulators [130, 131].

HEG In the homogeneous electron gas itself, these equations read:

$$\begin{aligned} \nu_{\text{SK}}^h(\omega) &= \Sigma_{n^h}^h(k(\omega), \omega) \\ \omega - \varepsilon_k^0 - \Sigma_{n^h}^h(k, \omega) \Big|_{k=k(\omega)} &= 0. \end{aligned}$$

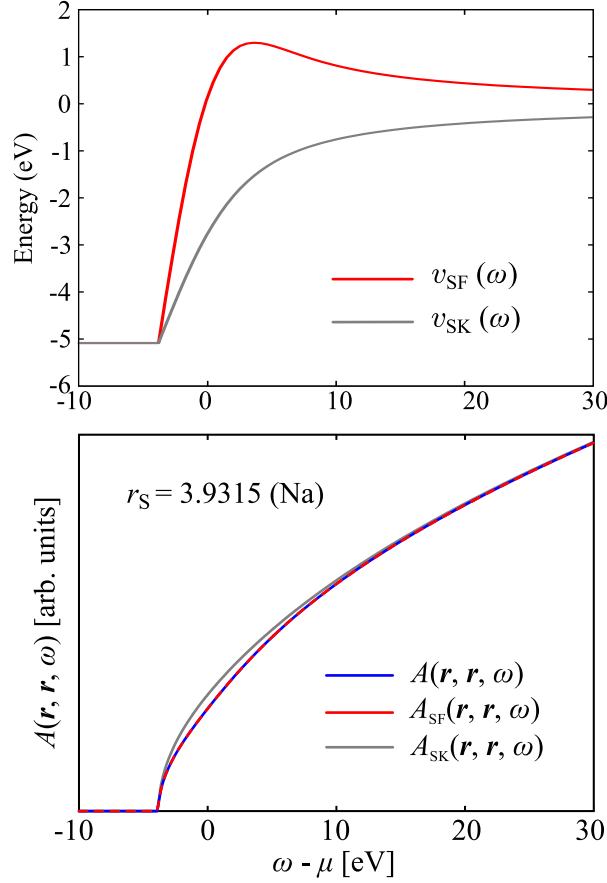


Figure 5.8: A comparison between the spectral potential $v_{\text{SF}}^h(\omega)$, eq. (4.63), and the Sham–Kohn potential $v_{\text{SK}}^h(\omega)$, eq. (5.27), in the HEG, corresponding to the HSE06 self energy. Above, the potentials, and below the spectral function they yield.

Considering a static self energy $\Sigma^h(k)$, the second equation is the definition of $k_0(\omega)$, see page 80. Therefore the Sham–Kohn potential can be written as:

$$v_{\text{SK}}^h(\omega) = \Sigma_{n^h}^h(k_0(\omega)) = \omega - 2 \left| \frac{\frac{k^2}{2}}{k+0} \right|_{k=k_0(\omega)}^2. \quad (5.27)$$

The last expression is extremely similar to the spectral potential $v_{\text{SF}}^h(\omega)$ of eq. (4.63), with the difference that here the derivative of the self energy has been replaced by a zero in the denominator. As the two expressions are different and the spectral potential $v_{\text{SF}}^h(\omega)$, eq. (4.63), is the only potential that yields the correct diagonal of the spectral function, it is clear that $v_{\text{SK}}^h(\omega)$ will not yield the exact spectral function of the HEG, as can be shown.

On the other hand, this potential is, in the homogeneous electron gas, the one of eq. (4.74), which we introduced to have the correct band structure, see fig. 4.23. There the exact spectral function, too, could be recovered, by changing the prescription on how to evaluate it. Since we were in an auxiliary system, having a new functional to get the spectral function was in principle admissible (compare with the total energy or the gap of the Kohn–Sham system). Here, on the other hand, since there are no auxiliary systems but $v_{\text{SK}}^h(\omega)$ is just an approximation to Σ , we cannot easily implement a different prescription, and we must conclude that the spectral function evaluated with $v_{\text{SK}}^h(\omega)$ is not the expected one, see fig. 4.22 and fig. 5.8.

After these three examples, we can appreciate the importance of having an auxiliary system, in between the real and the model systems.

The auxiliary system fixes the quantity of interest, and by doing so it states what it is possible to obtain in principle and what it is not. Furthermore, it leaves more freedom in defining functionals, as they do not have to be the same ones that one would define in the real system. Finally, it often already constitutes a good basis to start approximating.

The connector approach is extremely useful when some quantity is needed, but its exact expression is too difficult to evaluate. Therefore, one resorts to calculate that same quantity, or something very similar, in a model system, and then to import it. The prescription on how to import a particular quantity is the connector. It is based on physical insight, and it is the most delicate part of the method. In the next two chapters, I will test this approach for the asymmetric dimer and for realistic materials, showing how different can be the results depending on the choice of the particular connector.

The connector for the Hubbard dimer

Before passing to real materials and test the connector idea there, I present here another situation that presents non-trivial effect of inhomogeneity. In this case, the use of a model system is particularly suited. I will focus on the choice of which quantity should one import from the model system. Different choices clearly imply different performances.

The system I consider is a slightly modified version of the Hubbard dimer of section 4.2, in which the two sites 1 and 2 are here at different energy e_1 and e_2 , with $e_1 > e_2$:

$$\hat{H} = -t \sum_{\sigma} \left(\hat{c}_{1\sigma}^{\dagger} \hat{c}_{2\sigma} + \hat{c}_{2\sigma}^{\dagger} \hat{c}_{1\sigma} \right) + \sum_i e_i \hat{n}_i + U \sum_i \hat{n}_{i\uparrow} \hat{n}_{i\downarrow}. \quad (6.1)$$

The on-site energy term $e_1 \hat{n}_1 + e_2 \hat{n}_2$ can be recast in the form: $\bar{E} (\hat{n}_1 + \hat{n}_2) + \frac{D}{2} (\hat{n}_1 - \hat{n}_2)$, with $\bar{E} := \frac{e_1 + e_2}{2}$ the average energy and $D := e_1 - e_2$ their difference. Through a redefinition of energy (a shift of \hat{H}) we can always choose¹ $\bar{E} = 0$; in this way, the parameters that define the system are t , U and D , all positive. To simplify the notation, we measure the energy in units of t , defining the reduced quantities $\hat{H}/t := \hat{H}$, $U/t := U$ and $D/t := D$. Thus, the Hamiltonian reads:

$$\hat{H} = - \sum_{\sigma} \left(\hat{c}_{1\sigma}^{\dagger} \hat{c}_{2\sigma} + \hat{c}_{2\sigma}^{\dagger} \hat{c}_{1\sigma} \right) + \frac{D}{2} (\hat{n}_1 - \hat{n}_2) + U \sum_i \hat{n}_{i\uparrow} \hat{n}_{i\downarrow}, \quad (6.2)$$

which tends to the symmetric dimer Hamiltonian (4.10) in the limit $D \rightarrow 0$. D can be regarded as an external potential that alters the symmetry $site\ 1 \longleftrightarrow site\ 2$ and creates inhomogeneities in the dimer. Although it looks like an innocuous parameter, its non-zero value makes everything more complicated. Indeed, even if this Hamiltonian looks pretty close to the one of eq. (4.10), for $D \neq 0$ it is more difficult to obtain the Green's function, and from that the spectral function. The reason is the non-trivial interplay between the inhomogeneity set by D and the interaction U . This is where the model system idea will come into play.

Note, finally, that the situation I just sketched is similar to the one that I will discuss in the next chapter, when dealing with real materials. Also for real materials problems arise because of the interplay between inhomogeneity, set by $v^{ext}(\mathbf{r})$, and the Coulomb interaction between electrons; when the former is zero, we are in the homogeneous electron gas, which is easier to solve. As soon as the external potential is switched on, on the other hand, everything becomes more complicated and, in general, one cannot easily disentangle inhomogeneity from interaction effects.

¹This choice is different from the one we made in the symmetric case: there, we set $\mu = 0$. As a consequence, the two energy axis are shifted by the amount $\sqrt{1 + \frac{D^2}{4}}$.

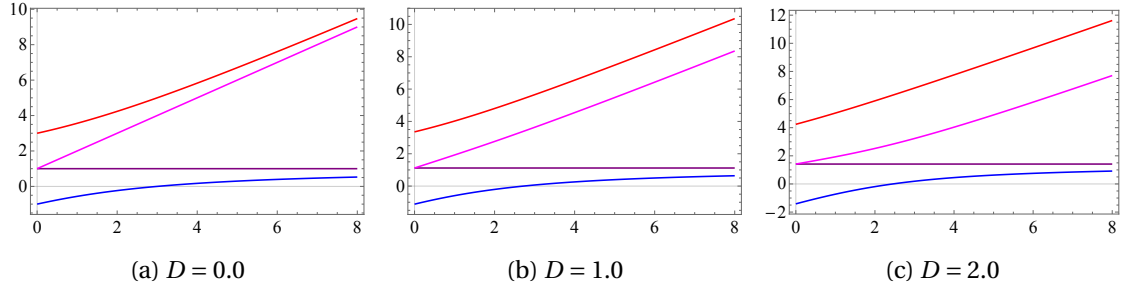


Figure 6.1: Position of the poles of the Green's function $\omega_\lambda = e_\lambda - e_-$, with e_λ in eq. (6.6), as a function of U , in units of t , for different values of D , as indicated.

6.1 The real system: one–fourth filling solution

As in the symmetric $D = 0$ case, we will focus on the case of $N = 1$ electrons. Diagonalizing the Hamiltonian (6.2), we get the eigenvalues $e_\pm = \pm \frac{1}{2}\sqrt{4 + D^2}$. The Fermi energy is thus $\mu = -\frac{1}{2}\sqrt{4 + D^2}$, and the associated eigenstates are:

$$|\pm, \sigma\rangle = \cos \rho_\pm |\sigma, 0\rangle + \sin \rho_\pm |0, \sigma\rangle, \quad (6.3)$$

with² $[\tan \rho_\pm]^{-1} := -\frac{1}{2}(D \pm \sqrt{4 + D^2})$. As in the symmetric case, we break the spin symmetry by choosing a spin-up electron as the ground state, $|GS\rangle \equiv |-, \uparrow\rangle$. The difference in the occupation of the two sites is given by: $n_1 - n_2 = \frac{1 - \tan^2 \rho_-}{1 + \tan^2 \rho_-}$, which is zero in the symmetric case and tends to $n_2 = 1$ for large D , as the assumption $e_1 > e_2$ favours the occupation of the second site, lower in energy.

The Green's function $G_{ij,\sigma}(t, t') := -i \langle GS | \hat{T} \hat{c}_{i\sigma}(t) \hat{c}_{j\sigma}^\dagger(t') | GS \rangle$ associated with this system is evaluated in appendix D, via the Lehmann representation. The result is trivial for the spin-up case: the single electron in the ground state can be removed, or another spin-up electron can be added to the system and it will go to the antibonding orbital, where it will not interact with the first. As a result, the spin-up Green's function is always non-interacting:

$$G_{ij,\uparrow}(\omega) = \frac{\Lambda_{ij}^{0(-)}}{\omega - e_- - i\eta} + \frac{\Lambda_{ij}^{0(+)}}{\omega - e_+ + i\eta}, \quad (6.4)$$

with weights defined as $\Lambda_{ij}^{0(\pm)} := [\delta_{i1} \cos \rho_\pm + \delta_{i2} \sin \rho_\pm] [\delta_{j1} \cos \rho_\pm + \delta_{j2} \sin \rho_\pm]$.

²In particular, $\cos \rho_+ = \sin \rho_-$ and $\sin \rho_+ = -\cos \rho_-$ and, for $D = 0$, $\cos \rho_{\pm=0} = \sin \rho_{\pm=0} = \frac{1}{\sqrt{2}}$. The matrix of change of basis, from the site basis $\{|i, \sigma\rangle\} \equiv \{|\uparrow, 0\rangle, |0, \uparrow\rangle, |\downarrow, 0\rangle, |0, \downarrow\rangle\}$ to the bonding–antibonding basis

$$\{|\alpha\rangle\} = \{|\pm, \sigma\rangle\} \equiv \{|-, \uparrow\rangle, |+, \uparrow\rangle, |-, \downarrow\rangle, |+, \downarrow\rangle\} \text{ is } \langle \alpha | i, \sigma \rangle = \begin{pmatrix} \cos \rho_- & \sin \rho_- & 0 & 0 \\ \sin \rho_- & -\cos \rho_- & 0 & 0 \\ 0 & 0 & \cos \rho_- & \sin \rho_- \\ 0 & 0 & \sin \rho_- & -\cos \rho_- \end{pmatrix}.$$

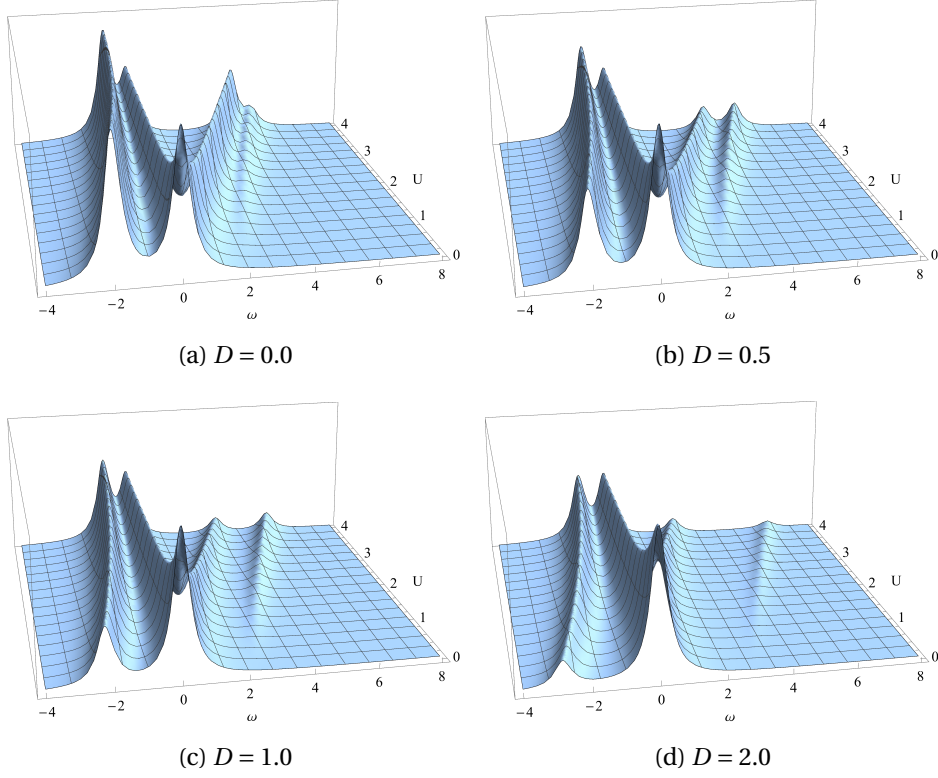


Figure 6.2: Diagonal of the spectral function $A_{ii,↓}(\omega)$ as a function of ω and U , in units of t , for different values of D , as indicated. A broadening $\eta = 0.3$ is added for clarity reasons. The behaviour of the poles as a function of U is the one of fig. (6.1).

On the contrary, the interaction enters the spin-down Green's function, that reads:

$$\begin{aligned}
 G_{11,↓}(\omega) &= \frac{\frac{1}{2} \sin^2 \rho_-}{\omega - (e_2 - e_-) + i\eta} + \sum_{\lambda=1,3,4} \frac{\frac{1}{|\mathcal{N}_\lambda|^2} \left[\cos \rho_- \left(\frac{2}{e_\lambda + (D-U)} - e_\lambda \right) + \sin \rho_- \right]^2}{\omega - (e_\lambda - e_-) + i\eta} \\
 G_{12,↓}(\omega) = G_{21,↓}(\omega) &= \frac{-\frac{1}{2} \sin \rho_- \cos \rho_-}{\omega - (e_2 - e_-) + i\eta} + \\
 &+ \sum_{\lambda=1,3,4} \frac{\frac{1}{|\mathcal{N}_\lambda|^2} \left[\cos \rho_- - \sin \rho_- \frac{2}{e_\lambda + (D-U)} \right] \left[\cos \rho_- \left(\frac{2}{e_\lambda + (D-U)} - e_\lambda \right) + \sin \rho_- \right]}{\omega - (e_\lambda - e_-) + i\eta} \\
 G_{22,↓}(\omega) &= \frac{\frac{1}{2} \cos^2 \rho_-}{\omega - (e_2 - e_-) + i\eta} + \sum_{\lambda=1,3,4} \frac{\frac{1}{|\mathcal{N}_\lambda|^2} \left[\cos \rho_- - \sin \rho_- \frac{2}{e_\lambda + (D-U)} \right]^2}{\omega - (e_\lambda - e_-) + i\eta},
 \end{aligned} \tag{6.5}$$

with the relevant $N = 2$ excitation energies defined by:

$$\begin{aligned}
 e_1 &= \frac{2}{3} \left[U - r \cos \left(\theta - \frac{\pi}{3} \right) \right] \\
 e_2 &= 0 \\
 e_3 &= \frac{2}{3} \left[U - r \cos \left(\theta + \frac{\pi}{3} \right) \right] \\
 e_4 &= \frac{2}{3} \left[U - r \cos (\theta + \pi) \right],
 \end{aligned} \tag{6.6}$$

with the parameters:

$$\begin{aligned} z^2 &:= 9D^2 - U^2 - 18 \\ r^2 &:= 3D^2 + U^2 + 12 \\ \cos 3\theta &:= \frac{z^2 U}{r^3}, \end{aligned}$$

and the normalization factor defined as $\frac{1}{2} \mathcal{N}_\lambda^2 = 1 + 2 \left(\frac{1}{e_\lambda + D - U} - \frac{e_\lambda}{2} \right)^2 + 2 \left(\frac{1}{e_\lambda + D - U} \right)^2$. The poles of the Green's function are $\omega_\lambda := e_\lambda - e_- \equiv e_\lambda + \frac{1}{2} \sqrt{4 + D^2}$, and they are shown in fig. 6.1. The diagonal of the spectral function $A_{ij,\sigma}(\omega) := \frac{1}{\pi} |\text{Im} G_{ij,\sigma}(\omega)|$ is shown in fig. 6.2. Although the Green's function (6.5) still presents four discrete poles, its expression is more complicated than its $D = 0$ counterpart; in particular, the poles ω_λ with $\lambda \neq 2$, real solutions of a third order equation, are *intrinsically* more sophisticated numbers than their $D = 0$ relatives, as, in general, they cannot be expressed in closed radical form without the use of complex numbers or trigonometry [132].

Therefore it is clear that, although the exact solution is at hand, one would like a quicker and more efficient way of obtaining the spectral function. Thus, one faces two alternatives: approximating the real system or building an auxiliary system.

6.2 Approximations to the self energy

When the exact solution is out of reach, the standard approach is building approximations, that can rely on an expansion of the self energy and a truncation of it.

The approximate self energy³ $\Sigma_{ij}^a(\omega)$ determines a frequency-dependent Hamiltonian $H_{ij}^a(\omega) = h_{ij}^0 + \Sigma_{ij}^a(\omega)$. Its eigenvalues $e_\lambda^a(\omega)$ enter the pole equation $\omega - e_\lambda^a(\omega) = 0$, whose solutions ω_λ^a are the position of the poles within the approximation Σ^a . In particular, from the form of $h_{ij}^0 = \begin{pmatrix} \frac{D}{2} & -1 \\ -1 & -\frac{D}{2} \end{pmatrix}$ and the fact that the off-diagonal elements of the self energy are equal, the pole equation reads:

$$\hat{0} = \omega \hat{1} - \hat{H}^a(\omega) \iff \omega - \left[\frac{\Sigma_{11}^a(\omega) + \Sigma_{22}^a(\omega)}{2} \pm \sqrt{\left[1 - \Sigma_{12}^a(\omega) \right]^2 + \left[\frac{D + \Sigma_{11}^a(\omega) - \Sigma_{22}^a(\omega)}{2} \right]^2} \right] = 0. \quad (6.7)$$

6.2.1 Hartree approximation

The simplest approximations to the full self energy are the Hartree and the exchange ones, that correspond to no correlation in the double occupation: $\langle \hat{n}_{i\uparrow} \hat{n}_{i\downarrow} \rangle \longrightarrow \langle \hat{n}_{i\uparrow} \rangle \langle \hat{n}_{i\downarrow} \rangle \equiv n_{i\uparrow} n_{i\downarrow}$. The interaction energy is thus $E_H + E_x = U \sum_i n_{i\uparrow} n_{i\downarrow}$. Since the Hartree term does depend only on the total density and, for $N = 1$, the exchange term is supposed to exactly balance and cancel it, we can define^{4 5}:

$$E_H = \frac{U}{2} \sum_i n_i^2 \quad E_x = -\frac{U}{2} \sum_i (n_{i\uparrow}^2 + n_{i\downarrow}^2),$$

from which the Hartree potential is:

$$v_i^H = \frac{\partial E_H}{\partial n_i} = U n_i. \quad (6.8)$$

³The self energy we consider here is the full one, and it also contains the Hartree term.

⁴For just one electron in the spin-polarized ground state that we have chosen, $n_{i\uparrow} \equiv n_i$ and $n_{i\downarrow} = 0$, thus $E_x = -E_H$ as expected. For unpolarized systems, $n_{i\uparrow} = n_{i\downarrow} = \frac{1}{2} n_i$ leading to $E_x = -\frac{U}{4} \sum_i n_i^2 = -\frac{1}{2} E_H$.

⁵An alternative definition of the Hartree potential, in which the latter is spin-dependent, is presented in appendix H.

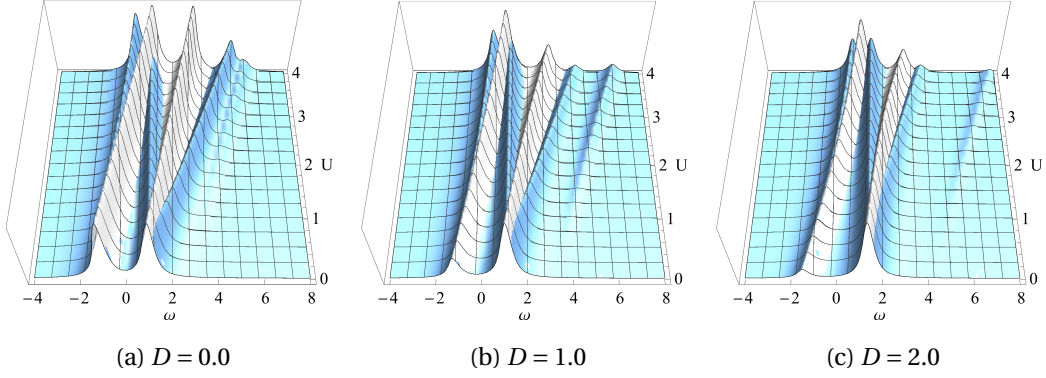


Figure 6.3: *The Hartree approximation. The blue surface is the exact spectral function, the same as in fig. 6.2, while in white the one evaluated with the Hartree approximation, eq. (6.8).*

This is a static potential, unable to split the number of peaks of the non-interacting spectral function. Indeed, from eq. (6.7) with $\Sigma_{ij}^a(\omega) = v_i^H \delta_{ij}$, the poles are:

$$\omega_\lambda^H = \frac{U}{2} \pm \sqrt{1 + h^2}, \quad (6.9)$$

with $h := \frac{D+U(n_1-n_2)}{2}$. The resulting spectral function is shown in fig. 6.3. The Hartree approximation is nonetheless already a good description of the system: it is an improvement with respect to the free-particle approximation $U = 0$, in which the position of the poles would be U -independent. Since the Hartree potential v_i^H depends on U , the two peaks ω_λ^H of the Hartree spectral function interpolate well between the four peaks of the spectral function of the real system. In particular, the Hartree approximation is always a good approximation for small U , independently of D . By contrast, for large U , where correlation effects become important, the correspondence is worse.

6.2.2 The GW approximation

The non-interacting Green's function has always two poles, in correspondence of the bonding and the antibonding eigenenergies. Any static approximation to the self energy will at most shift these two poles, but it will not change the number of them. To split the poles and have at least four of them, like in the real system, a frequency-dependent self energy must be considered.

The GW self energy is one of them: it is a non-local, complex and frequency dependent self-energy. In appendix H we propose two alternative GW-like approximations. In one of them the bare and the screened interactions are spin-dependent; this formulation is closer to the Feynman rules set by the Hubbard model (for instance, the exchange self energy is zero and the spin-up Green's function is always exact), and has the advantage of exactly solving the $D = 0$ model.

The other formulation, instead, employs a spin-independent interaction [96], and it is closer to usual GW in solids. It does treat spins on the same footing, adding additional poles to the spin-up Green's function (6.4). Moreover, it does not solve exactly the $D = 0$ system, and this is precisely the reason why we employ this formulation, and not the former, for the following discussion.

In particular, the self energy $\Sigma^{G_0 W_0}$ we consider is formed from the non-interacting Green's function G^0 and the RPA polarization $\Pi_0^{RPA} \sim -iG^0 G^0$, that dresses the bare interaction, evalu-

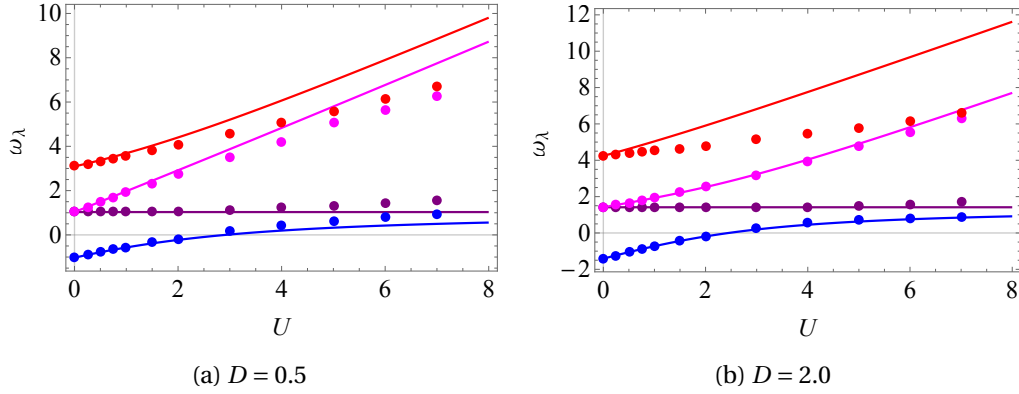


Figure 6.4: Position of the poles of the spin-down GW Green's function as a function of U . Solid line, exact results, as in fig. 6.1; dots, GW poles, from (H.25).

ated with non-interacting Green's function, too. It reads:

$$\begin{aligned} \Sigma_{ij,\sigma}^{G_0 W_0}(\omega) &= i \int \frac{d\omega'}{2\pi} e^{i\omega'\eta} G_{ij,\sigma}^0(\omega + \omega') W_{ij}^{RPA}(\omega') = \\ &= -\delta_{\sigma,\uparrow} \delta_{ij} U n_i + \frac{(-1)^{(i-j)} \frac{U^2}{2l}}{\sqrt{1 + \frac{D^2}{4}}} \left[\frac{\Lambda_{ij}^{0(-)}}{\omega - (e_- - l \text{sign } \sigma) - i\eta \text{sign } \sigma} + \frac{\Lambda_{ij}^{0(+)}}{\omega - (e_+ + l) + i\eta} \right], \end{aligned}$$

with $l^2 := 4(1 + \frac{D^2}{4}) + \frac{2U}{\sqrt{1 + \frac{D^2}{4}}}$. The poles of the Green's function evaluated with this self energy are the solution to the equation $\hat{\omega} = \omega \hat{1} - [\hat{h}_H + \hat{\Sigma}_{\sigma}^{G_0 W_0}(\omega)]$, explicitly given by eq. (H.25). In fig. 6.4, we show the GW poles of the spin-down Green's function for two values of D , as a function of U . This approximation works well for small interaction, while it tends to close the gap between the Hubbard bands for larger value of U . On the other hand, it seems that, apart from the fourth pole, its performances improve for larger values of D .

6.3 Dynamical Connector Approach (dynCA)

6.3.1 The auxiliary system

Instead of approximately solving the real system, we can work with an auxiliary system that, in principle, exactly targets the spectral function, precisely as we did in the symmetric case. We can define the auxiliary system (for the spin-down part of the spectral function) by replacing the self energy of the real system with a real and frequency-dependent potential $v_{\text{SF } i}(\omega)$, which in this case does truly depend on the site, as the two sites are no equivalent anymore:

$$G_{\text{SF } ij}^{-1}(\omega) = G_{ij}^{0-1}(\omega) - v_{\text{SF } i}(\omega). \quad (6.10)$$

The aim is reproducing the position of the poles. These are independent of the particular basis; therefore, it is useful to express the previous relation in the bonding-antibonding basis, where the non-interacting Green's function G^0 is diagonal, and the spectral potential reads:

$$v_{\alpha\beta}(\omega) = \sum_{i=1,2} \langle \alpha | i \rangle v_{\text{SF } i}(\omega) \langle i | \beta \rangle \rightarrow \begin{pmatrix} V(\omega) - \frac{\frac{D}{2}}{\sqrt{D^2+4}} \Delta v(\omega) & \frac{1}{\sqrt{D^2+4}} \Delta v(\omega) \\ \frac{1}{\sqrt{D^2+4}} \Delta v(\omega) & V(\omega) + \frac{\frac{D}{2}}{\sqrt{D^2+4}} \Delta v(\omega) \end{pmatrix}, \quad (6.11)$$

with $V(\omega) := \frac{1}{2}(v_{\text{SF } 1}(\omega) + v_{\text{SF } 2}(\omega))$ and $\Delta v(\omega) := v_{\text{SF } 1}(\omega) - v_{\text{SF } 2}(\omega)$. A local potential in the site basis, whose value depends on the particular site, is no local anymore in the bonding-

antibonding basis. In this basis, the equation that defines the auxiliary system becomes:

$$G_{\text{SF } \alpha\beta}^{-1}(\omega) = G_{\alpha}^{0-1}(\omega)\delta_{\alpha\beta} - \nu_{\text{SF } \alpha\beta}(\omega), \quad (6.12)$$

with $G_{\alpha}^{0-1}(\omega) = \omega - e_{\alpha}$, $e_{\alpha} = e_{\pm} = \pm \frac{1}{2}\sqrt{4 + D^2}$. The previous equation defines the frequency-dependent effective Hamiltonian in the auxiliary system, namely:

$$H_{\text{SF } \alpha\beta}(\omega) = e_{\alpha}\delta_{\alpha\beta} + \nu_{\text{SF } \alpha\beta}(\omega). \quad (6.13)$$

This Hamiltonian, which is not diagonal due to the presence of the local potential, can be diagonalized; it reads:

$$\hat{H}_{\text{SF}}(\omega) \rightarrow \begin{pmatrix} V(\omega) - \sqrt{1 + \left(\frac{D+\Delta\nu(\omega)}{2}\right)^2} & 0 \\ 0 & V(\omega) + \sqrt{1 + \left(\frac{D+\Delta\nu(\omega)}{2}\right)^2} \end{pmatrix} \quad (6.14)$$

In this third basis, the Green's function simply reads $\hat{G}_{\text{SF}}^{-1}(\omega) = \omega\hat{1} - \hat{H}_{\text{SF}}(\omega)$. Since, as already stated, the position of the poles in a discrete system does not depend on the basis, the poles of the Green's function $G_{\text{SF } ij}(\omega)$ are determined by the equation:

$$\hat{0} = \omega\hat{1} - \hat{H}_{\text{SF}}(\omega) \iff \begin{cases} \omega - \left[V(\omega) - \sqrt{1 + \left(\frac{D+\Delta\nu(\omega)}{2}\right)^2} \right] = 0 \\ \omega - \left[V(\omega) + \sqrt{1 + \left(\frac{D+\Delta\nu(\omega)}{2}\right)^2} \right] = 0 \end{cases} \quad (6.15)$$

If $\nu_{\text{SF } i}(\omega)$ is the exact potential, these two equations must possess the four⁶ solutions ω_{λ} , the poles of the Green's function of the real system.

However, we test the situation in which we would rather not solve the real system, because the solution is too complicated, or too time-consuming. Therefore, we will pretend not to know the exact position of the poles, solving the previous equations for $\nu_{\text{SF } i}(\omega)$.

On the contrary, we will find the potential somewhere else, put it in eq. (6.15) and obtain the resulting position of the poles $\omega_{\text{SF } \lambda}$. To benchmark our approach, we will compare $\omega_{\text{SF } \lambda}$ to the ones obtained via the reference calculation in the real system, ω_{λ} .

6.3.2 The model system

The approach we will follow here is to import the spectral potential $\nu_{\text{SF } i}(\omega)$ from a model system. The natural candidate for this role is the symmetric Hubbard dimer, in the same way as the homogeneous electron gas will be the model system for real crystals. In both cases, inhomogeneities (or asymmetries) are absent, and an exact solution of these models is easier to obtain (it is the solution of section 4.2). Once the potential is at hand in the model, we import it in the auxiliary system via a suitable connector.

The connector is a very general prescription that states *what* to import and *how* to do that. Both aspects are important. In this chapter we will focus on the first issue, while in the next one, when we will discuss real materials, we will mainly discuss the second. The reason is that, in this case, we do not have much freedom on choosing how to import things. Indeed, once t , U and N are considered as fixed, there is no tunable parameter in the symmetric Hubbard dimer.

We will adopt, as a connector, a *pole-by-pole* correspondence: that is a prescription on how to fix the *frequency* argument in the model system, for a certain value of frequency in the real system. As the two systems are discrete, the spectral function is zero for most of frequencies. There, the spectral potential has an undefined value. On the other hand, we can imagine that,

⁶Other solutions are allowed if the derivative of the potential diverges, as in the $D = 0$ case

switching on D from a $D = 0$ initial situation, the *nature* of the poles be unchanged, and the potential needed to reproduce a certain pole ω_λ is close to the potential we used to reproduce $\omega_\lambda^{(D=0)}$, even if $\omega_\lambda \neq \omega_\lambda^{(D=0)}$. Therefore, it is not the energy ω_λ that matters, but the *state* λ . We use the latter as a connector, namely we set:

$$v_{\text{SF } i}(\omega_\lambda) = v_{\text{SF}}^s(\omega_\lambda^s), \quad (6.16)$$

where s stands for the model system, the symmetric dimer. Note that the right hand side does not depend on the site i , as the model system we are using is not flexible enough to account for such a dependence. Note also that the same argument, a continuous behaviour of the position of the poles of the auxiliary system as a function of D , pushes to consider, also for $D \neq 0$, ω_1 and ω_4 as bonding poles, zeros of the first of eq. (6.15), while ω_2 and ω_3 as antibonding poles, zeros of the second of eq. (6.15).

The second issue is *what* to import: the whole spectral potential, as in eq. 6.16, or just a part of it? Clearly the idea is to treat exactly the spectral potential in the auxiliary system as far as possible, and import from the model system the smallest possible correction. We will investigate different prescriptions in the next section.

6.3.3 Different quantities to import

The strategy that we will follow is to provide a standard treatment of the real system up to a certain level we can get to, let's say Σ_a , with corresponding poles ω_λ^a . On top of this, we import some corrections from the model system, which, by contrast, we are able to solve not only up to Σ_a , but up to Σ , where Σ can be a higher-order approximation to the self energy, or even the exact self energy (like in the symmetric Hubbard dimer).

Concretely, if the model system $D = 0$ is solved by using $\Sigma_{aij}^s(\omega)$ as an approximated self energy, one can obtain the corresponding spectral potential $v_{\text{SF } a}^s(\omega)$ that yields the same spectral function as Σ_a^s , namely the same poles $\omega_\lambda^{a,s}$. If, in particular, the exact self energy Σ^s is at hand, the corresponding spectral potential is the exact one, $v_{\text{SF}}^s(\omega)$, with poles ω_λ^s . This is the content of section 4.2. Note that the poles stemming from the two self energies are in general different. However, as we have decided that the correspondence is set by the state λ and not by its energy ω_λ , we can compare the spectral potentials at the poles, and define their difference $\Xi_a^s(\omega_\lambda^s)$:

$$v_{\text{SF}}^s(\omega_\lambda^s) = v_{\text{SF } a}^s(\omega_\lambda^{a,s}) + \Xi_a^s(\omega_\lambda^s). \quad (6.17)$$

We can set up the same construction in the real $D \neq 0$ system. The exact spectral potential is the spectral potential corresponding to the a approximation, plus a correction:

$$v_{\text{SF } i}(\omega_\lambda) = v_{\text{SF } ai}(\omega_\lambda^a) + \Xi_{ai}(\omega_\lambda), \quad (6.18)$$

where $v_{\text{SF } ai}(\omega)$ is treated exactly within the $D \neq 0$ system, whereas $\Xi_{ai}(\omega)$ accounts for all the corrections beyond Σ_a , and it is not known. The idea of the model system approach is to import the unknown $\Xi_{ai}(\omega_\lambda)$ from the model system, which is here the symmetric dimer, namely to set:

$$\boxed{\Xi_{ai}^{a\text{-dLCA}}(\omega_\lambda) = \Xi_a^s(\omega_\lambda^s)} \quad (6.19)$$

where, as already said, the connection is made through the state label λ , which is indeed the only quantity which is shared by both sides. Note that the right hand side does not depend on the particular site i , but is a global quantity. This is due to the limitations imposed by this choice of the model, which does not offer much freedom in order to tune, *e.g.*, the density. By contrast, in the general approach of dynamical *local* density approximation, a different model system is considered for each point.

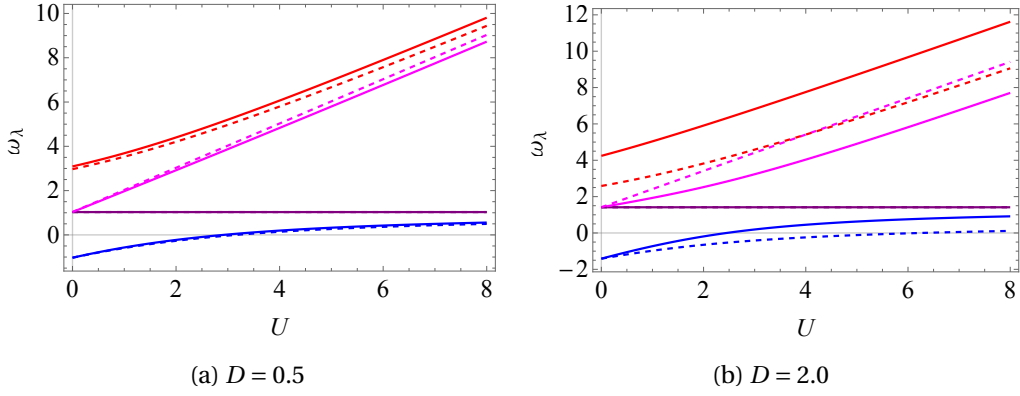


Figure 6.5: Position of the poles of the spin-down Green's function as a function of U . Solid line, exact results; dashed lines, the poles in eq. (6.21).

Different approximations depend on the different starting point Σ_a . We expect the connector approach to work better in situations in which most of the inhomogeneity is treated exactly within the real system, and all higher orders interaction corrections are provided by the model system.

No explicit potential In the simplest case $\Sigma_a = 0$ and, as a consequence, also $v_{\text{SF} a i}(\omega)$ and $v_{\text{SF} a}^s(\omega)$ are zero. From eq. (6.17), the quantity we import is $\Xi_0^s(\omega_\lambda^s) = v_{\text{SF}}^s(\omega_\lambda^s)$, the *whole* spectral potential of the model system; the prescription reads:

$$v_{\text{SF} i}^{0\text{-dLCA}}(\omega_\lambda) = v_{\text{SF}}^s(\omega_\lambda^s) \quad (6.20)$$

This is a *global* potential, independent of the site i . Still, inhomogeneity is accounted for by the external potential term that modifies the free-particle Green's function. By plugging expression (6.20) in the pole equation, eq. (6.15), and by using the same equation also in the model system, we get the four poles in this approximation:

$$\omega_\lambda^{0\text{-dLCA}} = \omega_\lambda^s \pm \left(\sqrt{1 + \frac{D^2}{4}} - 1 \right) \quad (6.21)$$

where the upper (lower) sign is for ω_2 and ω_3 (ω_1 and ω_4). We have achieved an exact disentanglement of interaction, accounted for by ω_λ^s , and inhomogeneity, that results from the second term. The performances of this relatively simple approach are pretty good, see fig. (6.5). Apart from the pole ω_4 , the results are exact in the $D \rightarrow 0$ limit. However, this expression is extremely simple and does not well reproduce the position of the poles for larger values of D or U .

Explicit Hartree potential In principle, a better solution is to have an explicit local dependence in the spectral potential, and import from the model system a smaller term. This is possible if the Hartree potential $v_i^H = U n_i$ is treated exactly in the real system (the asymmetric dimer), and therefore just the exchange-correlation part of the spectral potential is imported (from the symmetric dimer).

Indeed, from the separation $v_{\text{SF} i}(\omega) = v_i^H + v_{\text{SF} i}^{xc}(\omega)$, where $v_{\text{SF} i}^{xc}(\omega)$ is $\Xi_i^H(\omega)$ in the notation introduced above, we decide to take the unknown $v_{\text{SF} i}^{xc}(\omega)$ from the model system. There, the Hartree potential is simply $U/2$, hence $v_{\text{SF}}^{xc s}(\omega) = v_{\text{SF}}^s(\omega) - \frac{U}{2}$. Using the state λ as a connector, the analogous of eq. (6.18) and (6.19) reads:

$$v_{\text{SF} i}^{\text{H-dLCA}}(\omega_\lambda) = U n_i + v_{\text{SF}}^{xc s}(\omega_\lambda^s) \quad (6.22)$$

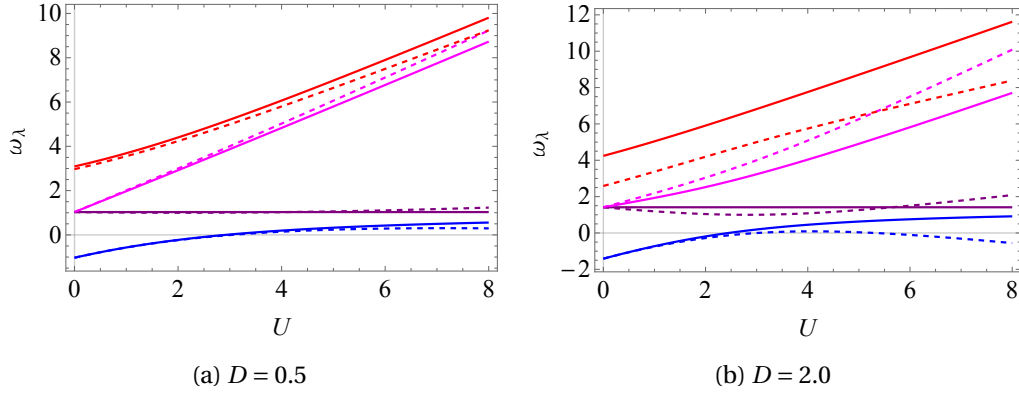


Figure 6.6: Position of the poles of the spin-down Green's function as a function of U . Solid line, exact results; dashed lines, the poles in eq. (6.23).

This is another connector, which again reduces to the exact result for $D \rightarrow 0$, and it explicitly treats some inhomogeneities in the interaction through the Hartree potential of the real system. Only the rest, namely the exchange–correlation part of the potential, is imported from the model.

Implementing this potential in eq. (6.15) to find the position of the poles, we get:

$$\omega_\lambda^{\text{H-dLCA}} = \omega_\lambda^s \pm \left(\sqrt{1 + h^2} - 1 \right), \quad (6.23)$$

which is very similar to the previous one, eq. (6.21) and it has the correct $D \rightarrow 0$ limit. Here, the interaction U enters also the square root, creating an interplay between inhomogeneity and interaction in the position of the poles, even if the two were disentangled in the definition of the potential, eq. (6.22). Still, as in the previous case, the pole ω_4 is not caught by this approximation for nonzero values of D .

Note, finally, that this approximation is an improvement with respect to:

1. The Hartree approximation itself, eq. (6.9). Indeed, with a frequency-dependent potential, the two poles (6.9) can be splitted. Furthermore, they are in good agreement with the expected result, at least for small D , because the correction is imported from the model system.
2. The model approach in which no Hartree term in the real system is explicitly considered, for small values of U . For large U , the previous approximation is a better approximation.

Explicit GW term In the same spirit of what we have just done, we would like to go on in the exact treatment of the real system up to the GW level⁷, and then add, on top, the correction from the model system.

We already evaluated the position of the poles in the GW approximation, eq. (H.25) and figure 6.4. These poles stem from the non-local and complex self energy $\Sigma_{ij}^{G_0 W_0}(\omega)$ and, equivalently, from the local and real spectral potential $v_{\text{SF}i}^{G_0 W_0}(\omega)$.

To find the latter in the model system is easy, as there is a one-to-one correspondence between the potential at the poles and the position of them. That is equation (4.32), that can be solved for the potential whenever the poles are given. For $D = 0$, the GW poles are the ones of

⁷One possible definition of GW: the important point is to use the same GW recipe in both the model and the auxiliary system.

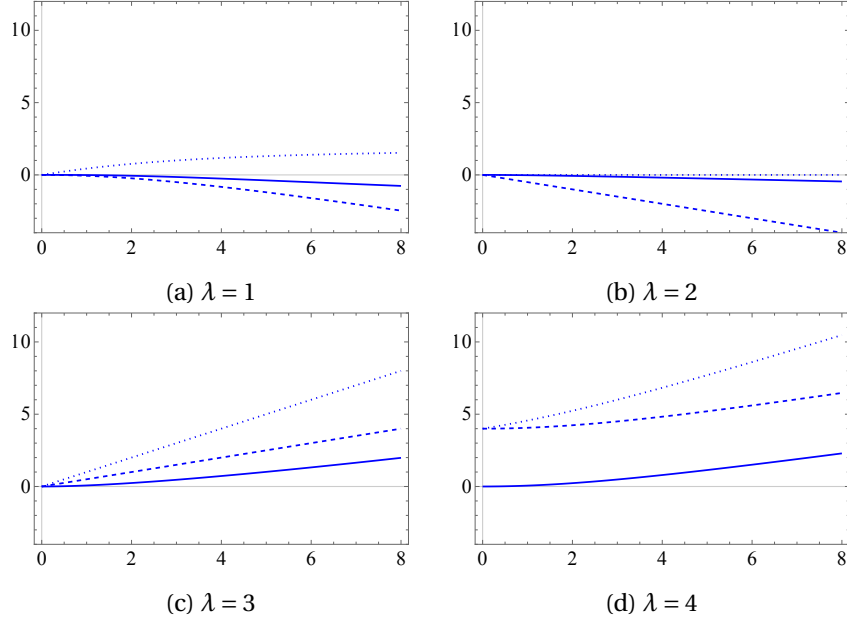


Figure 6.7: Corrections $\Xi_a^s(\omega_\lambda^s)$ for the potential of the model system $D = 0$ as a function of U , in units of t . Dotted lines are the corrections $\Xi_0^s(\omega_\lambda^s) \equiv v_{\text{SF}}^s(\omega_\lambda^s)$. Dashed lines represent the corrections to the Hartree potential, $\Xi_H^s(\omega_\lambda^s) \equiv v_{\text{SF}}^{\text{xc}s}(\omega_\lambda^s)$, while the continuous lines are the corrections $\Xi_{G_0W_0}^s(\omega_\lambda^s)$ to the GW potential of table 6.2 and

eq. (H.23):

$$\omega_\lambda^{G_0W_0s} = \frac{l + \frac{U}{2}}{2} \pm \frac{1}{2} \sqrt{\left(l \pm 2 - \frac{U}{2}\right)^2 + \frac{2U^2}{l}} \quad (6.24)$$

and they are shown in table 6.1.

λ	ω_λ^s	$\omega_\lambda^{G_0W_0s}$
1	$1 + \frac{U-c}{2}$	$\frac{l + \frac{U}{2}}{2} - \frac{1}{2} \sqrt{\left(l + 2 - \frac{U}{2}\right)^2 + \frac{2U^2}{l}}$
2	1	$\frac{l + \frac{U}{2}}{2} - \frac{1}{2} \sqrt{\left(l - 2 - \frac{U}{2}\right)^2 + \frac{2U^2}{l}}$
3	$1 + U$	$\frac{l + \frac{U}{2}}{2} + \frac{1}{2} \sqrt{\left(l - 2 - \frac{U}{2}\right)^2 + \frac{2U^2}{l}}$
4	$1 + \frac{U+c}{2}$	$\frac{l + \frac{U}{2}}{2} + \frac{1}{2} \sqrt{\left(l + 2 - \frac{U}{2}\right)^2 + \frac{2U^2}{l}}$

Table 6.1: Exact and GW poles of the spin-down Green's function in the model system.

The value of the potential that yields these poles, evaluated at the poles, is given by the relation $v_{\text{SF}}^{G_0W_0s}(\omega_\lambda^{G_0W_0s}) = \omega_\lambda^{G_0W_0s} \mp 1$, see eq. (4.32). It is shown in table 6.2.

Their differences $\Xi_{G_0W_0}^s(\omega_\lambda^s) = v_{\text{SF}}^s(\omega_\lambda^s) - v_{\text{SF}}^{G_0W_0s}(\omega_\lambda^{G_0W_0s})$ are the quantities we would like to import in the auxiliary system. Their value is shown in table 6.2, while their behaviour as a function of U is shown in fig. 6.7. In the same figure, I plot the analogous correction $\Xi_0^s(\omega_\lambda^s) \equiv v_{\text{SF}}^s(\omega_\lambda^s)$, occurring if no explicit potential is treated in the real system, and $\Xi_H^s(\omega_\lambda^s) \equiv v_{\text{SF}}^{\text{xc}s}(\omega_\lambda^s)$, if instead of GW we would have considered only the Hartree approximation: we can see that the more the spectral potential is treated exactly in the real system, the smaller the correction to import.

It is clear that GW is a great improvement over the simpler Hartree approximation. Indeed, the correction $\Xi_{G_0W_0}^s(\omega_\lambda^s)$ that one needs to get the exact potential is smaller. Moreover, that

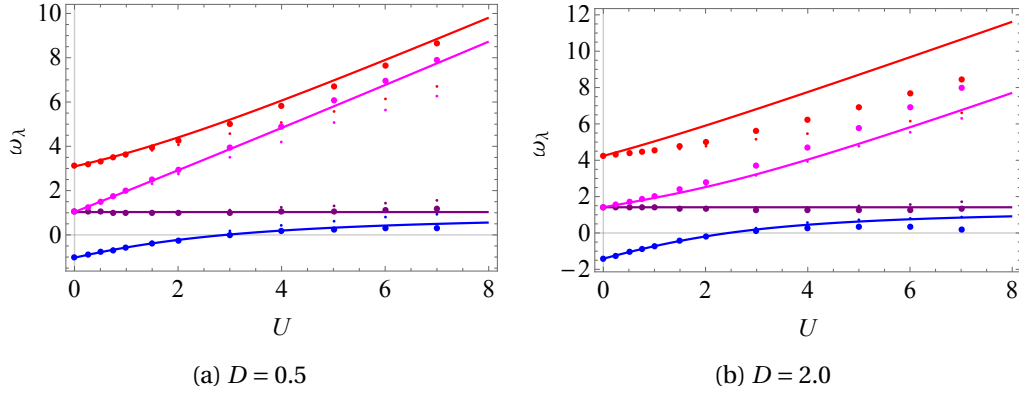


Figure 6.8: Position of the poles of the spin-down Green's function as a function of U . Solid line, exact results. Small dots, the G_0W_0 poles of eq. (H.25) and fig. 6.4. Large dots, the poles $\omega_\lambda^{G_0W_0\text{-dLCA}}$ in eq. (6.26), within the G_0W_0 -dynLCA approach.

λ	$v_{\text{SF}}^s(\omega_\lambda^s)$	$v_{\text{SF}}^{G_0W_0s}(\omega_\lambda^{G_0W_0s})$	$\Xi_{G_0W_0}^s(\omega_\lambda^s)$
1	$2 + \frac{U-c}{2}$	$\frac{l+\frac{U}{2}}{2} - \frac{1}{2}\sqrt{(l+2-\frac{U}{2})^2 + \frac{2U^2}{l}} + 1$	$1 + \frac{\frac{U}{2}-c-l}{2} + \frac{1}{2}\sqrt{(l+2-\frac{U}{2})^2 + \frac{2U^2}{l}}$
2	0	$\frac{l+\frac{U}{2}}{2} - \frac{1}{2}\sqrt{(l-2-\frac{U}{2})^2 + \frac{2U^2}{l}} - 1$	$1 - \frac{\frac{U}{2}+l}{2} + \frac{1}{2}\sqrt{(l-2-\frac{U}{2})^2 + \frac{2U^2}{l}}$
3	U	$\frac{l+\frac{U}{2}}{2} + \frac{1}{2}\sqrt{(l-2-\frac{U}{2})^2 + \frac{2U^2}{l}} - 1$	$1 + \frac{\frac{3}{2}U-l}{2} - \frac{1}{2}\sqrt{(l-2-\frac{U}{2})^2 + \frac{2U^2}{l}}$
4	$2 + \frac{U+c}{2}$	$\frac{l+\frac{U}{2}}{2} + \frac{1}{2}\sqrt{(l+2-\frac{U}{2})^2 + \frac{2U^2}{l}} + 1$	$1 + \frac{\frac{U}{2}+c-l}{2} - \frac{1}{2}\sqrt{(l+2-\frac{U}{2})^2 + \frac{2U^2}{l}}$

Table 6.2: Exact and GW potentials that give the poles of table 6.1, in the model system. Also their difference $\Xi_{G_0W_0}^s(\omega_\lambda^s) = v_{\text{SF}}^s(\omega_\lambda^s) - v_{\text{SF}}^{G_0W_0s}(\omega_\lambda^{G_0W_0s})$ is shown.

same correction is always asymptotically zero for $U \rightarrow 0$ (i.e., GW is asymptotically exact for $U \rightarrow 0$), even for the satellite ω_4 , whose physics is now clearly caught by the RPA polarization of GW.

Connection Got the term $\Xi_{G_0W_0}^s(\omega_\lambda^s)$ in the model system, we place it on top of the GW spectral potential $v_{\text{SF}i}^{G_0W_0}(\omega_\lambda)$ in the auxiliary system, and we obtain:

$$v_{\text{SF}i}^{G_0W_0\text{-dLCA}}(\omega_\lambda) = v_{\text{SF}i}^{G_0W_0}(\omega_\lambda) + \Xi_{G_0W_0}^s(\omega_\lambda^s) \quad (6.25)$$

The GW spectral potential $v_{\text{SF}i}^{G_0W_0}(\omega_\lambda)$ is the spectral potential that exactly yields the GW poles, eq. (H.25). In principle, it is found as the solution of the generalized Sham-Schlüter equation when the self energy is Σ_{GW} . In practice, we do not need its explicit form.

Indeed, plugging the previous expression in eq. (6.15) and using the fact that $\omega_\lambda^{G_0W_0}$ are the solutions of eq. (6.15) when the spectral potential is $v_{\text{SF}i}^{G_0W_0}(\omega_\lambda)$, we obtain the following simple expression for the poles:

$$\omega_\lambda^{G_0W_0\text{-dLCA}} = \omega_\lambda^{G_0W_0} + \Xi_{G_0W_0}^s(\omega_\lambda^s), \quad (6.26)$$

which, still, is exact in the limit of $D \rightarrow 0$. These poles are represented in fig. 6.8.

For small D , the GW approximation in the real system was closing the gap between the Hubbard bands, yielding poles that were blue-shifted in the lower band (ω_1 and ω_2) and red-shifted for the upper band (ω_3 and ω_4), see fig. 6.4. Adding the correction $\Xi_{G_0W_0}^s(\omega_\lambda^s)$ evaluated in the model system restores the expected position of the poles, and the agreement between our theory and the exact result is very good.

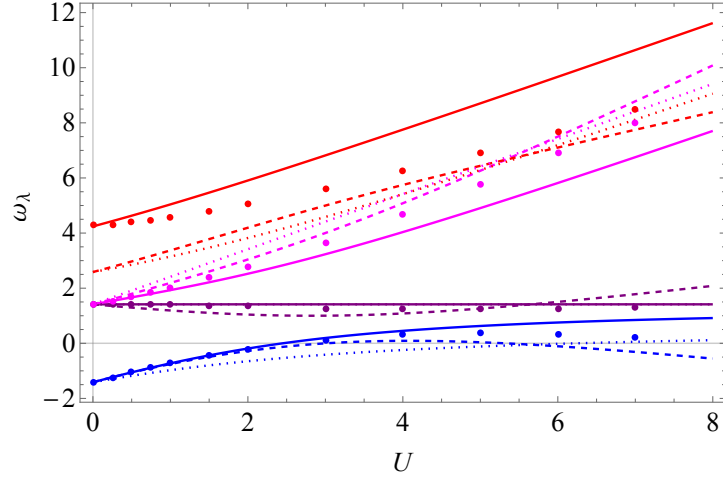


Figure 6.9: Position of the poles of the spin-down Green's function as a function of U , for $D = 2$. Solid line, exact results. Dotted lines for the poles of eq. (6.21), dynLCA on top of nothing. Dashed lines for the poles of eq. (6.23), dynLCA on top of Hartree. Dots, the poles of eq. (6.26), dynLCA on top of GW.

On the contrary, for larger values of D , the GW approximation was already extremely good for ω_1 , ω_2 and ω_3 , while it was not so good for ω_4 . With the model system approach, the agreement is spoiled for the first three poles while it is again improved for the fourth pole.

This behaviour is due to the choice of the model system and the connector. Indeed, the former is fixed, without possible parameters to tune. Therefore, the connector acts only on the frequency part of the potential, without giving any site-dependence to the correction imported from the model. As a consequence, the correction $\Xi_{G_0 W_0}^s(\omega_\lambda^s)$ that we import from the model system, eq. (6.26), does not depend on D , as can be seen from fig. 6.8.

This issue could be overcome by introducing a *local* connector between the model and the auxiliary system, like the local density of LDA. However, this is not straightforward, as the model system, the $N = 1$ symmetric Hubbard dimer, misses a density that could be tuned: there, $n_i = \frac{1}{2}$, and attempts to “localize” this value are not unequivocal.

I summarize the three different procedures of importing from a model system in fig. 6.9. In general, the more pieces of the potential are put into evidence and treated exactly in the auxiliary system, the more accurate the model system approach is. This is true when passing from eq. (6.20) to eq. (6.22), for not too-large interaction, $U \lesssim 2D$, and when passing from eq. (6.22) to eq. (6.25) for an even larger range of U .

The fact that, for small D , the dynLCA approximations work well is not surprising, as the real system is closer to the model system itself, and therefore the dynLDA prescription is better suited. Moreover, for small D , the real system is only slightly inhomogeneous, hence a mean field description as the one proposed here works well. On the contrary, for higher values of D , when properties are truly site-dependent, a *global* correction $\Xi_a^s(\omega_\lambda^s)$ shows its limits. In this regime, a *local* connector is expected to work better but, as already explained, the model system we have chosen is not flexible enough to account for this possibility (if t , U and N are kept fixed).

In this chapter, I have applied the strategy described in chapter 5 to a very simple model, the asymmetric Hubbard dimer. Indeed, despite its simplicity, obtaining the exact solution of the system is not elementary. Instead of exactly solving the real system, the dynLCA approach prescribes to solve a model system – the symmetric dimer, in this case – and then import the effective potential with a suitable connector. In this chapter, we have discussed the choice of the best quantity to import. We have examined three different possibilities: the whole spectral potential, its exchange–correlation part or, finally, only the term beyond GW. As expected, the smaller the correction to import, the better the agreement with the expected result. We have also considered the form of the connector, concluding that it is the state, and not its energy, that must be used to connect the model and the auxiliary system. We will find the same thing in real materials, where a shift of the frequency argument of the spectral potential will be implemented in order to pass from the model to the auxiliary system.

Dynamical Local Connector

Approximation in practice: real systems

The connector idea that we developed in the chapter 5 is theoretically very appealing: it allows one to bypass the calculation of the self energy for every different system, importing the relevant information from a database generated once and forever.

In this chapter we present the results of this approach for four very different real materials: bulk sodium, a nearly homogeneous metal; aluminum, still a metal but less homogeneous; silicon, a semiconductor with a small gap; and finally solid argon, a wide-gap insulator with very localized states. Their minimum, maximum and average densities, n_{\min} , n_{\max} and \bar{n} , are shown in table 7.1, as well as the standard deviation σ_n , defined via $\sigma_n^2 := (n_{\min} - \bar{n})^2 + (n_{\max} - \bar{n})^2$, and its value normalized to the average density σ_n / \bar{n} .

Inhomogeneity in the density stems from the presence of the lattice, which can modify to different extent the motion of electrons. In general, for bulk sodium, the presence of the lattice can be considered as a small perturbation to a free-electron motion, while this is less and less true for aluminum and silicon, till the limit case of argon, whose valence bands can be regarded as atomic-like, with very localized electrons. No matter to which degree, the homogeneous self energy $\Sigma^h(k, \omega)$ is modified by the lattice.

The standard approach is, thus, to build a self energy $\Sigma(\mathbf{k}, \omega)$ for every different system, suited to the particular lattice of that system. Our effective approach, on the contrary, accounts for the lattice inhomogeneity in the properties of the connector, but the electron-electron interaction described by the self energy is evaluated just once and forever in the model system, the homogeneous electron gas. The challenge is therefore to reproduce realistic results obtained via a \mathbf{k} -dependent self energy through a potential evaluated in a homogeneous system.

7.1 Implementation

Since they often offer a realistic representation of a system, and they are a true challenge to our local method, we consider the range-separated hybrids approximation for the self energy. It is given by eq. (4.47):

$$\Sigma_{\text{xc}}^{\text{HSE06}}(\mathbf{r}, \mathbf{r}') = h_{\text{xc}}^{\text{loc}}(\mathbf{r})\delta(\mathbf{r} - \mathbf{r}') + \alpha \Sigma_{\text{x}}^{\text{SR}}(\mathbf{r}, \mathbf{r}') \quad (7.1)$$

with the local part of it given by $h_{\text{xc}}^{\text{loc}}(\mathbf{r}) := v_{\text{xc}}^{\text{PBE}}(\mathbf{r}) - \alpha v_{\text{x}}^{\text{PBE,SR}}(\mathbf{r})$. The PBE functional is the one of ref. [108]. In the homogeneous electron gas, the self energy is expressed by eq. (4.50), and the corresponding spectral potential by eq. (4.63).

	$n_{\min}[a_0^{-3}]$	$n_{\max}[a_0^{-3}]$	$\bar{n}[a_0^{-3}]$	$r_s[a_0]$	$\omega_P[eV]$	$\sigma_n[a_0^{-3}]$	σ_n/\bar{n}
Na	$3.3344 \cdot 10^{-4}$	$4.3731 \cdot 10^{-3}$	$3.9306 \cdot 10^{-3}$	3.9312	6.0468	0.004	0.922
Al	$2.2456 \cdot 10^{-3}$	$3.1902 \cdot 10^{-2}$	$2.6768 \cdot 10^{-2}$	2.0738	15.7821	0.025	0.936
Si	$3.4131 \cdot 10^{-3}$	$8.3875 \cdot 10^{-2}$	$2.9601 \cdot 10^{-2}$	2.0054	16.5962	0.060	2.036
Ar	$4.7366 \cdot 10^{-4}$	$3.7761 \cdot 10^{-1}$	$3.2659 \cdot 10^{-2}$	1.9407	17.4325	0.346	10.608

Table 7.1: *Minimum, maximum, and average densities of the four materials considered; a measure of their inhomogeneity is given by the standard deviation σ_n and its value normalized to the average density σ_n/\bar{n} . Also the Wigner–Seitz radius r_s and the plasma frequency $\omega_P = \sqrt{4\pi\bar{n}}$ are shown.*

We will follow a perturbative approach with respect to a ground state Kohn–Sham calculation in the local density approximation. In other words, we will evaluate the various quantities using the Kohn–Sham density and orbitals, without updating the latter in a subsequent step, till eventually self-consistence. This procedure is analogous to the one-shot GW @LDA.

The self energy standard calculation For the purpose of the implementation, the self energy (7.1) can be expressed in the Bloch basis (see appendix I). In a perturbative approach, we consider only the diagonal elements in the bands. Therefore, the self energy reads:

$$\Sigma_n(\mathbf{k}) = h_{xcn}^{\text{loc}}(\mathbf{k}) + \alpha \Sigma_{xn}^{\text{SR}}(\mathbf{k})$$

As a consequence, a generic excitation reads:

$$\varepsilon_n(\mathbf{k}) = \left[\varepsilon_n^0(\mathbf{k}) + v_n^{\text{ext}}(\mathbf{k}) + v_n^{\text{H}}(\mathbf{k}) + h_{xcn}^{\text{loc}}(\mathbf{k}) \right] + \alpha \Sigma_{xn}^{\text{SR}}(\mathbf{k}) \quad (7.2)$$

This calculation, considered as a reference calculation to benchmark our approach, is done through the use of the open source code `Abinit`, version 7.10.5 [133, 134], for a certain number of \mathbf{k} -points in the irreducible part of the first Brillouin zone and for a certain number of bands. Since we are perturbative in the LDA Kohn–Sham orbitals, the quantity in square brackets is nothing but $\left[\varepsilon_n^{\text{KS-LDA}}(\mathbf{k}) - v_n^{\text{xc-LDA}}(\mathbf{k}) + h_{xcn}^{\text{loc(PBE)}}(\mathbf{k}) \right]$: it is the sum of simple quantities that can be obtained from a self consistent Kohn–Sham calculation, with little effort. On the contrary, the bottleneck in the calculation is the non-local self energy, hence the total computation time is similar to the one of a Hartree–Fock calculation.

Once the excitation energies $\varepsilon_n(\mathbf{k})$ are at hand, the spectral function in Bloch space is evaluated as:

$$A_n(\mathbf{k}, \omega) = \delta(\omega - \varepsilon_n(\mathbf{k})) \quad (7.3)$$

with the delta function represented by a Gaussian function with broadening $\eta = 0.1\text{eV}$. The bandstructure is obtained from it as $\omega = \varepsilon_n(\mathbf{k})$. From $A_n(\mathbf{k}, \omega)$ we have access both to the diagonal in real space of the spectral function:

$$A(\mathbf{r}, \mathbf{r}, \omega) = \frac{1}{V} \sum_{\mathbf{k} \in 1\text{BZ}} \sum_n u_{n\mathbf{k}}(\mathbf{r}) \delta(\omega - \varepsilon_n(\mathbf{k})) u_{n\mathbf{k}}^*(\mathbf{r}), \quad (7.4)$$

and to the interacting density of states $A(\omega) := \frac{1}{V} \int d^3r A(\mathbf{r}, \mathbf{r}, \omega)$, which is nothing but the integrated spectral function and reads:

$$A(\omega) = \frac{1}{V} \sum_{\mathbf{k} \in 1\text{BZ}} \sum_n \delta(\omega - \varepsilon_n(\mathbf{k})) \quad (7.5)$$

This last quantity is the one that we will consider to benchmark our approach.

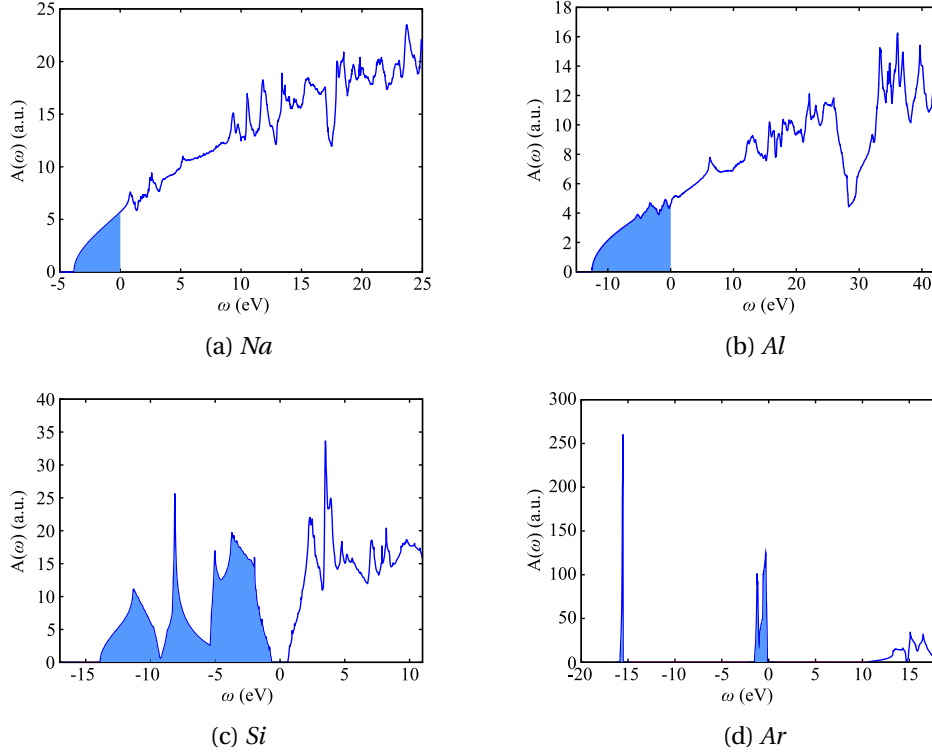


Figure 7.1: *Integrated spectral function $A(\omega)$ in the HSE06 approximation (in atomic units), as a function of frequency (in eV), aligned with $\mu = 0$ (for insulators, alternatively the mid-gap or the highest occupied level), for the four systems considered: sodium, aluminum, silicon and argon. The coloured area is the occupied band. Only for this picture, the tetrahedron method [135] is used to perform the sum in eq. (7.5), resulting in a very sharp integrated spectral function. This method has not yet been implemented for our approach, therefore, for the next figures, we will use a simple sum also for the self energy reference calculation.*

The calculation is carried out for the four prototypical systems mentioned above: sodium, aluminum, silicon and argon. Here are the physical and numerical characteristics of the four systems considered:

Sodium Sodium is a metal, whose density range is shown in table 7.1. It crystallizes in a body-centered cubic (BCC) lattice, with experimental [136] lattice constant $a = 4.225\text{\AA}$. To treat the ions (each one formed by a nucleus and the core electrons), we employ a Trouiller–Martins (TM) pseudopotential [137]. For the three calculations, LDA, reference and dynLCA, we use a Γ -centered grid of $30 \times 30 \times 30$ k -points, making 752 k -points in the irreducible part of the first Brillouin zone, and 20 bands. We use a common cut-off energy of 20.0 Hartree (Ha), and a gaussian smearing of 0.01 Ha to converge the k -integral. For the reference calculation, a cutoff of 4.0 Ha in the exchange part of the self energy is used, and 6.0 Ha for the wavefunctions.

Aluminum Aluminum is still a metal, but less homogeneous, see table 7.1. It crystallizes in a face-centered cubic (FCC) lattice, with a lattice constant $a = 4.049\text{\AA}$. In this case we use an optimized norm-conserving Vanderbilt (ONCV) pseudopotential [138]. To converge, we employed a Γ -centered grid of $38 \times 38 \times 38$ k -points, making 1440 k -points in the irreducible part of the first Brillouin zone, and 20 bands. Cutoff energy of 20.0 Ha, and a temperature smearing of 0.005 Ha. For the self energy calculation, a cutoff of 4.0 Ha for the exchange component is

	KS-LDA		HSE06	
	W [eV]	E_g [eV]	W [eV]	E_g [eV]
Na	3.25	0.00	3.83	0.00
Al	11.09	0.00	12.65	0.00
Si	11.96	0.56	13.26	1.20
Ar	14.41	8.31	15.71	10.74

Table 7.2: *The occupied band width W and band gap E_g , in eV, for the four materials considered (for Ar, also the s band is considered as a valence band), in DFT within the LDA approximation and with the HSE06 self energy.*

used, and 6.0 Ha for the wavefunctions.

Silicon Silicon is a semiconductor with a small experimental gap of 1.16 eV [139]. Its density range is wider than for aluminum, see table 7.1. Silicon crystallizes in a FCC lattice, and it has an experimental [136] lattice constant $a = 5.429 \text{ \AA}$. We use a TM pseudopotential [137]. A Monkhorst–Pack [140] grid of $14 \times 14 \times 14$ k -points with 4 shifts is considered, making 344 k -points in the irreducible part of the first Brillouin zone, and 12 bands. We consider a cutoff energy of 20.0 Ha. For the self energy calculation, we use a cutoff of 4.0 Ha in the exchange part of it, and 10.0 Ha for the wavefunctions.

Argon Argon is a wide gap insulator, and it is definitely not homogeneous: its density range is shown in table 7.1. It crystallizes into a FCC lattice, with an experimental [136] lattice constant $a = 5.256 \text{ \AA}$. We use a TM pseudopotential [137], and a Monkhorst–Pack [140] grid of $12 \times 12 \times 12$ k -points with 4 shifts, making 231 k -points in the irreducible part of the first Brillouin zone, and 12 bands. The cutoff energy is 20.0 Ha. For the reference calculation, a cutoff of 12.0 Ha in the exchange part of it is considered, and a cutoff of 16.0 Ha for the wavefunctions.

The results of the self energy calculation, which constitute the benchmark for our approach, are presented in fig. 7.1. Bandwidth W and gap E_g are given in table 7.2.

Implementation of dynLCA The self energy approach is what we have been referring to as the real system calculation. In the auxiliary system, the role of the self energy is played by the spectral potential. This is a local and frequency-dependent real potential which is nothing but the self energy whenever the latter is real and local, and differs from it otherwise. Therefore, as the self energy in eq. (7.1) contains a real and local part, it is natural to assume the following structure for the exchange–correlation spectral potential:

$$v_{\text{SF}}^{\text{xc}}(\mathbf{r}, \omega) = h_{\text{xc}}^{\text{loc}}(\mathbf{r}) + \alpha v_{\text{x}}^{\text{SR}}(\mathbf{r}, \omega), \quad (7.6)$$

which¹ in Bloch basis, see eq. (I.6), reads:

$$v_{\text{SF}n}^{\text{xc}}(\mathbf{k}, \omega) = h_{\text{xc}n}^{\text{loc}}(\mathbf{k}) + \alpha v_{\text{x}n}^{\text{SR}}(\mathbf{k}, \omega) \quad (7.7)$$

This potential yields, in a perturbative approach, the following excitation energies:

$$\varepsilon_n^{\text{SF}}(\mathbf{k}, \omega) = \left[\varepsilon_n^0(\mathbf{k}) + v_n^{\text{ext}}(\mathbf{k}) + v_n^{\text{H}}(\mathbf{k}) + h_{\text{xc}n}^{\text{loc}}(\mathbf{k}) \right] + \alpha v_{\text{x}n}^{\text{SR}}(\mathbf{k}, \omega) \quad (7.8)$$

¹In the purely frequency-dependent part of the spectral potential, $v_{\text{x}}^{\text{SR}}(\mathbf{r}, \omega)$, I drop the subscript SF for clarity reasons.

The quantity in square brackets is the same as in eq. (7.2), and it is evaluated in the real system through a simple Kohn–Sham calculation.

On the contrary, the role of the non–local self energy is played here by the purely frequency–dependent part of the spectral potential. We do not want to evaluate it exactly through the Sham–Schlüter equation (3.24), nor we want to find an approximation to it via the linearized Sham–Schlüter equation (3.25).

Here we stick to the connector approach, namely we import $v_x^{\text{SR}}(\mathbf{r}, \omega)$ from the homogeneous electron gas database, $\{v_x^{\text{SR}h}(\omega)\}_{nh}$, via different prescriptions that I illustrate below. Then we evaluate the matrix element $v_{xn}^{\text{SR}}(\mathbf{k}, \omega)$ and we plug it in eq. (7.8). Note that the calculation time is here drastically reduced: instead of the construction of a non–local self energy, we just have to read an external file.

The spectral function in Bloch space is not a simple delta function, as eq. (7.3), because the excitation energy is now frequency–dependent:

$$A_n^{\text{SF}}(\mathbf{k}, \omega) = \delta(\omega - \varepsilon_n^{\text{SF}}(\mathbf{k}, \omega)) \quad (7.9)$$

The band structure is obtained from solving the equation $\omega - \varepsilon_n^{\text{SF}}(\mathbf{k}, \omega) = 0$. The solution is $\omega = \varepsilon_n^{\text{SF}}(\mathbf{k})$. On the other hand, the integrated spectral function in the auxiliary system reads:

$$A_{\text{SF}}(\omega) = \frac{1}{V} \sum_{\mathbf{k} \in \text{1BZ}} \sum_n \delta(\omega - \varepsilon_n^{\text{SF}}(\mathbf{k}, \omega)) \quad (7.10)$$

We have implemented this procedure in `abinit`, version 7.10.5, and carried out the calculation for the same four prototypical materials, Na, Al, Si and Ar. To discuss the validity of this approach, we benchmark the resulting $A_{\text{SF}}(\omega)$ with its reference calculation counterpart $A(\omega)$.

Local density approximation We benchmark our results also to a simpler approach, Kohn–Sham in the standard local density approximation, in which the potential $v_{KS}^{\text{LDA}}(\mathbf{r})$, taken from ref. [120], is static. In general, as can be seen from table 7.2, LDA underestimates both gaps and the bandwidths with respect to HSE06.

LDA is very similar to an approximation to the Kohn–Sham potential that is on the same footing of `dynLCA` but with a static potential. It consists in importing the exchange–correlation potential $\tilde{v}_{xc}^{\text{KS}}(\mathbf{r})$ from the homogeneous electron gas at the local density. However, in the HEG, $\tilde{v}_{xc}^{\text{KS}h}$ reproduces the density obtained from an HSE06 calculation, and not the exact density of [103]. The potential $\tilde{v}_{xc}^{\text{KS}h}$ can be viewed as the exact exchange potential $\tilde{v}_{xc}^{\text{EX-HSE}h}$ in which the Fock self energy is replaced by the HSE06 one.

Such a potential, in the HEG, is given by:

$$\begin{aligned} \tilde{v}_{xc}^{\text{EX-HSE}} &= h_{xc}^{\text{loc}} + \alpha \Sigma_x^{\text{SR}}(k_F) \equiv h_{xc}^{\text{loc}} + \alpha v_x^{\text{SR}} = \\ &= v_{xc}^{\text{PBE}} + \alpha (v_x^{\text{SR}} - v_x^{\text{SR(PBE)}}) = v_{xc}^{\text{LDA}} \end{aligned}$$

as in the homogeneous electron gas PBE does not differ from LDA [141]. Therefore, importing in the auxiliary system via the local density, $\tilde{v}_{xc}^{\text{LDA}}(\mathbf{r}) = \tilde{v}_{xc}^{\text{EX-HSE}}|_{n^h=n(\mathbf{r})}$, we finally get that $\tilde{v}_{xc}^{\text{LDA}}(\mathbf{r}) = v_{xc}^{\text{LDA}}(\mathbf{r})$. Thus, $v_{KS}^{\text{LDA}}(\mathbf{r})$ can be considered as a static version of $v_{\text{SF}}(\mathbf{r}, \omega)$ and, by comparing our results to LDA, we appreciate the importance of frequency–dependence in $v_{\text{SF}}(\mathbf{r}, \omega)$.

7.2 The simplest connector: Fermi energy alignment

We start our investigation from the simplest connector applied to the simplest system. The simplest system we consider is bulk sodium, which is very close to the model system itself. As

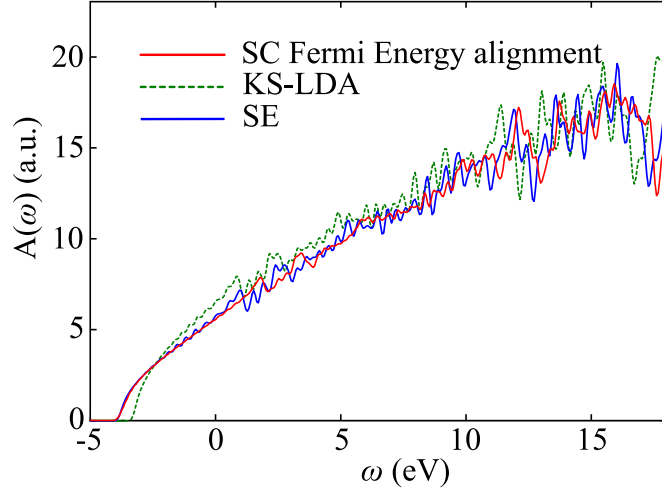


Figure 7.2: *Integrated spectral function of sodium, in eV, as a function of frequency, in eV. In blue the reference calculation with the self energy, in green LDA, in red our approach, dynLCA, with the connector of eq. (7.11). The three curves are aligned with $\mu = 0$.*

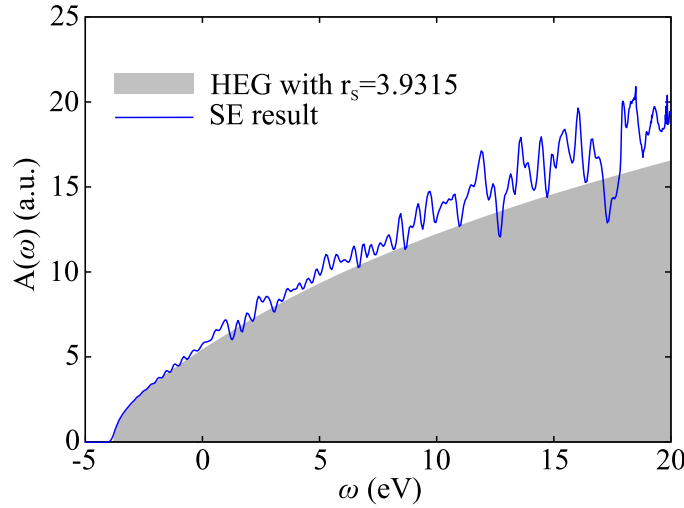


Figure 7.3: *Integrated spectral function of sodium, in eV, as a function of frequency, in eV. In blue the reference calculation with the self energy, in gray the homogeneous electron gas integrated spectral function with $r_s = 3.9315$ (Na average density).*

the homogeneous electron gas, indeed, sodium is a metal, and it is almost homogeneous (see table 7.1).

Since this system is almost homogeneous, we first implement the connector of eq. (5.17), applied to the purely frequency-dependent part of the hybrid spectral potential. In the spirit of eq. (5.15) (or of LDA), for each point \mathbf{r} we consider a homogeneous electron gas with the same local density $n(\mathbf{r})$ of the real system:

$$v_x^{\text{SR}}(\mathbf{r}, \omega) = v_{x n^h = n(\mathbf{r})}^{\text{SR}h}(\omega - \mu + \mu_{n^h = n(\mathbf{r})}^h) \quad (7.11)$$

This formula is extremely simple, and it is the most obvious connector for a system that is very close to the model. A drawback is that the Fermi energy μ of the auxiliary system appears, which is in principle an output result of the calculation done with $v_x^{\text{SR}}(\mathbf{r}, \omega)$ itself. To set its

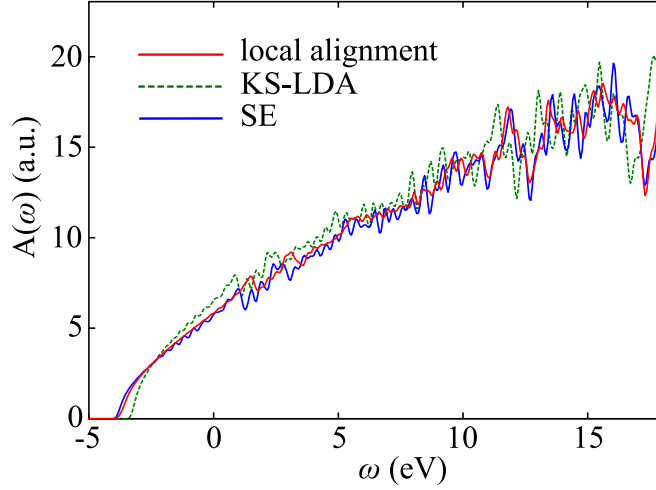


Figure 7.4: *Integrated spectral function of sodium, in eV, as a function of frequency, in eV. In blue the reference calculation with the self energy, in green LDA, in red our approach, dynLCA, with the connector of eq. (7.14). The three curves are aligned with $\mu = 0$.*

value, we here consider two possibilities: the first one is using the Fermi energy evaluated in the reference calculation. This is a quick recipe for the purpose of illustrating the results, but it is not efficient when studying real materials, as the aim of this whole thesis is to avoid a time consuming reference calculation with the self energy. Thus, we are left with the second possibility, namely finding the value of μ via an iteration cycle: one first guesses a value $\mu^{(\text{in})}$, plugs it into eq. (7.11), performs the calculation and evaluates the resulting Fermi energy $\mu^{(\text{out})}$, which becomes the new input parameter for the second cycle, until convergence is reached. For the materials we consider (in the HSE06 approximation), this procedure is converging after a few steps.

The result, shown in fig. 7.2, is already extremely promising: our approach reproduces the exact shape of the integrated spectral function, from the valence band to high unoccupied bands. It clearly overcomes the performances of LDA. In particular, the bandwidth is in excellent agreement with the reference calculation.

However, some shortcomings are still present: whenever the spectrum exhibits a spike (a *Van Hove singularity* [142]), in correspondence of high symmetry points in the Brillouin zone, this is always blue-shifted with respect to the reference calculation. It is a systematic shift, as opposed, *e.g.*, to the LDA one, which is a blue-shift for the valence band and a red-shift in the unoccupied region. By contrast, the dynLCA shift is always towards higher values of frequencies: it is zero at the bottom of the valence band, it increases for higher energies and then it decreases to zero for high bands.

To conclude, we have already obtained an important result: in fact, as the spectral potential of the homogeneous electron gas does not vary in a significant way over the density range of sodium, the local density in eq. (7.11) could be harmlessly replaced by an average density \bar{n} , and the result would not change. The corresponding connector, different from the one in eq. (7.11), would be:

$$v_x^{\text{SR}}(\mathbf{r}, \omega) = v_x^{\text{SR}h} n^{h=\bar{n}} (\omega - \mu + \mu_{n^h=\bar{n}}^h) \quad (7.12)$$

This prescription – and basically also the one in eq. (7.11) – is simply to *rigidly* move the model system on top of the real system by shifting the frequency argument and therefore aligning their energy scales to a common one. As the right hand side of eq. (7.12) does not depend on \mathbf{r} , *all* the inhomogeneities of sodium are accounted for by the previous terms, $v^{\text{ext}}(\mathbf{r}) +$

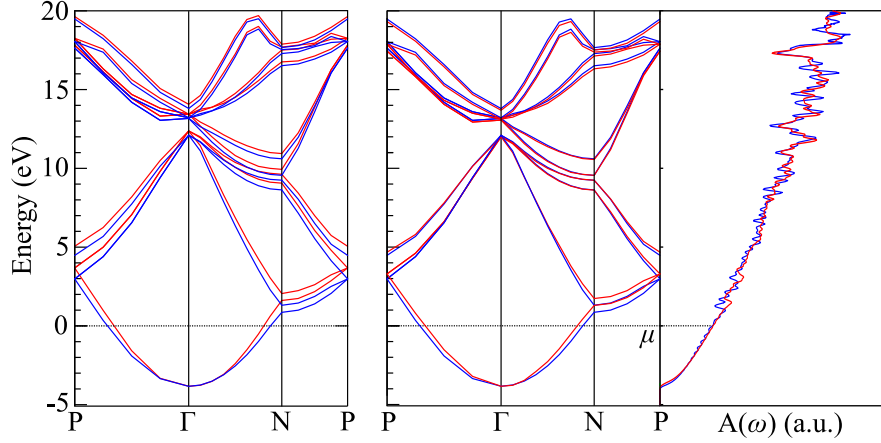


Figure 7.5: *Band structure in the real system $\varepsilon_{nn}(\mathbf{k})$, in blue, and in the auxiliary system, $\varepsilon_{nn}^{\text{SF}}(\mathbf{k})$, in red, for three paths in the first Brillouin zone of sodium. To the left, the spectral potential is the one of eq. (7.11), with the alignment of the Fermi energies; to the right the one of eq. (7.14), with a shift of the frequency argument by the external plus the Hartree potential. Also the corresponding integrated spectral function is shown.*

$v^{\text{H}}(\mathbf{r}) + h_{\text{xc}}^{\text{loc}}(\mathbf{r})$, and the electron–electron interaction effects described by $\Sigma_{\text{x}}^{\text{SR}}(\mathbf{r}, \mathbf{r}')$ are dealt with by $v_{\text{x}\bar{n}}^{\text{SR}h}$. This complete disentanglement of inhomogeneity from the non-trivial part of the electron–electron interaction works pretty well in this case, as the final result is astonishingly good. This will not be the case for less homogeneous systems, where a complete disentanglement is usually not achievable and indeed the right hand side of eq. (7.11) will acquire a strong local dependence.

Note, finally, the importance of evaluating most of the terms directly in the *real* system, the ones in square brackets in eq. (7.8): they constitute a valuable ground, already containing a lot of information on the real system, on top of which $v_{\text{x}\bar{n}}^{\text{SR}h}$ acts. The opposite limit, in which *everything* is imported from the model system (which is another way of saying that we approximate the system with a HEG at the average density), is shown as a shaded region in fig. 7.3. The valence part of the spectrum, as well as the value of the bandwidth, are well reproduced; the reason is that the valence band does not cross any high-symmetry point of the Brillouin zone, hence the dispersion is close to the one of the corresponding homogeneous electron gas. On the other hand, no feature coming from inhomogeneity (spikes, wells) is obviously caught by this procedure.

7.3 A shortcut: local alignment

The alignment of the static Fermi energy μ to the Fermi energy of the model system μ^h in eq. (7.11) depends on \mathbf{r} , as the latter is evaluated at the local density $n(\mathbf{r})$. On the other hand, μ is always just a number, and this does not leave much freedom to introduce locality in the frequency-dependence.

Another issue linked to the chemical potential is the self-consistent iterative procedure we discussed above: while the potential does not appreciably change over the density range of sodium, it still varies a lot with frequency, see fig. 5.5. Therefore, a precise value for μ is required. Especially for metals, this is difficult to get, as a large number of k -points is needed to locate the Fermi surface.

An alternative to the Fermi energy alignment is thus desirable. This is given by the Thomas–

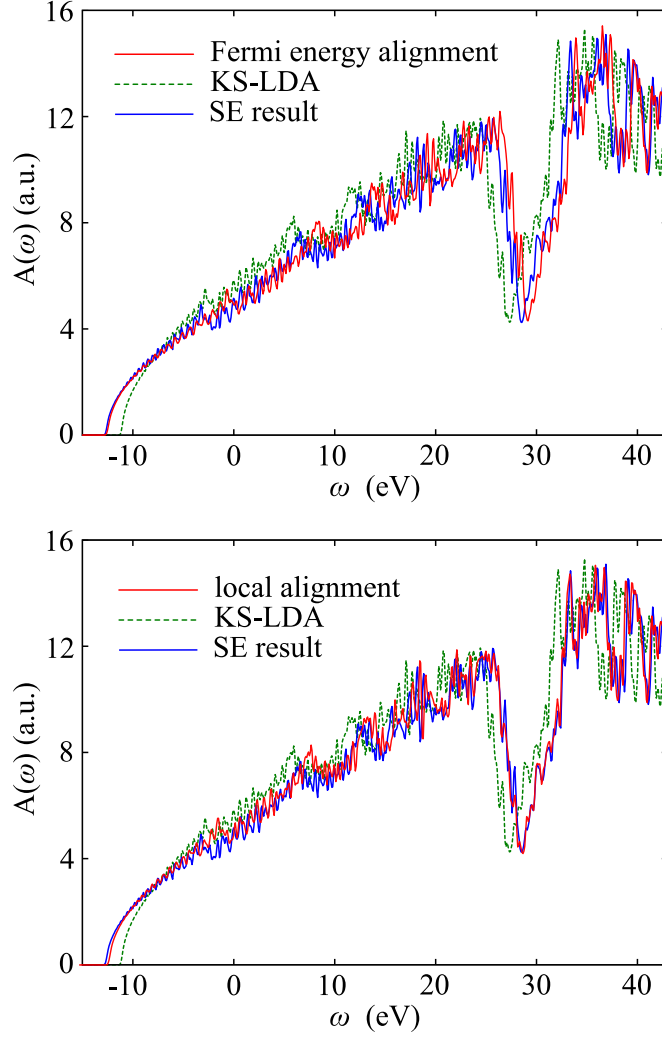


Figure 7.6: *Integrated spectral function of aluminum, in eV, as a function of frequency, in eV. In blue the reference calculation with the selfenergy, in green LDA, in red our approach, dynLCA, with the connector of eq. (7.11), above, and the one of eq. (7.14), below. The three curves are aligned with $\mu = 0$.*

Fermi relation, valid for slowly varying density [128]:

$$\mu = v^{\text{ext}}(\mathbf{r}) + v_{\text{H}}(\mathbf{r}) + \mu_{n^h=n(\mathbf{r})}^h \quad (7.13)$$

Therefore, we can switch from the Fermi energy alignment $\mu - \mu_{n^h=n(\mathbf{r})}^h$ in eq. (7.11) to the sum of the external and the Hartree potential, which are still functionals of the density:

$$v_{\text{x}}^{\text{SR}}(\mathbf{r}, \omega) = v_{\text{x}n^h=n(\mathbf{r})}^{\text{SR}h}(\omega - v^{\text{ext}}(\mathbf{r}) - v_{\text{H}}(\mathbf{r})) \quad (7.14)$$

This in *another* connector, in which the interplay between inhomogeneity and interaction is possibly stronger, as more local dependence enters the frequency argument. Note that the previous knowledge of the Fermi energy μ is no more needed here: we can avoid the self-consistent iteration cycle $\mu^{(\text{in})} \rightarrow \mu^{(\text{out})}$ as well as a precise evaluation of the chemical potential at the end of the calculation. Finally, this connector fits exactly the general form of eq. (5.15), with $c(\mathbf{r}, \omega) = v^{\text{ext}}(\mathbf{r}) + v_{\text{H}}(\mathbf{r})$, and no external correction is needed.

The resulting integrated spectral function $A(\omega)$ is shown in fig. 7.4. The dynLCA result is still on top of the reference calculation, and the blue-shift of the peaks has been reduced. This

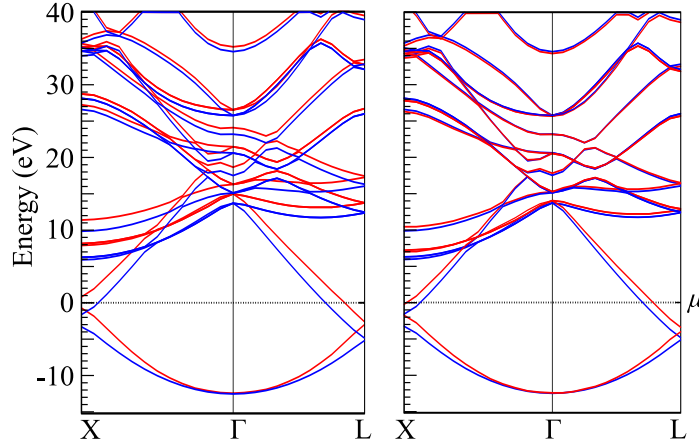


Figure 7.7: Band structure in the real system $\epsilon_{nn}(\mathbf{k})$, in blue, and in the auxiliary system, $\epsilon_{nn}^{\text{SF}}(\mathbf{k})$, in red, for two paths in the first Brillouin zone of aluminum. To the left, the spectral potential is the one of eq. (7.11), with the alignment of the Fermi energies; to the right the one of eq. (7.14), with a shift of the frequency argument by the external plus the Hartree potential.

is most evident if we consider the band structure, fig. 7.5: the discrepancies in the high energy region have almost disappeared, and they are reduced even in the low energy region. Still, these discrepancies are most evident at the high symmetry points of the first Brillouin zone. An interesting remark is that this is qualitatively the same blue-shift of the band structure of the homogeneous electron gas, fig. 4.21. We will come back to this point below.

Aluminum Aluminum, a less homogeneous metal, follows the same qualitative behaviour of sodium, see fig. 7.6: a pretty good reproduction of the shape of the integrated spectral function, in particular in the valence region, where the bandwidth is significantly improved with respect to LDA. Furthermore, the local alignment of eq. (7.14) is an improvement over the Fermi energy alignment of eq. (7.11), as in the case of sodium.

On the other hand, as well as in sodium, there is a systematic blue-shift of the intraband peaks towards higher frequencies. This is most evident in the peaks at -3.3 eV, 6.1 eV, 13.0 eV and for the deep dip at 28 eV for the Fermi energy alignment, and it still survives, even though reduced, in the local alignment connector for the low energy peaks.

This discrepancy is most evident in the band structure, fig. 7.7. In principle, the band structure is not a quantity which is reproduced in the auxiliary system; indeed, for the whole valence band in sodium and for the low energy region of the valence band of aluminum, although the band structure is not reproduced, the integrated spectral function $A_{\text{SF}}(\omega)$ is in excellent agreement with $A(\omega)$. On the other hand, as soon as a band crosses a high symmetry point in the Brillouin zone, the spectrum displays a peak and this is blue-shifted with respect to the reference calculation. Also for aluminum, as in sodium, this blue-shift is qualitatively the same that we had in the homogeneous electron gas, fig. 4.21.

We will come back to this issue in the next section. For the moment, let us focus on the general shape of the spectra, which is very well reproduced for the two metals we have considered. We can conclude that this second connector, eq. (7.14), is not only a shortcut with respect to the previous one, eq. (7.11), but also an improvement of it in the agreement with the reference calculation.

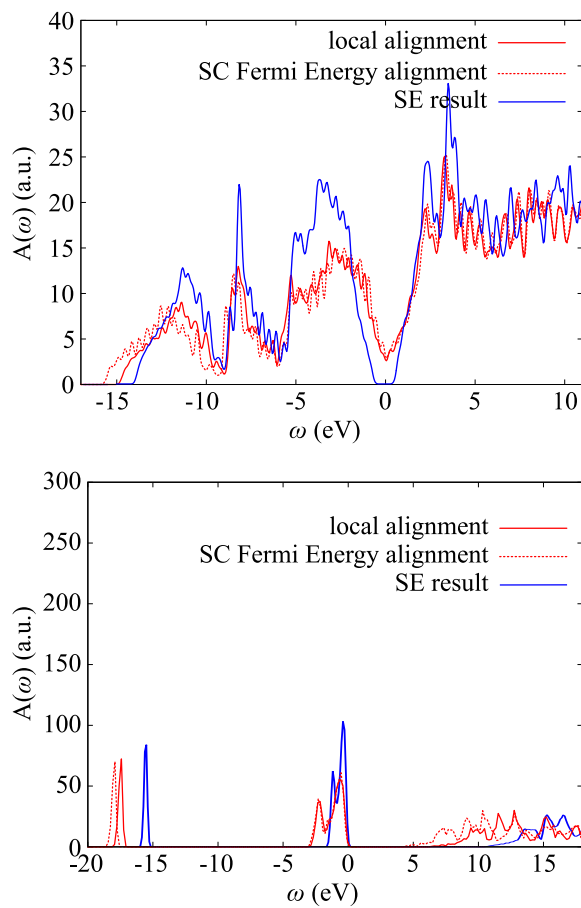


Figure 7.8: *Integrated spectral function of silicon (above) and argon (below) as a function of frequency. In blue the reference calculation with the self-energy, in red the dynLCA approach: dotted line for eq. (7.11), continuous line for the connector of eq. (7.14). The three curves are aligned with $\mu = 0$.*

Insulators On the other hand, not the Fermi energy alignment nor this simple local alignment are able to reproduce the integrated spectral function of non-zero gap systems, silicon and argon, as it is shown in fig. 7.8. As for silicon, we are not able to open the gap, and the bandwidth is overestimated with both procedures. In argon the behaviour is similar: the gap is not zero but largely underestimated, and the bandwidth is overestimated.

Note that, at least for silicon, which is not as inhomogeneous as argon (see table 7.1: actually, it is comparable to aluminum), we can still recover a HEG-like behaviour, as it is evident from fig. 7.9: as for sodium and aluminum, the intraband peaks are blue-shifted with respect to the reference calculation, resulting in an overestimation of the bandwidth; the shift increases for increasing energy in the low energy region, and then fades out for higher energy. On the contrary, argon is so inhomogeneous that this HEG-like picture breaks down and other effects appear.

As a final remark, for both silicon and aluminum, the connector of eq. (7.14) is an improvement over the one of eq. (7.11), but it is nevertheless clearly unsatisfactory.

A further refinement of the connector is required.

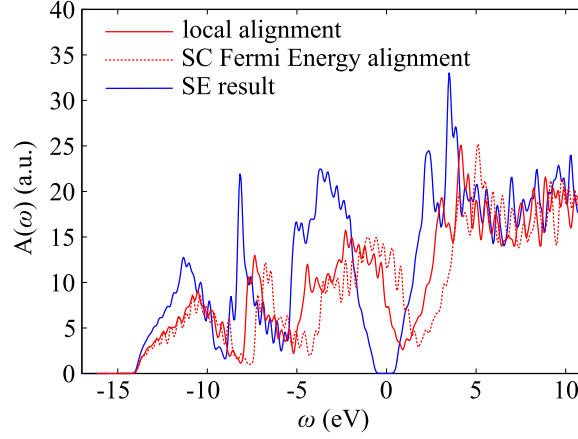


Figure 7.9: Silicon as in fig. 7.8, but with the *dynLCA* curves aligned to the bottom of the band: in this way it is clear that the behaviour of silicon, too, is similar to that of sodium and aluminum: a larger blue-shift with respect to the reference calculation for the connector of eq. (7.11), reduced by the connector of eq. (7.14). The shift, that increases at low energies, then becomes smaller for higher bands.

7.4 Band structure correction

To proceed further, we should gain a better understanding of how the HEG potential is modified in the solid. In order to do so and to avoid additional complications, it is useful to compare the homogeneous electron gas to the system which is the closest to it, sodium.

Here, the free particle dispersion $\omega_k = \frac{k^2}{2}$ is only slightly modified by the lattice, that opens small gaps in correspondence of some high-symmetry points, like N [101]. However, apart from this, the band structure remains generally close to the one of the homogeneous electron gas, see fig. 7.10, left panels².

The behaviour of the two band structures is so similar that we can try to make a parallelism between them. Indeed, roughly up to the Fermi energy μ , both in sodium as in the HEG the auxiliary system band structure (red line) is blue-shifted with respect to the real system one (blue line), more or less of the same amount. This discrepancy in the band structure does not prevent the resulting integrated spectral functions from matching. The reason for this in the HEG was analytically explained at pag. 86: we need a non-zero difference $\Delta_{\mathbf{k}}$, eq. (4.70), in the band structures, to allow a purely frequency-dependent potential to reproduce $A^h(\omega)$. The same holds true for sodium.

This argument, which holds also for higher bands, breaks down at the high-symmetry points N and P. There, the discrepancies in the band structure are not absorbed by the HEG $\Delta_{\mathbf{k}}$ -mechanism (that does not know what a gap is), and they become manifest in the integrated spectral function.

A very elaborated connector, that modifies the frequency-dependence of the spectral po-

²Note that, to avoid numerical issues due to the numerical implementation in `abinit`, we have here considered the homogeneous electron gas treated as a real material, hence the noise in the spectrum $A(\omega)$. No connector is needed for reproducing the HEG spectral function. Put it differently, the connectors we introduced smoothly tend towards the homogeneous spectral potential in the limit of constant density.

The homogeneous electron gas we have considered is the following: a fictitious *empty* simple cubic lattice with lattice parameter $a = 5.54a_0$ and $r_S = 3.9315a_0$ (Na average density). For the three calculations, LDA, self energy and *dynLCA*, we use an unshifted grid of $30 \times 30 \times 30$ k -points, making 2176 k -points in the first irreducible Brillouin zone, and 15 bands. Cut-off energy of 6.0 Ha, gaussian smearing of 0.01 Ha. For the self energy calculation, a cut-off of 4.0 Ha for both the exchange part of it and for the wavefunctions.

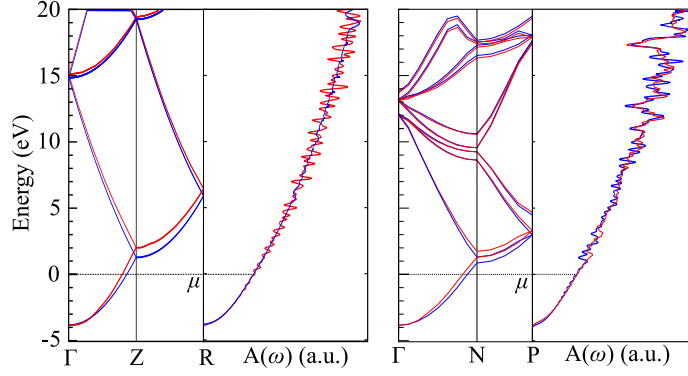


Figure 7.10: *Band structure and integrated spectral function of the homogeneous electron gas (left) and sodium (right), at the same average density. The homogeneous electron gas results are evaluated numerically as for real system.*

tential of the HEG in a non-trivial way, would be, in principle, able to overcome this issue and generate the exact spectral function even with a different band structure. In practice, finding such a connector can be extremely difficult. Therefore, we here propose a pragmatic solution.

It is clear that a *new* spectral potential $\tilde{v}_{\text{SF}}(\mathbf{r}, \omega)$, still real, local and frequency-dependent, that do not rest on the $\Delta_{\mathbf{k}}$ -mechanism but, on the contrary, explicitly reproduce the band structure (hence $\tilde{\Delta}_{\mathbf{k}} = 0$) and, through it, the integrated spectral function, would have more chances, when imported in the real material, to produce a band structure that *stick* to the true one and thus do not blue-shift features like intraband peaks.

This potential is, in the HEG, exactly the one we introduced in the end of section 4.3, as a trick to have both the band structure and the spectral function at once. It is connected to the old potential by eq. (4.75):

$$v_{\text{SF}}^h(\omega) \longrightarrow \tilde{v}_{\text{SF}}^h(\omega) = v_{\text{SF}}^h(\omega) - \Delta^h(\omega), \quad (7.15)$$

with $\Delta^h(\omega)$ defined by eq. (4.76):

$$\Delta^h(\omega) := v_{\text{SF}}^h(\omega) - \Sigma_{\text{xc}}^h(k_0(\omega)) = \alpha \Delta_{\text{x}}^{\text{SR}h}(\omega) \quad (7.16)$$

with:

$$\Delta_{\text{x}}^{\text{SR}h}(\omega) := v_{\text{x}}^{\text{SR}h}(\omega) - \Sigma_{\text{x}}^{\text{SR}h}(k_0(\omega)) \quad (7.17)$$

Working with $\tilde{v}_{\text{SF}}^h(\omega)$ in place of $v_{\text{SF}}^h(\omega)$ in the auxiliary system, its band structure is exactly the real system one by construction. To obtain also the exact value of the diagonal of the real system spectral function, one has to employ the prescription (4.78):

$$\tilde{A}_{\text{SF}}(\mathbf{r}, \mathbf{r}, \omega) := \frac{1}{2\pi^2} \int_0^{+\infty} dk k^2 \delta(\omega - \tilde{\varepsilon}_k^{\text{SF}}), \quad (7.18)$$

in place of (4.77), which is the homogeneous electron gas version of the more general equation (7.10), that we have used so far:

$$\tilde{A}_{\text{SF}}(\mathbf{r}, \mathbf{r}, \omega) = \frac{1}{2\pi^2} \int_0^{+\infty} dk k^2 \delta(\omega - \tilde{\varepsilon}_k^{\text{SF}}(\omega)) \quad (7.19)$$

with $\tilde{\varepsilon}_k^{\text{SF}}(\omega) = \varepsilon_k^0 + \tilde{v}_{\text{SF}}^h(\omega)$, and $\tilde{\varepsilon}_k^{\text{SF}}$ the solution of the equation $\omega - \tilde{\varepsilon}_k^{\text{SF}}(\omega) = 0$ for a given \mathbf{k} , namely, with a non-extraordinary notation, $\tilde{\varepsilon}_k^{\text{SF}} = \tilde{\varepsilon}_k^{\text{SF}}(\tilde{\varepsilon}_k^{\text{SF}})$.

The difference between the two prescriptions is subtle. In the latter, we first evaluate the k -integral, even without knowing the form of $\tilde{v}_{\text{SF}}^h(\omega)$, which results in $\frac{1}{2\pi^2} \tilde{k}_0^{\text{SF}}(\omega)$, see eq. (4.77);

only later (or independently) we fix the band structure by saying that $\tilde{k}_0^{\text{SF}}(\omega)$ is the solution to the equation $\omega - \tilde{\varepsilon}_k^{\text{SF}}(\omega) = 0$ (at fixed ω); the integrated spectral function takes priority over the band structure.

On the other hand, with the new prescription, eq. (7.18), we first fix the band structure by solving the equation $\omega - \tilde{\varepsilon}_k^{\text{SF}}(\omega) = 0$ (at fixed k) to find $\tilde{\varepsilon}_k^{\text{SF}}$ and then evaluate the spectral function. In this case, the band structure comes first and the spectral function follows.

If we stick to this new potential in the homogeneous electron gas, and import it in the real material through the connector (7.14), also the new prescription to evaluate the spectral function, eq. (7.18), must be implemented in the solid, or we would not be HEG-consistent when treating real materials (indeed – in our opinion – one of the most important criteria to design a connector is that it reduce to “the identity” in the uniform density limit, namely the HEG be exact as an auxiliary system as it is exact as a model system).

Therefore, we update the dynLCA approach in the following way: we use the potential (7.15) in place of $v_{\text{SF}}^h(\omega)$; the connector (7.14) thus reads³:

$$\boxed{v_{\mathbf{x}}^{\text{SR}}(\mathbf{r}, \omega) = [v_{\mathbf{x}}^{\text{SR}} - \Delta_{\mathbf{x}}^{\text{SR}}]_{n^h=n(\mathbf{r})}^h (\omega - v^{\text{ext}}(\mathbf{r}) - v_{\text{H}}(\mathbf{r}))} \quad (7.20)$$

From the potential $v_{\mathbf{x}}^{\text{SR}}(\mathbf{r}, \omega)$, we can build, via eq. (7.8), the frequency-dependent excitation energy $\varepsilon_{nn}^{\text{SF}}(\mathbf{k}, \omega)$. Solving the equation $\omega - \varepsilon_{nn}^{\text{SF}}(\mathbf{k}, \omega) = 0$ we get the band structure of the auxiliary system, $\omega = \varepsilon_{nn}^{\text{SF}}(\mathbf{k})$. Finally, from the band structure we obtain the diagonal of the spectral function via the formula:

$$A_{\text{SF}}(\omega) = \frac{1}{V} \sum_{\mathbf{k} \in \text{1BZ}} \sum_n \delta(\omega - \varepsilon_{nn}^{\text{SF}}(\mathbf{k})), \quad (7.21)$$

which replaces eq. (7.10). This new approach is still exact in the HEG limit, namely it yields the exact value of the diagonal of the real system spectral function. Furthermore, it also reproduces the exact band structure of the HEG.

Its performances for the two prototypical metals, sodium and aluminum, are shown in fig. 7.11. The agreement of the dynLCA curves with the reference results is excellent, both for sodium and for aluminum. Apart from a slight underestimation of the bandwidth, the dynLCA curve matches exactly the behaviour of the reference calculation and, in particular, the intra-band peaks – fingerprint of inhomogeneity – are in the expected position.

We can conclude that, at least for the two metals considered, the connector (7.20), together with the prescription (7.21), disentangles to a large extent the interaction described by the non-local self energy from inhomogeneity: the former is accounted for by the potential (and the Δ term) in the HEG, the latter by the local quantities $n(\mathbf{r})$, $v^{\text{ext}}(\mathbf{r})$ and $v_{\text{H}}(\mathbf{r})$ that enter the form of the connector.

Besides the theoretical insight, this result is also noteworthy on the computational side, as the cost for obtaining the dynLCA curves is similar to usual KS, much cheaper than the self energy calculation we implemented to obtain the reference curves.

Finally, also for the non-zero gap systems we studied, silicon and argon, the improvement with respect to the previous results, fig. 7.8, is impressive. This is shown in fig. 7.12. The first consideration is that dynLCA is now in good agreement with the reference calculation; it reproduces the shape of $A(\omega)$ and it definitely does a much better job than LDA. However, the bandwidth, in both cases, is slightly smaller than expected (as in sodium and aluminum), and the gap is underestimated.

³The meaning of the notation is that both quantities, $v_{\mathbf{x}}^{\text{SR}}$ and $\Delta_{\mathbf{x}}^{\text{SR}}$, are evaluated at the shifted frequency argument.

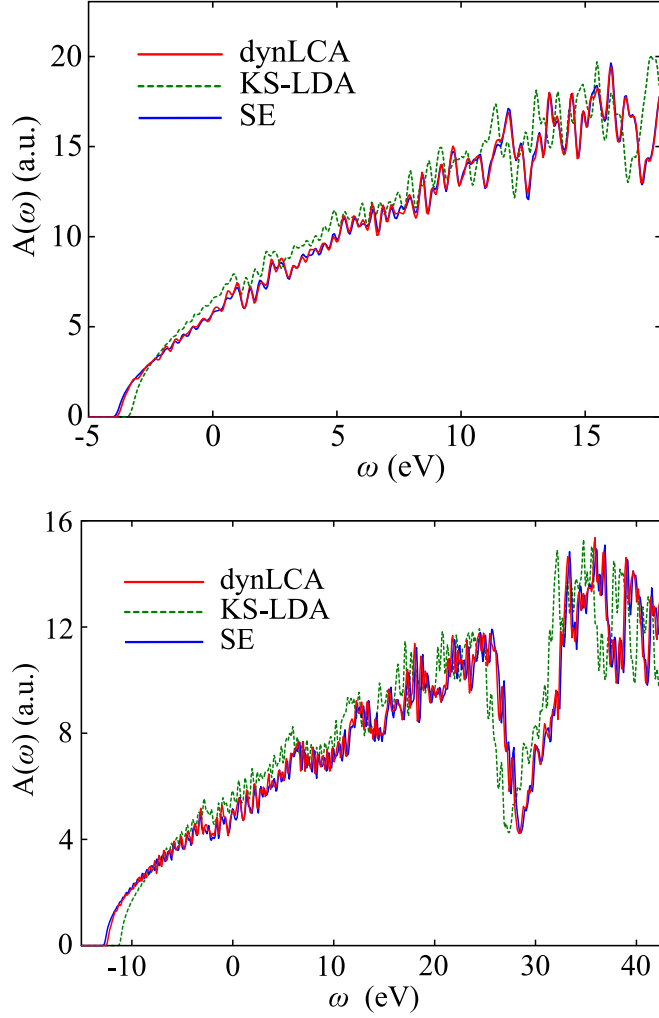


Figure 7.11: *Integrated spectral function of sodium (above) and aluminum (below) as a function of frequency, with $\mu = 0$. In blue the reference calculation with the self energy, in green LDA, in red the *dynLCA* approach of eq. (7.20) and eq. (7.21).*

That eq. (7.20) here shows its limits is expected. Its form is extremely simple, and it still yields a potential which is very close to the one in the HEG, as the connector prescription basically consists in a local shift of frequency. To better handle gapped systems, we look for a further refinement of the connector (7.20).

7.5 External correction

A hint for understanding the limitations of the simple connectors of the previous section when tackling non-zero gap systems is provided by the general discussion of section 5.5.1: whenever a gap, or a large depletion of spectral weight, shows up in the unoccupied band, a connector based on the Fermi energy alignment can hardly reproduce it: a stronger dependence on space is demanded.

Such a dependence is offered, formally, by the external correction to the HEG potential represented by the term $c(\mathbf{r}, \omega) - v^{\text{ext}}(\mathbf{r}) - v_{\text{H}}(\mathbf{r})$ in eq. (5.15). Such a term was zero for the connectors we have considered, in which $c(\mathbf{r}, \omega) = v^{\text{ext}}(\mathbf{r}) + v_{\text{H}}(\mathbf{r})$.

Therefore, to have an explicit non-zero correction, we generalize $c(\mathbf{r}, \omega)$ to $c(\mathbf{r}, \omega) = v_{\text{KS}}(\mathbf{r}) -$

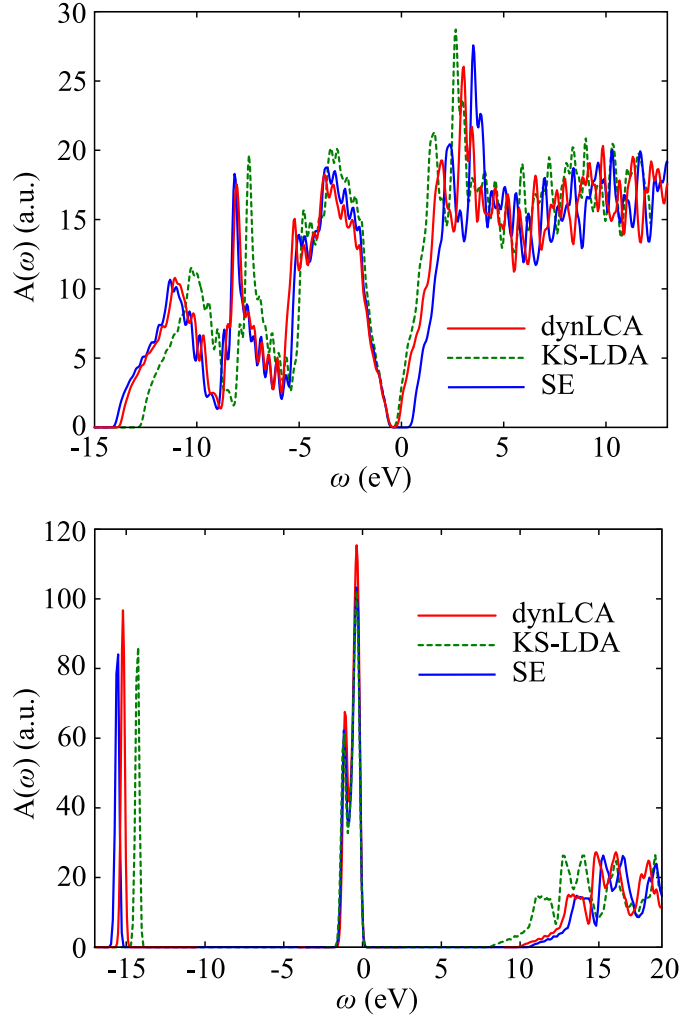


Figure 7.12: *Integrated spectral function of silicon (above) and argon (below) as a function of frequency, with $\mu = 0$. In blue the reference calculation with the selfenergy, in green LDA, in red the dynLCA approach of eq. (7.20) and eq. (7.21).*

$v_{\text{KS } n^h = \bar{n}}^h$, which tends to the previous value for slowly varying density. With such an ansatz, the external correction becomes $c(\mathbf{r}, \omega) - v^{\text{ext}}(\mathbf{r}) - v_{\text{H}}(\mathbf{r}) = v_{\text{KS}}^{\text{xc}}(\mathbf{r}) - v_{n^h = \bar{n}}^{\text{xc } h}$.

Finally, we rescale frequencies by the plasmon energies $\omega_{\text{P}} = \sqrt{4\pi n}$, which set the characteristic energy scales [143]; the final connector reads:

$$v_{\text{x}}^{\text{SR}}(\mathbf{r}, \omega) = [v_{\text{x}}^{\text{SR}} - \Delta_{\text{x}}^{\text{SR}}]_{n^h = n(\mathbf{r})}^h \left(\frac{\omega_{\text{P}}(n(\mathbf{r}))}{\omega_{\text{P}}(\bar{n})} (\omega - v_{\text{KS}}(\mathbf{r}) + v_{\text{KS } n^h = \bar{n}}^h) \right) + [v_{\text{KS}}^{\text{xc}}(\mathbf{r}) - v_{n^h = \bar{n}}^{\text{xc } h}] \quad (7.22)$$

This is still a fairly simple connector, in which all ingredients are evaluated from the HEG or from a cheap Kohn–Sham calculation on the real system. It is a generalization of the previous one, eq. (7.14), for systems with a density that spans a wider range; indeed, the application of this formula to sodium or aluminum is basically equivalent to the previous one, and yields the same results of fig. 7.11.

On the contrary, this formula shows its potential for silicon and argon, as it is shown in fig. 7.13. For argon, the LDA values for gap and bandwidth (8.31 eV and 14.41 eV, respectively) are increased to 10.74 eV and 15.71 eV, respectively, by the HSE06 calculation (see table 7.2). An application of the connector (7.22) yields a gap of 10.85 eV and a bandwidth of 15.70 eV. This

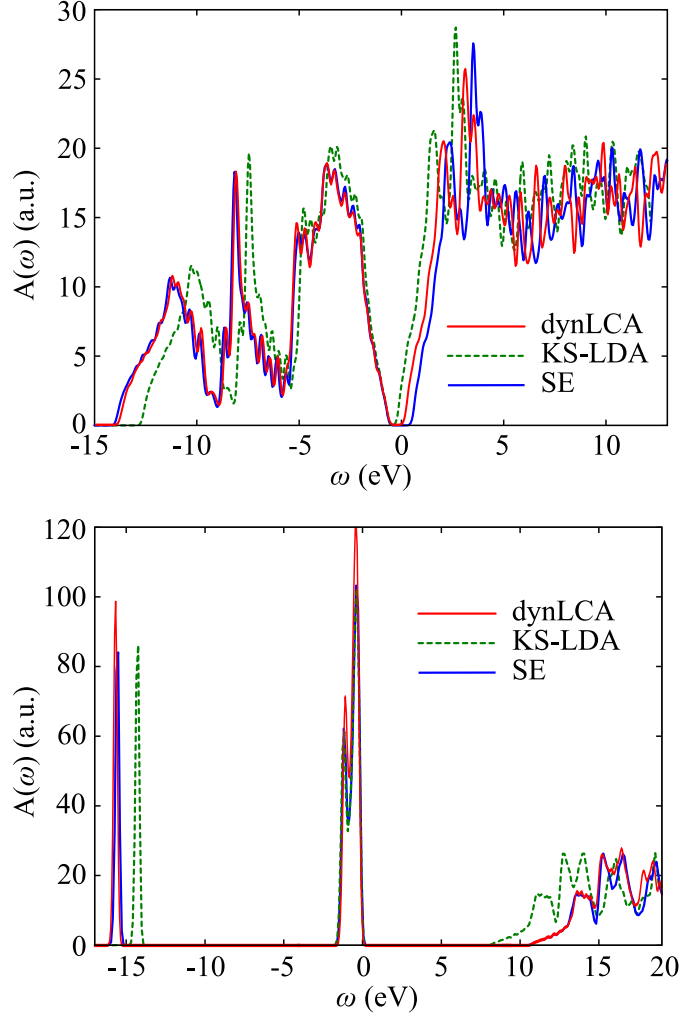


Figure 7.13: *Integrated spectral function of silicon (above) and argon (below) as a function of frequency, with $\mu = 0$. In blue the reference calculation with the self energy, in green LDA, in red the dynLCA approach of eq. (7.22).*

reduces the gap error from 22% in the LDA to 0.9% in dynLCA, and the bandwidth error from 8.3% in the LDA to 0.06% in dynLCA.

As for silicon, the LDA gap and valence bandwidth of respectively 0.56 eV and 11.96 eV are increased by the HSE06 calculation to the reference values of 1.20 eV and 13.26 eV. Implementing eq. (7.22) reduces the bandwidth error from 10% in the LDA to 1% (13.11 eV), and the gap error from 53% to 35% (0.78 eV); also the shape of the integrated spectral function is very good.

We argue that the better agreement we obtain in argon with respect to silicon is due to the fact that, in argon, electrons are quite localized and therefore they are more easily accessible by a local potential based on the local density. On the opposite side, metals are closer to the model system, the homogeneous electron gas. In an intermediate range, represented by silicon, deviations appear.

7.6 The dynLCA band structure

To obtain the quantity $A_{\text{SF}}(\omega)$, we passed through the band structure $\omega = \varepsilon_{nn}^{\text{SF}}(\mathbf{k})$, eq. (7.21). As already said, the excitation energies in the auxiliary system $\varepsilon_{nn}^{\text{SF}}(\mathbf{k})$ have no a direct physical meaning, in the same way as the Kohn–Sham excitation energies $\varepsilon_{nn}^{\text{KS}}(\mathbf{k})$ are not the exact

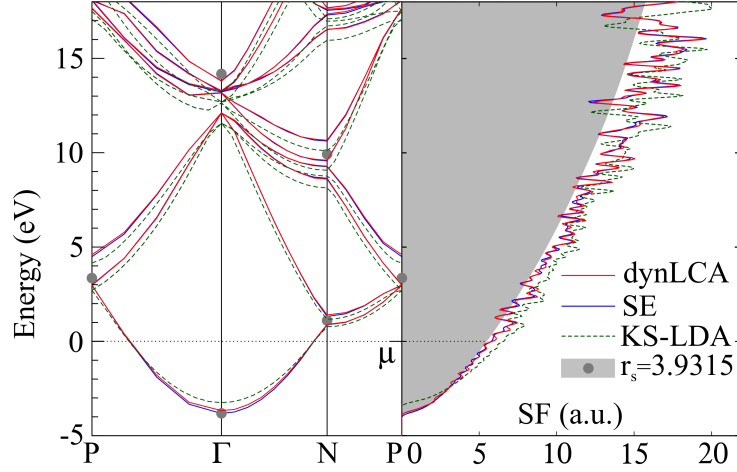


Figure 7.14: Sodium, band structure (left) and integrated spectral function (right). In blue the reference calculation with the self energy, in green LDA, in red the dynLCA approach of eq. (7.22). The gray dots and the gray shaded region represent the band structure and spectral function of a HEG with density equals to the average density of sodium ($r_s = 3.9315a_0$).

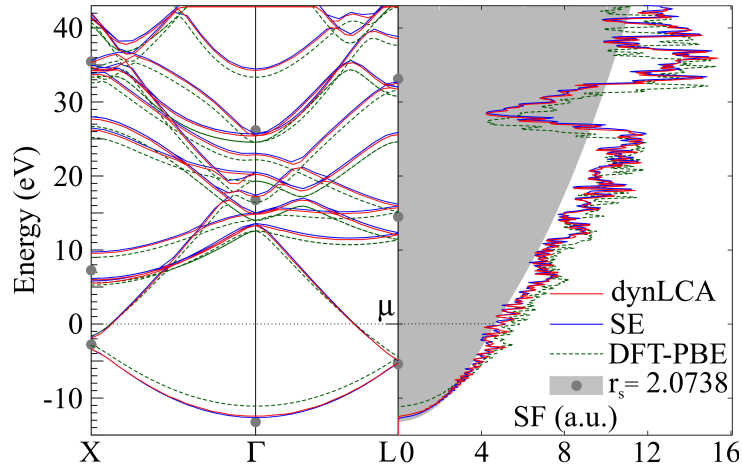


Figure 7.15: Aluminum, band structure (left) and integrated spectral function (right). In blue the reference calculation with the self energy, in green LDA, in red the dynLCA approach of eq. (7.22). The gray dots and the gray shaded region represent the band structure and spectral function of a HEG with density equals to the average density of aluminum ($r_s = 2.0738a_0$).

addition and removal energies. Both just represent an intermediate step to obtain what the auxiliary system is supposed to yield, the local density in Kohn–Sham and the diagonal of the spectral function in real space here.

In particular, to have the exact band structure from the relation $A_{nn}(\mathbf{k}, \omega) = \delta(\omega - \varepsilon_{nn}(\mathbf{k}))$, one must have also the exact off–diagonal elements of the spectral function in real space, as it is clear from the following inverse Fourier transform (see appendix I):

$$A_{nn}(\mathbf{k}, \omega) = \frac{1}{V} \int d^3r |u_{n\mathbf{k}}(\mathbf{r})|^2 A(\mathbf{r}, \mathbf{r}, \omega) + \frac{1}{V} \int d^3r d^3r' e^{-i\mathbf{k}\cdot(\mathbf{r}-\mathbf{r}')} u_{n\mathbf{k}}^*(\mathbf{r}) A(\mathbf{r}, \mathbf{r}', \omega) u_{n\mathbf{k}}(\mathbf{r}')$$

The auxiliary system, through the exact spectral potential, yields only the real system values of the diagonal elements $A(\mathbf{r}, \mathbf{r}, \omega)$, but not of the off–diagonal ones. These, in principle, can be

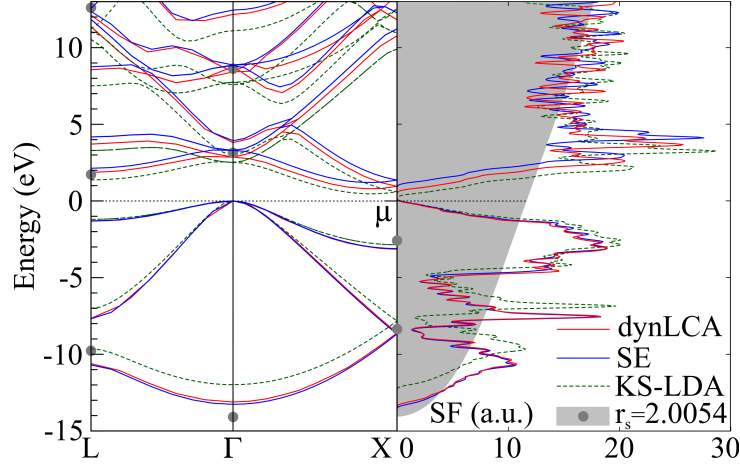


Figure 7.16: Silicon, band structure (left) and integrated spectral function (right). In blue the reference calculation with the self energy, in green LDA, in red the dynLCA approach of eq. (7.22). The gray dots and the gray shaded region represent the band structure and spectral function of a HEG with density equals to the average density of silicon ($r_s = 2.0054a_0$).

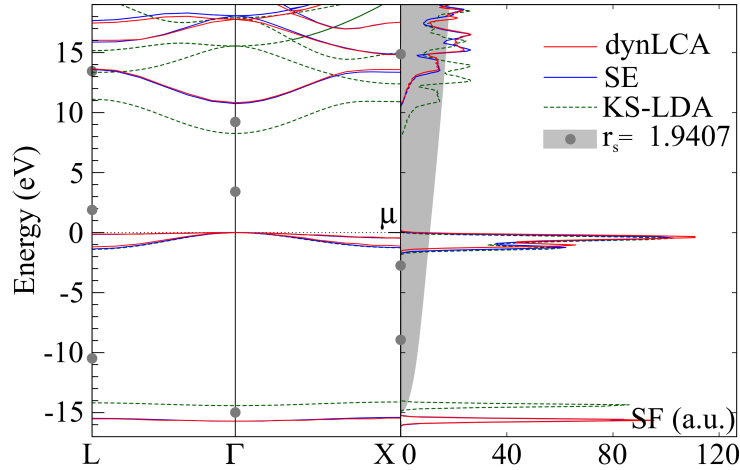


Figure 7.17: Argon, band structure (left) and integrated spectral function (right). In blue the reference calculation with the self energy, in green LDA, in red the dynLCA approach of eq. (7.22). The gray dots and the gray shaded region represent the band structure and spectral function of a HEG with density equals to the average density of argon ($r_s = 1.9407a_0$).

completely unrelated from the real system ones, resulting in a band structure which is different from the reference calculation.

Thus, it is remarkable that the band structures evaluated in the auxiliary systems of the four materials considered are in excellent agreement with their counterparts in the real systems, see fig. 7.14, 7.15, 7.16 and 7.17.

On the other hand, some aspects must be considered. The first is *symmetry*: as it was shown for the dimer and for the homogeneous electron gas, the off-diagonal elements of the spectral function are often connected to the diagonal elements by relations pertaining to the geometry of the system only (the dimer), or to the diagonal of the spectral function itself (the HEG). In these cases, an explicit knowledge of the off-diagonal elements $A(\mathbf{r}, \mathbf{r}', \omega)$ is not even needed, as all the information for the band structure is in $A(\mathbf{r}, \mathbf{r}, \omega)$ only. Therefore, if the latter is repro-

duced, also the former is in principle at hand.

Furthermore, the spectral potential in the HEG–connector approach is a dynamical generalization of LDA that targets, besides the density, also the diagonal of the spectral function. This means further constraints that the auxiliary system has to fulfill or, in other words, additional matches between auxiliary and real system quantities. Already the LDA band structure is not particularly weird, see the figures: it usually just needs a rigid shift – a scissor operator [144] – to match with the reference band structure. This shift is recovered in dynLCA by the fact that the diagonal of the spectral function must match its real system counterpart; hence, in practice, no much freedom is left to the band structure.

Finally, another element to consider is that the potential $v_{\text{SF}} - \Delta$, in the HEG, reproduces *also* the band structure by construction. Since the connectors (7.20) and (7.22) are HEG–consistent, namely they generate a potential that reduces to the HEG potential in the limit of uniform density, also the band structure that they produce reduces to the band structure of the HEG in that limit.

These considerations show that, although in principle the band structure can be crazier than expected, in practice this is not the case. One obtains, as a completely unforeseen by-product, a band structure in an extremely good agreement with the reference calculation. This result inaugurates the possibility of describing also angle resolved photoemission experiments, for which $A_{nn}(\mathbf{k}, \omega) = \delta(\omega - \varepsilon_{nn}(\mathbf{k}))$, hence the band structure, is needed (see eq. (1.10)).

We finally got the result we were looking for: a real, local and frequency–dependent potential, evaluated just once in a model system, is able to reproduce the integrated spectral function of real materials, at least for the four system we have considered, to a very good extent. Also the band structure, that was not expected to be recovered in the beginning, is indeed in surprisingly good agreement with the result obtained in the real system. As the computation time, one of the biggest issues in condensed matter physics, is drastically diminished, one could think – as far as spectral properties are concerned – to use this method instead of the standard one based on the self energy.

Conclusion

*We shall not cease from exploration
And the end of all our exploring
Will be to arrive where we started
And know the place for the first time*

THOMAS STEARNS ELIOT, Four Quartets

This thesis represents a modest contribution to the theoretical description of many–electron systems. I have presented the formulation of the problem in chapter 2, together with its standard approach in terms of Green’s functions. These are powerful intermediate objects, through which a full description of the many–body system can be accomplished. When focusing on photoemission processes (chapter 1), the one–particle Green’s function furnishes a complete description of the microscopic propagation of electrons and holes in the material. To obtain it, one usually introduces a non–local, complex and frequency–dependent self energy. However, to describe the outcome of an experiment, only the trace of the imaginary part of the Green’s function is needed. Therefore, once the Green’s function has been evaluated, which is a computationally expensive process because of the non–locality of the self energy, one integrates out most of the information gained. This, clearly, does not seem to be the most efficient approach.

In this thesis, I have presented two powerful shortcuts that are particularly suited to attack the many–body problem. The first is an effective way of focusing on a reduced quantity, through the introduction of an auxiliary system and the corresponding effective potential. The second is a practical method to find the potential in realistic calculations, without passing through the computationally heavy self energy but *connecting* to a model system, which is solved just once and for all. The results in the model system are tabulated and publicly available⁴.

I have applied these methods to the study of the diagonal of the spectral function $A(\mathbf{r}, \mathbf{r}, \omega)$, which is the fundamental many–body property that describes the outcome of direct and inverse photoemission experiments and, at the same time, yields the exact local density of the system.

The results are particularly promising for the four systems that we have considered, sodium, aluminum, silicon and solid argon, in the case in which the self energy is purely non–local and expressed by the HSE06 approximation [12]. In particular, one of the simplest possible forms of the connector, eq. (7.20), yields extremely accurate results for metals, while a more refined version, eq. (7.22), is able to account also for argon and, to a good approximation, for silicon. In the four cases, the results are in much better agreement with the reference self energy calculation than the Kohn–Sham LDA is, showing the importance of frequency dependence in

⁴<https://etsf.polytechnique.fr/research/connector/dynLCA>

the spectral potential.

The results that I have obtained for the four materials studied prove that this approach is feasible in practice. A real and local potential, obtained via a simple connector from a model system calculation, is able to reproduce – to a great extent – the diagonal of the spectral function of realistic materials. However, to establish this method as a reliable tool, a systematic analysis of different materials must be performed. In particular, is the final connector, eq. (7.22), always a good approximation for metals? Does it generally underestimate the gap of semiconductors? For which class of materials can we really abandon the self energy approach and completely trust the spectral potential method? To which extent can we disentangle properties of specific materials from the electron–electron interaction treated in the homogeneous electron gas? These are pertinent questions to which an analysis of many more different materials could answer.

Specifically, an attractive set of materials to examine is represented by transition metal oxides, paradigm of strongly correlated materials. Their valence states are strongly localized in space. Therefore, they are more suited, in principle, to an approach based on a local version of the self energy. On the contrary, their physics is very different from the one described by the homogeneous electron gas, the model system we use to import the potential from. However, the example of argon shows that the connector approach can work incredibly well even for highly inhomogeneous systems.

In chapter 7 I have focused on a real and static form of the self energy, the HSE06 one. We believe this to be the most challenging test for our method, as frequency dependence is not present in the standard approach, and must be introduced from scratch. The natural outlook is considering dynamical (and complex) generalizations for the self energy, like, *e.g.*, the GW one. A dynamical self energy yields, in general, a spectral function with more features. Besides a renormalized quasiparticle, satellites can show up in the spectrum. Obtaining the spectral function in the GW approximation is certainly more demanding than with the simpler HSE approach [124]. However, this calculation must be performed just in the homogeneous electron gas, and just one time (for different values of frequencies). Storing the results and importing them in the real material through a suitable connector would allow researchers to avoid time-consuming GW calculations.

Note also that an alternative strategy is possible. Indeed, one can break the spectral potential into one part that is treated exactly in the auxiliary system, plus a correction which is imported from the model system. This is the method that I implemented in chapter 6 for the Hubbard dimer. It is also – trivially – the method I used for real systems. There, the part treated exactly in the auxiliary system was the local contribution to the hybrids self energy; only the purely frequency-dependent part of the spectral potential, corresponding to the purely non-local part of the self energy, was imported from the model system. This idea can be generalized and applied, for instance, to hybrids and GW, or COHSEX and GW (or even GW and beyond [145]). The former could be treated exactly in the auxiliary system, by solving the generalized Sham–Schlüter equation (3.23) with $\Sigma = \Sigma_{\text{COHSEX}}$. The resulting spectral potential would account for the whole non-locality of Σ_{COHSEX} . The correction $\Sigma_{\text{GW}} - \Sigma_{\text{COHSEX}}$, instead, is expected to be dominated by its frequency dependence, and to be more local than the whole Σ_{GW} . It is this correction only, and not the whole Σ_{GW} , that is finally imported from the model system.

Finding the spectral potential in the HEG seems relatively straightforward. Indeed, eq. (4.62) still holds, even with a more accurate form of the spectral function. On the contrary, importing the potential through the same connector is less obvious. In this thesis I have presented different possible expressions for the connector. They are very simple, they are all dependent

CONCLUSION

on the local density and they are based on physical insight. However, a systematic derivation of a general expression for the connector is still missing. This is certainly a possible line of research for the future.

To conclude, this thesis represents only the first step towards an extensive use of the dynLCA approach in real materials. Many blanks are left to fill in and many results still need an explanation (the astonishing agreement in the band structure, for instance, or the analytic properties of the spectral potential). However, the agreement with the reference calculation that we obtained in the last chapter is an encouraging starting point.

Acknowledgments

*When we try to pick out anything
by itself, we find it hitched to
everything else in the Universe.*

JOHN MUIR,
My First Summer in the Sierra

*Il était assis seul et méditait là-dessus,
mais il ne pouvait rien y comprendre
lorsqu'une voix céleste se fit entendre et
lui dit : Veux-tu t'assimiler à moi? [...] toi,
en tant qu'être isolé, tu ne peux compren-
dre. Alors prends-toi un compagnon,
alors méditez tous les deux et vous com-
prendrez. Aussitôt Abraham alla chez son
Maître Sem, le fils de Noé, et ils restèrent
trois ans ensemble jusqu'à ce qu'ils aient
su créer le monde. Et jusqu'à maintenant
il n'y a personne qui puisse le comprendre
seul, mais deux savants sont nécessaires,
et encore ils ne le comprennent qu'au
bout de trois ans, sur quoi ils peuvent
faire tout ce que leur coeur demande.*

G. SCHOLEM,
La Kabbale et sa symbolique

This work – *ça va sans dire* – is the result of a collective effort.

Even before I first visited Palaiseau in summer 2014, the main points on which this thesis rests were already well focused in the minds of Lucia and Matteo.

On a surprisingly hot afternoon for a Parisian late September, indeed, sit on very old sofas while sipping coffee, Matteo and Lucia proposed me the task of looking for a potential no one had ever found before. And not just *a* potential, as the ones people are usually accustomed to, but a frequency dependent one. Funny enough, the only concept I disliked more than “potential”, at that time, was certainly “frequency”.

On the contrary, as I grew older in the group, I got fascinated by the power of frequency, which was able to split poles, generate new peaks, changing a dull delta into a realistic spectrum. I got enchanted by its origins, and finally won – and astonished – by the possibility of folding into it degrees of freedom people would rather bypass.

For opening my eyes, I owe a great debt of gratitude to Lucia Reining and Matteo Gatti, to their deep knowledge and their excellent teaching skills. They made me appreciate the power of simple reasoning and dirty derivations, of doubting anywhere and everywhere looking, they singled out the deepest physics in the simplest models.

Speaking about models, I acknowledge here the role of Prof. Sergio Ciuchi, who brought to my attention the CPA solution of the Hubbard model on the Bethe lattice. Dealing with it has been a challenging opportunity for our method. I also thank Stefano di Sabatino for the half-filled solution of the Hubbard dimer.

And Fausto must enter the stage now, with his *équipe* of experimentalists. They showed me that not only models, but even real systems do exist! And electrons as well, white dots on a black screen. And photoemission is not (only) a *gedankenexperiment*.

In between, the power of *ab initio* calculations. Many thanks to Andrea and Francesco for their constant help. I really needed it, they only know how much!

But a lab is much more than physics, and I'd like to thank everyone who made this statement true: besides the aforementioned folks, Sky, Marilena, Ilya, Jaakko, Martin, Azima, Giorgia, Walter, Pier Luigi, Claudia, Iaroslav, John and Tetiana: I learnt something from each of you! As well as from Lucie, Nicolas, Sophie, Christine, Valérie et Arnaud : le petit peu de français que je connais, c'est surtout grâce à vous ! Et merci aussi à Marylène, Élodie et Sylvie, pour ne pas m'avoir fait tomber dans le labyrinthe de la bureaucratie française.

Dans le labyrinthe qu'est Paris, par contre, je me suis perdu avec plaisir : je tiens à remercier tous ceux qui m'ont allumé les lumières de la ville. Ils m'ont permis de reprendre le RER, chaque lundi, jusqu'à Palaiseau !

Au-delà de Paris, my deepest gratitude goes to Andrea (said with a strict British accent): London-Paris exchanges could not have been more enjoyable; as well as to my M-list Italian anchor-friends (said with a lavish Italian accent), Vaner & Vane + Emy & Michael; and thanks to Fede e Ciccìa, who still tie me to kindergarten time.

Infine, un immenso grazie alla mia famiglia, che mi ha portato fin qui.

Appendices

Résumé en français

Cette thèse propose une méthode théorique innovante pour l'étude des spectres d'excitation à un électron, mesurée par spectroscopie de photoémission directe et inverse.

La plupart des calculs actuels au niveau de l'état de l'art reposent sur des fonctions de Green à plusieurs corps et des self-énergies complexes et non locales, évaluées spécifiquement pour chaque matériau. Même lorsque les spectres calculés sont en très bon accord avec les expériences, le coût de calcul est très important. La raison est que la méthode elle-même n'est pas efficace, car elle fournit beaucoup d'informations superflues qui ne sont pas nécessaires pour l'interprétation des données expérimentales.

Dans cette thèse, nous proposons deux raccourcis par rapport à la méthode standard. Le premier est l'introduction d'un système auxiliaire qui cible, en principe, le spectre d'excitation du système réel. L'exemple type est la théorie de la fonctionnelle de la densité, pour lequel le système auxiliaire est le système de Kohn-Sham : elle reproduit exactement la densité du système réel par l'intermédiaire d'un potentiel réel et statique, le potentiel de Kohn-Sham. La théorie de la fonctionnelle de la densité est, cependant, une théorie de l'état fondamental, qui ne fournit que rarement des propriétés pour les états excités : un exemple est le fameux problème de la sous-estimation de la bande interdite. Le potentiel que nous proposons (le potentiel spectral), local et dépendant de la fréquence, mais réel, peut être considéré comme une généralisation dynamique du potentiel de Kohn-Sham qui donne en principe le spectre exact.

Le deuxième raccourci est l'idée de calculer ce potentiel une fois pour toute dans un système modèle, le gaz d'électrons homogène, et de le tabuler. Pour étudier des matériaux réels, nous concevons un connecteur qui prescrit l'utilisation des résultats du gaz pour calculer les spectres électroniques.

La première partie de la thèse traite de l'idée de systèmes auxiliaires, montrant le cadre général dans lequel ils peuvent être introduits et les équations qu'ils doivent satisfaire. Nous utilisons des modèles de Hubbard solubles exactement pour mieux comprendre le rôle du potentiel spectral ; en particulier, il est démontré que le potentiel peut être défini de façon unique chaque fois que le spectre est non nul, et donne toujours les spectres attendus, même lorsque la partie imaginaire ou les contributions non locales de la self-énergie jouent un rôle de premier plan.

Dans la deuxième partie de la thèse, nous nous concentrons sur les calculs pour les systèmes réels. Nous évaluons d'abord le potentiel spectral dans le gaz d'électrons homogène, puis l'importons dans le système auxiliaire pour évaluer le spectre d'excitation. Toute l'interdépendance non triviale entre l'interaction électronique et l'inhomogénéité du système réel entre dans la forme du connecteur. Trouver une expression pour cela est le véritable défi de la procédure. Nous proposons une approximation raisonnable basée sur les propriétés locales du sys-

tème, que nous appelons approximation du connecteur dynamique local.

Nous mettons en œuvre cette procédure pour quatre prototypes de matériaux différents : le sodium, un métal presque homogène ; l'aluminium, encore un métal mais moins homogène ; le silicium, un semi-conducteur ; l'argon, un isolant inhomogène. Les spectres que nous obtenons avec cette approche concordent de manière impressionnante avec ceux qui sont évalués via la self-énergie, très coûteuse en temps de calcul, démontrant ainsi le potentiel de cette théorie.

Energy contributions

In this appendix we consider the different contributions to the total energy, proving eq. (2.7), (2.9), (2.10) and (2.13). While the Hartree and the exchange contribution rely on a factorized form for the wavefunction (independent particles), the kinetic and the whole interaction terms are completely general.

The kinetic term To express the kinetic energy contribution as a functional of $\gamma(\mathbf{r}, \mathbf{r}')$, we do not have to make any assumption on the structure of the wavefunction, apart from its antisymmetry:

$$\begin{aligned}
 \langle \Psi | \sum_i \left(-\frac{\nabla_i^2}{2} \right) | \Psi \rangle &= \sum_i \int d^3 r_1 \dots d^3 r_N d^3 r'_1 \dots d^3 r'_N \Psi^*(\mathbf{r}'_1, \dots, \mathbf{r}'_N) \delta(\mathbf{r}'_i - \mathbf{r}_i) \left(-\frac{\nabla_{\mathbf{r}'_i}^2}{2} \right) \Psi(\mathbf{r}_1, \dots, \mathbf{r}_N) = \\
 &= N \int d^3 r d^3 r' \delta(\mathbf{r}' - \mathbf{r}) \left(-\frac{\nabla_{\mathbf{r}}^2}{2} \right) \Psi(\mathbf{r}, \mathbf{r}_2, \dots, \mathbf{r}_N) \Psi^*(\mathbf{r}', \mathbf{r}_2, \dots, \mathbf{r}_N) = \\
 &= \int d^3 r d^3 r' \delta(\mathbf{r}' - \mathbf{r}) \left(-\frac{\nabla_{\mathbf{r}}^2}{2} \right) \gamma(\mathbf{r}, \mathbf{r}') \\
 &= \int d^3 r \lim_{\mathbf{r}' \rightarrow \mathbf{r}} \left(-\frac{\nabla^2}{2} \right) \gamma(\mathbf{r}, \mathbf{r}') \tag{2.10}
 \end{aligned}$$

Hartree Energy Assuming the “most classical” wavefunction, a *factorized* product of one-particle wavefunctions $u_i(\mathbf{r}_i)$, that is $\Psi^{(\text{H})}(\mathbf{r}_1, \dots, \mathbf{r}_N) := \prod_{i=1}^N u_i(\mathbf{r}_i)$, the expectation value of the interaction term in the Hamiltonian (2.3) is :

$$\begin{aligned}
 E_{\text{int}}^{(\text{H})} &:= \langle \Psi^{(\text{H})} | \frac{1}{2} \sum_{i \neq j} \frac{1}{|\hat{\mathbf{r}}_i - \hat{\mathbf{r}}_j|} | \Psi^{(\text{H})} \rangle = \\
 &= \frac{1}{2} \sum_{i \neq j} \int d^3 r_1 \dots d^3 r_N u_1^*(\mathbf{r}_1) \dots u_N^*(\mathbf{r}_N) \frac{1}{|\mathbf{r}_i - \mathbf{r}_j|} u_1(\mathbf{r}_1) \dots u_N(\mathbf{r}_N) = \\
 &= \frac{1}{2} \sum_{i \neq j} \int d^3 r d^3 r' \frac{u_i^*(\mathbf{r}) u_i(\mathbf{r}) u_j^*(\mathbf{r}') u_j(\mathbf{r}')}{|\mathbf{r} - \mathbf{r}'|} = \\
 &= \frac{1}{2} \int d^3 r d^3 r' \frac{n(\mathbf{r}) n(\mathbf{r}')}{|\mathbf{r} - \mathbf{r}'|} - \frac{1}{2} \sum_i \int d^3 r d^3 r' \frac{|u_i(\mathbf{r})|^2 |u_i(\mathbf{r}')|^2}{|\mathbf{r} - \mathbf{r}'|} \tag{2.7}
 \end{aligned}$$

where $n(\mathbf{r}) \equiv \langle \Psi^{(\text{H})} | \hat{n}(\mathbf{r}) | \Psi^{(\text{H})} \rangle = \sum_i |u_i(\mathbf{r})|^2$, with $\hat{n}(\mathbf{r}) := \sum_{i=1}^N \delta(\mathbf{r} - \hat{\mathbf{r}}_i)$. The very first term is the classical electrostatic contribution, eq. (2.7), while the second term is the strict self-interaction correction: a part of Fock is already here.

Exchange contribution We can derive the exchange term following the same reasoning of above, replacing the factorized wavefunction $\Psi^{(\text{H})}(\mathbf{r}_1, \dots, \mathbf{r}_N) := \prod_{i=1}^N u_i(\mathbf{r}_i)$ with its *antisym-*

metrized version $\Psi^{(\text{SL})}(\mathbf{r}_1, \dots, \mathbf{r}_N) := \frac{1}{\sqrt{N!}} \det \begin{vmatrix} u_1(\mathbf{r}_1) & \dots & u_1(\mathbf{r}_N) \\ \dots & \dots & \dots \\ u_N(\mathbf{r}_1) & \dots & u_N(\mathbf{r}_N) \end{vmatrix}$; the interaction energy is:

$$\begin{aligned} E_{\text{int}}^{(\text{HF})} &:= \langle \Psi^{(\text{SL})} | \frac{1}{2} \sum_{i \neq j} \frac{1}{|\hat{\mathbf{r}}_i - \hat{\mathbf{r}}_j|} | \Psi^{(\text{SL})} \rangle = \\ &= \frac{1}{2N!} \sum_{i \neq j} \int d^3 r_1 \dots d^3 r_N \left[u_1^*(\mathbf{r}_1) \dots u_N^*(\mathbf{r}_N) - \dots \right] \frac{1}{|\mathbf{r}_i - \mathbf{r}_j|} \left[u_1(\mathbf{r}_1) \dots u_N(\mathbf{r}_N) - \dots \right] = \\ &= \frac{1}{2} \sum_{ij} \int d^3 r d^3 r' \frac{u_i^*(\mathbf{r}) u_j^*(\mathbf{r}') [u_i(\mathbf{r}) u_j(\mathbf{r}') - u_i(\mathbf{r}') u_j(\mathbf{r})]}{|\mathbf{r} - \mathbf{r}'|} = \\ &= \frac{1}{2} \int d^3 r d^3 r' \frac{\gamma(\mathbf{r}, \mathbf{r}) \gamma(\mathbf{r}', \mathbf{r}') - \gamma(\mathbf{r}, \mathbf{r}') \gamma(\mathbf{r}', \mathbf{r})}{|\mathbf{r} - \mathbf{r}'|} \end{aligned} \quad (2.9)$$

with $\gamma(\mathbf{r}, \mathbf{r}') := \sum_i u_i(\mathbf{r}) u_i^*(\mathbf{r}')$. The self-interaction correction of above is here completely accounted for by the antisymmetry of the wavefunction, and generalized to the full exchange term of eq. (2.9).

Interaction energy The Hartree and the exchange contributions can be included in the whole interaction energy, expressed in terms of the pair density $n_2(\mathbf{r}, \mathbf{r}')$. As for the kinetic term, this procedure is independent of the particular form of the wavefunction:

$$\begin{aligned} \langle \Psi | \frac{1}{2} \sum_{i \neq j} \frac{1}{|\hat{\mathbf{r}}_i - \hat{\mathbf{r}}_j|} | \Psi \rangle &= \\ &= \int d^3 r_1 \dots d^3 r_N d^3 r'_1 \dots d^3 r'_N \Psi^*(\mathbf{r}'_1, \dots, \mathbf{r}'_N) \frac{1}{2} \sum_{i \neq j} \langle \mathbf{r}'_1, \dots, \mathbf{r}'_N | \frac{1}{|\hat{\mathbf{r}}_i - \hat{\mathbf{r}}_j|} | \mathbf{r}_1, \dots, \mathbf{r}_N \rangle \Psi(\mathbf{r}_1, \dots, \mathbf{r}_N) = \\ &= \frac{N(N-1)}{2} \int d^3 r d^3 r' d^3 r_3 \dots d^3 r_N \frac{1}{|\mathbf{r} - \mathbf{r}'|} \Psi(\mathbf{r}, \mathbf{r}', \mathbf{r}_3, \dots, \mathbf{r}_N) \Psi^*(\mathbf{r}, \mathbf{r}', \mathbf{r}_3, \dots, \mathbf{r}_N) = \\ &= \frac{1}{2} \int d^3 r d^3 r' \frac{n_2(\mathbf{r}, \mathbf{r}')}{|\mathbf{r} - \mathbf{r}'|} \end{aligned} \quad (2.13)$$

By comparing this exact relation with the corresponding ones (2.7) and (2.9), one can have access to the Hartree and Hartree–Fock contributions to $n_2(\mathbf{r}, \mathbf{r}')$:

$$\begin{aligned} n_2^{\text{H}}(\mathbf{r}, \mathbf{r}') &= n(\mathbf{r}) n(\mathbf{r}') - \sum_i |u_i(\mathbf{r})|^2 |u_i(\mathbf{r}')|^2 \\ n_2^{\text{HF}}(\mathbf{r}, \mathbf{r}') &= \gamma(\mathbf{r}, \mathbf{r}) \gamma(\mathbf{r}', \mathbf{r}') - \gamma(\mathbf{r}, \mathbf{r}') \gamma(\mathbf{r}', \mathbf{r}) \end{aligned}$$

From the last of these and eq. (2.12), the first-order (in e^2) contribution to the exchange–correlation hole is of purely exchange nature, and equal to:

$$n_{\text{xc}}^{(1)}(\mathbf{r}, \mathbf{r}') = -\gamma(\mathbf{r}, \mathbf{r}') \gamma(\mathbf{r}', \mathbf{r})$$

Some useful exact relations:

- By the Pauli principle, $\lim_{\mathbf{r}' \rightarrow \mathbf{r}} n_2(\mathbf{r}, \mathbf{r}') = 0$ (no two electrons in the same state), hence:

$$\lim_{\mathbf{r}' \rightarrow \mathbf{r}} n_{\text{xc}}(\mathbf{r}, \mathbf{r}') = -n(\mathbf{r})$$

from which it is clear that $n_{\text{xc}}^{(1)}(\mathbf{r}, \mathbf{r}')$ is “too much”: correlation reduces the hole.

- Two very far electrons can be considered as uncorrelated, hence:

$$\lim_{|\mathbf{r}-\mathbf{r}'|\rightarrow\infty} n_{\text{xc}}(\mathbf{r}, \mathbf{r}') = 0$$

- From the positivity of n and n_2 , we have:

$$n_{\text{xc}}(\mathbf{r}, \mathbf{r}') \leq n(\mathbf{r}')$$

- From the definition of $n(\mathbf{r})$ and $n_2(\mathbf{r}, \mathbf{r}')$, $\int d^3\mathbf{r} n(\mathbf{r}) = N$ and $\int d^3\mathbf{r}' n_2(\mathbf{r}, \mathbf{r}') = (N-1) n(\mathbf{r})$, hence integrating eq. (2.12) over \mathbf{r}' , we obtain:

$$\int d^3\mathbf{r}' n_{\text{xc}}(\mathbf{r}, \mathbf{r}') = -1$$

which says that the exchange–correlation hole contains exactly one electron: the electron and its hole constitute a globally neutral object.

Bethe lattice CPA solution

CPA solution of the Hubbard model on the Bethe lattice

In the infinite connectivity limit, the self energy becomes local and independent of the particular site i : $\Sigma_{ij}(\omega) \xrightarrow{z \rightarrow \infty} \delta_{ij} \Sigma(\omega)$; the Green's function in reciprocal space is thus $G_{\mathbf{k}}^{-1}(\omega) = \omega - \varepsilon_{\mathbf{k}}^0 - \Sigma(\omega)$: all the \mathbf{k} -dependence of the Green's function is due to the one-particle energy $\varepsilon_{\mathbf{k}}^0$ associated with the free Hamiltonian $U = 0$.

This constitutes an enormous simplification, as the on-site Green's function $G_{ii}(\omega) := G(\omega)$ can be evaluated as the Hilbert transform of the free density of states $A_0(\omega)$, evaluated at $\omega - \Sigma(\omega)$:

$$G(\omega) = \sum_{\mathbf{k}} \frac{1}{\omega - \varepsilon_{\mathbf{k}}^0 - \Sigma(\omega)} = \int_{\mathbb{R}} \frac{d\omega' A_0(\omega')}{\omega - \Sigma(\omega) - \omega'}.$$

Inserting the expression $A_0(\omega) = \theta(D - |\omega|) \frac{2}{\pi D} \sqrt{1 - (\frac{\omega}{D})^2}$, with $D = 2t$, the previous integral reads:

$$G(\omega) = \frac{2}{\pi D} \int_{-1}^{+1} dx \frac{\sqrt{1-x^2}}{\frac{\omega - \Sigma(\omega)}{D} - x} = \frac{2}{D^2} [\omega - \Sigma(\omega)] \pm \frac{2}{D} \sqrt{\frac{1}{D^2} [\omega - \Sigma(\omega)]^2 - 1}.$$

Squaring both sides and dividing by $G(\omega)$ we get:

$$\frac{D^2}{4} G(\omega) - [\omega - \Sigma(\omega)] + G^{-1}(\omega) = 0.$$

We now use the Dyson equation $G^{-1}(\omega) = \mathcal{G}_0^{-1}(\omega) - \Sigma(\omega)$ to arrive to the final result:

$$\mathcal{G}_0^{-1}(\omega) = \omega - \frac{D^2}{4} G(\omega) \tag{C.1}$$

which is eq. (4.2): it is just a consequence of the lattice taken into consideration (a Bethe lattice with $z \rightarrow \infty$), and the Dyson equation $G^{-1}(\omega) = \mathcal{G}_0^{-1}(\omega) - \Sigma(\omega)$, which relates the Bethe lattice local self energy $\Sigma(\omega)$ and the Bethe lattice on-site Green's function $G(\omega)$ to an impurity Green's function $\mathcal{G}_0(\omega)$; this is a self-consistent condition in DMFT, hence eq. (C.1) is called the self-consistent relation.

On the other hand, we have not given yet any expression for the self energy, and for *any* interaction term, the Hamiltonian (2.49) yields a Green's function fulfilling eq. (C.1). Therefore we supply eq. (C.1) with the Coherent Potential Approximation (CPA) expression for the Green's function, namely the relation [146, 147, 5]:

$$G(\omega) = \frac{1}{2} \left(\frac{1}{\mathcal{G}_0^{-1}(\omega) + \frac{U}{2}} + \frac{1}{\mathcal{G}_0^{-1}(\omega) - \frac{U}{2}} \right), \tag{C.2}$$

which is eq. (4.1).

Solution of the third order equation

Eq. (4.3) can be solved by standard methods; first, we set to one the coefficient of the G^3 term, with $G \equiv G(\omega)$, and eq. (4.3) becomes:

$$G^3 - \frac{8\omega}{D^2}G^2 + \frac{4}{D^2}\left(1 - \frac{U^2}{D^2} + \frac{4\omega^2}{D^2}\right)G - \left(\frac{4}{D^2}\right)^2\omega = 0 \quad (\text{C.3})$$

By referring to the cubic equation $x^3 + ax^2 + bx + c = 0$, we build the following quantities:

$$\begin{aligned} \Delta &\equiv 18abc - 4a^3c + a^2b^2 - 4b^3 - 27c^2 \\ \Delta_0 &\equiv a^2 - 3b = \left(\frac{4}{D^2}\right)^2\left(\omega^2 - \frac{3}{4}(D^2 - U^2)\right) \\ \Delta_1 &\equiv 2a^3 - 9ab + 27c = -\frac{\omega}{4}\left(\frac{4}{D^2}\right)^3(9D^2 + 18U^2 - 8\omega^2) \\ C &\equiv \left(\frac{\Delta_1 - \sqrt{\Delta_1^2 - 4\Delta_0^3}}{2}\right)^{\frac{1}{3}} \equiv \left(\frac{\Delta_1 - \sqrt{-27\Delta_0}}{2}\right)^{\frac{1}{3}} \end{aligned}$$

The three solutions of $x^3 + ax^2 + bx + c = 0$ are:

$$x^{(k)}(\omega) = -\frac{1}{3}\left[a + \xi^k C + \frac{\Delta_0}{\xi^k C}\right] \quad k = 0, 1, 2$$

with $\xi := \frac{1}{2}(-1 + \sqrt{3}i)$ cube root of unity. To apply it to our problem, we consider the following auxiliary quantities:

$$z_{\uparrow} = \omega + \frac{U}{2} + i\eta \quad z_{\downarrow} = \omega - \frac{U}{2} + i\eta$$

and the three parameters a , b and c become:

$$\begin{aligned} a &= -\frac{4}{D^2}(z_{\uparrow} + z_{\downarrow}) \\ b &= \frac{4}{D^2}\left[1 + \frac{4}{D^2}z_{\uparrow} \cdot z_{\downarrow}\right] \\ c &= -\frac{1}{2}\left(\frac{4}{D^2}\right)^2(z_{\uparrow} + z_{\downarrow}) \end{aligned}$$

For each value of frequency, of the three solutions $G^{(k)}(\omega)$ we choose, among the two conjugates, the one with negative imaginary part. The corresponding spectral function is:

$$A^{(k)}(\omega) = -\frac{1}{\pi}\text{Im} G^{(k)}(\omega) = \frac{1}{3\pi}\left[1 - \frac{\Delta_0}{|C|^2}\right]\text{Im}[\xi^k C]$$

which is positive, and zero if $\Delta_0 = |C|^2$ or if $\text{Im}[\xi^k C] = 0$.

Non-interacting system If $U = 0$, from eq. (4.1) $G^{(U=0)}(\omega) = \mathcal{G}_0^{(U=0)}(\omega) := G_0(\omega)$, and eq. (4.3) can be recast in the following form:

$$\left(\frac{D^2}{4}G_0 - \omega\right)\left[\left(\frac{D^2}{4}G_0 - \omega\right)G_0 + 1\right] = 0$$

with the solutions $G_0 = \frac{4\omega}{D^2}$ or $G_0 = \frac{2}{D^2}\left\{\omega \pm \sqrt{\omega^2 - D^2}\right\}$. The first one is purely real, hence we discard it, while among the other two we choose the one with negative imaginary part:

$$G_0(\omega) = \frac{2}{D^2}\left\{\omega - \sqrt{\omega^2 - D^2}\right\}.$$

The corresponding spectral function is:

$$A_0(\omega) = -\frac{1}{\pi} \text{Im} G_0(\omega) = \theta(D - |\omega|) \frac{2}{\pi D} \sqrt{1 - \left(\frac{\omega}{D}\right)^2}, \quad (\text{C.4})$$

normalized to 1 as: $\frac{2}{\pi D} \int_{-D}^D d\omega \sqrt{1 - \frac{\omega^2}{D^2}} = \frac{2}{\pi} \int_{-1}^1 dy \sqrt{1 - y^2} = \frac{2}{\pi} \int_{-\pi/2}^{\pi/2} d\theta \cos^2 \theta = 1$. Note that G_0 has no poles unless $\omega = 0$ for $D = 0$. The inverse of G_0 is:

$$G_0^{-1}(\omega) = \frac{1}{2} \left(\omega + \sqrt{\omega^2 - D^2} \right) \quad (\text{C.5})$$

Hubbard dimer at half filling

Symmetric case $D = 0$

Energy spectrum

We present the result of the diagonalization of Hamiltonian (4.10) in the half-filling case $N = 2$. A possible choice for the ordering of the site basis is $\{|\uparrow, \uparrow\rangle, |\uparrow, \downarrow\rangle, |\uparrow\downarrow, 0\rangle, |0, \uparrow\downarrow\rangle, |\downarrow, \uparrow\rangle, |\downarrow, \downarrow\rangle\}$. Symbolically, we refer to this basis as $|\sigma_{i=1}^{(1)} \sigma_{i=1}^{(2)}, \sigma_{i=2}^{(1)} \sigma_{i=2}^{(2)}\rangle$. In this basis, the Hamiltonian (2.49) is represented by the following matrix:

$$\hat{H} \longrightarrow H \equiv \begin{pmatrix} 2\varepsilon_0 & 0 & 0 & 0 & 0 & 0 \\ 0 & 2\varepsilon_0 & -t & -t & 0 & 0 \\ 0 & -t & 2\varepsilon_0 + U & 0 & +t & 0 \\ 0 & -t & 0 & 2\varepsilon_0 + U & +t & 0 \\ 0 & 0 & +t & +t & 2\varepsilon_0 & 0 \\ 0 & 0 & 0 & 0 & 0 & 2\varepsilon_0 \end{pmatrix}$$

The corresponding eigenvalues are $2\varepsilon_0$ (three times degenerate), $2\varepsilon_0 + U$ and $2\varepsilon_0 + \frac{U \pm c}{2}$, $c := \sqrt{(4t)^2 + U^2}$, with the following associated eigenvectors:

$$\begin{aligned} \{\hat{H} - 2\varepsilon_0\} |\uparrow, \uparrow\rangle &= 0 \\ \{\hat{H} - 2\varepsilon_0\} |\downarrow, \downarrow\rangle &= 0 \\ \{\hat{H} - 2\varepsilon_0\} \left[\frac{1}{\sqrt{2}} (|\uparrow, \downarrow\rangle + |\downarrow, \uparrow\rangle) \right] &= 0 \\ \{\hat{H} - [2\varepsilon_0 + U]\} \left[\frac{1}{\sqrt{2}} (|\uparrow\downarrow, 0\rangle - |0, \uparrow\downarrow\rangle) \right] &= 0 \\ \left\{ \hat{H} - \left[2\varepsilon_0 + \frac{U-c}{2} \right] \right\} \left[\frac{4t}{a(c-U)} (|\uparrow, \downarrow\rangle - |\downarrow, \uparrow\rangle) + \frac{1}{a} (|\uparrow\downarrow, 0\rangle + |0, \uparrow\downarrow\rangle) \right] &= 0 \\ \left\{ \hat{H} - \left[2\varepsilon_0 + \frac{U+c}{2} \right] \right\} \left[\frac{4t}{b(c+U)} (|\uparrow, \downarrow\rangle - |\downarrow, \uparrow\rangle) - \frac{1}{b} (|\uparrow\downarrow, 0\rangle + |0, \uparrow\downarrow\rangle) \right] &= 0 \end{aligned} \tag{D.1}$$

with $\frac{a^2}{2} := 1 + \left(\frac{4t}{c-U}\right)^2$ and $\frac{b^2}{2} := 1 + \left(\frac{4t}{c+U}\right)^2$.

The lower energy is represented by the fifth state, which is the ground state, completely symmetric in spin:

$$|\text{GS}\rangle^{(N=2)} = \frac{4t}{a(c-U)} (|\uparrow, \downarrow\rangle - |\downarrow, \uparrow\rangle) + \frac{1}{a} (|\uparrow\downarrow, 0\rangle + |0, \uparrow\downarrow\rangle)$$

One can introduce also for $N = 2$ a bonding-antibonding basis [148] $|\alpha_1 \sigma_1, \alpha_2 \sigma_2\rangle$, namely an electron in the state α_1 with spin σ_1 and another in state α_2 with spin σ_2 ; this new basis is

conventionally ordered as follows: $\{|-\uparrow, +\uparrow\rangle, |-\uparrow, +\downarrow\rangle, |-\uparrow, -\downarrow\rangle, |+\uparrow, +\downarrow\rangle, |-\downarrow, +\uparrow\rangle, |-\downarrow, +\downarrow\rangle\}$, and the matrix of change of basis is:

$$\langle \sigma_{i=1}^{(1)} \sigma_{i=1}^{(2)}, \sigma_{i=2}^{(1)} \sigma_{i=2}^{(2)} | \alpha_1 \sigma_1, \alpha_2 \sigma_2 \rangle = \begin{pmatrix} -1 & 0 & 0 & 0 & 0 & 0 \\ 0 & -\frac{1}{2} & \frac{1}{2} & -\frac{1}{2} & -\frac{1}{2} & 0 \\ 0 & \frac{1}{2} & \frac{1}{2} & \frac{1}{2} & -\frac{1}{2} & 0 \\ 0 & -\frac{1}{2} & \frac{1}{2} & \frac{1}{2} & \frac{1}{2} & 0 \\ 0 & -\frac{1}{2} & -\frac{1}{2} & \frac{1}{2} & -\frac{1}{2} & 0 \\ 0 & 0 & 0 & 0 & 0 & -1 \end{pmatrix}$$

In this new basis the ground state reads:

$$|\text{GS}\rangle^{(N=2)} = \sqrt{\frac{1}{2} + \frac{2t}{c}} |-\uparrow, -\downarrow\rangle - \sqrt{\frac{1}{2} - \frac{2t}{c}} |+\uparrow, +\downarrow\rangle$$

Green's function

One can build the Green's function with the usual Lehmann decomposition; the $N = 3$ sector is analogous to the already diagonalized $N = 1$ sector (particle-hole symmetry). The result is symmetric in spin, which we omit, and reads:

$$G_-(\omega) = \frac{\frac{1}{2} - \frac{2t}{c}}{\omega - (\varepsilon_0 + t + \frac{U+c}{2}) + i\eta} + \frac{\frac{1}{2} + \frac{2t}{c}}{\omega - (\varepsilon_0 + t + \frac{U-c}{2}) - i\eta}$$

$$G_+(\omega) = \frac{\frac{1}{2} + \frac{2t}{c}}{\omega - (\varepsilon_0 - t + \frac{U+c}{2}) + i\eta} + \frac{\frac{1}{2} - \frac{2t}{c}}{\omega - (\varepsilon_0 - t + \frac{U-c}{2}) - i\eta}$$

The non-interacting Green's function is:

$$G_-^0(\omega) = \frac{1}{\omega - (\varepsilon_0 - t) - i\eta}$$

$$G_+^0(\omega) = \frac{1}{\omega - (\varepsilon_0 + t) + i\eta}$$

Therefore, the self energy reads:

$$\Sigma_-(\omega) = \frac{U}{2} + \frac{\frac{U^2}{4}}{\omega - (\varepsilon_0 + 3t + \frac{U}{2}) + i\eta}$$

$$\Sigma_+(\omega) = \frac{U}{2} + \frac{\frac{U^2}{4}}{\omega - (\varepsilon_0 - 3t + \frac{U}{2}) - i\eta}$$

Asymmetric case

We repeat the analysis for the Hamiltonian (6.2), with $D \neq 0$, $t = 1$ and $N = 2$.

Energy spectrum

To get the Green's function, we must diagonalize the Hamiltonian in its sector relative to the addition of a spin-down electron (the spin-up situation or the removal of a spin-down electron are trivial). Therefore, we can restrict ourselves to the Hilbert space spanned by the basis $\{|\uparrow, \downarrow\rangle, |\uparrow\downarrow, 0\rangle, |0, \uparrow\downarrow\rangle, |\downarrow, \uparrow\rangle\}$, where the Hamiltonian (6.2) reads:

$$\hat{H}^{(N=2, S_z=0)} \longrightarrow \begin{pmatrix} 0 & -1 & -1 & 0 \\ -1 & U+D & 0 & 1 \\ -1 & 0 & U-D & 1 \\ 0 & 1 & 1 & 0 \end{pmatrix} \quad (\text{D.2})$$

The eigenvalue equation $\det[\hat{H} - e_\lambda \hat{1}] = 0$ reads $e_\lambda \{e_\lambda^3 - 2Ue_\lambda^2 + (U^2 - D^2 - 4)e_\lambda + 4U\} = 0$, which has the solution $e_\lambda = 0 := e_2$ plus the three solutions of the third order equation $e_\lambda^3 - 2Ue_\lambda^2 - e_\lambda(D^2 - U^2 + 4) + 4U = 0$:

$$\begin{aligned} e_1 &= \frac{2}{3} \left[U - r \cos\left(\theta - \frac{\pi}{3}\right) \right] \\ e_2 &= 0 \\ e_3 &= \frac{2}{3} \left[U - r \cos\left(\theta + \frac{\pi}{3}\right) \right] \\ e_4 &= \frac{2}{3} \left[U - r \cos(\theta + \pi) \right] \end{aligned}$$

with:

$$\begin{aligned} z^2 &:= 9D^2 - U^2 - 18 \\ r^2 &:= 3D^2 + U^2 + 12, \\ \cos 3\theta &:= \frac{z^2 U}{r^3} \end{aligned}$$

The corresponding normalized eigenvectors are:

$$|\phi_\lambda\rangle = \begin{cases} \frac{1}{\mathcal{N}_\lambda} \left[(|\uparrow, \downarrow\rangle - |\downarrow, \uparrow\rangle) + \frac{2}{e_\lambda + (D-U)} (|\uparrow\downarrow, 0\rangle - |0, \uparrow\downarrow\rangle) - e_\lambda |\uparrow\downarrow, 0\rangle \right] & \lambda = 1, 3, 4 \\ \frac{1}{\sqrt{2}} (|\uparrow, \downarrow\rangle + |\downarrow, \uparrow\rangle) & \lambda = 2 \end{cases}$$

with $\mathcal{N}_\lambda = \sqrt{2} \left[1 + 2 \left(\frac{1}{e_\lambda + D - U} - \frac{e_\lambda}{2} \right)^2 + 2 \left(\frac{1}{e_\lambda + D - U} \right)^2 \right]^{\frac{1}{2}}$, with the expected behaviour in the limit $D \rightarrow 0$, see eq. (D.1). Finally, I show the action of the creation and annihilation operators¹ on the ground state $|-, \uparrow\rangle \equiv \cos \rho_- |\uparrow, 0\rangle + \sin \rho_- |0, \uparrow\rangle$:

$$\begin{aligned} \hat{c}_{1\uparrow}^\dagger |-, \uparrow\rangle &= -\sin \rho_- |\uparrow, \uparrow\rangle & \hat{c}_{1\downarrow}^\dagger |-, \uparrow\rangle &= \cos \rho_- |\uparrow\downarrow, 0\rangle - \sin \rho_- |\downarrow, \uparrow\rangle \\ \hat{c}_{2\uparrow}^\dagger |-, \uparrow\rangle &= \cos \rho_- |\uparrow, \uparrow\rangle & \hat{c}_{2\downarrow}^\dagger |-, \uparrow\rangle &= \cos \rho_- |\uparrow, \downarrow\rangle + \sin \rho_- |0, \uparrow\downarrow\rangle \\ \hat{c}_{1\uparrow} |-, \uparrow\rangle &= \cos \rho_- |0, 0\rangle & \hat{c}_{1\downarrow} |-, \uparrow\rangle &= 0 \\ \hat{c}_{2\uparrow} |-, \uparrow\rangle &= \sin \rho_- |0, 0\rangle & \hat{c}_{2\downarrow} |-, \uparrow\rangle &= 0 \end{aligned}$$

The Green's function for $N = 1$

The spin-up case is trivial, since an additional spin-up electron would not interact with the other one, and one would therefore get a non-interacting two-poles Green's function:

$$\begin{aligned} G_{ij,\uparrow}(\omega) &= \frac{[\delta_{i1} \cos \rho_+ + \delta_{i2} \sin \rho_+][\delta_{j1} \cos \rho_+ + \delta_{j2} \sin \rho_+]}{\omega - e_+ + i\eta} + \\ &\quad + \frac{[\delta_{i1} \cos \rho_- + \delta_{i2} \sin \rho_-][\delta_{j1} \cos \rho_- + \delta_{j2} \sin \rho_-]}{\omega - e_- - i\eta} \end{aligned}$$

The corresponding spectral function has two peaks:

$$A_{ij,\uparrow}(\omega) = \Lambda_{ij,\uparrow}^{(+)} \delta(\omega - e_+) + \Lambda_{ij,\uparrow}^{(-)} \delta(\omega - e_-) \quad (\text{D.3})$$

with weights:

$$\Lambda_{ij,\uparrow}^{(\pm)} := [\delta_{i1} \cos \rho_\pm + \delta_{i2} \sin \rho_\pm][\delta_{j1} \cos \rho_\pm + \delta_{j2} \sin \rho_\pm] = \begin{cases} \frac{1}{2} \left[1 \mp (-)^i \frac{D}{\sqrt{D^2+4}} \right] & i = j \\ \mp \frac{1}{\sqrt{D^2+4}} & i \neq j \end{cases}$$

¹As a convention, $|\uparrow\downarrow, \uparrow\rangle = c_{2\uparrow}^\dagger c_{1\downarrow}^\dagger c_{1\uparrow}^\dagger |0, 0\rangle$.

Spin-down case: the Lehmann representation For the spin-down case, we must use the exact diagonalization results to explicitly build the Green's function via the Lehmann representation. The spin-down Green's function involves a sum over the four eigenvectors ϕ_λ of the $N = 2$ Hamiltonian, that generate the four poles of the Green's function:

$$G_{ij,\downarrow}(\omega) = \sum_{\lambda=1}^4 \frac{\langle \phi_\lambda | \hat{c}_{j\downarrow}^\dagger | -, \uparrow \rangle \langle -, \uparrow | \hat{c}_{i\downarrow} | \phi_\lambda \rangle}{\omega - (e_\lambda - e_-) + i\eta} := \sum_{\lambda=1}^4 G_{ij,\downarrow}^{(e_\lambda)}(\omega)$$

The contributions relative to the transitions from the ground state to the e_1 , e_3 and e_4 excited state are:

$$\begin{aligned} G_{11,\downarrow}^{(e_\lambda)}(\omega) &= \frac{\langle \phi_\lambda | \hat{c}_{1\downarrow}^\dagger | -, \uparrow \rangle \langle -, \uparrow | \hat{c}_{1\downarrow} | \phi_\lambda \rangle}{\omega - (e_\lambda - e_-) + i\eta} = \frac{\frac{1}{|\mathcal{N}_\lambda|^2} \left[\cos \rho_- \left(\frac{2}{e_\lambda + (D-U)} - e_\lambda \right) + \sin \rho_- \right]^2}{\omega - (e_\lambda - e_-) + i\eta} \\ G_{12,\downarrow}^{(e_\lambda)}(\omega) &= G_{21,\downarrow}^{(e_\lambda)}(\omega) = \frac{\langle \phi_\lambda | \hat{c}_{2\downarrow}^\dagger | -, \uparrow \rangle \langle -, \uparrow | \hat{c}_{1\downarrow} | \phi_\lambda \rangle}{\omega - (e_\lambda - e_-) + i\eta} = \\ &= \frac{\frac{1}{|\mathcal{N}_\lambda|^2} \left[\cos \rho_- - \sin \rho_- \frac{2}{e_\lambda + (D-U)} \right] \left[\cos \rho_- \left(\frac{2}{e_\lambda + (D-U)} - e_\lambda \right) + \sin \rho_- \right]}{\omega - (e_\lambda - e_-) + i\eta} \\ G_{22,\downarrow}^{(e_\lambda)}(\omega) &= \frac{\langle \phi_\lambda | \hat{c}_{2\downarrow}^\dagger | -, \uparrow \rangle \langle -, \uparrow | \hat{c}_{2\downarrow} | \phi_\lambda \rangle}{\omega - (e_\lambda - e_-) + i\eta} = \frac{\frac{1}{|\mathcal{N}_\lambda|^2} \left[\cos \rho_- - \sin \rho_- \frac{2}{e_\lambda + (D-U)} \right]^2}{\omega - (e_\lambda - e_-) + i\eta} \end{aligned}$$

while for the second pole:

$$\begin{aligned} G_{11,\downarrow}^{(e_2)}(\omega) &= \frac{\langle \phi_2 | \hat{c}_{1\downarrow}^\dagger | -, \uparrow \rangle \langle -, \uparrow | \hat{c}_{1\downarrow} | \phi_2 \rangle}{\omega - (e_2 - e_-) + i\eta} = \frac{\frac{1}{2} \sin^2 \rho_-}{\omega - (e_2 - e_-) + i\eta} \\ G_{12,\downarrow}^{(e_2)}(\omega) &= G_{21,\downarrow}^{(e_2)}(\omega) = \frac{\langle \phi_2 | \hat{c}_{2\downarrow}^\dagger | -, \uparrow \rangle \langle -, \uparrow | \hat{c}_{1\downarrow} | \phi_2 \rangle}{\omega - (e_2 - e_-) + i\eta} = \\ &= \frac{-\frac{1}{2} \sin \rho_- \cos \rho_-}{\omega - (e_2 - e_-) + i\eta} \\ G_{22,\downarrow}^{(e_2)}(\omega) &= \frac{\langle \phi_2 | \hat{c}_{2\downarrow}^\dagger | -, \uparrow \rangle \langle -, \uparrow | \hat{c}_{2\downarrow} | \phi_2 \rangle}{\omega - (e_2 - e_-) + i\eta} = \frac{\frac{1}{2} \cos^2 \rho_-}{\omega - (e_2 - e_-) + i\eta} \end{aligned}$$

Putting everything together, the total Green's function reads:

$$\begin{aligned} G_{11,\downarrow}(\omega) &= \frac{\frac{1}{2} \sin^2 \rho_-}{\omega - (e_2 - e_-) + i\eta} + \sum_{\lambda=1,3,4} \frac{\frac{1}{|\mathcal{N}_\lambda|^2} \left[\cos \rho_- \left(\frac{2}{e_\lambda + (D-U)} - e_\lambda \right) + \sin \rho_- \right]^2}{\omega - (e_\lambda - e_-) + i\eta} \\ G_{12,\downarrow}(\omega) &= G_{21,\downarrow}(\omega) = \frac{-\frac{1}{2} \sin \rho_- \cos \rho_-}{\omega - (e_2 - e_-) + i\eta} + \\ &+ \sum_{\lambda=1,3,4} \frac{\frac{1}{|\mathcal{N}_\lambda|^2} \left[\cos \rho_- - \sin \rho_- \frac{2}{e_\lambda + (D-U)} \right] \left[\cos \rho_- \left(\frac{2}{e_\lambda + (D-U)} - e_\lambda \right) + \sin \rho_- \right]}{\omega - (e_\lambda - e_-) + i\eta} \\ G_{22,\downarrow}(\omega) &= \frac{\frac{1}{2} \cos^2 \rho_-}{\omega - (e_2 - e_-) + i\eta} + \sum_{\lambda=1,3,4} \frac{\frac{1}{|\mathcal{N}_\lambda|^2} \left[\cos \rho_- - \sin \rho_- \frac{2}{e_\lambda + (D-U)} \right]^2}{\omega - (e_\lambda - e_-) + i\eta} \end{aligned}$$

from which the spectral function can be written as:

$$A_{ij,\downarrow}(\omega) = \sum_{\lambda=1}^4 \Lambda_{ij,\downarrow}^{(\lambda)} \delta(\omega - \omega_\lambda)$$

where the poles are $\omega_\lambda := e_\lambda - e_- \equiv e_\lambda + \sqrt{1 + \frac{D^2}{4}}$ and the intensities are:

$$\Lambda_{ij,\downarrow}^{(\lambda=2)} = \frac{1}{2} [\sin \rho_- \delta_{i1} - \cos \rho_- \delta_{i2}] [\sin \rho_- \delta_{j1} - \cos \rho_- \delta_{j2}]$$

$$\begin{aligned} \Lambda_{ij,\downarrow}^{(\lambda \neq 2)} = \frac{1}{|\mathcal{N}_\lambda|^2} & \left[\left(\cos \rho_- \left(\frac{2}{e_\lambda + (D-U)} - e_\lambda \right) + \sin \rho_- \right) \delta_{i1} + \right. \\ & \left. + \left(\cos \rho_- - \sin \rho_- \frac{2}{e_\lambda + (D-U)} \right) \delta_{i2} \right] \cdot \left[\left(\cos \rho_- \left(\frac{2}{e_\lambda + (D-U)} - e_\lambda \right) + \sin \rho_- \right) \delta_{j1} + \right. \\ & \left. + \left(\cos \rho_- - \sin \rho_- \frac{2}{e_\lambda + (D-U)} \right) \delta_{j2} \right] \end{aligned}$$

Non-interacting system

Setting $U = 0$, we have:

$$\begin{aligned} e_1^{(U=0)} &= -\sqrt{D^2 + 4} \\ e_2^{(U=0)} &= 0 \\ e_3^{(U=0)} &= 0 \\ e_4^{(U=0)} &= \sqrt{D^2 + 4} \end{aligned}$$

while the eigenvectors become:

$$\begin{aligned} |\phi_1\rangle^{(U=0)} &= \frac{1}{\sqrt{D^2 + 4}} \left[(|\uparrow, \downarrow\rangle - |\downarrow, \uparrow\rangle) + \frac{1}{2} \left((\sqrt{D^2 + 4} - D) |\uparrow\downarrow, 0\rangle + (\sqrt{D^2 + 4} + D) |0, \uparrow\downarrow\rangle \right) \right] \\ |\phi_2\rangle^{(U=0)} &= \frac{1}{\sqrt{2}} (|\uparrow, \downarrow\rangle + |\downarrow, \uparrow\rangle) \\ |\phi_3\rangle^{(U=0)} &= \frac{1}{\sqrt{D^2 + 4}} \left[\frac{D}{\sqrt{2}} (|\uparrow, \downarrow\rangle - |\downarrow, \uparrow\rangle) + \sqrt{2} (|\uparrow\downarrow, 0\rangle - |0, \uparrow\downarrow\rangle) \right] \\ |\phi_4\rangle^{(U=0)} &= \frac{1}{\sqrt{D^2 + 4}} \left[(|\uparrow, \downarrow\rangle - |\downarrow, \uparrow\rangle) - \frac{1}{2} \left((\sqrt{D^2 + 4} + D) |\uparrow\downarrow, 0\rangle + (\sqrt{D^2 + 4} - D) |0, \uparrow\downarrow\rangle \right) \right] \end{aligned}$$

The amplitudes of the peaks of the SF are:

$$\begin{aligned} \Lambda_{ij,\downarrow}^{(\lambda \neq 2)} = \frac{\sin^2 \rho_-}{|\mathcal{N}_\lambda|^2} & \left[\left(\tan^{-1} \rho_- \left(\frac{2}{e_\lambda + D} - e_\lambda \right) + 1 \right) \delta_{i1} + \left(\tan^{-1} \rho_- - \frac{2}{e_\lambda + D} \right) \delta_{i2} \right] \cdot \\ & \cdot \left[\left(\tan^{-1} \rho_- \left(\frac{2}{e_\lambda + D} - e_\lambda \right) + 1 \right) \delta_{j1} + \left(\tan^{-1} \rho_- - \frac{2}{e_\lambda + D} \right) \delta_{j2} \right] \end{aligned}$$

that is, finally, a non-interacting two-peaks SF:

$$\begin{aligned} A_{11,\downarrow}^{(U=0)}(\omega) &= \frac{1}{2} \left(1 - \frac{D}{\sqrt{D^2 + 4}} \right) \delta(\omega - \omega_1) + \frac{1}{2} \left(1 + \frac{D}{\sqrt{D^2 + 4}} \right) \delta(\omega - \omega_2) \\ A_{12,\downarrow}^{(U=0)}(\omega) &= \frac{1}{\sqrt{D^2 + 4}} \delta(\omega - \omega_1) - \frac{1}{\sqrt{D^2 + 4}} \delta(\omega - \omega_2) \\ A_{22,\downarrow}^{(U=0)}(\omega) &= \frac{1}{2} \left(1 + \frac{D}{\sqrt{D^2 + 4}} \right) \delta(\omega - \omega_1) + \frac{1}{2} \left(1 - \frac{D}{\sqrt{D^2 + 4}} \right) \delta(\omega - \omega_2) \end{aligned}$$

having used the fact that $e_2^{(U=0)} = e_1^{(U=0)}$. As expected, the fourth pole $e_4^{(U=0)} = \sqrt{D^2 + 4}$ has a vanishing amplitude in the limit $U \rightarrow 0$, and doesn't show up in the previous expressions. Moreover, the spectral weights depend on the site: for $D \gg t$, $A_{11,\downarrow}^{(U=0)}(\omega) \sim \delta(\omega - \omega_2)$, while $A_{22,\downarrow}^{(U=0)}(\omega) \sim \delta(\omega - \omega_1)$. By contrast, for $D \sim 0$ one is back to the symmetric result.

Symmetric system Setting $D = 0$, we're supposed to go back to the symmetric dimer results. Solving the equation $\cos 3\theta_{D=0} = -U \frac{U^2+18}{(U^2+12)^{3/2}}$, we are left with three solutions, namely:

$$\begin{aligned}\cos\theta_{D=0} &= \frac{3\sqrt{U^2+16}-U}{4\sqrt{U^2+12}} \\ \cos\theta_{D=0} &= \frac{-3\sqrt{U^2+16}-U}{4\sqrt{U^2+12}} \\ \cos\theta_{D=0} &= \frac{U}{2\sqrt{U^2+12}}\end{aligned}$$

These different solutions correspond to different orderings of the $D = 0$ poles: chosen one of the previous $\theta_{D=0}$, the poles derived from it are always the same: in this sense, there is no ambiguity.

Small displacement If $D \ll 1$, a power-series expansion in D is convenient; here is the behaviour of the position of the poles:

$$\begin{aligned}\omega_1 &\stackrel{D \sim 0}{\sim} \left(1 + \frac{U-c}{2}\right) + \frac{D^2}{8} \left(1 + \frac{\frac{\sqrt{2}U}{c}(U^2+14)\sqrt{U^2-Uc+8} - 2(U+3c)}{U^2+12}\right) + \mathcal{O}(D^4) \\ \omega_2 &\stackrel{D \sim 0}{\sim} 1 + \frac{D^2}{8} + \mathcal{O}(D^4) \\ \omega_3 &\stackrel{D \sim 0}{\sim} (1+U) + \frac{D^2}{8} \left(1 + \frac{1}{\sqrt{6}} \frac{12\sqrt{U^2-Uc+8} - \frac{\sqrt{2}U}{c}(U^2+14)(U+3c)}{U^2+12}\right) + \mathcal{O}(D^4) \\ \omega_4 &\stackrel{D \sim 0}{\sim} \left(1 + \frac{U+c}{2}\right) + \frac{D^2}{8} \left(1 + \frac{\frac{\sqrt{2}U}{c}(U^2+14)\sqrt{U^2-Uc+8} + 2(U+3c)}{U^2+12}\right) + \mathcal{O}(D^4)\end{aligned}$$

or:

$$\omega_i \stackrel{D \sim 0}{\sim} \omega_i^{(h)} + \frac{D^2}{8} (1 + \Delta^{(2)} \omega_i) + \mathcal{O}(D^4)$$

where $\Delta^{(2)} \omega_i \equiv 4 \partial^2 \omega_i / \partial D^2 \big|_{D=0} - 1$.

Sham–Schlüter equation for the density matrix

Hubbard dimer at half filling

If continuous space is discretized into lattice sites i , the analogous of the generalized Sham–Schlüter equation (3.17) for the density matrix $\gamma_{ij} = \int \frac{d\omega}{2\pi i} e^{i\omega\eta} G_{ij}(\omega)$ is:

$$\sum_{kl} \int \frac{d\omega}{2\pi i} e^{i\omega\eta} G_{ik}^\gamma(\omega) \Sigma_{kl}(\omega) G_{lj}(\omega) = \sum_{kl} v_{kl}^\gamma \int \frac{d\omega}{2\pi i} e^{i\omega\eta} G_{ik}^\gamma(\omega) G_{lj}(\omega) \quad (\text{E.1})$$

with the non-local γ -effective potential v_{ij}^γ . We take the Hubbard dimer, eq. (4.10), as a model to which applying the previous equation. As both Green's function and self energy are diagonal in the bonding–antibonding basis $\{\alpha\} = \{\pm\}$, with $\alpha = \pm$ in the antibonding and the bonding state respectively, we express the Sham–Schlüter equation in that basis, with $v_{ij}^\gamma = \sum_\alpha \langle i|\alpha\rangle v_\alpha^\gamma \langle \alpha|j\rangle$:

$$\int \frac{d\omega}{2\pi i} e^{i\omega\eta} G_\alpha^\gamma(\omega) \Sigma_\alpha(\omega) G_\alpha(\omega) = v_\alpha^\gamma \int \frac{d\omega}{2\pi i} e^{i\omega\eta} G_\alpha^\gamma(\omega) G_\alpha(\omega) \quad (\text{E.2})$$

Note that its DFT counterpart would involve a local potential v_i^{KS} , which corresponds to an α -independent v^{KS} . The Sham–Schlüter equation for the density would be:

$$\int \frac{d\omega}{2\pi i} e^{i\omega\eta} \sum_\alpha G_\alpha^{\text{KS}}(\omega) \Sigma_\alpha(\omega) G_\alpha(\omega) = v^{\text{KS}} \int \frac{d\omega}{2\pi i} e^{i\omega\eta} \sum_\alpha G_\alpha^{\text{KS}}(\omega) G_\alpha(\omega) \quad (\text{E.3})$$

which is more likely to have a solution as a sum over α is performed.

Let us check if a solution to eq. (E.2) exists. If the ground state is composed of a single electron in the ground state, as we considered in chapter 4.2, the previous equation will always have an undetermined solution v_{ij}^γ . Indeed, with a single spin-up electron, the ground state is a trivial Slater determinant, and the density matrix is already idempotent and independent of the interaction: $\gamma_{\alpha\beta,\sigma} = \delta_{\sigma,\uparrow} \delta_{\alpha\beta} \delta_{\alpha,-}$ or $\gamma_{ij,\sigma} = \frac{1}{2} \delta_{\sigma,\uparrow}$.

Therefore, to check if non-trivial solutions of eq. (E.2) exist, we have to move to the $N = 2$ sector (half-filling): the result is displayed in appendix D:

$$G_-(\omega) = \frac{\frac{1}{2} - \frac{2t}{c}}{\omega - (\varepsilon_0 + t + \frac{U+c}{2}) + i\eta} + \frac{\frac{1}{2} + \frac{2t}{c}}{\omega - (\varepsilon_0 + t + \frac{U-c}{2}) - i\eta}$$

$$G_+(\omega) = \frac{\frac{1}{2} + \frac{2t}{c}}{\omega - (\varepsilon_0 - t + \frac{U+c}{2}) + i\eta} + \frac{\frac{1}{2} - \frac{2t}{c}}{\omega - (\varepsilon_0 - t + \frac{U-c}{2}) - i\eta}$$

with the self energy:

$$\begin{aligned}\Sigma_-(\omega) &= \frac{U}{2} + \frac{\frac{U^2}{4}}{\omega - (\varepsilon_0 + 3t + \frac{U}{2}) + i\eta} \\ \Sigma_+(\omega) &= \frac{U}{2} + \frac{\frac{U^2}{4}}{\omega - (\varepsilon_0 - 3t + \frac{U}{2}) - i\eta}\end{aligned}$$

The auxiliary system Green's function $G_\alpha^\gamma(\omega)$ can be read from the real system Green's function, by setting $U = 0$ and introducing an state-dependent potential v_α^γ :

$$\begin{aligned}G_-^\gamma(\omega) &= \frac{1}{\omega - (\varepsilon_0 - t + v_-^\gamma) - i\eta} \\ G_+^\gamma(\omega) &= \frac{1}{\omega - (\varepsilon_0 + t + v_+^\gamma) + i\eta}\end{aligned}$$

Let us now plug all these quantities in eq. (E.2), assuming $t = 1$ and $\varepsilon_0 = 0$ for simplicity. We first consider the bonding state; the right hand side reads:

$$\begin{aligned}v_-^\gamma \int \frac{d\omega}{2\pi i} e^{i\omega\eta} G_-^\gamma(\omega) G_-(\omega) &= \\ v_-^\gamma \int \frac{d\omega}{2\pi i} \frac{e^{i\omega\eta}}{\omega - (-1 + v_-^\gamma) - i\eta} \left[\frac{\frac{1}{2}(1 - \frac{4}{c})}{\omega - (1 + \frac{c+U}{2}) + i\eta} + \frac{\frac{1}{2}(1 + \frac{4}{c})}{\omega - (1 - \frac{c-U}{2}) - i\eta} \right] &= \frac{v_-^\gamma}{v_-^\gamma - 2 - \frac{c+U}{2}} \left(1 - \frac{4}{c}\right)\end{aligned}$$

As for the left hand side, it reads:

$$\begin{aligned}& \int \frac{d\omega}{2\pi i} e^{i\omega\eta} G_-^\gamma(\omega) \Sigma_-(\omega) G_-(\omega) = \\ &= \int \frac{d\omega}{2\pi i} \frac{e^{i\omega\eta}}{\omega - (-1 + v_-^\gamma) - i\eta} \left[\frac{U}{2} + \frac{\frac{U^2}{4}}{\omega - (3 + \frac{U}{2}) + i\eta} \right] \left[\frac{\frac{1}{2}(1 - \frac{4}{c})}{\omega - (1 + \frac{c+U}{2}) + i\eta} + \frac{\frac{1}{2}(1 + \frac{4}{c})}{\omega - (1 - \frac{c-U}{2}) - i\eta} \right] = \\ &= \frac{\frac{U}{4}(1 - \frac{4}{c})}{v_-^\gamma - 2 - \frac{c+U}{2}} + \frac{U^2}{8} \left(1 - \frac{4}{c}\right) \int \frac{d\omega}{2\pi i} \frac{e^{i\omega\eta}}{\omega - (-1 + v_-^\gamma) - i\eta} \frac{1}{\omega - (3 + \frac{U}{2}) + i\eta} \frac{1}{\omega - (1 + \frac{c+U}{2}) + i\eta} + \\ &+ \frac{U^2}{8} \left(1 + \frac{4}{c}\right) \int \frac{d\omega}{2\pi i} \frac{e^{i\omega\eta}}{\omega - (-1 + v_-^\gamma) - i\eta} \frac{1}{\omega - (3 + \frac{U}{2}) + i\eta} \frac{1}{\omega - (1 - \frac{c-U}{2}) - i\eta} = \\ &= \frac{\frac{U}{4}(1 - \frac{4}{c})}{v_-^\gamma - 2 - \frac{c+U}{2}} + \frac{U^2}{8} \left(1 - \frac{4}{c}\right) \frac{1}{v_-^\gamma - 4 - \frac{U}{2}} \frac{1}{v_-^\gamma - 2 - \frac{U+c}{2}} + \\ &+ \frac{U^2}{8} \left(1 + \frac{4}{c}\right) \left[\frac{1}{v_-^\gamma - 4 - \frac{U}{2}} \frac{1}{v_-^\gamma - 2 - \frac{U-c}{2}} + \frac{1}{v_-^\gamma - 2 - \frac{U-c}{2}} \frac{1}{2 + \frac{c}{2}} \right] = \\ &= \frac{U}{4} \left(1 - \frac{4}{c}\right) \left\{ \frac{1}{[v_-^\gamma - 2 - \frac{c+U}{2}]} + \frac{\frac{U}{2}}{[v_-^\gamma - 4 - \frac{U}{2}][v_-^\gamma - 2 - \frac{c+U}{2}]} + \right. \\ &\quad \left. + \frac{U}{2} \left(\frac{1 + \frac{4}{c}}{1 - \frac{4}{c}}\right) \left[\frac{1}{[v_-^\gamma - 4 - \frac{U}{2}][v_-^\gamma - 2 - \frac{U-c}{2}]} + \frac{1}{[2 + \frac{c}{2}][v_-^\gamma - 2 - \frac{U-c}{2}]} \right] \right\}\end{aligned}$$

Therefore, the Sham-Schlüter equation reads:

$$\begin{aligned}0 &= \frac{U}{4} \left(1 - \frac{4}{c}\right) \left\{ \frac{1 - \frac{2v_-^\gamma}{U}}{[v_-^\gamma - 2 - \frac{c+U}{2}]} + \frac{\frac{U}{2}}{[v_-^\gamma - 4 - \frac{U}{2}][v_-^\gamma - 2 - \frac{c+U}{2}]} + \right. \\ &\quad \left. + \frac{U}{2} \left(\frac{1 + \frac{4}{c}}{1 - \frac{4}{c}}\right) \left[\frac{1}{[v_-^\gamma - 4 - \frac{U}{2}][v_-^\gamma - 2 - \frac{U-c}{2}]} + \frac{1}{[2 + \frac{c}{2}][v_-^\gamma - 2 - \frac{U-c}{2}]} \right] \right\}\end{aligned}$$

which simplifies to:

$$0 = -\frac{1}{2} \left(1 - \frac{4}{c} \right) \frac{v_k^\gamma - \left(2 + \frac{U+c}{2} \right)}{v_k^\gamma - \left(2 + \frac{U+c}{2} \right)}$$

which never holds, apart when $U = 0$, when it displays an undetermined solution. Of course, this is a trivial case as the density matrix is already idempotent. Note that, even with a complex-valued auxiliary system potential $v_k^\gamma \in \mathbb{C}$, we would arrive at the same conclusions.

Homogeneous electron gas

In the case of the homogeneous electron gas, the non-local potential $v^\gamma(\mathbf{r}, \mathbf{r}') = v^\gamma(|\mathbf{r} - \mathbf{r}'|)$ can be written in reciprocal space as a k -dependent function $v^\gamma(k)$, and the density matrix of the auxiliary system in reciprocal space reads:

$$\gamma_\gamma(k) = \int_{-\infty}^{\mu} d\omega A_\gamma(k, \omega) = \int_{-\infty}^{+\infty} d\omega \theta(\mu - \omega) \delta(\omega - \varepsilon_k^0 - v^\gamma(k)) = \theta(\mu - \varepsilon_k^0 - v^\gamma(k))$$

On the contrary, using the standard self-energy, the density matrix is:

$$\gamma(k) = \int_{-\infty}^{\mu} d\omega A(k, \omega) = \int_{-\infty}^{+\infty} d\omega \theta(\mu - \omega) \delta(\omega - \varepsilon_k^0 - \Sigma(k, \omega))$$

In the most general case, when there is correlation and the self energy is frequency-dependent, there exists more than one single solution $\omega_0(k)$ to the pole equation $\omega - \varepsilon_k^0 - \Sigma(k, \omega) \Big|_{\omega=\omega_0(k)} = 0$; therefore, the delta function splits into:

$$\delta(\omega - \varepsilon_k^0 - \Sigma(k, \omega)) = \sum_{\omega_0(k)} \frac{\delta(\omega - \omega_0(k))}{\left| 1 - \frac{\partial \Sigma(k, \omega)}{\partial \omega} \right|_{\omega=\omega_0(k)}}$$

and the density matrix becomes:

$$\gamma(k) = \sum_{\omega_0(k)} \frac{\theta(\mu - \omega_0(k))}{\left| 1 - \frac{\partial \Sigma(k, \omega)}{\partial \omega} \right|_{\omega=\omega_0(k)}}$$

Thus, the generalized Sham–Schlüter equation 3.17 for the density matrix becomes:

$$\theta(\mu - \varepsilon_k^0 - v^\gamma(k)) = \sum_{\omega_0(k)} \frac{\theta(\mu - \omega_0(k))}{\left| 1 - \frac{\partial \Sigma(k, \omega)}{\partial \omega} \right|_{\omega=\omega_0(k)}}$$

or, introducing the excitation energies of both the auxiliary and the real system, $\varepsilon_k^\gamma := \varepsilon_k^0 - v^\gamma(k)$ and $\varepsilon_k^{(i)} = \omega_0^{(i)}(k)$, and the renormalization factors $Z_i^{-1} := \left| 1 - \frac{\partial \Sigma(k, \omega)}{\partial \omega} \right|_{\omega=\omega_0^{(i)}(k)}$:

$$\theta(\mu - \varepsilon_k^\gamma) = \sum_i Z_i \theta(\mu - \varepsilon_k^{(i)})$$

This equation cannot hold in general for any k : the left hand side is a simple theta function that is alternatively one or zero, depending on k . This single theta function cannot stem from the sum of different thetas: their weights must sum to one, resulting in a step function that starts with one and goes to zero as $\omega_0(k)$ goes from lower to higher values. Indeed, for very small k , the energies $\varepsilon_k^{(i)}$ lie inside the Fermi sphere, hence the sum is over all the terms and results in $\sum_i Z_i = 1$: the equality can hold. By contrast, for larger values of k , some terms will not be inside the Fermi sphere and will not be included in the summation, hence a resulting value less than one (the steps), that cannot be reproduced by the single theta function on the left hand side. Finally, for larger k , there will be no terms in the summation, yielding a zero density matrix that, again, can be reproduced by v_k^γ .

Homogeneous Electron Gas integrals

We will prove here some expressions given in the text relative to the homogeneous electron gas; such a system is homogeneous and isotropic: local quantities like $f(\mathbf{r})$ cannot depend on a specific location \mathbf{r} , hence they are constant; bilocal quantities like $f(\mathbf{r}, \mathbf{r}')$ will depend just on the distance between the arguments, $f(\mathbf{r}, \mathbf{r}') = f(|\mathbf{r} - \mathbf{r}'|)$; the same holds true when performing Fourier transforms into reciprocal space.

Screened exchange self energy

I will prove here eq. (4.50), the Fock self energy evaluated with a Coulomb potential multiplied by a screening function; in particular, I will first consider the screened potential in reciprocal space, then I will evaluate the long range contribution $\Sigma_{x,\lambda}^{\text{LR}}(k)$, from which the pure Fock self energy $\Sigma_x(k)$ as its limit for $\lambda \rightarrow 0$, and finally, from the relation $\text{erfc}(x) \equiv 1 - \text{erf}(x)$, the short range part $\Sigma_{x,\lambda}^{\text{SR}}(k)$, which is equals to $\Sigma_x(k) - \Sigma_{x,\lambda}^{\text{LR}}(k)$.

The screened potential Consider the long range part of the Coulomb potential in the error function parametrization, $v_{\text{LR}}(\mathbf{r}) = \frac{\text{erf}(|\mathbf{r}|/\lambda)}{|\mathbf{r}|}$; its Fourier transform is $v_{\text{LR}}(\mathbf{k}) = \int d^3r e^{-i\mathbf{k}\cdot\mathbf{r}} v_{\text{LR}}(\mathbf{r})$. For $r := |\mathbf{r}| \gg \lambda$, $v_{\text{LR}}(\mathbf{r})$ asymptotically goes as $1/r$, whose Fourier transform is ill-defined; we therefore add an artificial Yukawa damping $e^{-\mu r}$ to the function $v_{\text{LR}}(\mathbf{r})$, that becomes $v_{\text{LR}}^\mu(\mathbf{r}) = v_{\text{LR}}(\mathbf{r})e^{-\mu r}$, keeping in mind to take the limit $\mu \rightarrow 0^+$ at the end of the calculation [4].

The Fourier transform of $v_{\text{LR}}^\mu(\mathbf{r})$ is therefore:

$$\begin{aligned} v_{\text{LR}}^\mu(\mathbf{k}) &= \int d^3r e^{-i\mathbf{k}\cdot\mathbf{r}} v_{\text{LR}}^\mu(\mathbf{r}) = 2\pi \int_0^{+\infty} dr r^2 \frac{\text{erf}(r/\lambda)}{r} e^{-\mu r} \int_{-1}^{+1} d\xi e^{-i|\mathbf{k}|r\xi} = \\ &= \frac{2\pi i \lambda}{|\mathbf{k}|} \int_0^{+\infty} dx \text{erf}(x) \left\{ e^{-\lambda(\mu+ik)x} - e^{-\lambda(\mu-ik)x} \right\} \end{aligned} \quad (\text{E1})$$

with $x = r/\lambda$. The integral $\int_0^{+\infty} dx \text{erf}(x) e^{-zx}$ with $\text{Re}z > 0$ can be evaluated by parts [149], and the result is $\int_0^{+\infty} dx \text{erf}(x) e^{-zx} = \frac{1}{z} e^{z^2/4} \text{erfc}\frac{z}{2}$. Therefore, eq. (E1) becomes:

$$v_{\text{LR}}^\mu(\mathbf{k}) = \frac{2\pi i \lambda}{|\mathbf{k}|} \left\{ \frac{e^{\frac{\lambda^2}{4}(\mu+ik)^2}}{\lambda(\mu+ik)} \text{erfc}\left(\frac{\lambda(\mu+ik)}{2}\right) - \frac{e^{\frac{\lambda^2}{4}(\mu-ik)^2}}{\lambda(\mu-ik)} \text{erfc}\left(\frac{\lambda(\mu-ik)}{2}\right) \right\} \quad (\text{E2})$$

One can now take the limit $\mu \rightarrow 0$ and recover the original potential $v_{\text{LR}}(k)$, which reads:

$$v_{\text{LR}}(k) = \frac{4\pi}{k^2} e^{-\frac{\lambda^2 k^2}{4}} \quad (\text{E3})$$

having used the property that, since $\operatorname{erf}(-x) = -\operatorname{erf}(x)$, $\operatorname{erfc}(-x) = 2 - \operatorname{erfc}(x)$. Its short range counterpart $v_{\text{SR}}(k)$ is $v(k) - v_{\text{LR}}(k)$, with $v(k)$ the Fourier transform of the Coulomb potential:

$$v_{\text{SR}}(k) = \frac{4\pi}{k^2} \left(1 - e^{-\frac{\lambda^2 k^2}{4}} \right) \quad (\text{F.4})$$

The behaviour of the potentials $v_{\text{LR}}(k)$ and $v_{\text{SR}}(k)$ as functions of k are shown in fig. 4.14b.

The long range self energy The general form of a screened Fock self energy is given by eq. (2.47) with $v_C(\mathbf{r})$ replaced by $v_{\text{screened}}(\mathbf{r})$; in particular, using $\operatorname{erf}(r/\lambda)$ as a screening function results in the long range potential $v_{\text{LR}}(\mathbf{r})$ introduced in eq. (4.45); transforming to reciprocal and frequency space, the self energy thus reads:

$$\Sigma_{\text{x}}^{\text{LR}}(k) = i \int \frac{d^3 q}{(2\pi)^3} \frac{d\omega'}{2\pi} e^{i\omega'\eta} G(|\mathbf{k} + \mathbf{q}|, \omega + \omega') v_{\text{LR}}(q)$$

with $v_{\text{LR}}(q)$ given by eq. (F.3): since that is a static potential, the frequency integral can be done straightforwardly by moving to the complex plane: the convergence factor $e^{i\omega'\eta}$ selects the upper half plane, where the poles of the Green's function refer to occupied states; therefore it is not surprising that the occupation number $n_{\mathbf{p}} = \int_{-\infty}^{\mu} d\omega A(\mathbf{p}, \omega) = \theta(k_{\text{F}} - |\mathbf{p}|)$ pops up, and the previous expression simplifies to:

$$\Sigma_{\text{x}}^{\text{LR}}(k) = - \int \frac{d^3 q}{(2\pi)^3} v_{\text{LR}}(q) n_{|\mathbf{k} + \mathbf{q}|}$$

or, in polar coordinates, with $\mathbf{k} \cdot \mathbf{q} = kq \cos \vartheta := kq\xi$:

$$\Sigma_{\text{x}}^{\text{LR}}(k) = - \frac{1}{\pi} \int_0^{k_{\text{F}}} dq q^2 \int_{-1}^{+1} d\xi \frac{e^{-\frac{\lambda^2}{4} |\mathbf{q} - \mathbf{k}|^2}}{|\mathbf{q} - \mathbf{k}|^2}$$

Replacing ξ by the variable $t := \frac{\lambda^2}{4} |\mathbf{q} - \mathbf{k}|^2$, the last integral becomes:

$$\int_{-1}^{+1} d\xi \frac{e^{-\frac{\lambda^2}{4} |\mathbf{q} - \mathbf{k}|^2}}{|\mathbf{q} - \mathbf{k}|^2} = \frac{1}{2kq} \int_{\frac{\lambda^2}{4}(q-k)^2}^{\frac{\lambda^2}{4}(q+k)^2} dt \frac{e^{-t}}{t} = \frac{1}{2kq} \left\{ \operatorname{Ei} \left(-\frac{\lambda^2}{4} (q+k)^2 \right) - \operatorname{Ei} \left(-\frac{\lambda^2}{4} (q-k)^2 \right) \right\}$$

having introduced the *Exponential Integral* function, defined for $x \in \mathbb{R} \setminus 0$ as $\operatorname{Ei}(x) := - \int_{-x}^{+\infty} dt \frac{e^{-t}}{t}$. Its derivative is $\frac{d}{dx} \operatorname{Ei}(x) = \frac{e^x}{x}$. Therefore, the self energy becomes:

$$\Sigma_{\text{x}}^{\text{LR}}(k) = - \frac{1}{2\pi k} \int_0^{k_{\text{F}}} dq q \left\{ \operatorname{Ei} \left(-\frac{\lambda^2}{4} (q+k)^2 \right) - \operatorname{Ei} \left(-\frac{\lambda^2}{4} (q-k)^2 \right) \right\}$$

It is useful to introduce the dimensionless variables $x := \frac{\lambda}{2} (k \pm q)$ in the first and the second term respectively; the self energy assumes the compact form:

$$\Sigma_{\text{x}}^{\text{LR}}(k) = - \frac{\left(\frac{2}{\lambda}\right)^2}{2\pi k} \int_{\frac{\lambda}{2}(k-k_{\text{F}})}^{\frac{\lambda}{2}(k+k_{\text{F}})} dx \left(x - \frac{\lambda}{2} k \right) \operatorname{Ei}(-x^2)$$

We now use the integrals [150]:

$$\begin{aligned} \int dx x \operatorname{Ei}(-x^2) &= \frac{x^2}{2} \operatorname{Ei}(-x^2) - \int dx \frac{x^2}{2} \left(\frac{2}{x} e^{-x^2} \right) = \frac{x^2}{2} \operatorname{Ei}(-x^2) + \frac{1}{2} e^{-x^2} \\ \int dx \operatorname{Ei}(-x^2) &= x \operatorname{Ei}(-x^2) - \int dx x \left(\frac{2}{x} e^{-x^2} \right) = x \operatorname{Ei}(-x^2) - \sqrt{\pi} \operatorname{erf}(x) \end{aligned}$$

and the previous expression becomes:

$$\Sigma_{\mathbf{x}}^{\text{LR}}(k) = -\frac{1}{\pi\lambda^2 k} \left\{ e^{-x^2} + \sqrt{\pi}\lambda k \operatorname{erf}(x) + x(x - \lambda k) \operatorname{Ei}(-x^2) \right\}^{\frac{\lambda}{2}(k+k_{\text{F}})}_{\frac{\lambda}{2}(k-k_{\text{F}})}$$

namely:

$$\begin{aligned} \Sigma_{\mathbf{x}}^{\text{LR}}(k) = & -\frac{1}{\pi\lambda^2 k} \left\{ e^{-\frac{\lambda^2}{4}(k+k_{\text{F}})^2} - e^{-\frac{\lambda^2}{4}(k-k_{\text{F}})^2} + \sqrt{\pi}\lambda k \left[\operatorname{erf}\left(\frac{\lambda(k+k_{\text{F}})}{2}\right) - \operatorname{erf}\left(\frac{\lambda(k-k_{\text{F}})}{2}\right) \right] + \right. \\ & \left. + \frac{\lambda^2}{4}(k^2 - k_{\text{F}}^2) \left[\operatorname{Ei}\left(-\frac{\lambda^2}{4}(k-k_{\text{F}})^2\right) - \operatorname{Ei}\left(-\frac{\lambda^2}{4}(k+k_{\text{F}})^2\right) \right] \right\} \quad (\text{E.5}) \end{aligned}$$

which is an even function of k : $\Sigma_{\mathbf{x}}^{\text{LR}}(-k) = \Sigma_{\mathbf{x}}^{\text{LR}}(k)$. Note that, like the Fock self energy, also the derivative of $\Sigma_{\mathbf{x}}^{\text{LR}}(k)$ is singular for $k = k_{\text{F}}$; indeed, both $\nu_{\text{LR}}(\mathbf{r})$ and the full Coulomb potential have the same unscreened long range behaviour.

Some properties of $\Sigma_{\mathbf{x}}^{\text{LR}}(k)$ are the following:

$$\begin{aligned} \Sigma_{\mathbf{x}}^{\text{LR}}(k=0) &= -\frac{1}{\sqrt{\pi}\lambda} \left[\operatorname{erf}\left(\frac{\lambda k_{\text{F}}}{2}\right) - \operatorname{erf}\left(-\frac{\lambda k_{\text{F}}}{2}\right) \right] \xrightarrow{\lambda \rightarrow 0} -\frac{2k_{\text{F}}}{\pi} \\ \Sigma_{\mathbf{x}}^{\text{LR}}(k=k_{\text{F}}) &= -\frac{k_{\text{F}}}{\pi} \left[\sqrt{\pi} \frac{\operatorname{erf}(\lambda k_{\text{F}})}{\lambda k_{\text{F}}} - \frac{1}{\lambda^2 k_{\text{F}}^2} (1 - e^{-\lambda^2 k_{\text{F}}^2}) \right] \xrightarrow{\lambda \rightarrow 0} -\frac{k_{\text{F}}}{\pi} \end{aligned}$$

The Fock self energy Taking the limit $\lambda \rightarrow 0$, the long range part of the Coulomb potential (E.3) tends to the full Coulomb potential, and eq. (E.5) becomes the usual Fock self energy; using the limits $\operatorname{erf}(x) \xrightarrow{x \rightarrow 0} \frac{2}{\sqrt{\pi}}x$ and $\operatorname{Ei}(x) \xrightarrow{x \rightarrow 0} \gamma + \ln|x| + \mathcal{O}(x)$, with $\gamma = 0.577\dots$ Euler–Mascheroni constant, eq. (E.5) becomes:

$$\Sigma_{\mathbf{x}}(k) = \lim_{\lambda \rightarrow 0} \Sigma_{\mathbf{x}}^{\text{LR}}(k) = -\frac{k_{\text{F}}}{\pi} \left\{ 1 + \frac{k^2 - k_{\text{F}}^2}{2k_{\text{F}}k} \ln \left| \frac{k - k_{\text{F}}}{k + k_{\text{F}}} \right| \right\} \quad (\text{E.6})$$

which is the usual Fock self energy [99].

The short range self energy Finally, as $\nu_{\text{SR}}(\mathbf{r}) = \nu(\mathbf{r}) - \nu_{\text{LR}}(\mathbf{r})$, the short range self energy can be found from $\Sigma_{\mathbf{x},\lambda}^{\text{SR}}(k) = \Sigma_{\mathbf{x}}(k) - \Sigma_{\mathbf{x},\lambda}^{\text{LR}}(k)$. The result is:

$$\begin{aligned} \Sigma_{\mathbf{x}}^{\text{SR}}(k) = & -\frac{k_{\text{F}}}{\pi} \left[1 - \frac{k^2 - k_{\text{F}}^2}{2k_{\text{F}}k} \ln \left| \frac{k_{\text{F}} + k}{k_{\text{F}} - k} \right| \right] + \\ & + \frac{1}{\pi\lambda^2 k} \left\{ e^{-\frac{\lambda^2}{4}(k+k_{\text{F}})^2} - e^{-\frac{\lambda^2}{4}(k-k_{\text{F}})^2} + \sqrt{\pi}\lambda k \left[\operatorname{erf}\left(\frac{\lambda(k+k_{\text{F}})}{2}\right) - \operatorname{erf}\left(\frac{\lambda(k-k_{\text{F}})}{2}\right) \right] + \right. \\ & \left. + \frac{\lambda^2}{4}(k^2 - k_{\text{F}}^2) \left[\operatorname{Ei}\left(-\frac{\lambda^2}{4}(k-k_{\text{F}})^2\right) - \operatorname{Ei}\left(-\frac{\lambda^2}{4}(k+k_{\text{F}})^2\right) \right] \right\} \quad (\text{4.50}) \end{aligned}$$

Some properties of $\Sigma_{\mathbf{x}}^{\text{SR}}(k)$ are:

$$\begin{aligned} \Sigma_{\mathbf{x}}^{\text{SR}}(k=0) &= -\frac{2k_{\text{F}}}{\pi} \left[1 - \frac{\sqrt{\pi}}{2} \frac{\operatorname{erf}\left(\frac{\lambda k_{\text{F}}}{2}\right)}{\left(\frac{\lambda k_{\text{F}}}{2}\right)} \right] \\ \Sigma_{\mathbf{x}}^{\text{SR}}(k=k_{\text{F}}) &= -\frac{k_{\text{F}}}{\pi} \left[1 - \sqrt{\pi} \frac{\operatorname{erf}(\lambda k_{\text{F}})}{\lambda k_{\text{F}}} + \frac{1}{\lambda^2 k_{\text{F}}^2} (1 - e^{-\lambda^2 k_{\text{F}}^2}) \right] \end{aligned}$$

Note that, as the Kohn–Sham potential in the homogeneous electron gas is the self energy at the Fermi level, $\nu_{\text{xc}}^{\text{DFT}} = \Sigma_{\text{xc}}(k_{\text{F}}, \mu)$, the last line represents also the short range exchange potential of DFT: $\nu_{\text{x}}^{\text{DFT,SR}} = \Sigma_{\text{x}}^{\text{SR}}(k_{\text{F}})$, that we will need for defining the HSE06 hybrids self energy.

Moreover, from the definition of the Fermi energy μ as the single particle energy ε_k at the Fermi wave vector k_F , namely $\mu = \varepsilon_{k_F} = \varepsilon_{k_F}^0 + h_{xc}^{\text{loc}} + \alpha \Sigma_x^{\text{SR}}(k = k_F)$, since $h_{xc}^{\text{loc}} = v_{xc}^{\text{DFT}} - \alpha v_x^{\text{DFT,SR}}$ and $v_x^{\text{DFT,SR}} = \Sigma_x^{\text{SR}}(k_F)$, we obtain the important result that the Fermi energy in the HSE06 approximation is the same as the Fermi energy in DFT: $\mu = \mu^{\text{DFT}} = \varepsilon_{k_F}^0 + v_{xc}^{\text{DFT}}$.

Also the *bandwidth* $W = \mu - \varepsilon_{k=0}$ can be directly related to the self energy: in the free as well as in the DFT case, the bandwidth is $W^{\text{DFT}} = \varepsilon_{k_F}^0$. In the HSE06 case, the bandwidth is smaller:

$$\begin{aligned} W^{\text{HSE06}} &= W^{\text{DFT}} - \alpha [\Sigma_x^{\text{SR}}(k=0) - \Sigma_x^{\text{SR}}(k=k_F)] = \\ &= W^{\text{DFT}} - \alpha \frac{k_F}{\pi} \left[\left(\frac{1 - e^{-\lambda^2 k_F^2}}{\lambda^2 k_F^2} - 1 \right) + \frac{\sqrt{\pi}}{\lambda k_F} \left(2 \operatorname{erf} \left(\frac{\lambda k_F}{2} \right) - \operatorname{erf}(\lambda k_F) \right) \right] \end{aligned} \quad (\text{F7})$$

The correction in square brackets is zero for $\lambda k_F = 0$ (pure DFT limit) and goes asymptotically to 1 for $\lambda k_F \rightarrow \infty$ (the correction of the PBE0 functional).

The first and second derivatives of $\Sigma_x^{\text{SR}}(k)$ are:

$$\begin{aligned} \frac{d\Sigma_x^{\text{SR}}(k)}{dk} &= \frac{1}{\pi} \left\{ \frac{1}{4} \left(1 + \frac{k_F^2}{k^2} \right) \left[\operatorname{Ei} \left(-\frac{\lambda^2}{4} (k - k_F)^2 \right) - \operatorname{Ei} \left(-\frac{\lambda^2}{4} (k + k_F)^2 \right) - \ln \left| \frac{k - k_F}{k + k_F} \right|^2 \right] + \right. \\ &\quad \left. - \frac{k_F}{k} + \frac{1}{\lambda^2 k^2} e^{-\frac{\lambda^2}{4} (k + k_F)^2} \left(e^{\lambda^2 k_F k} - 1 \right) \right\} \end{aligned} \quad (\text{F8})$$

$$\begin{aligned} \frac{d^2 \Sigma_x^{\text{SR}}(k)}{dk^2} &= \frac{1}{2\pi k^3 (k^2 - k_F^2)} \left\{ k_F^2 (k_F^2 - k^2) \left[\operatorname{Ei} \left(-\frac{\lambda^2}{4} (k - k_F)^2 \right) - \operatorname{Ei} \left(-\frac{\lambda^2}{4} (k + k_F)^2 \right) - \ln \left| \frac{k - k_F}{k + k_F} \right|^2 \right] + \right. \\ &\quad \left. - 4k_F^3 k + 2e^{-\frac{\lambda^2}{4} (k + k_F)^2} \left[\left(e^{\lambda^2 k_F k} - 1 \right) (k + k_F) \left[k_F k^2 - \frac{2(k - k_F)}{\lambda^2} \right] + 2k_F k^3 \right] \right\} \end{aligned} \quad (\text{F9})$$

Their values at the Fermi wave vector are:

$$\begin{aligned} \left. \frac{d\Sigma_x^{\text{SR}}(k)}{dk} \right|_{k=k_F} &= \frac{1}{\pi} \left\{ \frac{\gamma}{2} - 1 + \frac{1}{2} \ln(-\lambda^2 k_F^2) - \frac{1}{2} \operatorname{Ei}(-\lambda^2 k_F^2) + \frac{1}{\lambda^2 k_F^2} \left(1 - e^{-\lambda^2 k_F^2} \right) \right\} \\ \left. \frac{d^2 \Sigma_x^{\text{SR}}(k)}{dk^2} \right|_{k=k_F} &= -\frac{1}{k_F} \left. \frac{d\Sigma_x^{\text{SR}}(k)}{dk} \right|_{k=k_F} + \frac{1}{\pi k_F} \left\{ \frac{1 + e^{-\lambda^2 k_F^2}}{2} - \frac{1 - e^{-\lambda^2 k_F^2}}{\lambda^2 k_F^2} \right\} \end{aligned}$$

which diverge for $\lambda \rightarrow 0$ (Hartree–Fock limit). Finally, also the short range self energy Σ_x^{SR} is an even function of k : $\Sigma_x^{\text{SR}}(-k) = \Sigma_x^{\text{SR}}(k)$; as a consequence, its derivative is odd. We will use these properties in the next section.

Spectral function

I will consider here the full spectral function defined in eq. (4.52), which reads:

$$A(\mathbf{r}, \mathbf{r}', \omega) = \int \frac{d^3 k}{(2\pi)^3} e^{i\mathbf{k} \cdot (\mathbf{r} - \mathbf{r}')} A(k, \omega) = \frac{1}{(2\pi)^2} \int_0^{+\infty} dk k^2 \delta(\omega - \varepsilon_k) \int_{-1}^{+1} d\xi e^{ik\Delta r \xi}$$

having introduced $\Delta r := |\mathbf{r} - \mathbf{r}'|$ and $\xi = \cos \vartheta$ with ϑ the angle between \mathbf{k} and the vector $\mathbf{r} - \mathbf{r}'$. Evaluating the last integral, $A(\Delta r, \omega)$ becomes:

$$A(\mathbf{r}, \mathbf{r}', \omega) = \frac{1}{4i\pi^2 \Delta r} \int_{-\infty}^{+\infty} dk k e^{ik\Delta r} \delta(\omega - \varepsilon_k)$$

The delta function can be expressed as a sum over the two symmetric (ε_k is an even function of k) zeros $\pm k_0(\omega)$, solutions of the equation $0 = \omega - \varepsilon_k^0 - h_{xc}^{\text{loc}} - \alpha \Sigma_x^{\text{SR}}(k) \Big|_{k=\pm k_0(\omega)}$, with $+k_0(\omega)$ the

positive one; such a solution exists whenever $\omega \geq \min_k \varepsilon_k = \mu - W$, with the bandwidth given by eq. (E.7); if no solution exists, the spectral function is identically zero. Therefore:

$$A(\mathbf{r}, \mathbf{r}', \omega) = \frac{\theta(\omega - \mu + W)}{4i\pi^2 \Delta r} \int_{-\infty}^{+\infty} dk k e^{ik\Delta r} \left\{ \frac{\delta(k - k_0(\omega))}{\left| k + \alpha \frac{d\Sigma_x^{\text{SR}}(k)}{dk} \right|_{k_0(\omega)}} + \frac{\delta(k + k_0(\omega))}{\left| k + \alpha \frac{d\Sigma_x^{\text{SR}}(k)}{dk} \right|_{-k_0(\omega)}} \right\}$$

Since both k and $\frac{d\Sigma_x^{\text{SR}}(k)}{dk}$ are odd functions of k , the previous expression simplifies to:

$$A(\mathbf{r}, \mathbf{r}', \omega) = \frac{\theta(\omega - \mu + W)}{4i\pi^2 \Delta r} \int_{-\infty}^{+\infty} dk \frac{k e^{ik\Delta r}}{\left| k + \alpha \frac{d\Sigma_x^{\text{SR}}(k)}{dk} \right|_{k_0(\omega)}} \left\{ \delta(k - k_0(\omega)) + \delta(k + k_0(\omega)) \right\}$$

Finally, we can integrate out the delta functions and obtain:

$$A(\mathbf{r}, \mathbf{r}', \omega) = \frac{\theta(\omega - \mu + W)}{2\pi^2} \frac{k_0^2(\omega)}{\left| k_0(\omega) + \alpha \frac{d\Sigma_x^{\text{SR}}(k)}{dk} \right|_{k_0(\omega)}} \frac{e^{ik_0(\omega)\Delta r} - e^{-ik_0(\omega)\Delta r}}{2i k_0(\omega) \Delta r}$$

or:

$$A(\mathbf{r}, \mathbf{r}', \omega) = \frac{\theta(\omega - \mu + W)}{\pi^2} \left| \frac{\frac{k^2}{2}}{k + \alpha \frac{d\Sigma_x^{\text{SR}}(k)}{dk}} \right| \frac{\sin(k\Delta r)}{k\Delta r} \Big|_{k=k_0(\omega)}$$

which is eq. (4.53).

First order perturbation in v^{ext} of the generalized Sham–Schlüter equation

In this appendix, from the viewpoint of the generalized Sham–Schlüter equation, we derive a relation between the spectral potentials of a homogeneous system in which $v^{\text{ext}} + v_{\text{H}} = 0$ and a system in which the external potential is considered as a small perturbation $\delta v^{\text{ext}}(\mathbf{r})$ to v^{ext} .

We therefore consider four systems: the homogeneous electron gas G^h and its auxiliary system G_{SF}^h on the one hand; the actual system G in which we turn on $\delta v^{\text{ext}}(\mathbf{r})$ with its auxiliary system G_{SF} on the other.

A first consequence of turning on δv^{ext} is the modification of the Hartree Green’s function, which becomes:

$$\begin{aligned} G_{\text{H}}^{-1}(\mathbf{r}, \mathbf{r}', \omega) &= \delta(\mathbf{r} - \mathbf{r}') \left[\omega - \left(-\frac{\nabla^2}{2} + v^{\text{ext}} + \delta v^{\text{ext}}(\mathbf{r}) + v_{\text{H}} + \delta v_{\text{H}}(\mathbf{r}) \right) \right] = \\ &= G_0^{h-1}(\mathbf{r}, \mathbf{r}', \omega) - [\delta v^{\text{ext}}(\mathbf{r}) + \delta v_{\text{H}}(\mathbf{r})] \delta(\mathbf{r} - \mathbf{r}') \end{aligned}$$

Consider now the actual system Green’s function G ; its inverse is given by $G^{-1} = G_{\text{H}}^{-1} - \Sigma$, where the self energy can be written as $\Sigma = \Sigma^h + \delta\Sigma$, and $\delta\Sigma \sim \mathcal{O}(\delta v^{\text{ext}})$. It follows that (variables and integrations implied):

$$\begin{aligned} G^{-1} &= G_0^{h-1} - [\delta v^{\text{ext}} + \delta v_{\text{H}} + \Sigma^h + \delta\Sigma] = \\ &= G^{h-1} - [\delta v^{\text{ext}} + \delta v_{\text{H}} + \delta\Sigma] \end{aligned}$$

being $G^{h-1} = G_0^{h-1} - [v^{\text{ext}} + v_{\text{H}} + \Sigma^h]$ and $v^{\text{ext}} + v_{\text{H}} = 0$. Inverting this equation we get:

$$G = G^h + G^h [\delta v^{\text{ext}} + \delta v_{\text{H}} + \delta\Sigma] G$$

and to its first order in δv^{ext} :

$$G \approx G^h + G^h [\delta v^{\text{ext}} + \delta v_{\text{H}} + \delta\Sigma] G^h \tag{G.1}$$

The same proceeding for the auxiliary systems G_{SF}^h and G_{SF} yields, to its first order in δv^{ext} :

$$G_{\text{SF}} \approx G_{\text{SF}}^h + G_{\text{SF}}^h (\delta v^{\text{ext}} + \delta v_{\text{H}} + \delta v_{\text{SF}}^{\text{xc}}) G_{\text{SF}}^h \tag{G.2}$$

having written the exchange–correlation part of the spectral potential as $v_{\text{SF}}^{\text{xc}} = v_{\text{SF}}^{\text{xc}h} + \delta v_{\text{SF}}^{\text{xc}}$, and $\delta v_{\text{SF}}^{\text{xc}} \sim \mathcal{O}(\delta v^{\text{ext}})$.

Require now $\text{Im}[G]_{r,r} = \text{Im}[G_{\text{SF}}]_{r,r}$ and alike in the homogeneous system: $\text{Im}[G^h]_{r,r} = \text{Im}[G_{\text{SF}}^h]_{r,r}$. Using the expansions (G.1) and (G.2), the zero order terms (the spectral function of the homogeneous system) cancel exactly and we are left with the following relation:

$$\text{Im}\left[G^h(\delta v^{\text{ext}} + \delta v_{\text{H}} + \delta \Sigma)G^h\right]_{r,r} = \text{Im}\left[G_{\text{SF}}^h(\delta v^{\text{ext}} + \delta v_{\text{H}} + \delta v_{\text{SF}}^{\text{xc}})G_{\text{SF}}^h\right]_{r,r} \quad (\text{G.3})$$

which is the first order perturbation term to the generalized Sham–Schlüter equation (3.23). Introducing the quantity $\tilde{\zeta}_{\text{SF}}^h(\mathbf{r}, \mathbf{r}', \omega) := \text{Im}[G_{\text{SF}}^h(\mathbf{r}, \mathbf{r}', \omega)G_{\text{SF}}^h(\mathbf{r}', \mathbf{r}, \omega)]$, its solution is:

$$\begin{aligned} \delta v_{\text{SF}}^{\text{xc}}(\mathbf{r}, \omega) = \int_{\mathbf{x}} \tilde{\zeta}_{\text{SF}}^{h-1}(\mathbf{r}, \mathbf{x}, \omega) \int_{\mathbf{y}, \mathbf{z}} \text{Im}\left[G^h(\mathbf{x}, \mathbf{y}, \omega) [(\delta v^{\text{ext}}(\mathbf{y}) + \delta v_{\text{H}}(\mathbf{y}))\delta(\mathbf{y} - \mathbf{z}) + \right. \\ \left. + \delta \Sigma(\mathbf{y}, \mathbf{z}, \omega)] G^h(\mathbf{z}, \mathbf{x}, \omega)\right] - (\delta v^{\text{ext}}(\mathbf{r}) + \delta v_{\text{H}}(\mathbf{r})) \end{aligned} \quad (\text{G.4})$$

Therefore, the full spectral potential in the actual system $v_{\text{SF}}^{\text{xc}}(\mathbf{r}, \omega) = v_{\text{SF}}^h(\omega) + \delta v_{\text{SF}}^{\text{xc}}(\mathbf{r}, \omega)$ reads:

$$\begin{aligned} v_{\text{SF}}^{\text{xc}}(\mathbf{r}, \omega) = v_{\text{SF}}^h(\omega) + \int_{\mathbf{x}, \mathbf{y}, \mathbf{z}} \tilde{\zeta}_{\text{SF}}^{h-1}(\mathbf{r}, \mathbf{x}, \omega) \text{Im}\left[G^h(\mathbf{x}, \mathbf{y}, \omega) [(\delta v^{\text{ext}}(\mathbf{y}) + \delta v_{\text{H}}(\mathbf{y}))\delta(\mathbf{y} - \mathbf{z}) + \right. \\ \left. + \delta \Sigma(\mathbf{y}, \mathbf{z}, \omega)] G^h(\mathbf{z}, \mathbf{x}, \omega)\right] - (\delta v^{\text{ext}}(\mathbf{r}) + \delta v_{\text{H}}(\mathbf{r})) \end{aligned} \quad (\text{G.5})$$

Possibly, one could consider the linearized form of eq. (G.3) by replacing G^h with G_{SF}^h everywhere (also in the definition of Σ), and get the following simplified version:

$$\text{Im}\left[\tilde{G}_{\text{SF}}^h \delta \tilde{\Sigma} \tilde{G}_{\text{SF}}^h\right]_{r,r} = \text{Im}\left[\tilde{G}_{\text{SF}}^h \delta \tilde{v}_{\text{SF}}^{\text{xc}} \tilde{G}_{\text{SF}}^h\right]_{r,r}, \quad (\text{G.6})$$

whose solution is:

$$\delta \tilde{v}_{\text{SF}}^{\text{xc}}(\mathbf{r}, \omega) = \int_{\mathbf{x}} \tilde{\zeta}_{\text{SF}}^{h-1}(\mathbf{r}, \mathbf{x}, \omega) \int_{\mathbf{y}, \mathbf{z}} \text{Im}\left[\tilde{G}^h(\mathbf{x}, \mathbf{y}, \omega) \delta \tilde{\Sigma}(\mathbf{y}, \mathbf{z}, \omega) \tilde{G}^h(\mathbf{z}, \mathbf{x}, \omega)\right]. \quad (\text{G.7})$$

which is similar to eq. (G.5) but the external and the Hartree potential do not explicitly appear.

The previous solutions, eq. (G.7) and eq. (G.4), have been achieved by directly relating the real system Green's functions to their homogeneous counterparts; on the other hand, one can first relate them to their common Hartree Green's function G_{H} , and the Sham–Schlüter equation would read $\text{Im}[G_{\text{H}}\Sigma G]_{r,r} = \text{Im}[G_{\text{H}}v_{\text{SF}}^{\text{xc}}G_{\text{SF}}]_{r,r}$, with:

$$\begin{aligned} G_{\text{H}}\Sigma G &= \left[G_0^h + G_0^h(\delta v^{\text{ext}} + \delta v_{\text{H}})G_0^h\right] \left[\Sigma^h + \delta \Sigma\right] \left[G^h + G^h(\delta v^{\text{ext}} + \delta v_{\text{H}} + \delta \Sigma)G^h\right] = \\ &\approx G_0^h \Sigma^h G^h + G_0^h \delta \Sigma G^h + G_0^h \Sigma^h G^h (\delta v^{\text{ext}} + \delta v_{\text{H}} + \delta \Sigma) G^h + G_0^h (\delta v^{\text{ext}} + \delta v_{\text{H}}) G_0^h \Sigma^h G^h = \\ &= G_0^h \Sigma^h G^h + G_0^h \left[\delta \Sigma + \Sigma^h G^h (\delta v^{\text{ext}} + \delta v_{\text{H}} + \delta \Sigma) + (\delta v^{\text{ext}} + \delta v_{\text{H}}) G_0^h \Sigma^h\right] G^h = \\ &= G_0^h \Sigma^h G^h + G_0^h \left[\left(1 + \Sigma^h G^h\right) \delta \Sigma + \Sigma^h G^h (\delta v^{\text{ext}} + \delta v_{\text{H}}) + (\delta v^{\text{ext}} + \delta v_{\text{H}}) G_0^h \Sigma^h\right] G^h = \\ &= G_0^h \Sigma^h G^h + G^h \delta \Sigma G^h + \left(G^h - G_0^h\right) (\delta v^{\text{ext}} + \delta v_{\text{H}}) G^h + G_0^h (\delta v^{\text{ext}} + \delta v_{\text{H}}) \left(G^h - G_0^h\right) = \\ &= G_0^h \Sigma^h G^h + G^h (\delta v^{\text{ext}} + \delta v_{\text{H}} + \delta \Sigma) G^h - G_0^h (\delta v^{\text{ext}} + \delta v_{\text{H}}) G_0^h \end{aligned}$$

and:

$$\begin{aligned} G_{\text{H}}v_{\text{SF}}^{\text{xc}}G_{\text{SF}} &= \left[G_0^h + G_0^h(\delta v^{\text{ext}} + \delta v_{\text{H}})G_0^h\right] \left[v_{\text{SF}}^h + \delta v_{\text{SF}}^{\text{xc}}\right] \left[G_{\text{SF}}^h + G_{\text{SF}}^h(\delta v^{\text{ext}} + \delta v_{\text{H}} + \delta v_{\text{SF}}^{\text{xc}})G_{\text{SF}}^h\right] = \\ &\approx G_0^h v_{\text{SF}}^h G_{\text{SF}}^h + G_0^h \left[\left(1 + v_{\text{SF}}^h G_{\text{SF}}^h\right) \delta v_{\text{SF}}^{\text{xc}} + v_{\text{SF}}^h G_{\text{SF}}^h (\delta v^{\text{ext}} + \delta v_{\text{H}}) + (\delta v^{\text{ext}} + \delta v_{\text{H}}) G_0^h v_{\text{SF}}^h\right] G_{\text{SF}}^h = \\ &= G_0^h v_{\text{SF}}^h G_{\text{SF}}^h + G_{\text{SF}}^h \delta v_{\text{SF}}^{\text{xc}} G_{\text{SF}}^h + \left(G_{\text{SF}}^h - G_0^h\right) (\delta v^{\text{ext}} + \delta v_{\text{H}}) G_{\text{SF}}^h + G_0^h (\delta v^{\text{ext}} + \delta v_{\text{H}}) \left(G_{\text{SF}}^h - G_0^h\right) = \\ &= G_0^h v_{\text{SF}}^h G_{\text{SF}}^h + G_{\text{SF}}^h (\delta v^{\text{ext}} + \delta v_{\text{H}} + \delta v_{\text{SF}}^{\text{xc}}) G_{\text{SF}}^h - G_0^h (\delta v^{\text{ext}} + \delta v_{\text{H}}) G_0^h \end{aligned}$$

Assuming the Sham–Schlüter equation to hold in the homogeneous system, $\text{Im} [G_{\text{H}}^h \Sigma^h G^h]_{r,r} = \text{Im} [G_{\text{H}}^h \nu_{\text{SF}}^h G_{\text{SF}}^h]_{r,r}$, we are left with the relation:

$$\text{Im} [G^h (\delta \nu^{\text{ext}} + \delta \nu_{\text{H}} + \delta \Sigma) G^h]_{r,r} = \text{Im} [G_{\text{SF}}^h (\delta \nu^{\text{ext}} + \delta \nu_{\text{H}} + \delta \nu_{\text{SF}}^{\text{xc}}) G_{\text{SF}}^h]_{r,r}$$

which is exactly eq. (G.3), again.

Appendix H

GW for the Hubbard dimer

In this appendix, I will present two different diagrammatic approaches for studying the Green's function of the Hubbard dimer. They rely on two different ways of considering the on-site interaction.

As the diagrammatic approach has been carried out for Coulomb systems in an external potential, it is useful to start from the link between the Hubbard model and the many-body Hamiltonian.

The Hubbard dimer as a simplified electron gas

Taking explicitly spin into account, which will be important for the Hubbard model, the many-body Hamiltonian (2.3a) reads:

$$\hat{H} = \sum_{\sigma} \int d^3 r \hat{\psi}_{\sigma}^{\dagger}(\mathbf{r}) h_0(\mathbf{r}) \hat{\psi}_{\sigma}(\mathbf{r}) + \frac{1}{2} \sum_{\sigma\sigma'} \int d^3 r d^3 r' \hat{\psi}_{\sigma}^{\dagger}(\mathbf{r}) \hat{\psi}_{\sigma'}^{\dagger}(\mathbf{r}') v_C(|\mathbf{r} - \mathbf{r}'|) \hat{\psi}_{\sigma'}(\mathbf{r}') \hat{\psi}_{\sigma}(\mathbf{r})$$

We rewrite this Hamiltonian in a new basis, using the expansion: $\hat{\psi}_{\sigma}^{\dagger}(\mathbf{r}) := \hat{\psi}^{\dagger}(\mathbf{x}) = \sum_I \chi_I^*(\mathbf{x}) \hat{c}_I^{\dagger}$, with $\chi_I(\mathbf{x}) := \langle \mathbf{x} | I \rangle \equiv \langle \mathbf{r}, \sigma | R_I, \sigma_I \rangle$, and the compact notation $\mathbf{x} \equiv (\mathbf{r}, \sigma)$ and $I \equiv (R_I, \sigma_I) \equiv (i, \sigma_I)$. We then define the following parameters:

$$\begin{aligned} h_{IJ} &:= \sum_{\sigma} \int d^3 r \chi_I^*(\mathbf{x}) h_0(\mathbf{r}) \chi_J(\mathbf{x}) \\ U_{IJKL} &:= \sum_{\sigma\sigma'} \int d^3 r d^3 r' \chi_I^*(\mathbf{x}) \chi_J^*(\mathbf{x}') v_C(|\mathbf{r} - \mathbf{r}'|) \chi_K(\mathbf{x}') \chi_L(\mathbf{x}) \end{aligned} \quad (\text{H.1})$$

through which the many-body Hamiltonian becomes:

$$\hat{H} = \sum_{IJ} h_{IJ} \hat{c}_I^{\dagger} \hat{c}_J + \frac{1}{2} \sum_{IJKL} U_{IJKL} \hat{c}_I^{\dagger} \hat{c}_J^{\dagger} \hat{c}_K \hat{c}_L \quad (\text{H.2})$$

To finally obtain the asymmetric Hubbard dimer, the indices I, J, K and L run over the discrete set $\{(i_1, \sigma_1), (i_2, \sigma_2)\}$, with i called "site", and:

$$\begin{aligned} h_{IJ} &= e_i \delta_{ij} \delta_{\sigma_i \sigma_j} - t(1 - \delta_{ij}) \delta_{\sigma_i \sigma_j} \\ U_{IJKL} &= U_{IJ} \delta_{iL} \delta_{jK} \\ U_{IJ} &= U \delta_{ij} (1 - \delta_{\sigma_i \sigma_j}) \end{aligned} \quad (\text{H.3})$$

The Hamiltonian finally becomes the dimer one, eq. (6.1):

$$\hat{H} = -t \sum_{\sigma} \left(\hat{c}_{1\sigma}^{\dagger} \hat{c}_{2\sigma} + \hat{c}_{2\sigma}^{\dagger} \hat{c}_{1\sigma} \right) + \sum_i e_i \hat{n}_i + U \sum_i \hat{n}_{i\uparrow} \hat{n}_{i\downarrow} \quad (\text{6.1})$$

The connection between real space quantities and site quantities can be done via eq. (H.1). For example, the spin density in real space is:

$$n_{\sigma}(\mathbf{r}) := \langle GS | \hat{\psi}_{\sigma}^{\dagger}(\mathbf{r}) \hat{\psi}_{\sigma}(\mathbf{r}) | GS \rangle = \sum_{IJ} \chi_I^*(\mathbf{r}, \sigma) \chi_J(\mathbf{r}, \sigma) n_{IJ} \quad (\text{H.4})$$

while the spin density matrix is:

$$\gamma_{\sigma\sigma'}(\mathbf{r}, \mathbf{r}') := \langle GS | \hat{\psi}_{\sigma}^{\dagger}(\mathbf{r}) \hat{\psi}_{\sigma'}(\mathbf{r}') | GS \rangle = \sum_{IJ} \chi_I^*(\mathbf{r}, \sigma) \chi_J(\mathbf{r}', \sigma') n_{IJ} \quad (\text{H.5})$$

with $n_{IJ} = \langle GS | \hat{c}_I^{\dagger} \hat{c}_J | GS \rangle = \delta_{\sigma_I, \uparrow} \delta_{\sigma_J, \uparrow} (\cos \rho - \delta_{i1} + \sin \rho - \delta_{i2}) (\cos \rho - \delta_{j1} + \sin \rho - \delta_{j2}) \equiv \delta_{\sigma_I, \uparrow} \delta_{\sigma_J, \uparrow} \Lambda_{ij}^{0(-)}$ and $n_I := n_{II} = \delta_{\sigma_I, \uparrow} (\cos^2 \rho - \delta_{i1} + \sin^2 \rho - \delta_{i2})$.

Spin-dependent GW

Hartree and exchange energy contributions With the rules (H.3) to connect the Hubbard dimer Hamiltonian to the many body Hamiltonian, we can address the Hartree energy:

$$\begin{aligned} E_H &= \frac{1}{2} \int d^3 r d^3 r' \frac{n(\mathbf{r}) n(\mathbf{r}')}{|\mathbf{r} - \mathbf{r}'|} = \frac{1}{2} \sum_{IJKL} n_{IJ} n_{KL} \int d^3 r d^3 r' \chi_I^*(\mathbf{r}) \chi_J(\mathbf{r}) v_C(|\mathbf{r} - \mathbf{r}'|) \chi_K^*(\mathbf{r}') \chi_L(\mathbf{r}') = \\ &= \frac{1}{2} \sum_{IJKL} U_{IJKL} n_{IL} n_{JK} = \frac{1}{2} \sum_{IJ} U_{IJ} n_{II} n_{JJ} = \frac{U}{2} \sum_{i, \sigma} n_{(i, \sigma), (i, \sigma)} n_{(i, -\sigma), (i, -\sigma)} = \\ &= U \sum_i n_{i\uparrow, i\uparrow} n_{i\downarrow, i\downarrow} \equiv U \sum_i n_{i\uparrow} n_{i\downarrow} \end{aligned}$$

From this derivation, the Hartree term is responsible for the whole mean field energy (which is zero, for one-fourth filling), that one obtains disregarding correlation, as explained in the main text.

In the same way, the exchange energy is:

$$\begin{aligned} E_X &= -\frac{1}{2} \int d^3 r d^3 r' \frac{\gamma(\mathbf{r}, \mathbf{r}') \gamma(\mathbf{r}', \mathbf{r})}{|\mathbf{r} - \mathbf{r}'|} = -\frac{1}{2} \sum_{IJKL} U_{IJKL} n_{IK} n_{JL} = -\frac{1}{2} \sum_{IJ} U_{IJ} n_{IJ} n_{JI} = \\ &= -\frac{U}{2} \sum_{i, \sigma} n_{(i, \sigma), (i, -\sigma)} n_{(i, -\sigma), (i, \sigma)} \equiv -U \sum_i n_{i\uparrow, i\downarrow} n_{i\downarrow, i\uparrow} \end{aligned}$$

which is zero because the density matrix n_{IJ} is diagonal in spin space, and “for the Hubbard model with only one orbital per site, there is no exchange energy, $E_x = 0$, because only unlike spins interact” [151]. This result is consistent with the fact that the whole mean field energy is due to the Hartree term, and no additional contribution is required at a mean field level.

Hartree potential and Exchange self energy

The Green’s function in the basis $\{I\}$ is defined as:

$$iG_{IJ}(t, t') := \langle GS | \hat{\mathcal{T}} \hat{c}_I(t) \hat{c}_J^{\dagger}(t') | GS \rangle$$

Applying the Gell-Mann and Low theorem [4], we have:

$$iG_{IJ}(t, t') = \langle GS | \hat{\mathcal{T}} \hat{c}_I(t) \hat{c}_J^{\dagger}(t') \exp -i \int d\tau d\tau' \sum_{KL} \hat{u}_{KL}(\tau, \tau') | GS \rangle$$

where now ground state and operators are referred to the $U = 0$ Hamiltonian, and $\hat{u}_{KL}(\tau, \tau') := \frac{1}{2} \hat{c}_K^{\dagger}(\tau) \hat{c}_L^{\dagger}(\tau') U_{KL} \delta(\tau - \tau') \hat{c}_L(\tau') \hat{c}_K(\tau)$. At zero order in U , we get the following non-interacting Green’s function:

$$G_{ij, \sigma}^0(\omega) = \frac{\Lambda_{ij}^{0(-)}}{\omega - e_- - i\eta \text{sign} \sigma} + \frac{\Lambda_{ij}^{0(+)}}{\omega - e_+ + i\eta}$$

with weights defined as $\Lambda_{ij}^{0(\pm)} := \left[\delta_{i1} \cos \rho_{\pm} + \delta_{i2} \sin \rho_{\pm} \right] \left[\delta_{j1} \cos \rho_{\pm} + \delta_{j2} \sin \rho_{\pm} \right]$.

First order diagrams At first order in U , we have:

$$iG_{IJ}^{(1)}(t, t') = iG_{IJ}^0(t, t') - i \int d\tau d\tau' \sum_{KL} \langle GS | \hat{\mathcal{F}} \hat{c}_I(t) \hat{c}_J^\dagger(t') \hat{u}_{KL}(\tau, \tau') | GS \rangle$$

so that the six-points function we have to evaluate is:

$$\langle GS | \hat{\mathcal{F}} \hat{c}_I(t) \hat{c}_J^\dagger(t') \hat{c}_K^\dagger(\tau^+) \hat{c}_L^\dagger(\tau'^+) \hat{c}_L(\tau') \hat{c}_K(\tau) | GS \rangle$$

Contracting via Wick's theorem and disregarding vacuum diagrams, we are left with:

$$\begin{aligned} & -\frac{i}{2} \int d\tau d\tau' \sum_{KL} U_{KL} \delta(\tau - \tau') \langle GS | \hat{\mathcal{F}} \hat{c}_I(t) \hat{c}_J^\dagger(t') \hat{c}_K^\dagger(\tau^+) \hat{c}_L^\dagger(\tau'^+) \hat{c}_L(\tau') \hat{c}_K(\tau) | GS \rangle = \\ & = \int d\tau d\tau' \sum_{KL} U_{KL} \delta(\tau - \tau') [G_{IK}^0(t, \tau^+) G_{LL}^0(\tau', \tau'^+) G_{KJ}^0(\tau, t') + \\ & \qquad \qquad \qquad - G_{IK}^0(t, \tau^+) G_{KL}^0(\tau, \tau'^+) G_{LJ}^0(\tau', t')] \end{aligned}$$

That is, finally:

$$\begin{aligned} G_{IJ}(t, t') &= G_{IJ}^0(t, t') - i \int d\tau d\tau' \sum_{KL} U_{KL} \delta(\tau - \tau') \cdot \\ & \cdot [G_{IK}^0(t, \tau^+) G_{LL}^0(\tau', \tau'^+) G_{KJ}^0(\tau, t') - G_{IK}^0(t, \tau^+) G_{KL}^0(\tau, \tau'^+) G_{LJ}^0(\tau', t')] \end{aligned}$$

Since, at first order in the interaction, the Dyson equation is $G = G^0 + G^0 \Sigma G^0$, the first order self energy, identified with the Hartree plus the exchange one, is given by:

$$\begin{aligned} \Sigma_{IJ}^{(H)}(t, t') &= -i\delta(t - t') \delta_{IJ} \sum_K U_{IK} G_{KK}^0(\tau', \tau'^+) \\ \Sigma_{IJ}^{(X)}(t, t') &= i\delta(t - t') U_{IJ} G_{IJ}^0(t, t'^+) \end{aligned}$$

In frequency space we get static self energies, depending only on occupied orbitals:

$$\begin{aligned} \Sigma_{IJ}^{(H)} &= -i\delta_{IJ} \sum_K U_{IK} \int \frac{d\omega}{2\pi} e^{i\omega\eta} G_{KK}^0(\omega) \\ \Sigma_{IJ}^{(X)} &= iU_{IJ} \int \frac{d\omega}{2\pi} e^{i\omega\eta} G_{IJ}^0(\omega) \end{aligned}$$

If we apply these results to the dimer in the spin-up ground state, via eq. (H.3), we get the following results:

$$\begin{aligned} \Sigma_{ij,\sigma}^{(H)} &= -iU\delta_{ij} \int \frac{d\omega}{2\pi} e^{i\omega\eta} G_{ii,-\sigma}^0(\omega) = \delta_{ij} \delta_{\sigma,\downarrow} U n_i \\ \Sigma_{ij,\sigma\sigma'}^{(X)} &= iU_{ij,\sigma\sigma'} \int \frac{d\omega}{2\pi} e^{i\omega\eta} G_{IJ}^0(\omega) = -U_{ij,\sigma\sigma'} \delta_{\sigma\sigma'} \delta_{\sigma,\downarrow} n_{ij} = 0 \end{aligned} \tag{H.6}$$

where the last equality can be understood by the fact that a spin-conserving Green's function is multiplied by an interaction which is purely off-diagonal in spin-space. Stated differently, adding a spin-down electron to a spin-up ground state doesn't require any exchange term, since the two particles are distinguishable.

Therefore, in this formulation, the Hartree potential is spin-dependent¹. It reads:

$$v_{i,\sigma}^H := \frac{\partial E_H}{\partial n_{i,\sigma}} = U n_{i,-\sigma} = \begin{cases} U n_{i,\downarrow} = 0 & \sigma = \uparrow \\ U n_{i,\uparrow} = U n_i & \sigma = \downarrow \end{cases} \quad (\text{H.7})$$

Hartree Green's function For later use, it is useful to introduce the Green's function associated to the Hartree potential, $G_{ij,\sigma}^{H-1}(\omega) = G_{ij,\sigma}^{0-1}(\omega) - v_{i,\sigma}^H$. The Hartree Hamiltonian, spin-dependent because of the spin-dependent Hartree potential, is $h_{ij,\sigma}^H = (e_i + \delta_{\sigma,\downarrow} U n_i) \delta_{ij} - t(1 - \delta_{ij})$. Diagonalizing it, its eigenvalues are $e_{\pm,\uparrow}^H = \pm \sqrt{1 + \frac{D^2}{4}} \equiv e_{\pm}$ and $e_{\pm,\downarrow}^H = \frac{U}{2} \pm \sqrt{1 + \left(\frac{D+U\Delta n}{2}\right)^2}$, with $\Delta n := n_1 - n_2$. Note that the Hartree potential does not modify the spin-up eigenvalues, which are already the poles of the fully interacting spin-up Green's function.

The eigenvectors of $h_{ij,\sigma}^H$ define a new bonding-antibonding basis, with the parameter α_{\pm}^H in place of ρ_{\pm} , defined by $[\tan \alpha_{\pm,\sigma}^H]^{-1} = -\frac{D+U\Delta n}{2} \mp \sqrt{1 + \left(\frac{D+U\Delta n}{2}\right)^2}$. In this basis, the Hartree Green's function reads:

$$G_{\pm,\uparrow}^H(\omega) = \frac{1}{\omega - e_{\pm,\uparrow}^H \pm i\eta} \quad G_{\pm,\downarrow}^H(\omega) = \frac{1}{\omega - e_{\pm,\downarrow}^H + i\eta}$$

In the site basis, the Green's function is $G_{ij,\sigma}^H(\omega) = \sum_{\pm} \langle i, \sigma | \pm, \sigma \rangle G_{\pm,\sigma}^H(\omega) \langle \pm, \sigma | j, \sigma \rangle$, with the matrix of change of basis $\langle i, \sigma | \pm, \sigma \rangle = \delta_{i1} \cos \alpha_{\pm,\sigma}^H + \delta_{i2} \sin \alpha_{\pm,\sigma}^H$. Thus, for the spin-down sector:

$$G_{ij,\downarrow}^H(\omega) = \frac{\Lambda_{ij}^{H(-)}}{\omega - e_{-,\downarrow}^H + i\eta} + \frac{\Lambda_{ij}^{H(+)}}{\omega - e_{+,\downarrow}^H + i\eta} \quad (\text{H.8})$$

with $\Lambda_{ij}^{H(\pm)} = \begin{pmatrix} \cos^2 \alpha_{\pm,\downarrow}^H & \cos \alpha_{\pm,\downarrow}^H \sin \alpha_{\pm,\downarrow}^H \\ \cos \alpha_{\pm,\downarrow}^H \sin \alpha_{\pm,\downarrow}^H & \sin^2 \alpha_{\pm,\downarrow}^H \end{pmatrix}$. It is useful to introduce the parameter $h := \frac{D+U\Delta n}{2} \equiv \frac{D+U\Delta n}{2}$, through which $\Lambda_{ij}^{H(\pm)}$ assumes the following compact form:

$$\Lambda_{ij}^{H(\pm)} = \frac{1}{2} \begin{pmatrix} 1 \pm \frac{h}{\sqrt{1+h^2}} & \mp \frac{1}{\sqrt{1+h^2}} \\ \mp \frac{1}{\sqrt{1+h^2}} & 1 \mp \frac{h}{\sqrt{1+h^2}} \end{pmatrix} \quad (\text{H.9})$$

whose limit for $U \rightarrow 0$ is $\Lambda_{ij}^{0(\pm)} = \left[\delta_{i1} \cos \rho_{\pm} + \delta_{i2} \sin \rho_{\pm} \right] \left[\delta_{j1} \cos \rho_{\pm} + \delta_{j2} \sin \rho_{\pm} \right]$, with $D/2$ in place of h , or ρ_{\pm} in place of α_{\pm}^H .

Trivially, $G_{ij,\uparrow}^H(\omega) \equiv G_{ij,\uparrow}^0(\omega)$ so that, in general:

$$G_{ij,\sigma}^H(\omega) = \frac{\Lambda_{ij,\sigma}^{H(-)}}{\omega - e_{-,\sigma}^H - i\eta \text{sign} \sigma} + \frac{\Lambda_{ij,\sigma}^{H(+)}}{\omega - e_{+,\sigma}^H + i\eta} \quad (\text{H.10})$$

with $\Lambda_{ij,\uparrow}^{H(\pm)} = \Lambda_{ij}^{0(\pm)}$ and $\Lambda_{ij,\downarrow}^{H(\pm)} = \Lambda_{ij}^{H(\pm)}$. With respect to the non-interacting Green's function, the Hartree approximation (H.10) modifies the amplitudes and the position of the poles, but keeps the structure (two poles, spin-diagonal) of it.

¹Note that, although in the site basis the Hartree potential depends on spin, the real space Hartree potential is still spin-independent:

$$v^H(\mathbf{r}) := \frac{\delta E_H}{\delta n(\mathbf{r})} = U \sum_{i,\sigma} \frac{\delta n_{i,\sigma}}{\delta n(\mathbf{r})} n_{i,-\sigma}$$

and the connection between the two is provided by:

$$v_{i,\sigma}^H = \frac{\partial E_H}{\partial n_{i,\sigma}} = \sum_{\sigma'} \int d^3 r \frac{\delta E_H}{\delta n(\mathbf{r})} \frac{\partial n_{\sigma'}(\mathbf{r})}{\partial n_{i,\sigma}} = \int d^3 r v^H(\mathbf{r}) \sum_{\sigma'} \frac{\partial n_{\sigma'}(\mathbf{r})}{\partial n_{i,\sigma}}$$

The GW self energy

We build GW in the usual way, as the dressed–interaction counterpart of the exchange self energy. We consider the Hartree approximation as our starting point. The RPA polarizability evaluated with Hartree Green’s functions, $i\Pi_{\sigma\sigma'}^H(1,2) := \sum_{\rho} G_{\sigma\rho}^H(1,2)G_{\rho\sigma'}^H(2,1^+)$, with $1 \equiv (i_1, t_1)$, is spin-diagonal and, in frequency space, it reads:

$$i\Pi_{ij,\sigma}^H(\omega) = \int \frac{d\omega'}{2\pi} e^{i\omega'\eta} G_{ij,\sigma}^H(\omega + \omega') G_{ji,\sigma}^H(\omega')$$

where $G_{ji,\sigma}^H(\omega)$ is given by eq. (H.10). As expected, only the occupied states do contribute, hence $\Pi_{ij,\sigma}^H(\omega) \equiv \Pi_{ij,\sigma}^{(0)}(\omega)$, the non-interacting polarizability:

$$\begin{aligned} \Pi_{ij,\sigma}^{(0)}(\omega) &= \delta_{\sigma,\uparrow} \Lambda_{ij}^{0(+)} \Lambda_{ij}^{0(-)} \left[\frac{1}{\omega - (e_+ - e_-) + 2i\eta} - \frac{1}{\omega + (e_+ - e_-) - 2i\eta} \right] \equiv \\ &\equiv \frac{(-1)^{(i-j)} \delta_{\sigma,\uparrow}}{D^2 + 4} \Pi^{(0)}(\omega) \end{aligned} \quad (\text{H.11})$$

where $\Pi^{(0)}(\omega)$ is the quantity in square brackets, $e_+ - e_- = \sqrt{D^2 + 4}$ is the gap between the excited (antibonding) and the ground (bonding) states, and we used the fact that $\Lambda_{ij}^{0(+)} \Lambda_{ij}^{0(-)} = (-1)^{(i-j)} / (D^2 + 4)$. As it is a non-interacting quantity, this result is consistent with the definition of GW that we will give in the next section [96].

The polarization screens the bare interaction $U_{IJ} = U\delta_{ij}\delta_{\sigma_i,-\sigma_j}$ via the Dyson equation $W_{IJ} = U_{IJ} + U_{IK}\Pi_{KL}W_{LJ}$ that, for the asymmetric dimer at one-fourth filling, reads:

$$W_{ij,\sigma\sigma'}^{RPA}(\omega) = U\delta_{ij}\delta_{\sigma,-\sigma'} + \frac{U\delta_{\sigma,\uparrow}}{D^2 + 4} \Pi^{(0)}(\omega) \sum_l (-1)^{(i-l)} W_{lj,\uparrow\sigma'}^{RPA}(\omega).$$

Considering the four possible spin combinations:

$$\begin{aligned} W_{ij,\uparrow\uparrow}^{RPA}(\omega) &= 0 \\ W_{ij,\uparrow\downarrow}^{RPA}(\omega) &= U\delta_{ij} \\ W_{ij,\downarrow\uparrow}^{RPA}(\omega) &= U\delta_{ij} + \frac{U}{D^2 + 4} \Pi^{(0)}(\omega) \sum_l (-1)^{(i-l)} W_{lj,\uparrow\uparrow}^{RPA}(\omega) = U\delta_{ij} + 0 = U\delta_{ij} \\ W_{ij,\downarrow\downarrow}^{RPA}(\omega) &= \frac{U}{D^2 + 4} \Pi^{(0)}(\omega) \sum_l (-1)^{(i-l)} W_{lj,\uparrow\uparrow}^{RPA}(\omega) = \frac{U}{D^2 + 4} \Pi^{(0)}(\omega) \sum_l (-1)^{(i-l)} U\delta_{lj} = \\ &= (-1)^{(i-j)} \frac{U^2}{D^2 + 4} \Pi^{(0)}(\omega) \end{aligned} \quad (\text{H.12})$$

which is an expected result: at the RPA level, where just a simple spin–up bubble polarization is present, two spin–up electrons cannot interact ($W_{ij,\uparrow\uparrow}^{RPA}(\omega) = 0$), different spins interact through the bare interaction ($W_{ij,\uparrow\downarrow}^{RPA}(\omega) = W_{ij,\downarrow\uparrow}^{RPA}(\omega) = U\delta_{ij}$) but now two spin–down electrons are allowed to interact through the polarization of the medium, which reflects in a non–zero value for $W_{ij,\downarrow\downarrow}^{RPA}(\omega)$; in this last case, the dressed interaction is proportional to U^2 because *two* vertices are needed for the interaction to take place. Finally, the “perturbation” expansion that led us to the closed form of the screened interaction has been possible in just “one step” because only a single bubble can be formed. In this sense, RPA is a second–order expansion in U , and not an infinite expansion in e^2 as in the continuum.

Note that here, in order to remain as close as possible to the Feynman rules of the model, we have obtained a (not even diagonal) spin-dependent screened interaction, as in ref. [152], whereas in [96] a spin-independent potential is used. For a comparison between the two approaches, see [153, 152, 154, 155, 156].

Let us now consider, with $G = G^H$, the self energy induced by this screened interaction at the GW level, namely $\Sigma_{\sigma}^{GW}(1,2) := iG_{\sigma}^H(1,2)W_{\sigma}^{RPA}(2,1^+)$ which is diagonal in spin-space because G^H is; in frequency space, it becomes:

$$\Sigma_{ij,\sigma}^{GW}(\omega) = i \int \frac{d\omega'}{2\pi} e^{i\omega'\eta} G_{ij,\sigma}^H(\omega + \omega') W_{ji,\sigma}^{RPA}(\omega')$$

From the form of the screened interaction, only the spin-down block is non-zero:

$$\begin{aligned} \Sigma_{ij,\downarrow}^{GW}(\omega) &= i \int \frac{d\omega'}{2\pi} e^{i\omega'\eta} G_{ij,\downarrow}^H(\omega + \omega') W_{ji,\downarrow}^{RPA}(\omega') = \\ &= i(-1)^{(i-j)} \frac{U^2}{D^2 + 4} \int \frac{d\omega'}{2\pi} e^{i\omega'\eta} G_{ij,\downarrow}^H(\omega + \omega') \Pi^{(0)}(\omega') = \\ &= (-1)^{(i-j)} \frac{U^2}{D^2 + 4} \left[\frac{\Lambda_{ij}^{H(-)}}{\omega - (e_{-, \downarrow}^H - 2e_F) + 3i\eta} + \frac{\Lambda_{ij}^{H(+)}}{\omega - (e_{+, \downarrow}^H - 2e_F) + 3i\eta} \right] \end{aligned} \quad (\text{H.13})$$

This contribution to the self energy corresponds to a dynamic exchange term due to the polarization of the medium (the direct exchange term – the Fock term – was ruled out by the very form of the interaction). From an analysis of the second-order Feynman diagrams, the RPA term is the only non-zero proper one (see, e.g., fig. 9.8 of ref. [4]: (e), (g), (h) and (j) have spin-diagonal interactions, while (f) is zero for $n_{i,\downarrow} = 0$).

Once the self energy is at hand, the poles of the corresponding Green's function are the solution to the equation $0 = \det[G_H^{-1}(\omega) - \Sigma^{GW}(\omega)]$, which can be solved numerically for different values of D and U . The result is shown in fig. H.1: while this GW approximation is exact for $D = 0$ (see below), it departs from the expected result for larger D , for the spin-down case. On the contrary, since the self energy is zero for the spin-up sector, the result for the poles of the spin-up Green's function is always exact (non-interacting poles).

GW for the symmetric dimer In the symmetric case, restoring a $t \neq 1$ in the poles, the self energy (H.13) reads:

$$\Sigma_{ij,\downarrow}^{GW}(\omega) \stackrel{D=0}{=} \frac{U^2}{8} \left[\frac{(-1)^{(i-j)}}{\omega - (t + \frac{U}{2}) + i\eta} + \frac{1}{\omega - (3t + \frac{U}{2}) + i\eta} \right] \quad (\text{H.14})$$

Adding the Hartree contribution, we have precisely obtained the exact result of eq. (4.24):

$$\Sigma_{ij,\downarrow}(\omega) = v_{i,\downarrow}^H \delta_{ij} + \Sigma_{ij,\downarrow}^{GW}(\omega).$$

This is an extremely nice and unexpected result which holds only for the symmetric case $D = 0$. It is the consequence of *exact* cancellations between vertex corrections and self-consistency in the Green's function, as already pointed out in an approximate way in [152, 154, 156].

GW with spin-independent interaction

The issue with a diagrammatic approach to the Hubbard model is the choice of the Feynman rules to apply; in this section we will stick to the standard GW approach in which a spin-independent interaction is considered [96]: therefore, among other things, exchange diagrams will arise, in order to cancel the spurious interaction introduced in the model (e.g., a non-zero spin-up self energy will show up, and a corresponding exchange term as well).

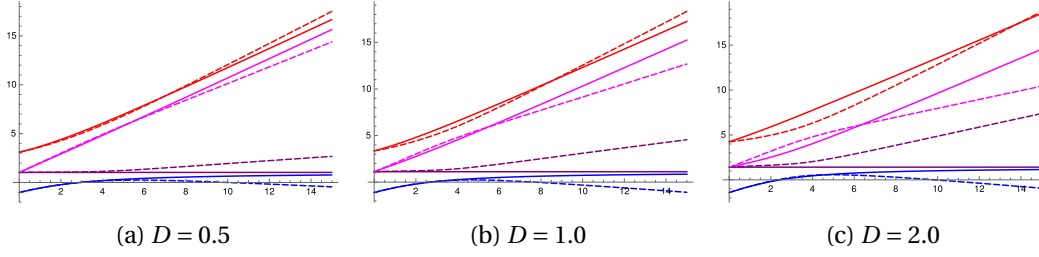


Figure H.1: *The four poles of the spin-down Green's function as a function of U , in the GW approximation which is exact for $D = 0$. The solid lines are the expected result, from eq. (6.6), while the dashed ones the numerical solutions to the pole equation $0 = \det [G_H^{-1}(\omega) - \Sigma^{GW}(\omega)]$.*

Hartree and Exchange re-defined

We introduce a spin-independent Hartree potential, $v_i^H = Un_i$. It must be balanced by a spin-dependent exchange contribution, $v_{i,\sigma}^X$, which reads:

$$\Sigma_{ij,\sigma}^X(\omega) = i \int \frac{d\omega'}{2\pi} e^{i\omega'\eta} G_{ij,\sigma}^0(\omega + \omega') v_{ij} = -\delta_{\sigma,\uparrow} n_{ij} v_{ij} = -\delta_{\sigma,\uparrow} \delta_{ij} Un_i$$

having used a spin-independent bare interaction $v_{ij} = U\delta_{ij}$. At this level this approach can be considered as a rearrangement of the previous one, as the sum of the Hartree and the exchange term is still the same. On the contrary, going to higher orders, we expect a different behaviour of the two, since they are built on top of different Hartree terms.

The Hartree Green's function will now be different from the non-interacting one also in its spin-up component. In place of eq. (H.10), we have:

$$G_{ij,\sigma}^H(\omega) = \frac{\Lambda_{ij}^{H(-)}}{\omega - e_{-1}^H - i\eta \text{sign} \sigma} + \frac{\Lambda_{ij}^{H(+)}}{\omega - e_{+1}^H + i\eta} \quad (\text{H.15})$$

As it is clear from these expressions, the spin does not influence any more the position of the poles or the height of the peaks, but only tells us if the state is occupied or empty.

Polarization and Screened Interaction

If we decide to build the polarization from the Hartree Green's function (H.15), its expression $\Pi_{\sigma\sigma'}^H(1,2) := -i \sum_{\rho} G_{\sigma\rho}^H(1,2) G_{\rho\sigma'}^H(2,1^+)$ is still diagonal in spin and, in frequency space, it reads:

$$i\Pi_{ij,\sigma}^H(\omega) = \int \frac{d\omega'}{2\pi} e^{i\omega'\eta} G_{ij,\sigma}^H(\omega + \omega') G_{ji,\sigma}^H(\omega')$$

Still, only the occupied states do contribute, hence:

$$\begin{aligned} \Pi_{ij,\sigma}^H(\omega) &= \delta_{\sigma,\uparrow} \Lambda_{ij}^{H(+)} \Lambda_{ij}^{H(-)} \left[\frac{1}{\omega - (e_{+1}^H - e_{-1}^H) + 2i\eta} - \frac{1}{\omega + (e_{+1}^H - e_{-1}^H) - 2i\eta} \right] \equiv \\ &\equiv \frac{(-1)^{(i-j)}}{4} \frac{\delta_{\sigma,\uparrow}}{1+h^2} \Pi^H(\omega) \end{aligned} \quad (\text{H.16})$$

where $\Pi^H(\omega)$ is the quantity in square brackets and $e_{+1}^H - e_{-1}^H = 2\sqrt{1+h^2}$ is now the gap between the Hartree antibonding and bonding states.

We define the screened interaction as a spin-independent quantity, like its bare counterpart. To do so, we introduce the spin-independent polarization $\Pi_{ij}^H(\omega) := \sum_{\sigma} \Pi_{ij,\sigma}^H(\omega) \equiv \Pi_{ij,\uparrow}^H(\omega)$.

The Dyson equation $W_{ij}^{RPA}(\omega) = U\delta_{ij} + U\Pi_{ik}^H(\omega)W_{kj}^{RPA}(\omega)$ can be inverted, and yields:

$$W_{ij}^{RPA}(\omega) = U\delta_{ij} + (-1)^{(i-j)} \frac{\frac{U^2}{\sqrt{1+h^2}}}{\omega^2 - 4(1+h^2) - \frac{2U}{\sqrt{1+h^2}}} \quad (\text{H.17})$$

where the first term $U\delta_{ij}$ represents the exchange interaction and the rest is the screening due to the polarization of the spin-up electron (only a single bubble). Manipulating the previous expression and treating with care the $\pm i\eta$ terms, we finally get:

$$W_{ij}^{RPA}(\omega) = U\delta_{ij} + (-1)^{(i-j)} \frac{\frac{U^2}{2k}}{\sqrt{1+h^2}} \left[\frac{1}{\omega - k + i\eta} - \frac{1}{\omega + k - i\eta} \right] \quad (\text{H.18})$$

with $k := \sqrt{4(1+h^2) + \frac{2U}{\sqrt{1+h^2}}}$.

GW self energy

In a G_0W_0 approach, the self energy reads:

$$\begin{aligned} \Sigma_{ij,\sigma}^{GHW}(\omega) &= i \int \frac{d\omega'}{2\pi} e^{i\omega'\eta} G_{ij,\sigma}^H(\omega + \omega') W_{ij}^{RPA}(\omega') = \\ &= \Sigma_{ij,\sigma}^X - \frac{(-1)^{(i-j)} \frac{U^2}{2k}}{\sqrt{1+h^2}} \int \frac{d\omega'}{2\pi i} e^{i\omega'\eta} G_{ij,\sigma}^H(\omega + \omega') \left[\frac{1}{\omega' - k + i\eta} - \frac{1}{\omega' + k - i\eta} \right] = \\ &= \Sigma_{ij,\sigma}^X + \frac{(-1)^{(i-j)} \frac{U^2}{2k}}{\sqrt{1+h^2}} \left[\frac{\Lambda_{ij}^{H(-)}}{\omega - (e_{-1}^H - k \text{sign } \sigma) - i\eta \text{sign } \sigma} + \frac{\Lambda_{ij}^{H(+)}}{\omega - (e_{+1}^H + k) + i\eta} \right] \end{aligned}$$

which, for $D \rightarrow 0$ and restoring a $t \neq 1$, reduces to:

$$\Sigma_{ij,\sigma}^{GHW}(\omega) \stackrel{D=0}{=} \Sigma_{ij,\sigma}^X + \frac{U^2 t}{4k} \left[\frac{(-1)^{(i-j)}}{\omega - (\frac{U}{2} - t - k \text{sign } \sigma) - i\eta \text{sign } \sigma} + \frac{1}{\omega - (\frac{U}{2} + t + k) + i\eta} \right] \quad (\text{H.19})$$

with $k_{D=0}^2 = 4t^2 + 2Ut$. Note that inserting a non-interacting $k \rightarrow k^0 = 2t$ in the previous expression, we would obtain the exact spin-down self energy for the symmetric dimer.

Let us use this $D = 0$ self energy to build the corresponding Green's function. As for the position of the poles, it suffices to solve the equation $0 = \det [G_H^{-1} - \Sigma^{GHW}]$, with $(G_H^{-1})_{ij,\sigma} = (\omega - e_i - Un_i)\delta_{ij} + t(1 - \delta_{ij})$. The result is:

$$\omega_{1,2,3,4}^{GHW \downarrow D=0} = \frac{k+U}{2} \pm \frac{1}{2} \sqrt{\left(k \pm 2\right)^2 + \frac{2U^2}{l}} \quad (\text{H.20})$$

for the spin-down part, with the two sets of “ \pm ” signs unrelated (four poles), while for the spin-up component, the poles are:

$$\omega_{1,2,3,4}^{GHW \uparrow D=0} = \frac{\pm k + \frac{U}{2}}{2} \pm \frac{1}{2} \sqrt{\left(k + 2 \pm \frac{U}{2}\right)^2 + \frac{2U^2}{k}} \quad (\text{H.21})$$

where the second “ \pm ” is unrelated from the other two (which are related among themselves).

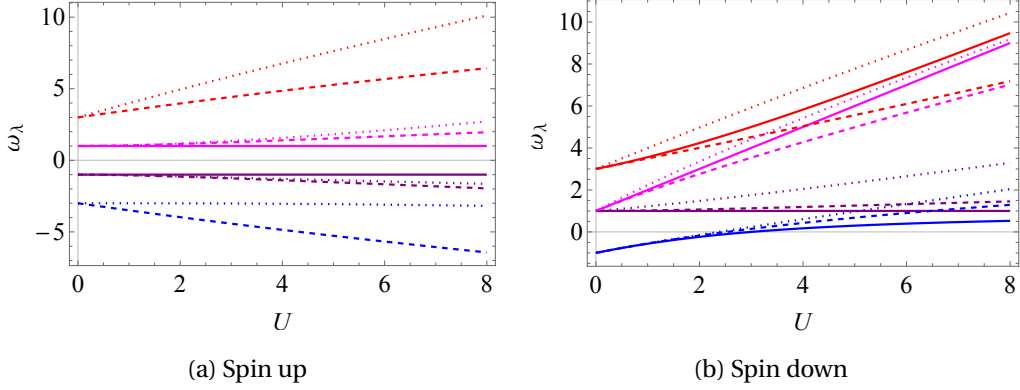


Figure H.2: Position of the poles of the $D = 0$ Green's function as a function of U . Solid line, exact results; dotted lines, $\tilde{G}_H \tilde{W}^{RPA}$, eq. (H.21) and (H.20); dashed lines, $G_0 \tilde{W}^{RPA^0}$, eq. (H.24) and (H.23).

Another approach is building a GW self energy with G^0 as the Green's function and with the polarization built from G^0 and not from G^H , as it has been done in [96]. What we get for polarization and RPA interaction is:

$$\Pi_{ij,\sigma}^0(\omega) = \frac{(-1)^{(i-j)}}{4} \frac{\delta_{\sigma,\uparrow}}{1 + \frac{D^2}{4}} \left[\frac{1}{\omega - (e_+ - e_-) + i\eta} - \frac{1}{\omega + (e_+ - e_-) - i\eta} \right]$$

$$W_{ij}^{RPA^0}(\omega) = U \delta_{ij} + (-1)^{(i-j)} \frac{\frac{U^2}{2l}}{\sqrt{1 + \frac{D^2}{4}}} \left[\frac{1}{\omega - l + i\eta} - \frac{1}{\omega + l - i\eta} \right]$$

with $l^2 := 4(1 + \frac{D^2}{4}) + \frac{2U}{\sqrt{1 + \frac{D^2}{4}}}$. The corresponding GW self energy is:

$$\begin{aligned} \Sigma_{ij,\sigma}^{G_0 W}(\omega) &= i \int \frac{d\omega'}{2\pi} e^{i\omega'\eta} G_{ij,\sigma}^0(\omega + \omega') W_{ij}^{RPA^0}(\omega') = \\ &= \Sigma_{ij,\sigma}^X + \frac{(-1)^{(i-j)} \frac{U^2}{2l}}{\sqrt{1 + \frac{D^2}{4}}} \left[\frac{\Lambda_{ij}^{0(-)}}{\omega - (e_- - l \text{sign } \sigma) - i\eta \text{sign } \sigma} + \frac{\Lambda_{ij}^{0(+)}}{\omega - (e_+ + l) + i\eta} \right] \end{aligned}$$

which, for $D \rightarrow 0$ and restoring a $t \neq 1$, reduces to:

$$\Sigma_{ij,\sigma}^{G_0 W}(\omega) \stackrel{D=0}{=} \Sigma_{ij,\sigma}^X + \frac{U^2 t}{4l} \left[\frac{(-1)^{(i-j)}}{\omega + (t + l \text{sign } \sigma) - i\eta \text{sign } \sigma} + \frac{1}{\omega - (t + l) + i\eta} \right] \quad (\text{H.22})$$

with $l_{D=0}^2 = 4t^2 + 2Ut \equiv k_{D=0}^2$ [96]. Solving the equation $\det[G_H^{-1} - \Sigma^{G_0 W}] = 0$, one gets, for the spin-down symmetric dimer Green's function, the following four pole positions:

$$\omega_{1,2,3,4}^{G_0 W \downarrow} \stackrel{D=0}{=} \frac{l + \frac{U}{2}}{2} \pm \frac{1}{2} \sqrt{\left(l \pm 2 - \frac{U}{2}\right)^2 + \frac{2U^2}{l}} \quad (\text{H.23})$$

while for the spin-up part:

$$\omega_{1,2,3,4}^{G_0 W \uparrow} \stackrel{D=0}{=} \pm \frac{l}{2} \pm \frac{1}{2} \sqrt{(l+2)^2 + \frac{2U^2}{l}} \quad (\text{H.24})$$

where in both expressions the “ \pm ” signs are unrelated in order to form four poles each.

The poles we end up with are presented in figure H.2. The behaviour is similar for the two GW approaches: they both shrink the (atomic limit) gap for the spin-down component and

open it in the spin-up case. A difference is that the spin-down $G_0 W^{RPA^0}$ has level-crossing, while $G_H W^{RPA}$ does not, as the exact solution. Furthermore, $G_0 W^{RPA^0}$ is very good for ω_1 and ω_2 , but not that good for ω_3 and ω_4 , while the opposite is true for $G_H W^{RPA}$.

Back to the asymmetric case in the $G_0 W^{RPA^0}$ approximation, the spin-down poles are the solutions to the following equation:

$$\det \left[\begin{pmatrix} \omega - (\frac{U}{2} + h) & 1 \\ 1 & \omega - (\frac{U}{2} - h) \end{pmatrix} - \frac{\frac{U^2}{2l} \frac{1}{\sqrt{1 + \frac{D^2}{4}}}}{(\omega - l)^2 - (1 + \frac{D^2}{4})} \begin{pmatrix} \omega - l + \frac{D^2}{4} & 1 \\ 1 & \omega - l - \frac{D^2}{4} \end{pmatrix} \right] = 0 \quad (\text{H.25})$$

Bilocal functions in Bloch basis

In this appendix, I show the form of generic non-local functions $f(\mathbf{r}, \mathbf{r}')$ when expressed in the Bloch basis, for functions $f(\mathbf{r}, \mathbf{r}')$ describing some physical property of a Bravais lattice.

In general, $f(\mathbf{r}, \mathbf{r}')$ can be seen as a matrix whose change of basis transformation from the set $\{\alpha\}$ to the set $\{\mathbf{r}\}$ reads:

$$f(\mathbf{r}, \mathbf{r}') = \sum_{\alpha\beta} \langle \mathbf{r} | \alpha \rangle f_{\alpha\beta} \langle \beta | \mathbf{r}' \rangle$$

We now consider the set $\{\mathbf{k}\}$ of momenta for the basis $\{\alpha\}$, with $|\mathbf{k}| \in [0, +\infty)$. A generic element of the matrix of change of basis is $\langle \mathbf{r} | \mathbf{k} \rangle = \frac{1}{\sqrt{V}} e^{i\mathbf{k}\cdot\mathbf{r}}$. The previous equation reads:

$$f(\mathbf{r}, \mathbf{r}') = \frac{1}{V} \sum_{\mathbf{k}\mathbf{k}'} e^{i\mathbf{k}\cdot\mathbf{r}} f(\mathbf{k}, \mathbf{k}') e^{-i\mathbf{k}'\cdot\mathbf{r}'}$$

This is nothing but the usual Fourier transform of a non-local function. For a lattice, a Brillouin zone in reciprocal space is defined: each sum over \mathbf{k} can be decomposed into a sum over vectors \mathbf{k} belonging to the first Brillouin zone (1BZ) and another sum over reciprocal lattice vectors \mathbf{G} : $\sum_{\mathbf{k}} = \sum_{\mathbf{k} \in 1\text{BZ}} \sum_{\mathbf{G}}$, with $\mathbf{k} = \mathbf{k} + \mathbf{G}$:

$$f(\mathbf{r}, \mathbf{r}') = \frac{1}{V} \sum_{\mathbf{k}\mathbf{k}' \in 1\text{BZ}} \sum_{\mathbf{G}\mathbf{G}' } e^{i(\mathbf{k}+\mathbf{G})\cdot\mathbf{r}} f_{\mathbf{G}\mathbf{G}'}(\mathbf{k}, \mathbf{k}') e^{-i(\mathbf{k}'+\mathbf{G}')\cdot\mathbf{r}'}$$

where $f_{\mathbf{G}\mathbf{G}'}(\mathbf{k}, \mathbf{k}')$ is just a standard convention of writing $f(\mathbf{k} + \mathbf{G}, \mathbf{k}' + \mathbf{G}')$.

We now focus on the fact that $f(\mathbf{r}, \mathbf{r}')$ describes some physical property of a Bravais lattice. It follows that it must be invariant under the simultaneous shift of both its arguments by a generic lattice vector \mathbf{R} :

$$f(\mathbf{r} + \mathbf{R}, \mathbf{r}' + \mathbf{R}) = \frac{1}{V} \sum_{\mathbf{k}\mathbf{k}' \in 1\text{BZ}} \sum_{\mathbf{G}\mathbf{G}' } e^{i(\mathbf{k}-\mathbf{k}')\cdot\mathbf{R}} e^{i(\mathbf{k}+\mathbf{G})\cdot\mathbf{r}} f_{\mathbf{G}\mathbf{G}'}(\mathbf{k}, \mathbf{k}') e^{-i(\mathbf{k}'+\mathbf{G}')\cdot\mathbf{r}'} \stackrel{!}{=} f(\mathbf{r}, \mathbf{r}')$$

having used the fact that $e^{i\mathbf{G}\cdot\mathbf{R}} = 1$. Therefore, we are left with the requirement $e^{i(\mathbf{k}-\mathbf{k}')\cdot\mathbf{R}} = 1$, which holds whenever $\mathbf{k} - \mathbf{k}'$ is a reciprocal lattice vector; since both vectors are in the 1BZ, it follows that $\mathbf{k} - \mathbf{k}' = \mathbf{0}$, and the Fourier transform becomes diagonal in \mathbf{k} :

$$f(\mathbf{r}, \mathbf{r}') = \frac{1}{V} \sum_{\mathbf{k} \in 1\text{BZ}} \sum_{\mathbf{G}\mathbf{G}' } e^{i\mathbf{k}\cdot(\mathbf{r}-\mathbf{r}')} e^{i\mathbf{G}\cdot\mathbf{r}} f_{\mathbf{G}\mathbf{G}'}(\mathbf{k}) e^{-i\mathbf{G}'\cdot\mathbf{r}'} \quad (\text{I.1})$$

This expression is valid also in the non-periodic case, in which the unit cell covers the whole system, the Brillouin zone disappears and the \mathbf{G} vectors are unrestricted vectors in \mathbb{R}^3 .

An equivalent expression can be given in terms of bands and Bloch states, instead of \mathbf{G} vectors and plane waves; in fact a \mathbf{G} vector is equivalent to a \mathbf{k} vector in the 1BZ with a certain

band index n : $\sum_{\mathbf{k} \in 1\text{BZ}} \sum_{\mathbf{G}\mathbf{G}'} \rightarrow \sum_{\mathbf{k} \in 1\text{BZ}} \sum_{nn'}$; the matrix element of change of basis is now a Bloch wavefunction [101] $\langle \mathbf{r} | \mathbf{k}n \rangle = \varphi_{n\mathbf{k}}(\mathbf{r}) = e^{i\mathbf{k} \cdot \mathbf{r}} u_{n\mathbf{k}}(\mathbf{r})$, with $u_{n\mathbf{k}}(\mathbf{r} + \mathbf{R}) = u_{n\mathbf{k}}(\mathbf{r})$. Therefore, the previous expression can equivalently be written as:

$$f(\mathbf{r}, \mathbf{r}') = \frac{1}{V} \sum_{\mathbf{k} \in 1\text{BZ}} \sum_{nn'} e^{i\mathbf{k} \cdot (\mathbf{r} - \mathbf{r}')} u_{n\mathbf{k}}(\mathbf{r}) f_{nn'}(\mathbf{k}) u_{n'\mathbf{k}}^*(\mathbf{r}') \quad (\text{I.2})$$

which is the expression we use to implement our theory. Note that the diagonal elements $\mathbf{r}' = \mathbf{r}$ are still non-diagonal in the bands:

$$f(\mathbf{r}, \mathbf{r}) = \frac{1}{V} \sum_{\mathbf{k} \in 1\text{BZ}} \sum_{nn'} u_{n\mathbf{k}}(\mathbf{r}) f_{nn'}(\mathbf{k}) u_{n'\mathbf{k}}^*(\mathbf{r}) \quad (\text{I.3})$$

By contrast, integrating over space results in a diagonal expression also in the band indices:

$$\frac{1}{V} \int d^3r f(\mathbf{r}, \mathbf{r}) = \frac{1}{V} \sum_{\mathbf{k} \in 1\text{BZ}} \sum_n f_{nn}(\mathbf{k}) \quad (\text{I.4})$$

having used the orthogonality of the functions $u_{n\mathbf{k}}(\mathbf{r})$.

The inverse transformation reads:

$$f_{nn'}(\mathbf{k}) = \frac{1}{V} \int d^3r d^3r' e^{-i\mathbf{k} \cdot (\mathbf{r} - \mathbf{r}')} u_{n\mathbf{k}}^*(\mathbf{r}) f(\mathbf{r}, \mathbf{r}') u_{n'\mathbf{k}}(\mathbf{r}') \quad (\text{I.5})$$

and, for a local quantity $f(\mathbf{r}, \mathbf{r}') = v(\mathbf{r})\delta(\mathbf{r} - \mathbf{r}')$, it simplifies to:

$$v_{nn'}(\mathbf{k}) = \frac{1}{V} \int d^3r u_{n\mathbf{k}}^*(\mathbf{r}) v(\mathbf{r}) u_{n'\mathbf{k}}(\mathbf{r}) \quad (\text{I.6})$$

Bibliography

- [1] P. W. Anderson, “More Is Different,” *Science*, vol. 177, no. 4047, pp. 393–396, 1972.
- [2] L. D. Landau, “The Theory of a Fermi Liquid,” *Soviet Physics JETP*, vol. 3, pp. 920–925, Jan 1957.
- [3] A. A. Abrikosov, L. P. Gorkov, and I. E. Dzyaloshinski, *Methods of Quantum Field Theory in Statistical Physics*. Dover, 1963.
- [4] A. L. Fetter and J. D. Walecka, *Quantum Theory of Many Particle Systems*. Dover, 1971.
- [5] R. M. Martin, L. Reining, and D. M. Ceperley, *Interacting Electrons: Theory and Computational Approaches*. Cambridge University Press, June 2016.
- [6] M. Gatti, V. Olevano, L. Reining, and I. V. Tokatly, “Transforming Nonlocality into a Frequency Dependence: A Shortcut to Spectroscopy,” *Phys. Rev. Lett.*, vol. 99, p. 057401, Aug 2007.
- [7] W. Kohn and L. J. Sham, “Self-Consistent Equations Including Exchange and Correlation Effects,” *Phys. Rev.*, vol. 140, pp. A1133–A1138, Nov 1965.
- [8] S. Y. Savrasov and G. Kotliar, “Spectral density functionals for electronic structure calculations,” *Phys. Rev. B*, vol. 69, p. 245101, Jun 2004.
- [9] A. Georges and G. Kotliar, “Hubbard model in infinite dimensions,” *Phys. Rev. B*, vol. 45, pp. 6479–6483, Mar 1992.
- [10] E. Runge and E. K. U. Gross, “Density-Functional Theory for Time-Dependent Systems,” *Phys. Rev. Lett.*, vol. 52, pp. 997–1000, Mar 1984.
- [11] L. J. Sham and M. Schlüter, “Density-Functional Theory of the Energy Gap,” *Phys. Rev. Lett.*, vol. 51, pp. 1888–1891, Nov 1983.
- [12] J. Heyd, G. E. Scuseria, and M. Ernzerhof, “Erratum: “Hybrid functionals based on a screened Coulomb potential” [J. Chem. Phys. 118, 8207 (2003)],” *The Journal of Chemical Physics*, vol. 124, no. 21, p. 219906, 2006.
- [13] A. Einstein, “Über einen die Erzeugung und Verwandlung des Lichtes betreffenden heuristischen Gesichtspunkt,” *Annalen der Physik*, vol. 322, no. 6, pp. 132–148, 1905.
- [14] K. M. Siegbahn, “Nobel Lecture: Electron Spectroscopy for Atoms, Molecules and Condensed Matter,” Dec 1981.

- [15] J. S. Zhou *et al.*, “ARPES on valence aluminum.” in preparation.
- [16] L. Venema, B. Verberck, I. Georgescu, G. Prando, E. Couderc, S. Milana, M. Maragkou, L. Persechini, G. Pacchioni, and L. Fleet, “The quasiparticle zoo,” *Nat. Phys.*, vol. 12, no. 12, pp. 1085–1089, 2016.
- [17] S. Hüfner, *Photoelectron Spectroscopy, Principles and Applications*. Springer-Verlag Berlin Heidelberg, 2003.
- [18] C. N. Berglund and W. E. Spicer, “Photoemission Studies of Copper and Silver: Theory,” *Phys. Rev.*, vol. 136, pp. A1030–A1044, Nov 1964.
- [19] A. Damascelli, “Probing the Electronic Structure of Complex Systems by ARPES,” *Physica Scripta*, vol. 2004, no. T109, p. 61, 2004.
- [20] P. A. M. Dirac, “The Quantum Theory of the Emission and Absorption of Radiation,” *Proceedings of the Royal Society of London A: Mathematical, Physical and Engineering Sciences*, vol. 114, no. 767, pp. 243–265, 1927.
- [21] E. Fermi, *Nuclear Physics*. University of Chicago Press, 1950.
- [22] L. Hedin, “On correlation effects in electron spectroscopies and the GW approximation,” *Journal of Physics: Condensed Matter*, vol. 11, no. 42, p. R489, 1999.
- [23] A. Damascelli, Z. Hussain, and Z.-X. Shen, “Angle-resolved photoemission studies of the cuprate superconductors,” *Rev. Mod. Phys.*, vol. 75, pp. 473–541, Apr 2003.
- [24] G. Binnig and H. Rohrer, “Scanning tunneling microscopy—from birth to adolescence,” *Rev. Mod. Phys.*, vol. 59, pp. 615–625, Jul 1987.
- [25] E. Ruska, “The development of the electron microscope and of electron microscopy,” *Rev. Mod. Phys.*, vol. 59, pp. 627–638, Jul 1987.
- [26] J. Stroscio and D. M. Eigler, “Atomic and Molecular Manipulation with the Scanning Tunneling Microscope,” *Science*, vol. 254, no. 5036, pp. 1319–1326, 1991.
- [27] C. Hellenthal, R. Heimbuch, K. Sotthewes, E. S. Kooij, and H. J. W. Zandvliet, “Determining the local density of states in the constant current STM mode,” *Phys. Rev. B*, vol. 88, p. 035425, Jul 2013.
- [28] J. Tersoff and D. R. Hamann, “Theory and Application for the Scanning Tunneling Microscope,” *Phys. Rev. Lett.*, vol. 50, pp. 1998–2001, Jun 1983.
- [29] J. R. Schrieffer, D. J. Scalapino, and J. W. Wilkins, “Effective tunneling density of states in superconductors,” *Phys. Rev. Lett.*, vol. 10, pp. 336–339, Apr 1963.
- [30] M. M. Ervasti, F. Schulz, P. Liljeroth, and A. Harju, “Single- and many-particle description of scanning tunneling spectroscopy,” *Journal of Electron Spectroscopy and Related Phenomena*, vol. 219, no. Supplement C, pp. 63 – 71, 2017.
- [31] R. P. Feynman, R. B. Leighton, and M. L. Sands, *The Feynman lectures on physics*. Reading, Mass, Addison-Wesley Pub. Co., 1964-1966.
- [32] E. Rutherford, “LXXIX. The Scattering of α - and β - Particles by Matter and the Structure of the Atom,” *Philosophical Magazine*, vol. 21, no. 6, pp. 669 – 688, 1911.

- [33] M. Born, W. Heisenberg, and P. Z. Jordan, “Zur Quantenmechanik. II.,” *Zeitschrift für Physik*, vol. 35, pp. 557–615, 1926.
- [34] P. A. M. Dirac, “The Fundamental Equations of Quantum Mechanics,” *Proc. R. Soc. Lond. A*, vol. 109, pp. 642–653, 1925.
- [35] E. Schrödinger, “An Undulatory Theory of the Mechanics of Atoms and Molecules,” *Phys. Rev.*, vol. 28, pp. 1049–1070, Dec 1926.
- [36] M. Born and R. Oppenheimer, “Zur Quantentheorie der Molekeln,” *Annalen der Physik*, vol. 389, no. 20, pp. 457–484, 1927.
- [37] N. I. Gidopoulos and E. K. U. Gross, “Electronic non-adiabatic states: towards a density functional theory beyond the Born–Oppenheimer approximation,” *Philosophical transactions. Series A, Mathematical, physical, and engineering sciences*, vol. 372, p. 20130059, 03 2014.
- [38] S. Pisana, M. Lazzeri, C. Casiraghi, K. S. Novoselov, A. K. Geim, A. C. Ferrari, and F. Mauri, “Breakdown of the adiabatic Born–Oppenheimer approximation in graphene,” *Nature Materials*, vol. 6, pp. 198 – 201, 2007.
- [39] F. Sottile, *Response functions of semiconductors and insulators: from the Bethe-Salpeter equation to time-dependent density functional theory*. PhD thesis, École Polytechnique, 2003.
- [40] J. E. Jones, “On the Determination of Molecular Fields. II. From the Equation of State of a Gas,” *Proceedings of the Royal Society of London. Series A*, vol. 106, p. 463, 10 1924.
- [41] P. M. Morse, “Diatomic Molecules According to the Wave Mechanics. II. Vibrational Levels,” *Phys. Rev.*, vol. 34, pp. 57–64, Jul 1929.
- [42] P. A. M. Dirac, “Quantum Mechanics of Many-Electron Systems,” *Proceedings of the Royal Society of London. Series A, Containing Papers of a Mathematical and Physical Character*, vol. 123, Apr 1929.
- [43] W. Kohn, “Nobel Lecture: Electronic structure of matter—wave functions and density functionals,” *Rev. Mod. Phys.*, vol. 71, pp. 1253–1266, Oct 1999.
- [44] J. H. van Vleck, “Nonorthogonality and Ferromagnetism,” *Phys. Rev.*, vol. 49, pp. 232–240, Feb 1936.
- [45] M. Schlosshauer, J. Kofler, and A. Zeilinger, “A snapshot of foundational attitudes toward quantum mechanics,” *Studies in History and Philosophy of Science Part B: Studies in History and Philosophy of Modern Physics*, vol. 44, no. 3, pp. 222 – 230, 2013.
- [46] R. O. Jones and O. Gunnarsson, “The density functional formalism, its applications and prospects,” *Rev. Mod. Phys.*, vol. 61, pp. 689–746, Jul 1989.
- [47] G. F. Giuliani and G. Vignale, *Quantum Theory of the Electron Liquid*. Cambridge University Press, 2005.
- [48] P. A. M. Dirac, “Note on Exchange Phenomena in the Thomas Atom,” *Mathematical Proceedings of the Cambridge Philosophical Society*, vol. 26, no. 3, p. 376–385, 1930.
- [49] R. G. Parr and W. Yang, *Density-Functional Theory of Atoms and Molecules*. Oxford University Press, 1989.

- [50] R. M. Martin, *Electronic Structure: Basic Theory and Applications*. Cambridge University Press, 2004.
- [51] M. Levy, “Universal variational functionals of electron densities, first-order density matrices, and natural spin-orbitals and solution of the v -representability problem,” *Proceedings of the National Academy of Sciences*, vol. 76, no. 12, pp. 6062–6065, 1979.
- [52] P. Hohenberg and W. Kohn, “Inhomogeneous electron gas,” *Phys. Rev.*, vol. 136, pp. B864–B871, 1964.
- [53] T. L. Gilbert, “Hohenberg-Kohn theorem for nonlocal external potentials,” *Phys. Rev. B*, vol. 12, pp. 2111–2120, Sep 1975.
- [54] A. M. K. Müller, “Explicit approximate relation between reduced two- and one-particle density matrices,” *Phys. Lett. A*, vol. 105, pp. 446–452, Nov 1984.
- [55] S. Sharma, J. K. Dewhurst, S. Shallcross, and E. K. U. Gross, “Spectral Density and Metal-Insulator Phase Transition in Mott Insulators within Reduced Density Matrix Functional Theory,” *Phys. Rev. Lett.*, vol. 110, p. 116403, Mar 2013.
- [56] S. Di Sabatino, J. A. Berger, L. Reining, and P. Romaniello, “Photoemission spectra from reduced density matrices: The band gap in strongly correlated systems,” *Phys. Rev. B*, vol. 94, p. 155141, Oct 2016.
- [57] E. K. U. Gross, J. F. Dobson, and M. Petersilka, *Density functional theory of time-dependent phenomena*, vol. 181. Springer, 1996.
- [58] P. Nozières, *Theory of Interacting Fermi Systems*. Westview Press, 1964.
- [59] V. M. Galitskii and A. B. Migdal, “Application of Quantum Field Theory Methods to the Many Body Problem,” *Sov. Phys. JETP*, vol. 34, p. 96, July 1958.
- [60] W. Tarantino, P. Romaniello, J. A. Berger, and L. Reining, “Self-consistent Dyson equation and self-energy functionals: An analysis and illustration on the example of the Hubbard atom,” *Phys. Rev. B*, vol. 96, p. 045124, Jul 2017.
- [61] H. Lehmann, “Über Eigenschaften von Ausbreitungsfunktionen und Renormierungskonstanten quantisierter Felder,” *Nuovo Cim.*, vol. 11, p. 342, 1954.
- [62] B. Farid, *Towards ab initio calculation of electron energies in semiconductors*. PhD thesis, Technische Universiteit Eindhoven, 1989.
- [63] B. Farid, “Ground and Low-Lying Excited States of Interacting Electron Systems: A Survey and Some Critical Analyses,” in *Electron Correlation in the Solid State* (N. H. March, ed.), pp. 103–261, Imperial College Press, 2011.
- [64] J. M. Luttinger, “Analytic Properties of Single-Particle Propagators for Many-Fermion Systems,” *Phys. Rev.*, vol. 121, pp. 942–949, Feb 1961.
- [65] G. Onida, L. Reining, and A. Rubio, “Electronic excitations: density-functional versus many-body Green’s-function approaches,” *Rev. Mod. Phys.*, vol. 74, pp. 601–659, Jun 2002.
- [66] L. Hedin, “New Method for Calculating the One-Particle Green’s Function with Application to the Electron-Gas Problem,” *Phys. Rev.*, vol. 139, pp. A796–A823, Aug 1965.

- [67] F. Aryasetiawan and O. Gunnarsson, “The GW method,” *Reports on Progress in Physics*, vol. 61, no. 3, p. 237, 1998.
- [68] E. Jensen and E. W. Plummer, “Experimental Band Structure of Na,” *Phys. Rev. Lett.*, vol. 55, pp. 1912–1915, Oct 1985.
- [69] E. G. Dalla Torre, D. Benjamin, Y. He, D. Dentelski, and E. Demler, “Friedel oscillations as a probe of fermionic quasiparticles,” *Phys. Rev. B*, vol. 93, p. 205117, May 2016.
- [70] N. F. Mott, “The Basis of the Electron Theory of Metals, with Special Reference to the Transition Metals,” *Proceedings of the Physical Society. Section A*, vol. 62, no. 7, p. 416, 1949.
- [71] N. F. Mott, “Metal-Insulator Transition,” *Rev. Mod. Phys.*, vol. 40, pp. 677–683, Oct 1968.
- [72] A. Georges, “Strongly Correlated Electron Materials: Dynamical Mean-Field Theory and Electronic Structure,” *AIP Conference Proceedings*, vol. 715, no. 1, pp. 3–74, 2004.
- [73] M. C. Gutzwiller, “Effect of Correlation on the Ferromagnetism of Transition Metals,” *Phys. Rev. Lett.*, vol. 10, pp. 159–162, Mar 1963.
- [74] J. Kanamori, “Electron Correlation and Ferromagnetism of Transition Metals,” *Progress of Theoretical Physics*, vol. 30, pp. 275–289, Sep 1963.
- [75] J. Hubbard, “Electron correlations in narrow energy bands,” *Proceedings of the Royal Society of London A: Mathematical, Physical and Engineering Sciences*, vol. 276, pp. 238–257, Nov 1963.
- [76] D. Vollhardt, “Dynamical Mean-Field Theory of Electronic Correlations in Models and Materials,” *AIP Conference Proceedings*, vol. 1297, no. 1, pp. 339–403, 2010.
- [77] J. P. F. LeBlanc, A. E. Antipov, F. Becca, I. W. Bulik, G. K.-L. Chan, C.-M. Chung, Y. Deng, M. Ferrero, T. M. Henderson, C. A. Jiménez-Hoyos, E. Kozik, X.-W. Liu, A. J. Millis, N. V. Prokof’ev, M. Qin, G. E. Scuseria, H. Shi, B. V. Svistunov, L. F. Tocchio, I. S. Tupitsyn, S. R. White, S. Zhang, B.-X. Zheng, Z. Zhu, and E. Gull, “Solutions of the Two-Dimensional Hubbard Model: Benchmarks and Results from a Wide Range of Numerical Algorithms,” *Phys. Rev. X*, vol. 5, p. 041041, Dec 2015.
- [78] H. Bethe, “Zur theorie der metalle,” *Zeitschrift für Physik*, vol. 71, pp. 205–226, Mar 1931.
- [79] M. Gatti, *Correlation effects in valence-electron spectroscopy of transition-metal oxides: many-body perturbation theory and alternative approaches*. PhD thesis, École Polytechnique, 2007.
- [80] J. P. Perdew, R. G. Parr, M. Levy, and J. L. Balduz, “Density-Functional Theory for Fractional Particle Number: Derivative Discontinuities of the Energy,” *Phys. Rev. Lett.*, vol. 49, pp. 1691–1694, Dec 1982.
- [81] J. P. Perdew and M. Levy, “Physical Content of the Exact Kohn-Sham Orbital Energies: Band Gaps and Derivative Discontinuities,” *Phys. Rev. Lett.*, vol. 51, pp. 1884–1887, Nov 1983.
- [82] L. J. Sham, “Exchange and correlation in density-functional theory,” *Phys. Rev. B*, vol. 32, pp. 3876–3882, Sep 1985.

- [83] M. E. Casida, “Generalization of the optimized-effective-potential model to include electron correlation: A variational derivation of the Sham-Schlüter equation for the exact exchange-correlation potential,” *Phys. Rev. A*, vol. 51, pp. 2005–2013, Mar 1995.
- [84] R. T. Sharp and G. K. Horton, “A Variational Approach to the Unipotential Many-Electron Problem,” *Phys. Rev.*, vol. 90, pp. 317–317, Apr 1953.
- [85] J. D. Talman and W. F. Shadwick, “Optimized effective atomic central potential,” *Phys. Rev. A*, vol. 14, pp. 36–40, Jul 1976.
- [86] P. Rinke, A. Qteish, J. Neugebauer, and M. Scheffler, “Exciting prospects for solids: Exact-exchange based functionals meet quasiparticle energy calculations,” *phys. stat. sol. (b)*, vol. 245, pp. 929–945, 2008.
- [87] A. Ferretti, I. Dabo, M. Cococcioni, and N. Marzari, “Bridging density-functional and many-body perturbation theory: Orbital-density dependence in electronic-structure functionals,” *Phys. Rev. B*, vol. 89, p. 195134, May 2014.
- [88] W. Metzner and D. Vollhardt, “Correlated Lattice Fermions in $d = \infty$ Dimensions,” *Phys. Rev. Lett.*, vol. 62, pp. 324–327, Jan 1989.
- [89] M. Jarrell, “Hubbard model in infinite dimensions: A quantum Monte Carlo study,” *Phys. Rev. Lett.*, vol. 69, pp. 168–171, Jul 1992.
- [90] M. Ostili, “Cayley trees and bethe lattices: A concise analysis for mathematicians and physicists,” *Physica A*, vol. 391, no. 12, pp. 3417 – 3423, 2012.
- [91] W. Metzner and D. Vollhardt, “Correlated Lattice Fermions in $d = \infty$ Dimensions,” *Phys. Rev. Lett.*, vol. 62, pp. 324–327, Jan 1989.
- [92] M. Eckstein, M. Kollar, K. Byczuk, and D. Vollhardt, “Hopping on the Bethe lattice: Exact results for densities of states and dynamical mean-field theory,” *Phys. Rev. B*, vol. 71, p. 235119, Jun 2005.
- [93] E. Economou, *Green’s Functions in Quantum Physics*. Springer Series in Solid-State Sciences, Springer, 2006.
- [94] R. Bulla, “Zero Temperature Metal-Insulator Transition in the Infinite-Dimensional Hubbard Model,” *Phys. Rev. Lett.*, vol. 83, pp. 136–139, Jul 1999.
- [95] D. J. Carrascal, J. Ferrer, J. C. Smith, and K. Burke, “The Hubbard dimer: a density functional case study of a many-body problem,” *Journal of Physics: Condensed Matter*, vol. 27, no. 39, p. 393001, 2015.
- [96] P. Romaniello, F. Bechstedt, and L. Reining, “Beyond the *GW* approximation: Combining correlation channels,” *Phys. Rev. B*, vol. 85, p. 155131, Apr 2012.
- [97] E. Wigner, “On the Interaction of Electrons in Metals,” *Phys. Rev.*, vol. 46, pp. 1002–1011, Dec 1934.
- [98] M. Gell-Mann and K. A. Brueckner, “Correlation Energy of an Electron Gas at High Density,” *Phys. Rev.*, vol. 106, pp. 364–368, Apr 1957.
- [99] P. A. M. Dirac, “Note on Exchange Phenomena in the Thomas Atom,” *Mathematical Proceedings of the Cambridge Philosophical Society*, vol. 26, no. 3, p. 376–385, 1930.

- [100] J. C. Slater, "A Simplification of the Hartree–Fock Method," *Phys. Rev.*, vol. 81, pp. 385–390, Feb 1951.
- [101] N. W. Ashcroft and N. D. Mermin, *Solid State Physics*. Saunders College, 1976.
- [102] R. M. Dreizler and E. K. U. Gross, *Density Functional Theory*. Springer Verlag, 1990.
- [103] D. M. Ceperley and B. J. Alder, "Ground state of the electron gas by a stochastic method," *Phys. Rev. Lett.*, vol. 45, pp. 566–569, Aug 1980.
- [104] J. Heyd, G. E. Scuseria, and M. Ernzerhof, "Hybrid functionals based on a screened Coulomb potential," *The Journal of Chemical Physics*, vol. 118, no. 18, pp. 8207–8215, 2003.
- [105] T. M. Henderson, J. Paier, and G. E. Scuseria, "Accurate treatment of solids with the HSE screened hybrid," *physica status solidi (b)*, vol. 248, no. 4, pp. 767–774, 2011.
- [106] K. Hummer, J. Harl, and G. Kresse, "Heyd-scuseria-ernzerhof hybrid functional for calculating the lattice dynamics of semiconductors," *Phys. Rev. B*, vol. 80, p. 115205, Sep 2009.
- [107] A. Sharan, Z. Gui, and A. Janotti, "Hybrid-Functional Calculations of the Copper Impurity in Silicon," *Phys. Rev. Applied*, vol. 8, p. 024023, Aug 2017.
- [108] J. P. Perdew, K. Burke, and M. Ernzerhof, "Generalized Gradient Approximation Made Simple," *Phys. Rev. Lett.*, vol. 77, pp. 3865–3868, Oct 1996.
- [109] A. D. Becke, "Density functional thermochemistry. III. The role of exact exchange," *The Journal of Chemical Physics*, vol. 98, no. 7, pp. 5648–5652, 1993.
- [110] A. D. Becke, "A new mixing of hartree–fock and local density–functional theories," *The Journal of Chemical Physics*, vol. 98, no. 2, pp. 1372–1377, 1993.
- [111] J. P. Perdew, M. Ernzerhof, and K. Burke, "Rationale for mixing exact exchange with density functional approximations," *The Journal of Chemical Physics*, vol. 105, no. 22, pp. 9982–9985, 1996.
- [112] M. A. L. Marques, J. Vidal, M. J. T. Oliveira, L. Reining, and S. Botti, "Density-based mixing parameter for hybrid functionals," *Phys. Rev. B*, vol. 83, p. 035119, Jan 2011.
- [113] J. Toulouse, I. C. Gerber, G. Jansen, A. Savin, and J. G. Ángyán, "Adiabatic-Connection Fluctuation-Dissipation Density-Functional Theory Based on Range Separation," *Phys. Rev. Lett.*, vol. 102, p. 096404, Mar 2009.
- [114] T. Stein, H. Eisenberg, L. Kronik, and R. Baer, "Fundamental Gaps in Finite Systems from Eigenvalues of a Generalized Kohn-Sham Method," *Phys. Rev. Lett.*, vol. 105, p. 266802, Dec 2010.
- [115] J. Harris and R. O. Jones, "The surface energy of a bounded electron gas," *Journal of Physics F: Metal Physics*, vol. 4, no. 8, p. 1170, 1974.
- [116] O. Gunnarsson and B. I. Lundqvist, "Exchange and correlation in atoms, molecules, and solids by the spin-density-functional formalism," *Phys. Rev. B*, vol. 13, pp. 4274–4298, May 1976.

- [117] W. Kohn, "Density Functional and Density Matrix Method Scaling Linearly with the Number of Atoms," *Phys. Rev. Lett.*, vol. 76, pp. 3168–3171, Apr 1996.
- [118] E. Prodan and W. Kohn, "Nearsightedness of electronic matter," *Proceedings of the National Academy of Sciences of the United States of America*, vol. 102, no. 33, pp. 11635–11638, 2005.
- [119] O. Gunnarsson, M. Jonson, and B. I. Lundqvist, "Descriptions of exchange and correlation effects in inhomogeneous electron systems," *Phys. Rev. B*, vol. 20, pp. 3136–3164, Oct 1979.
- [120] S. Goedecker, M. Teter, and J. Hutter, "Separable dual-space Gaussian pseudopotentials," *Phys. Rev. B*, vol. 54, pp. 1703–1710, Jul 1996.
- [121] B. I. Lundqvist, "Single-particle spectrum of the degenerate electron gas," *Physik der kondensierten Materie*, vol. 6, pp. 193–205, Sep 1967.
- [122] B. I. Lundqvist, "Single-particle spectrum of the degenerate electron gas," *Physik der kondensierten Materie*, vol. 6, pp. 206–217, Sep 1967.
- [123] B. I. Lundqvist, "Single-particle spectrum of the degenerate electron gas," *Physik der kondensierten Materie*, vol. 7, pp. 117–123, Mar 1968.
- [124] U. von Barth and B. Holm, "Self-consistent GW_0 results for the electron gas: Fixed screened potential W_0 within the random-phase approximation," *Phys. Rev. B*, vol. 54, pp. 8411–8419, Sep 1996.
- [125] L. H. Thomas, "The calculation of atomic fields," *Mathematical Proceedings of the Cambridge Philosophical Society*, vol. 23, no. 5, p. 542–548, 1927.
- [126] E. Fermi, "Un Metodo Statistico per la Determinazione di alcune Proprietà dell'Atomo," *Rend. Accad. Naz. Lincei*, vol. 6, pp. 602–607, 1927.
- [127] E. Teller, "On the Stability of Molecules in the Thomas-Fermi Theory," *Rev. Mod. Phys.*, vol. 34, pp. 627–631, Oct 1962.
- [128] L. J. Sham and W. Kohn, "One-Particle Properties of an Inhomogeneous Interacting Electron Gas," *Phys. Rev.*, vol. 145, pp. 561–567, May 1966.
- [129] L. Hedin and B. I. Lundqvist, "Explicit local exchange-correlation potentials," *Journal of Physics C: Solid State Physics*, vol. 4, no. 14, p. 2064, 1971.
- [130] C. S. Wang and W. E. Pickett, "Density-Functional Theory of Excitation Spectra of Semiconductors: Application to Si," *Phys. Rev. Lett.*, vol. 51, pp. 597–600, Aug 1983.
- [131] W. E. Pickett and C. S. Wang, "Local-density approximation for dynamical correlation corrections to single-particle excitations in insulators," *Phys. Rev. B*, vol. 30, pp. 4719–4733, Oct 1984.
- [132] L. Wantzel, "Classification des nombres incommensurables d'origine algébrique," *Nouvelles annales de mathématiques : journal des candidats aux écoles polytechnique et normale, Série 1*, vol. 2, pp. 117–127, 1843.

- [133] X. Gonze, B. Amadon, P.-M. Anglade, J.-M. Beuken, F. Bottin, P. Boulanger, F. Bruneval, D. Caliste, R. Caracas, M. Côté, T. Deutsch, L. Genovese, P. Ghosez, M. Giantomassi, S. Goedecker, D. Hamann, P. Hermet, F. Jollet, G. Jomard, S. Leroux, M. Mancini, S. Mazevet, M. Oliveira, G. Onida, Y. Pouillon, T. Rangel, G.-M. Rignanese, D. Sangalli, R. Shaltaf, M. Torrent, M. Verstraete, G. Zerah, and J. Zwanziger, “Abinit: First-principles approach to material and nanosystem properties,” *Computer Physics Communications*, vol. 180, no. 12, pp. 2582 – 2615, 2009.
- [134] X. Gonze, G. Rignanese, M. Verstraete, J. Betiken, Y. Pouillon, R. Caracas, F. Jollet, M. Torrent, G. Zerah, M. Mikami, P. Ghosez, M. Veithen, J.-Y. Raty, V. Olevano, F. Bruneval, L. Reining, R. Godby, G. Onida, D. Hamann, and D. Allan, “A brief introduction to the ABINIT software package,” *Zeitschrift für Kristallographie. (Special issue on Computational Crystallography.)*, vol. 220, pp. 558–562, 2005.
- [135] P. E. Blöchl, O. Jepsen, and O. K. Andersen, “Improved tetrahedron method for Brillouin-zone integrations,” *Phys. Rev. B*, vol. 49, pp. 16223–16233, Jun 1994.
- [136] R. Wyckoff, *Crystal structures*, vol. 1. New York: Interscience Publishers, second ed., 1963.
- [137] N. Troullier and J. L. Martins, “Efficient pseudopotentials for plane-wave calculations,” *Phys. Rev. B*, vol. 43, pp. 1993–2006, Jan 1991.
- [138] D. R. Hamann, “Optimized norm-conserving Vanderbilt pseudopotentials,” *Phys. Rev. B*, vol. 88, p. 085117, Aug 2013.
- [139] J. W. Precker and M. A. da Silva, “Experimental estimation of the band gap in silicon and germanium from the temperature–voltage curve of diode thermometers,” *American Journal of Physics*, vol. 70, no. 11, pp. 1150–1153, 2002.
- [140] H. J. Monkhorst and J. D. Pack, “Special points for Brillouin-zone integrations,” *Phys. Rev. B*, vol. 13, pp. 5188–5192, Jun 1976.
- [141] J. P. Perdew and S. Kurth, “Density functionals for non-relativistic coulomb systems in the new century,” in *A Primer in Density Functional Theory*, Springer, 2003.
- [142] L. Van Hove, “The Occurrence of Singularities in the Elastic Frequency Distribution of a Crystal,” *Phys. Rev.*, vol. 89, pp. 1189–1193, Mar 1953.
- [143] G. Cappellini, R. Del Sole, L. Reining, and F. Bechstedt, “Model dielectric function for semiconductors,” *Phys. Rev. B*, vol. 47, pp. 9892–9895, Apr 1993.
- [144] G. A. Baraff and M. Schlüter, “Migration of interstitials in silicon,” *Phys. Rev. B*, vol. 30, pp. 3460–3469, Sep 1984.
- [145] A. Schindlmayr and R. W. Godby, “Systematic Vertex Corrections through Iterative Solution of Hedin’s Equations Beyond the *GW* Approximation,” *Phys. Rev. Lett.*, vol. 80, pp. 1702–1705, Feb 1998.
- [146] “Electron correlations in narrow energy bands III. An improved solution,” *Proceedings of the Royal Society of London A: Mathematical, Physical and Engineering Sciences*, vol. 281, no. 1386, pp. 401–419, 1964.
- [147] F. Gebhard, *The Mott Metal–Insulator Transition, Models and Methods*. Springer, 1997.

- [148] J. M. Tomczak, *Spectral and Optical Properties of Correlated Materials*. PhD thesis, École Polytechnique, 2007.
- [149] E. W. Ng and M. Geller, “A table of Integrals of the Error Functions,” *J. Res. Natl. Bur. Stand., Sec. B: Math. Sci.*, vol. 73B, no. 1, p. 1, 1969.
- [150] M. Geller and E. W. Ng, “A table of Integrals of the Exponential Integral,” *J. Res. Natl. Bur. Stand., Sec. B: Math. Sci.*, vol. 73B, no. 3, p. 191, 1969.
- [151] K. Capelle and V. L. Campo, “Density functionals and model hamiltonians: Pillars of many-particle physics,” *Physics Reports*, vol. 528, no. 3, pp. 91 – 159, 2013.
- [152] X. Wang, C. D. Spataru, M. S. Hybertsen, and A. J. Millis, “Electronic correlation in nanoscale junctions: Comparison of the GW approximation to a numerically exact solution of the single-impurity Anderson model,” *Phys. Rev. B*, vol. 77, p. 045119, Jan 2008.
- [153] K. S. Thygesen, “Impact of Exchange-Correlation Effects on the *IV* Characteristics of a Molecular Junction,” *Phys. Rev. Lett.*, vol. 100, p. 166804, Apr 2008.
- [154] C. Verdozzi, R. W. Godby, and S. Holloway, “Evaluation of *GW* Approximations for the Self-Energy of a Hubbard Cluster,” *Phys. Rev. Lett.*, vol. 74, pp. 2327–2330, Mar 1995.
- [155] K. S. Thygesen and A. Rubio, “Conserving *GW* scheme for nonequilibrium quantum transport in molecular contacts,” *Phys. Rev. B*, vol. 77, p. 115333, Mar 2008.
- [156] M. P. von Friesen, C. Verdozzi, and C.-O. Almbladh, “Successes and Failures of Kadanoff-Baym Dynamics in Hubbard Nanoclusters,” *Phys. Rev. Lett.*, vol. 103, p. 176404, Oct 2009.

TITRE : SYSTÈMES AUXILIAIRES POUR LES OBSERVABLES : APPROXIMATION DU CONNECTEUR DYNAMIQUE LOCAL POUR LES SPECTRES D'ADDITION ET D'ÉMISSION D'ÉLECTRONS.

MOTS-CLÉS : APPROCHES EFFICACES, FONCTION SPECTRALE, SPECTROSCOPIE THÉORIQUE.

RÉSUMÉ : cette thèse propose une méthode théorique innovante pour l'étude des spectres d'excitation à un électron.

Nous proposons deux raccourcis par rapport à la méthode standard, qui repose sur des self-énergies complexes et non locales. Le premier est l'introduction d'un système auxiliaire qui cible précisément le spectre d'excitation du système réel via un potentiel réel, local et dynamique, le potentiel spectral. Le deuxième consiste à ne calculer ce potentiel qu'une fois pour toute dans un système modèle, le gaz d'électrons ho-

mogène. Pour étudier des matériaux réels, nous concevons un connecteur qui prescrit l'utilisation des résultats du gaz pour calculer les spectres électroniques. Nous proposons une approximation basée sur les propriétés locales du système: l'approximation du connecteur dynamique local. Nous mettons en œuvre cette procédure pour quatre matériaux: le sodium, l'aluminium, le silicium et l'argon. Les spectres que nous obtenons démontrent le potentiel de cette théorie.

TITLE: AUXILIARY SYSTEMS FOR OBSERVABLES: DYNAMICAL LOCAL CONNECTOR APPROXIMATION FOR ELECTRON ADDITION AND REMOVAL SPECTRA.

KEYWORDS: EFFECTIVE APPROACHES, SPECTRAL FUNCTION, THEORETICAL SPECTROSCOPY.

ABSTRACT: this thesis proposes an innovative theoretical method for studying one-electron excitation spectra.

We propose two shortcuts to the standard method, which relies on complex, non-local self energies evaluated specifically for each material. The first one is the introduction of an auxiliary system that exactly targets, in principle, the excitation spectrum of the real system, via a local and frequency-dependent, yet real, potential (the spectral potential). The second shortcut consists in

calculating this potential just once and forever in a model system, the homogeneous electron gas. To study real materials, we design a connector which prescribes the use of the gas results for calculating electronic spectra. We propose an approximation for it, based on local properties of the system: the dynamical local connector approximation. We implement this procedure for four prototypical materials: sodium, aluminum, silicon and argon. The spectra we obtain demonstrate the potential of this theory.

